An investigation into the role of cannabinoid and group 1 metabotropic glutamate receptors in the control of rhythmic locomotion in hatchling *Xenopus Laevis*

A thesis submitted for the degree of. Doctor of Philosophy (PhD)

by

Jack West Gibson

School of Science and Technology,

Abertay University.

September, 2018

Declaration

Candidate's declarations:

I, Jack West Gibson, hereby certify that this thesis submitted in partial fulfilment of the requirements for the award of Doctor of Philosophy (PhD) at Abertay University, is wholly my own work unless otherwise referenced or acknowledged. This work has not been submitted for any other qualification at any other academic institution.

Signed [candidates' signature]…… [redacted] …….

Date……30/09/18……..

Supervisor's declaration:

I, Anne Savage, hereby certify that the candidate has fulfilled the conditions of the Resolution and Regulations appropriate for the degree of PhD in Abertay University and that the candidate is qualified to submit this thesis in application for that degree.

Signed [Principal Supervisors signature] … … [redacted] ..

Date……30/09/18……..

Certificate of Approval

I certify that this is a true and accurate version of the thesis approved by the examiners, and that all relevant ordinance regulations have been fulfilled.

Supervisor…… [redacted] ……..

Date……30/09/18……..

Acknowledgements

I would like to thank Dr Peter Moult for his help, support and encouragement in getting me to this stage I wouldn't be here without you. Secondly I would like to thank everyone in the graduate school who helped and supported me and all the other students particularly I would like to thank Dr Nia White for managing to care for all the students equally, it's great to have someone in your corner at all times, I would also like to thank Wendy for dealing with all the numerous queries thrown her way.

A huge thank you to Dr Anne Savage who came on to the supervisory team at the last minute and was a big help in getting me across the line.

Finally, I would like to thank my partner Billie, without whom I would have gone mad a long time ago. Your help, support and love through all the ups and downs has enabled me to get to the end.

Abbreviations

2-archidonyl glycerol (2-AG),

α-amino-3-hydroxy-5-methyl-4-isoxazolepropionic acid (AMPA),

Ascending interneurons (aINs),

Brain derived neurotrophic factor (BDNF),

Calcium/calmodulin-dependent protein kinase II (CaMKII),

$Ca^{2+/}Mg^{2+}$ free solution (CMF),

Cannabidiol (CBD)

Central nervous system (CNS),

Central pattern generators (CPGs),

C-Jun N-terminal kinases (JNK),

Commissural interneurons (cIN),

Descending interneurons (dINs),

Dihydroxyphenylglycine (DHPG)

Cyclic GMP-dependent protein kinase (PKG),

Diacylglycerol (DAG),

Dorsolateral ascending (dla),

Dorsolateral commissural interneuron (dlc),

Fatty acid amide hydrolase (FAAH),

Fragile X mental retardation 1 (FMR1),

Fragile X mental retardation protein (FMRP),

Fragile X syndrome (FXS),

γ-aminobutyric acid (GABA),

G-protein coupled receptors (GPCRs),

Long-term depression (LTD),

Long-term potentiation (LTP),

2-Methyl-6-(phenylethynyl)pyridine (MPEP)

Monoacylglycerol lipase (MAGL),

Motoneuron (mn),

NAPE –Phospholipase D (NAPE-PLD),

N-arachidonoylethanolamide (AEA),

N-arachidonoyl-dopamine (NADA),

Nicotinic acetylcholine receptors (nAchRs),

Normal Frog ringer (NFR),

N-Methyl-D-aspartic acid (NMDA),

N-oleoylethanolamide (OEA),

N-palmitoylethanolamine (PEA),

Peripheral nervous system (PNS),

Phosphatidylinositol 4,5-bisphosphate (PIP2),

Phospholipase C- β (PLC-β),

Post-synaptic density (PSD),

Precursor N-Arachidonoyl-phosphatidylethanolamine (NAPE),

Protein kinase A (PKA),

Protein kinase C (PKC),

Proto-oncogene tyrosine-protein kinase (FYN),

Rohon-beard (RB),

Tetrahydrocannabinol (THC),

Abstract

The group 1 metabotropic glutamate receptors ($mGluR_{1/5}$) are of key interest in the synaptic plasticity that underlies learning and memory and have been implicated as a cause or target in many disease models such as Parkinson's, Huntington's, Alzheimer's, depression, schizophrenia and fragile X syndrome. Alongside this, group 1 mGluRs are linked, via the production endocannabinoid 2-archidonyl glycerol (2-AG), to cannabinoid receptor 1 (CB1). CB1 is one of the most highly expressed G-protein coupled receptors (GPCRs) in the central nervous system (CNS) and its function has not been confirmed in *Xenopus laevis* tadpoles. Debate and research are still ongoing as to how CB1 can be targeted to improve disease outcomes and the extent of its effect *in vivo*.

The pattern of neuronal signalling in the *X. laevis* central pattern generator (CPG) has been well categorised using electrophysiological recording in the immobilised tadpole at stages 37-42. We sought to build on these previous experiments to assess the swimming behaviour of the *X. laevis* tadpole *in vivo* using slow-motion high frame rate video (400 frames per second) to determine the frequency of tail swim cycles and the angle of tail flexion achieved during these swim cycles. Using this well-characterised model the effects of the two GPCRs can be determined in the unadulterated swimming behaviour. *X. laevis* tadpoles are also advantageous because of low cost in maintenance, a simple primary culture that can be set up at room temperature and an ectothermic development meaning large batches can be staggered in age.

We looked to assess well-known plasticity inducing modulatory receptors $mGluR_{1/5}$ and corroborate electrophysiological recordings previously showing $mGluR_{1/5}$ activation via Dihydroxyphenylglycine (DHPG) increased motoneuron output frequency. We tested if, as in other models such as lamprey, this increase is partly mediated by retrograde cannabinoid signalling.

Our results show group 1 metabotropic glutamate receptors cause increases in the frequency of *X. laevis* swim-cycles at stage 40-42 evidenced through the application of DHPG, a group 1 mGluR agonist. This increase appears to be mainly through $mGluR_1$ as inhibition of this receptor via LY367385 caused significant decreases in swim cycle frequency whereas inhibition of $mGluR_5$ with 2-Methyl-6-(phenylethynyl)pyridine (MPEP) caused no significant decreases, indicating an intrinsic role for $mGluR_1$ over $mGluR_5$ in the maintenance of normal swim cycle frequency. Antagonism of CB1 with AM-251 caused significant decreases at 50µM and 10µM. However, a significant

increase was observed at 2µM indicating a biphasic effect dependent on concentration. Inhibition of CB1 with AM-251 (10µM) followed by application of DHPG (50µM) had no significant effect on the frequency of swim cycles when compared with vehicle control, indicating that the increase seen with DHPG application may be blocked by CB1 inhibition. Application of endogenous CB1 agonist N-arachidonoylethanolamide (AEA) decreased frequency of swim cycles at lower concentrations (0.1-10µM), but no significant change was observed at the highest concentration (50µM). This may be some form of partial antagonism due to a higher affinity of AEA than other endogenous ligand 2-AG, but lower efficacy, effectively occupying the CB1 receptor without activation. Our data suggest that $mGluR_5$ and CB1 may be involved in the normal muscle flexion during swimming with the application of MPEP alone or with AM-251 causing significant decreases in the angle of tail flexion.

We wanted to see if these changes in behaviour reflect in the morphology of neurons, particularly the dendritic spines dimension and membrane viscoelasticity. To do this, a primary *X. laevis* neuron-muscle co-culture was developed from the literature. The cultures were treated with the same pharmacological treatments and fixed in glutaraldehyde 5%. The dendritic spines of the neurons were scanned with an Atomic Force Microscope (AFM). From these scans the dendritic spine dimensions measured were; radius, volume, cross-sectional area, and membrane roughness. Using the phase contrast images, the loss tangent was calculated to give a unitless ratio of membrane stiffness. This measure of the stiffness/viscosity of the sample was used to determine if the dendritic spine head changed significantly in stiffness after group 1 mGluR or CB1 targeted drug treatment.

With AFM analysis of dendritic spine morphology and membrane stiffness, we found that group 1 mGluR activation elongated dendritic spines corroborating previous evidence in immature developing spines and in mature hippocampal cultures. Interestingly inhibition of $mGluR_5$ also elongated the spines alongside increasing the volume of the spines. Both $mGluR_5$ inhibition with MPEP and group 1 mGluR activation with DHPG caused significant increases in dendritic spine membrane stiffness compared with vehicle controls.

We aimed to investigate if the 20-minute application of treatments induced changes in protein expression, particularly postsynaptic density protein-95 (PSD-95) a postsynaptic structural protein present in glutamate synapses linked to NMDAR function, a key receptor in the glutamate excitation of descending interneurons (dINs).

After the behavioural assessment, the tadpoles were fixed and embedded in paraffin wax for microtome sections, which enabled observation of the spinal cord, which was investigated for changes in PSD-95 density using immunohistochemical means.
After scanning with AFM, the cultures were stained with anti-PSD-95 antibodies and changes in fluorescence were measured. The results of this investigation were inconclusive due to large autofluorescence meaning a clear positive signal could not be identified.
The *in vivo* swimming analysis gives almost completely unadulterated tadpoles for analysis of swim-cycle output with a very well understood neuronal network that serves as an excellent model for the interplay between excitatory and inhibitory signalling of CPG networks.
In future AFM scanning can be used alongside fluorescent confocal microscopy to build a detailed picture of morphology and changes in membrane dynamics that may aid our understanding of synapse formation in normal development and in genetic disease such as fragile X.

Table of Contents

List of Figures

List of Tables

1 Introduction

Neurons are the main signalling cells in the central and peripheral nervous system that enable the co-ordination of our various biological functions. The higher brain regions are a complex array of over 3 billion neurons that store our memories, control our emotional response to events and allow cognitional processing that gives us decision making abilities and control over our lives. As we move towards the centre of the brain more primitive structures in the pons, medulla and hypothalamus regulate everything that keeps us alive such as heart rate, breathing and temperature. As we move down through the brainstem, neurons of the spinal cord and periphery initiate actions such as movement in muscle and stimulate or inhibit organs in the production of hormones. They do all this and more by communicating with each other and their target tissues via the release of neurotransmitters across the synaptic cleft. Although the outcome of neural signalling can be drastically different, whether they are creating and storing memories in the hippocampus or regulating the antagonistic contractions of muscle groups, the primary principles with which they operate is universal from humans to tadpoles.

Neuron structure varies dependent on location in the central nervous system (CNS) and peripheral nervous system (PNS) but all neurons have some form of dendritic projections which receive inputs, a soma containing the nucleus and an axon. Neurons enable function through tight regulation of ion channels and receptor systems, meaning that through rapid changes in the net charge of the membrane potential, summation of these inputs generate an action potential once the threshold for that neuron is reached. Figure 1.1.1 demonstrates the classic structure of a neuron, the dendritic tree of most neurons has dendritic spines, tiny protrusions that receive the signals across the small gap termed the synapse, from another neuron's axon terminal. However, the axon does not have to synapse onto dendritic spines and can synapse with the soma or dendritic tree. Dendritic spines are currently thought to only receive excitatory signals although some emerging evidence of dendritic spines receiving inhibitory neurotransmission has been provided (Chen *et al.*, 2012; van Versendaal *et al.*, 2012).

The internal charge of a neuron at rest usually exist at -70mV in comparison to the extracellular space. When the dendrite receives an input in the form of a neurotransmitter or a physical phenomenon such as pressure change or light, sodium (Na^+) channels open allowing Na^+ to diffuse into the cell along the electrochemical gradient in a localised area close to that input. This increases the net charge of the neuron. If the signal is large enough or enough signals summate together Na^+ channels will open in a wave like fashion along the membrane

and the internal charge of the neuron will eventually reach the threshold potential. Once this occurs an action potential will fire. This involves sodium channels opening in a wave down the axon rapidly propagating the signal to the axon terminal. At the axon terminal the final step is the opening of calcium (Ca^{2+}) channels which initiate the release (exocytosis) of neurotransmitters. These neurotransmitters will diffuse across the synapse and either cause the excitation or inhibition of the receiving neuron. If the excitation is a strong enough signal it will repeat the process and fire another action potential, continuing the process, or inhibition will stop it from firing an action potential. Once the action potential has fired membrane bound sodium/potassium ATPase pumps return the internal net charge of the neuron to resting -70mV after a brief hyperpolarisation (Figure 1.1.1).

Although there is a wide variety of neurotransmitters and their corresponding receptors the principle of all of them is the same: they either depolarise the neuron in events of excitatory postsynaptic currents (EPSC), which summate to excitatory postsynaptic potentials (EPSP), or hyperpolarise the neuron inhibiting or reducing the likelihood of action potential generation with inhibitory postsynaptic currents (IPSC), which summate to inhibitory postsynaptic potentials (IPSP).

In this thesis I will predominantly focus on glutamate and glycine neurotransmitter releasing neurons of the *Xenopus laevis* tadpole, stages 37-42, in the central pattern generator (CPG) of

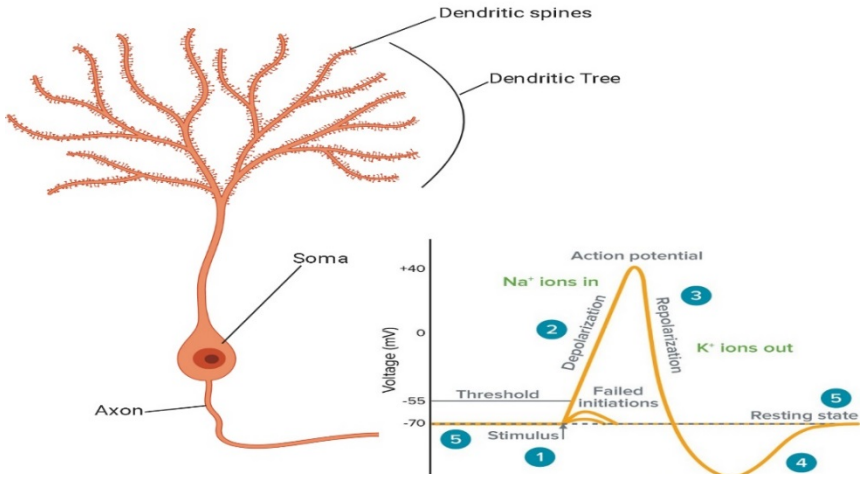

Figure 1.1.1*- Neuron structure and action potential generation. Left schematic of a neuron its dendritic tree with many dendritic spines, soma and axon. Right- classic representation of the net charge change of the intracellular space of the neuron during an action potential. 1 Stimulus and summation -if the inputs received at the dendritic spines, dendritic tree and soma summate to a large enough change in charge the threshold potential is reached, 2. Depolarisation- once passed threshold ion channels (mainly sodium) rapidly open causing massive influx of positively charged ions until action potential is reached. 3 repolarisation- potassium channels open and sodium channels inactivated leads to efflux of K^+ alongside K^+/Na^+ pumps reducing internal charge of neuron. 4 hyperpolarisation – the efflux of K^+ overshoots inhibiting neuron from firing action potential in this time. 5 return to resting potential ready to fire another action potential. Image produced using biorender.com, action potential graph reproduced form https://www.moleculardevices.com/applications/patch-clamp-electrophysiology/what-action-potential#gref*

the hindbrain and spinal cord. We have focussed on these two neurotransmitter systems because they are the main neurotransmitters that regulate the speed of left-right alternating contractions of the tadpole tail during swimming. However, they are also ubiquitous systems that are implicated in diseased systems such as neurodegeneration, excitotoxity, anxiety, depression, loss of memory function and motor control.

We will investigate if the group 1 metabotropic glutamate receptors (mGluRs) and cannabinoid receptor 1 (CB1) affect the frequency of swim-cycles and the flexion of the tail during swimming *in vivo.* These are two receptor systems that modulate glutamate signalling and CB1 can also reduce glycine release. We will ask whether the manipulation of these receptor systems affect changes in behaviour, and if this is transient through short term ion channel changes or by changing the morphology of dendritic spines in culture, assessed using atomic force microscopy. We will then investigate if these changes are reflected in the expression of a key post-synaptic density protein PSD-95 assessed using immunohistochemistry. Morphology of dendritic spines is a key marker to function (discussed in section 1.7) and has implications for neuron recovery from injury and abnormal systems, such as fragile X and autism. PSD-95 is a key structural protein in excitatory synapses and increases in expression may be an indicator of enhanced excitatory post synaptic density efficiency.

1.1 Central Pattern Generators

CPGs are neural networks that control rhythmic motor patterns such as breathing, walking, flying and swimming (Marder and Bucher, 2001; Ijspeert, 2008). When maintaining a rhythmic motion antagonistic muscle groups are excited near simultaneously, and the regulation of alternation between them is controlled by inhibitory interneurons. While one side contracts the other side is inhibited. In walking, once the thought to stimulate walking has occurred the process of alternating legs is controlled by a CPG meaning the signal from the brain can be thought of as always on, while inhibitory interneurons regulate the timing of when and which legs move. This process of maintaining a complex motor pattern with low-level input from higher brain regions means CPGs are an excellent model for investigation into the fundamental interplay between interneurons that regulate motor output. Their ubiquitous nature from *drosophila* to humans means that more accessible models such as *Drosophila*, *X. laevis* and *Petromyzontiformes* can be useful studies for disease models such as spinal cord injury, fragile X and autism. The ease of genetic manipulation and pharmacological intervention makes these models, which have predictable and well-characterised patterns of CPG output, essential if we want to improve disease outcomes in humans. Further to this, as we enter the realm of

robotics (Ijspeert, 2008), understanding the CPG networks' regulation of motor patterns such as walking will be key to producing functional robots that can perform the complex function of walking upright, something many of us take for granted. CPG networks offer a reliable output measurable by electrophysiological recording and, as we will show, high-speed video, that means fundamental question can be answered. Questions relating to the structure and function of neuron groups, the effect of receptor signalling and elucidating the integral role of excitation-inhibition balance present throughout the CNS, dysregulation of which is implicated in many neurological disorders such as schizophrenia, depression and autism.

1.2 The synapse and plasticity

Synaptic plasticity is a term used to define the activity-dependent change in synapse configuration. This involves changes in receptor expression, changes in the probability of neurotransmitter released and changes in protein expression that can result in structural changes, which either enhance receptor position and enable more efficient signalling or decrease receptor expression, change dendritic spine morphology and depress/reduce efficiency in signalling. The change in synapse organisation requires structural changes which enable efficiency and stability. These changes are separated into short-term and long-term changes (Bosch and Hayashi, 2012; Hunt and Castillo, 2012; Huganir and Nicoll, 2013; Sala and Segal, 2014).

1.3 Group 1 metabotropic glutamate receptors in health and disease

Group 1 mGluRs have been implicated in neurological disease. Most prominently in the study of fragile X syndrome (FXS) a form of autism (Dölen and Bear, 2008). FXS is caused by a mutation that leads to transcriptional silencing of the FMR1 gene which transcribes FMRP, a key downstream protein initiated by group 1 mGluR activation that is thought to suppress gene transcription. It was shown in FMR1 knockout mice that mGluR-LTD was increased. When mice were generated that either lacked the FMR1 gene or the $mGluR_5$ receptor it was found that a 50% reduction in $mGluR_5$ expression in FMR1 knockout mice almost corrected the FXS phenotype, providing more evidence that $mGluR_5$ increases protein synthesis and FMRP negatively regulates this protein synthesis (Dölen and Bear, 2008). The current theory suggests that lacking FMRP produces an LTD phenotype similar to DHPG-LTD (100μM) because unregulated/massive increases in mGluR induced protein synthesis, produce an LTD phenotype without regulation of these genes or high-frequency stimulation. This is somewhat corroborated by *in vitro* evidence of the geometric changes in dendritic spine shape observed with DHPG-LTD (Vanderklish and Edelman, 2002). Antagonism of $mGluR_5$ inhibited elongation

of developing dendritic spines in a similar way to FMR1 knockout mice, in contrast to the healthy mouse brain, where DHPG or glutamate-induced elongation and stabilisation of developing dendritic spines (Cruz-Martín, Crespo and Portera-Cailliau, 2012). This also highlights the possibility of different roles for group 1 mGluRs during development compared with the maintenance of dendritic spines in mature organisms.

Group 1 mGluRs are also of keen interest to the treatment of epilepsy (Ure, Baudry and Perassolo, 2006), Alzheimer's disease (Kumar, Dhull and Mishra, 2015), Parkinson's (Amalric, 2015) and prion toxicity (Goniotaki et al., 2017).

1.4 Glutamate and excitatory signalling

Glutamate is the main excitatory neurotransmitter in the CNS. It was first acknowledged to be an excitatory neurotransmitter in the 1980s (Fonnum, 1984). L-glutamate, the amino acid, is the starting block for the two most abundant signalling systems in the CNS: the excitatory glutamate releasing neurons, and the inhibitory γ-aminobutyric acid (GABA) releasing neurons. This is achieved through the enzyme L-glutamic acid decarboxylase. L-glutamate is modified to GABA, which when released produces inhibitory effects in the postsynaptic neuron through activation of GABARs and subsequent influx of chlorine ions. Glutamate signalling is of key interest in synaptic plasticity involved in learning and memory, and genetic disorders, such as anxiety, depression, fragile X and excitotoxicity induced by stroke or neuron death.

Being such a ubiquitous neurotransmitter in the CNS it stands to reason there are several receptors activated by glutamate (Jahr and Stevens, 1987). These are typically split into two categories: ionotropic and metabotropic. The ionotropic receptors encompass the N-Methyl-D-aspartic acid (NMDA), α-amino-3-hydroxy-5-methyl-4-isoxazolepropionic acid (AMPA) and kainite receptors, which differ in their synthetic agonist specificities and ions they allow into the cell. Each receptor has multiple subunits which combine differently dependent on cell type, and the combination of these subunits changes their ionic conductance properties. The similarity is their function as gated ion channels, enabling depolarisation after activation by glutamate (Glutamate receptors summarised in table 1.4.1).

AMPARs have four subunits GluA1-4 that form heteromeric tetrameric complexes. When activated by glutamate AMPARs allow conductance of Na^+ through its ion channel and a small efflux of K^+ (termed the leak current). AMPARs are the main excitatory glutamate receptor, they are the first receptor activated in a glutamate postsynaptic density (PSD) and initiate the depolarisation of the membrane. The position and density of AMPARs are linked to the state of the synapse (Matsuzaki et al., 2004). A key area for research is how AMPARs are cycled in and out of the PSD. Current evidence suggests that large rafts of AMPARs are tethered to the PSD

in a potentiated synapse (Matsuzaki et al., 2001, 2004; Huganir and Nicoll, 2013). The GluA1-4 subunits are phosphorylated on serine, threonine, and tyrosine residues by several protein kinases including calcium/calmodulin-dependent protein kinase II (CaMKII), protein kinase A (PKA), protein kinase C (PKC), cyclic GMP-dependent protein kinase (PKG), proto-oncogene tyrosine-protein kinase (FYN), and c-Jun N-terminal kinases (JNK) on over 20 different phosphorylation sites (Shepherd and Huganir, 2007; Lu and Roche, 2012). The differences in phosphorylation of AMPARs are numerous, but they can be thought of in two categories: either enhancing synaptic transmission or decreasing synaptic transmission.

The NMDAR has subunits GluN1-3, with each subunit having several splice variants. At resting potential NMDAR is blocked by Mg^{2+} in the channel pore of the receptor. NMDARs are only activated when the Mg^{2+} block is removed by AMPAR-mediated depolarisation or voltage-clamp experiments where the potential of the membrane is increased. Then, the binding of glutamate and glycine to the active site in the extracellular N-terminus (Mayer, Westbrook and Guthrie, 1984) opens the channel and allows Ca^{2+} and Na^{+} into the cell. NMDARs are thought to be the key to the enhancement or reduction in the size of the PSD, structural changes which are thought to underlie learning and memory (Li and Tsien, 2009). Their activation allows Ca^{2+} influx through which CAMKII is activated stimulating a series of phosphorylation events which are linked to synapse growth (Herring and Nicoll, 2016). CAMKII was originally thought to be the sole molecule responsible for potentiation. However, evidence showed that calcium spikes only caused transient increases in CAMKII activity and it was the downstream effectors that are phosphorylated by CAMKII that cause potentiation (Lee et al., 2009). PSD-95 (postsynaptic density protein-95) binds directly to the carboxy-terminal tails of GluN2 subunits of NMDARs (Kornau et al., 1995; Niethammer, Kim and Sheng, 1996). In this way, PSD-95 appears to stabilize NMDARs at the cell surface. Phosphorylation of GluN2 subunits affects their interaction with PSD-95 and regulates GluN2 subunit composition at synapses (Sanz-Clemente et al., 2010).

NMDAR dysfunction is linked to many psychiatric disorders such as schizophrenia. It was discovered that the illicit drug ‘angel dust’ is an antagonist of NMDAR and causes severe hallucinations similar to psychosis (Luby et al., 1959; Bowers and Hoffman, 1984; Freeman and Bunney, 1984; Moghaddam and Krystal, 2012). Although the Na^{+} flow across the cell membrane is essential, it is the regulation of Ca^{2+} that is linked to many biological processes. In the post-synaptic density concentration of Ca^{2+} is essential. Dysregulation of Ca^{2+} can cause cell death, which can be initiated by excessive glutamate stimulation of neurons, termed excitotoxicity (Kornau et al., 1995).

Modulating the activity of excitatory glutamate releasing neurons are the inhibitory neurons, which produce neurotransmitters GABA or glycine. Unlike excitatory synapses, inhibitory neurons usually release their inhibitory neurotransmitters onto the neuron soma, although emerging evidence suggests they may also synapse with dendritic spines (Chen et al., 2012). When inhibitory neurotransmitters (GABA or glycine) are released across the synapse they activate their respective ionic receptors (GABAR or GlyR) allowing Cl^- into the cell, hyperpolarising the membrane potential. The Cl^- influx counteracts the future influx of positive ions (Na^+ and Ca^{2+}) and disables the ability of the cell to depolarise and fire an action potential (Mody and Pearce, 2004). The interplay between excitatory glutamate and inhibitory GABA/Glycine signalling regulates the firing frequency of the majority of the CNS and are the two most studied systems involved in synaptic plasticity.

Table 1.4.1- The Glutamate receptors

Receptor	**Type**	**Location in relation to synapse**	**Effect on neurotransmitter release and firing rate**
AMPAR	Ionotropic (Na^+ channel)	Predominantly Postsynaptic, also presynaptic	Increase in Na^+ entry to the cell which begins depolarisation. As activation increases will increase the rate of fire of neuron
NMDAR	Ionotropic (Ca^{2+} channel)	Predominantly Postsynaptic, also presynaptic	AMPAR activation required to remove Mg^{2+} block once open Ca^{2+} and Na^+ entry enhances final push to depolarisation and action potential. On its own constitutive activity would not increase fire rate without AMPAR
Group 1 mGluRs (mGluR1, mGluR5)	Metabotropic GPCR	Predominantly post-synaptic, also presynaptic discoveries. Often exist extra-synaptically	Increased release of internal calcium will increase rate of depolarisation to action potential. May decrease adjacent inhibitory signalling via 2-AG production. May also enhance IPSP

			through inward rectifying GIRK channels
Group 2 mGluRs (mGluR2, mGluR3)	Metabotropic GPCR	Presynaptic and post-synaptic	Inhibits neurotransmitter release (when on presynaptic terminal) via inhibition of calcium channels. Activation of K^+ channels, inhibition of adenylyl cyclase
Group 3 mGluRs (mGluR4, mGluR6, mGluR7, mGluR8)	Metabotropic GPCR	Predominantly presynaptic. mGluR6 is post-synaptic	Inhibits neurotransmitter release (when on presynaptic terminal) via inhibition of calcium channels. Activation of K+ channels, inhibition of adenylyl cyclase mGluR6-stimulates cGMP phosphodiesterase
Kainate	Ionotropic (Na^+, Ca^{2+} & K^+)	Post-synaptic and presynaptic	Na^+ Ca^{2+} and K^+ ion entry largely dependent on subunit assembly and location

1.4.1 Metabotropic glutamate receptors

The metabotropic glutamate receptors (mGluRs) have 8 subtypes ($mGluR_{1-8}$) that are split into three groups depending on their structure and function. They are all GPCRs with seven transmembrane loops and different second messenger signalling pathways regulated by the g-proteins they couple to. Group 2 and 3 mGluRs are predominantly coupled to $G_{i/o}$ proteins. $G_{i/o}$ linked receptors are classically coupled to the inhibition of adenylyl cyclase. Through the action of Gβγ subunits they also directly regulate ion channels, such as g protein-coupled inwardly rectifying potassium channels (GIRKs). They have also been shown to affect many other downstream signalling pathways, such as activation of MAPK and phosphatidyl Inositol trisphosphate (IP3) and Phosphoinositide 3-kinase (PI3K) pathways (Iacovelli *et al.*, 2002; Niswender and Conn, 2010). They are predominantly presynaptic, although many instances of

postsynaptic group 2 and 3 mGluRs have been documented, their activation is generally linked to inhibition of neurotransmitter release, although this can vary depending on cell type.

1.4.2 Group 1 metabotropic glutamate receptors

There are two group 1 mGluR sub-types, $mGluR_1$ and $mGluR_5$ (summarised in Table 1.4.2), predominantly found in the extra-synaptic location of dendritic spines, although they are also commonly found on glia and presynaptically on axon terminals (Watabe, Carlisle and O'Dell, 2002). Many splice variants have been categorised (mGluR1a,b,c,d,e,f; mGluR5a,b, (Niswender and Conn, 2010). mGluRs contain a large N-terminal domain named the Venus Fly Trap domain (VDF). The VDF is the active site of glutamate binding (Kunishima *et al.*, 2000; Bessis *et al.*, 2002). As shown in Figure 1.4.1, when glutamate binds to $mGluR_{1/5}$ the signal propagates through the cysteine-rich domain causing a conformational change, which liberates the g-proteins coupled intra-cellularly. They couple to G_q /G_{11} and activate phospholipase Cβ (PLCβ), resulting in the hydrolysis of phosphoinositides and generation of inositol 1,4,5-trisphosphate (IP3) and diacylglycerol (DAG) (Hermans and Challiss, 2001). IP3 releases Ca^{2+} from intracellular stores of the endoplasmic reticulum, that enhances depolarisation and activates protein kinase C (PKC). Depending on the cell type or neuronal population, group I mGluRs can activate a range of downstream effectors, including phospholipase D (PLD), protein kinase pathways such as casein kinase 1, Jun kinase, cyclin-dependent protein kinase, the mitogen-activated protein kinase extracellular receptor kinase (MAPK/ERK) pathway, and the mammalian target of rapamycin (MTOR)/p70 S6 kinase pathway (Page *et al.*, 2006; Li *et al.*, 2007). Their main function is to enhance the signal, whether it be depression or potentiation of the dendritic spine. Through interaction with the main ionic glutamate receptors (AMPAR and NMDAR), they can enhance depolarisation or ensure depression. It is also thought that through activation of GIRK channels they can enhance IPSPs.

***Table 1.4.2**- The group 1 metabotropic glutamate receptors agonist and antagonist and signalling cascades*

Receptor	Main exogenous Agonists	Main exogenous Antagonists	Signalling cascades and ion channel activation
$mGluR_1$	DHPG	LY367385	Phospholipase C-IP3-Ca^{2+} release from endoplasmic reticulum, adenylyl cyclase activation, DAG lipase activation GIRK channel opening
$mGluR_5$	DHPG	MPEP	

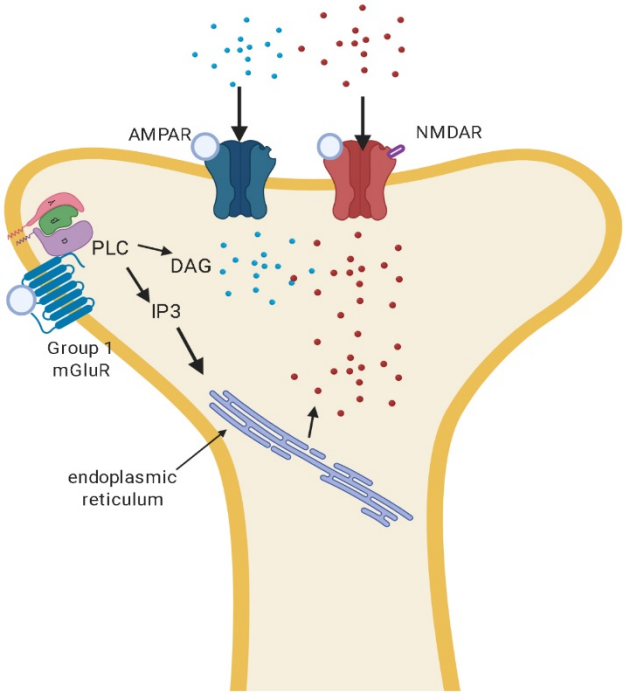

***Figure 1.4.1**- Schematic of the glutamate receptors AMPAR, NMDAR and group 1 mGluRs. Once glutamate (blue circles large) bind to the AMPAR the channel opens and allow influx of Na^+ (blue dots). This depolarisation in the membrane removes the magnesium block from the NMDAR channel. Glutamate and glycine (purple) bind to the receptor opening the channel and allowing Ca^{2+} (red dots) to enter increasing the postivie internal charge of the neuron enhancing the likelyhood of action potential generation. Group 1 mGluR's are a GPCR activated by glutamate. The g-proteins release PLCβ from the membrane which activates DAG and IP3. IP3 releases Ca^{2+} from internal stores in the endoplasmic reticulum.*

1.5 The endocannabinoid system: Background and basics

The cannabinoid system has been shown to affect many processes in the body, some of which are: hunger and metabolism (DiPatrizio and Piomelli, 2012); sleep (Vaughn *et al.*, 2010); learning and plasticity (Marsicano and Lafenêtre, 2009; Yang and Calakos, 2013); and motor control (El Manira and Kyriakatos, 2010; Chaouloff *et al.*, 2011; Polissidis *et al.*, 2013). It may also be a new therapeutic target for obesity, inflammation and neurodegeneration, schizophrenia and autism (Younts and Castillo, 2014).

The endocannabinoid system has been of keen interest to research since the discovery of the cannabinoid receptors (Devane *et al.*, 1988) and the subsequent discovery of endogenous ligand N-arachidonoylethanolamide (AEA) from the porcine brain (Devane *et al.*, 1992). Successive ligands have been discovered the most studied of which is 2-archidonyl glycerol (2-AG) (Mechoulam *et al.*, 1995). The cannabinoid receptors are G-protein coupled receptors (GPCRs) and their ligands are eicosanoids, lipid-based, that are cleaved from membrane precursors and the metabolised products of both ligands feed into the arachidonic acid prostaglandin signalling system. The cannabinoid system is best known in society for the recreational plant marijuana, which contains Tetrahydrocannabinol (THC). THC produces a "high" when smoked or consumed orally in large quantities and is linked to psychosis and schizophrenia in vulnerable/at-risk users, most likely through a process of NMDAR hypofunction (Sánchez-Blázquez, Rodríguez-Muñoz and Garzón, 2014). Its use is also linked to short term memory loss (Mallet and Beninger, 1998; Robinson *et al.*, 2007). However, there are many studies that show that cannabinoids may help with insomnia, anorexia (Støving *et al.*, 2009), depression and anxiety(Huang, Chen and Zhang, 2016). And cannabidiol (CBD) (another component of the marijuana plant) may even combat psychosis (Schubart *et al.*, 2014), due to an inverse agonist/ functional selectivity effect (essentially having the opposite effect at the CB1 receptor, it recruits the stimulatory alpha subunit stimulating adenylyl cyclase conversion of ATP to cAMP).

There are two known cannabinoid receptors named CB1 and CB2, though other orphan receptors have been suggested, such as GPR55 and GPR119 (Brown, 2007; Ryberg *et al.*, 2007; Godlewski *et al.*, 2009). CB1 has been identified mainly in the CNS and periphery (Tsou *et al.*, 1998) with CB2 found in tissues and immune cells. However, recent evidence suggests their presence in neurons (Morgan, Stanford and Woodhall, 2009). CB1 is a presynaptic receptor and its ligands are produced from postsynaptic membrane based on its activity. The short term function of CB1 was first determined in Purkinje cells (Vincent, Armstrong and Marty, 1992) and confirmed in hippocampal slices (Pitler and Alger, 1992). The process is termed

depolarisation induced suppression of inhibition/excitation (DSI/E), due to its ability to inhibit the future release of neurotransmitter from the inhibitory/excitatory presynaptic terminals on which it resides. As summarised in Figure 1.5.1, the CB1 receptor achieves DSI/E primarily by inhibiting the N, P/Q and L-type Ca^{2+} channels (Howlett, Blume and Dalton, 2010), reducing calcium influx at axon terminals and stopping neurotransmitter release. CB1 also activates inwardly rectifying K^{+} Channels (Diana and Marty, 2003)(Augustine, 2001). This function means that CB1 can alter the glutamate excitation of postsynaptic cells and thus affect the development of LTP and LTD at synapses (Cui *et al.*, 2015). As a $GPCR_{\alpha i/o}$ the CB1 receptor also decreases cyclic AMP (cAMP) response element binding protein (CREB) transcription through the inhibition of adenylyl cyclase by its alpha subunit. It also activates MAPK signalling and modulates the phosphoinositide-3-kinase (PI3K)-mediated signalling cascade (Castillo *et al.*, 2012; Huang, Chen and Zhang, 2016).

The synthesis of the endocannabinoids is dependent on postsynaptic conditions with production linked to calcium influx, group 1 mGluR activation and NMDAR activation (Kettunen *et al.*, 2005; Liu *et al.*, 2006; Sánchez-Blázquez, Rodríguez-Muñoz and Garzón, 2014). AEA synthesis has multiple pathways from the membrane precursor N-Arachidonoyl-phosphatidylethanolamine (NAPE). Its synthesis from NAPE is normally mediated by NAPE – Phospholipase D (NAPE-PLD), although AEA levels in most tissues were found unchanged in NAPE-PLD knockout mice (Leung *et al.*, 2006), which has led to the proposal of other pathways. The catabolism of AEA is carried out by fatty acid amide hydrolase (FAAH) to give arachidonic acid and ethanolamine. 2-AG has a much simpler synthetic pathway cleaved from the membrane precursor Phosphatidylinositol 4,5-bisphosphate (PIP2) via the phospholipase C- β (PLC-β) pathway to diacylglycerol (DAG). This is converted to 2-AG mediated by DAG lipase and is catabolised by monoacylglycerol lipase (MAGL) to arachidonic acid and glycerol (figure 1.5.1) (Bisogno *et al.*, 2003; Gao *et al.*, 2010) Interestingly FAAH is located primarily in postsynaptic regions of dendrites and somata with MAGL localised in axon terminals (Gulyas *et al.*, 2004). There is some controversy over the transport of AEA. It has been reported that inhibition of the FAAH-like anandamide transporter (FLAT) increases levels of AEA, indicating this protein was involved in carrying AEA back across the synapse to FAAH in the postsynaptic neuron. This has recently been disputed (Leung *et al.*, 2013) as it was found that FLAT does not leave the postsynaptic cell and is mainly located in intracellular membranes and cytoplasm, suggesting that its effects to speed up the catabolism are enzymatic signalling from within the cell.

There have been other endocannabinoids discovered and characterized which are: virodhamine (Porter *et al.*, 2002), N-arachidonoyl-dopamine (NADA)(Huang *et al.*, 2002), 2-

arachidonyl glycerol ether (Hanus *et al.*, 2001), N-palmitoylethanolamine (PEA) and N-oleoylethanolamide (OEA). Virodhamine is the same atomic make-up as AEA with the amide bond changed to an ester bond and this change makes it an antagonist at CB1, but a full agonist at CB2 (Porter *et al.*, 2002). The experiment quantifying virodhamine in the rat and human hippocampus found it to be similar in concentration to that of anandamide. This suggests a complex control mechanism of AEA activation and virodhamine inhibition of CB1 in the brain. N-arachidonoyl-dopamine is an agonist of CB1 and not an agonist of the dopamine receptors. It acts like capsaicin (the active component of chilli peppers) and activates the receptor transient receptor potential vanilloid 1 (TRPV1) causing the production of substance P involved in nociception (Huang *et al.*, 2002). Anandamide has been investigated as an analgesic, even suggested to be an endovanniloid (Tóth, Blumberg and Boczán, 2009) due to its endogenous agonist activity at TRVP1. This receptor is an unspecific cation channel that is linked to pain perception, and often referred to as the capsaicin receptor or vanilloid receptor 1. NADAs discovery suggests further roles for the cannabinoids in pain regulation. 2-arachidonyl glycerol ether has been shown to be an endogenous ligand of CB1 causing hypothermia and mild anti-nociception (Hanus *et al.*, 2001). N-palmitoylethanolamine (PEA) and N-oleoylethanolamide (OEA) although classed as endocannabinoids do not activate either receptor. Their effects are classed as “entourage effects” and are thought to be synthesised alongside AEA, enhancing or regulating the outcome of AEA induced CB1 activation (Okamoto *et al.*, 2004). They have been shown to activate peroxisome proliferator-activated receptor alpha (PPARα), although this receptor did not account for all of their physiological effects. Recently, they have been shown to have an affinity to the orphan GPCRs GPR55 and GPR119, whose function is still being explored. Although deletion displays no clear disease phenotypes they appear to have some role in development (Godlewski *et al.*, 2009). PPARα is nuclear receptor transcription factor, the activation of which upregulates genes that co-ordinate the transport, uptake and utilisation of fatty acids. The endocannabinoid system has effects on energy metabolism and this receptor may contribute to this through the entourage effects of OEA and PEA (ligand function and receptor affinity summarised in Table 1.5.1).

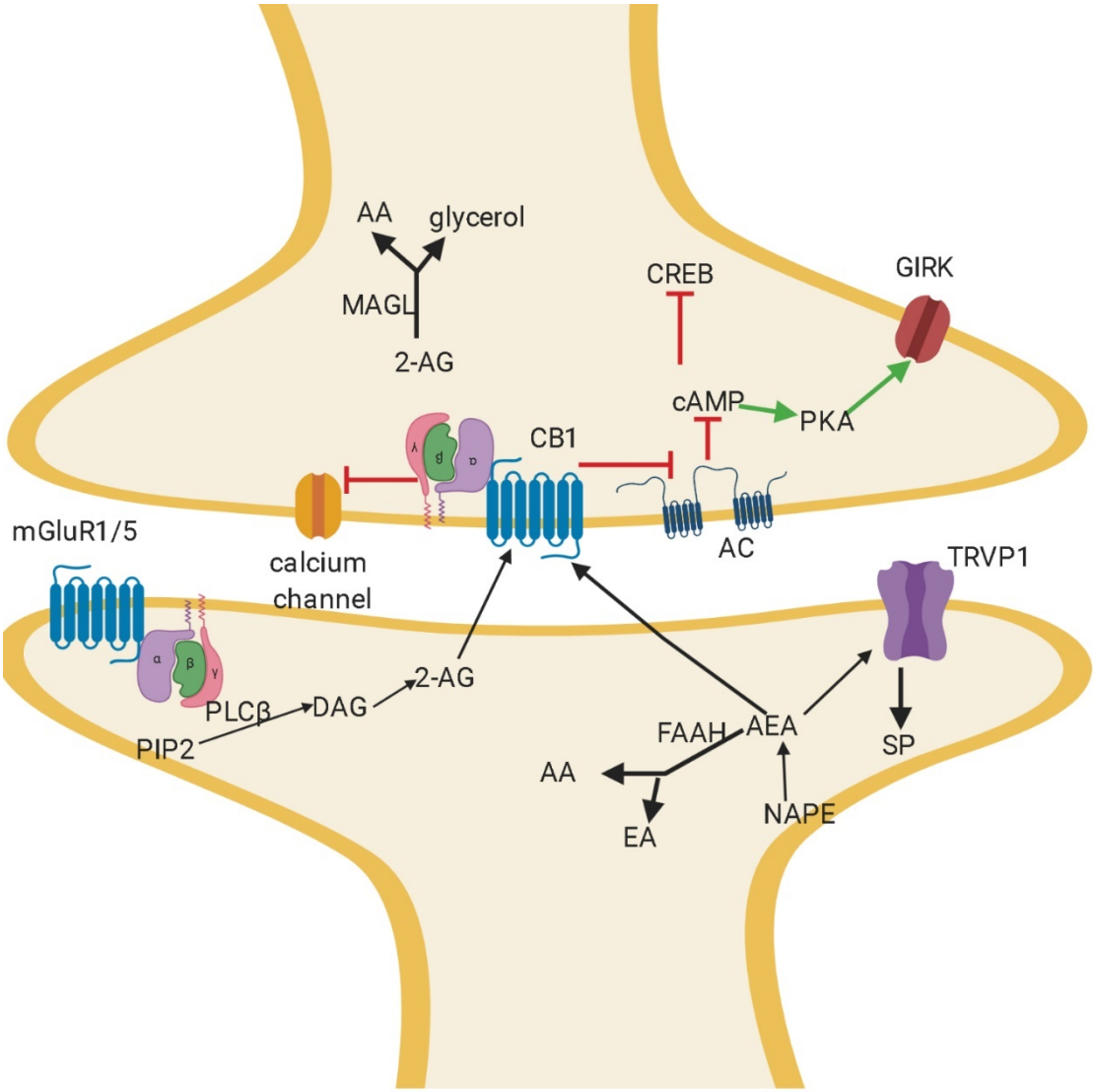

Figure 1.5.1*-Retrograde endocannabinoid signalling and signal transduction of CB1. Endocannabinoids 2-AG and AEA are synthesised in response to post-synaptic density stimulation. For AEA, calcium increases activate NAPE-PLD to cleave membrane precursor NAPE to AEA. From here it can activate TRVP1, travel to presynaptic terminal to activate CB1, be degraded immediately by FAAH to arachidonic acid (AA) and ethanolamine (EA) or activate internal CB1 possibly mitochondrial CB1 (not shown). TRVP1 has been identified as a receptor responsible for the production of substance P (SP) involved in the perception of pain particularly with regards to heat, high pH or capsicum. 2-AG is synthesised by the cleavage of membrane precursor PIP2 to DAG by PLCβ (which can be activated by group 1 mGluR activation). DAG is converted to 2-AG by DAG lipase. 2-AG can travel retrogradely to presynaptic CB1. 2-AG is broken down in the presynaptic terminal by MAGL to AA and glycerol. CB1 activation inhibits adenylyl cyclase via its α subunit. This stops the conversion of ATP to cAMP. This reduction in cAMP activates protein kinase A (PKA) which activates inwardly rectifying potassium channels (GIRKs) aiding hyperpolarisation. The βγ subunits inhibit calcium channels further hyperpolarising the axon terminal and inhibiting neurotransmitter release. The reduction in cAMP also effects the transcription factor CREB. Other downstream effects of CB1 activation are activation of MAPK and PI3K signal cascade.*

Table 1.5.1*-Table of the endocannabinoid ligands, receptors they can activate and their effects in neurons with those receptors*

Endocannabinoids	Effects the Receptor(s)	Effects in neurons
N-arachidonoylethanolamine (AEA or anandamide)	CB1 (agonist) CB2 (partial agonist) TRPV1 (agonist)	-Inhibits release of neurotransmitters -anti-inflammatory -increase in post-synaptic ion flow into cell linked to nociception
2-Arachidonoylglycerol (2-AG)	CB1 (agonist) CB2 (agonist)	-Inhibits the release of neurotransmitters - anti-inflammatory
O-arachidonoyl ethanolamine (O-AEA or virodhamine)	CB2 (agonist) GPR55 (agonist) CB1 (antagonist)	-anti-inflammatory -G_{13} GPCR leads to stimulation of rhoA, cdc42 and rac1. -may antagonise CB1 allowing neurotransmitter release
N-arachidonoyl-dopamine (NADA)	CB1 (agonist) TRPV1 (agonist)	-inhibits neurotransmitter release - increase in post-synaptic ion flow into cell linked to nociception
2-achidonyl-glycerol-ether (2-AGE)	CB1 (agonist) CB2 (agonist) TRPV1 (partial agonist)	- inhibits neurotransmitter release - anti-inflammatory - increase in post-synaptic ion flow into cell linked to nociception
N-palmitoylethanolamine (PEA)	Peroxisome proliferator-activated receptor alpha (PPAR-α) (agonist) GPR55 (agonist) GPR19 (agonist)	-nuclear receptor gating expression of genes involved in energy homeostasis - G_{13} GPCR leads to stimulation of rhoA, cdc42 and rac1 -possibly regulates E-cadherin and involved in metastasis. Highly expressed in developing brain function still unclear
N-oleoylethanolamide (OEA)	Peroxisome proliferator-activated receptor alpha (PPAR-α) (agonist) GPR55 (agonist) GPR19 (agonist)	-nuclear receptor gating expression of genes involved in energy homeostasis - G_{13} GPCR leads to stimulation of rhoA, cdc42 and rac1 -possibly regulates E-cadherin and involved in metastasis. Highly expressed in developing brain function still unclear

1.5.1 Cannabinoids in Motor studies affect outcomes in a biphasic manner

In motor output studies cannabinoid agonists and antagonists have opposing effects between high and low concentrations. Many studies have reported the decreased activity with cannabinoid agonist application usually at very high exogenous concentrations, which one would expect considering the primary function of CB1 is to inhibit neurotransmitter release and this is especially the case when looking at voluntary movement. However, the picture becomes far more complicated when the concentration range is expanded and can depend on the neural network assessed (i.e. motor cortex vs spinal cord). Studies in mice (Sulcova 1998) analysed AEA effects on catalepsy on a ring, horizontal ambulation, vertical rearing, defecation, analgesia on a hotplate, the aggressiveness of interaction with other mice and chemiluminescence of leukocytes. All areas were tested with a range of concentrations from 0.001mg/kg to 100mg/kg increasing in factors of 10 and all areas except analgesia on the hotplate gave a biphasic result. In ambulation and rearing, lowest dose increased activity with high doses decreasing activity. Catalepsy on the ring was decreased in low dose and increased in high dose. Similarly, leukocyte phagocytic activity was increased at low does and decreased at high dose. These interesting results are made more so by the knowledge that all these behaviours and cellular events are controlled by different pathways, yet the overall pattern is the same. The consistency of results throughout various analysis methods points to an intrinsic function of the cannabinoid receptors that enable dual-action dependent on dose and environmental physiology. Following this study a similar analysis in rats was performed using Δ^9-THC, which also recorded a biphasic interaction in voluntary movement recorded by light beams broken, catalepsy on ring and faecal boluses produced (Sañudo-Peña *et al.*, 2000). In this study low doses (0.2-0.5mg/kg) decreased activity, middle doses (1.5-2mg/kg) increased activity and high doses (2.5-5mg/kg) decreased movement and increased catalepsy with no concentrations affecting autonomic activity of faecal boluses. The synthetic agonist WIN 55,212-2 also induced a biphasic result in rats with low dose 0.1M increasing voluntary ambulation and 1M decreasing ambulation. This was the same in vertical counts and all significant changes were negated with the application of 0.3M of synthetic antagonist SR-121716A (Polissidis *et al.*, 2013). This group went further than previous studies and performed micro dialysis of dopamine and glutamate release in the striatum, nucleus accumbens and prefrontal cortex. The dopamine release in the striatum was increased by both doses of WIN with 1M increasing more than 0.1M. Interestingly, glutamate was decreased by 1M WIN with no change in 0.1M. This result could go some way in explaining the biphasic effect of dose as glutamate release in the brain region is likely the driving force behind voluntary movement.

To explain this, we first must look at the distribution of CB1 which is found primarily on inhibitory GABAergic/Glycinergic or excitatory glutamatergic terminals. Studies in rat medial prefrontal cortex (mPFC) estimate the ratio of glutamate neurons to GABA producing neurons as 80:20% however the ratio of excitation: inhibition% (E: I%) release is reversed at 18:82 due to the nature of feed forward and feedback regulation. One study showed that exogenous cannabinoid (WIN 55) application super infused into the mPFC shifted the E:I% in favour of excitation as far as 30:70% (den Boon *et al.*, 2014). It was noted in this study that the overall production of both IPSC and EPSCs were decreased, although the inhibitory currents decreased more. This is evidence that CB1 activation reduces all neurotransmission, but, due to higher expression at inhibitory neuron terminals reduces inhibitory signalling to a greater extent, thus enabling more excitatory signalling to take place.

1.6 Long-term synaptic plasticity

The famous theory of Donald Hebb has dominated neuroscience since 1949- “Neurons that fire together wire together” (Hebb, 1949). Behind the simplicity of this statement is a truth that neuroscientists have been trying to fully understand since. From this theory and through extensive experimentation, synaptic plasticity is now often thought of in short-term changes (0-30 minutes) and long-term changes (30 minutes-10 hours). Short-term changes may be increased fire rate of a motoneuron due to increased glutamate at the synapse. How these immediate changes then reflect into long-term changes have been well characterised. Long term changes are divided into two categories: long-term potentiation (LTP) and long-term depression (LTD). If 2 neurons forming a synapse are stimulated repeatedly (general protocol states that 100 paired- pulses at 100Hz induces LTP (Dudek and Bear, 1993)) the synapse between the neurons will become potentiated. To do this involves synaptic plasticity changes, in receptor expression (AMPAR) and glutamate expression, but, most crucially of all, NMDAR activation. This will mean for the long-term future (30 mins -10 hours *in vitro*, 1 month or longer *in vivo*) this synapse will signal more efficiently, it will grow larger, and the rate of action potential generation will be increased. The key tenets of LTP are association and convergence, input specificity and cooperativity. Specifically, to induce LTP both the pre and post synapse must be stimulated by high-frequency stimulation (HFS). Mechanistically the AMPARs initiate depolarisation, relieving the magnesium block of the NMDAR allowing conductance and the subsequent secondary signalling that follows. If this is experienced repetitively in a short time period (HFS) LTP will occur, this is defined as NMDAR-dependent-LTP. Previously, it was thought NMDAR-independent-LTP was only regulated by increased Ca^{2+} channel conductance. However, recent evidence provided a role for group 1 metabotropic glutamate receptors in this process (Wang *et al.*, 2016).

Long-term depression of synaptic transmission is defined by a long-lasting decrease in efficacy and strength of signalling. LTD has a number of forms, it was first observed in heterosynaptic transmission where stimulating potentiation between two neurons induced depression of a nearby non-stimulated pathway (Lynch, Dunwiddie and Gribkoff, 1977). Depotentiation or homosynaptic depression is another form of LTD that is induced by low-frequency stimulation (LFS-5-10Hz to the presynaptic neuron) (Staubli and Lynch, 1990). After this discovery in the hippocampus, LTD was confirmed in many other brain regions *in vivo* and it is now considered a key function of regulating neuronal systems.

1.6.1 Group 1 mGluR-dependent-LTD

LTD can also be induced chemically through group 1 mGluRs (mGluR-LTD) (Ito, Sakurai and Tongroach, 1982). The key requisites for this induction are calcium increase and mGluR activation. Since then the complexity has increased and it is now well accepted that low-frequency stimulation (LFS) induces LTD through low NMDAR activity and group 1 mGluRs. mGluR-LTD requires mGLuR activation without NMDAR, although in some brain regions, such as the amygdala and perirhinal cortex (Wang and Gean, 1999; Cho *et al.*, 2000), it requires NMDAR activation.

Two of the key signalling mechanisms that underlie mGluR-LTD are p38 MAPK activation alongside tyrosine dephosphorylation (Moult *et al.*, 2008), the inhibition of these two events was found to occlude mGluR-LTD. Gene transcription events lead to activated proteins, such as eEF2, Arc/Arg3.1, which are involved in AMPAR endocytosis. Other proteins synthesized during mGluR-LTD include; Striatal-Enriched protein tyrosine Phosphatase (STEP), fragile X mental retardation protein (FMRP), and microtubule-associated protein 1B (MAP1B), which may also regulate AMPAR synaptic trafficking (Beattie *et al.*, 2000; Lee, Simonetta and Sheng, 2004). The key difference in LTP or LTD induction usually lies with the rate of activation. As shown LTD can be chemically induced with 100µM DHPG. However, this is in neurons with a low or negligible fire rate, combined with the high level of activation of proteins, that negatively regulate the dendritic spine, such as FMRP transcription.

1.7 Dendritic spines in plasticity

Dendritic spines are tiny protrusions from the dendritic tree that receive excitatory inputs. They were first proposed by Ramon y Cajal over 100 years ago, who recognised them as a structure in cultured hippocampal neurons stained with the Golgi method (García-López, García-Marín and Freire, 2007). Dendritic spines are generally split into four categories based on morphology; mushroom, filopodia, thin and stubby (Matsuzaki *et al.*, 2004; Basu *et al.*, 2018). Evidence has shown that the structure of a dendritic spine may be a determinant for the state of the spine (potentiated or depressed) (Matsuzaki *et al.*, 2001, 2004; Bosch *et al.*, 2014; On *et al.*, 2017; Basu *et al.*, 2018). Dendritic spines consist of a thin neck protruding from the dendrite with a head containing the post-synaptic density (PSD). The PSD is located directly behind the synapse membrane and consists of a dense and complex array of structural proteins to which the receptors are tethered (figure 1.7.1). The PSD proteins are linked to actin filaments (primarily f-actin) which define the structure of the spine and are key targets for structural plasticity.

When quantifying the structure of dendritic spines under different conditions it has been shown that mushroom spines with a larger surface area and volume represent potentiated spines and that under conditions that induce LTD in hippocampal neurons, the spines elongate in length but do not change in volume (Vanderklish and Edelman, 2002). This is evidence that the shape of the spine and the volume are critical determinants of potentiated vs depressed spines (Matsuzaki *et al.*, 2004). In a mushroom spine, the surface area is primed to receive neurotransmitters, presenting AMPA receptor rafts on the surface for fast synaptic transmission of glutamate. In an elongated spine, the surface area at the head of the spine is decreased allowing less space for AMPA receptor expression. This is supported by other work which shows the location of AMPA receptors to be a predictor of the state of the dendritic spine (Matsuzaki *et al.*, 2001, 2004) When a spine becomes depressed the AMPARs are located extrasynaptically trafficked away from the head surface.

Depolarisation events have been shown to provoke gene transcription through double strand DNA break inducing transcription of growth causing actors such as c-fos almost immediately (Madabhushi *et al.*, 2015). Recent high-speed atomic force microscope scans show dendrites forming within 20 minutes (Shibata *et al.*, 2015). Investigations into the remodelling of spines undergoing potentiation defined the key events of potentiation into 3 phases. In the first phase, reorganisation of the actin cytoskeleton occurs. This happens in the first 1-7 minutes after LTP induction, where it was observed that actin fills the spine and it is quickly polymerised to F-actin. During this period there is a transient decrease in G3 proteins

(CAMKIIβ, α-actinin and drebrin), that are responsible for the stabilisation of F-actin through binding it to the PSD. At the same time, there is an increase in G1 and G2 proteins, such as cofilin and Arp2/3, proteins responsible for severing and branching F-actin. The increased cofilin in the spine is triggered by NMDAR activation. The second phase is defined by the stabilisation of the newly remodelled cytoskeleton. This occurs over the next 7-60 minutes, during which time cofilin continues to rise. G2 and G3 proteins return to their normal levels and increase in proportion with spine volume. The G3 proteins such as CAMKIIβ are thought to stabilise the increasing F-actin which is the key driver of growth. The third phase was defined as delayed PSD protein synthesis. It was found that during phase 1 and 2 the PSD structure and protein density remained unchanged. It was after 1 hour that increases in G4 proteins, such as Homer and Shank, were observed (Bosch *et al.*, 2014; Bosch *et al.*, 2015).

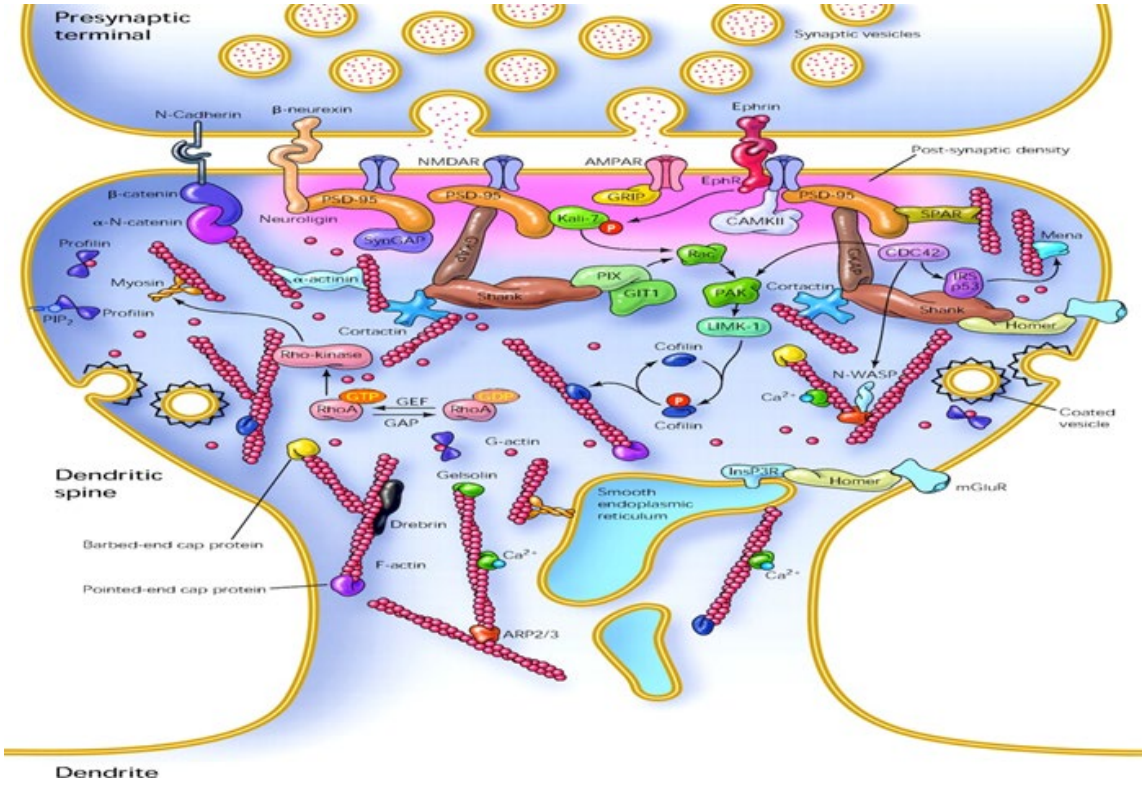

Figure 1.7.1 *-Example schematic of the protein organisation and maintenance of dendritic spines (reproduced from Calabrese, Wilson and Halpain, 2006)*

1.7.1 Summary of plasticity in dendritic spines

LTP induction- Glutamate released from the presynaptic terminal activates the glutamate receptors NMDAR, AMPAR and mGluR. AMPAR and NMDAR are connected to PSD-95, Homer and SHANK (as shown in figure 1.7.1). Increased Ca^{2+} influx via NMDARs activates CAMKII which translocates to the PSD where it phosphorylates synapse proteins including receptors, MAGUKS and other synapse proteins. Calcium released from intracellular stores in the endoplasmic reticulum induced by mGluR g-protein-mediated activation of IP3 enhances the depolarisation event and trigger second messenger systems. Repetitive increases in signalling (100 pulse pairs LTP) and persistent Ca^{2+} increases, lead to local gene transcription events, which over the first 1-7 minutes after LTP induction, increase the concentration of cofilin and ARP2/3, which cleave and branch actin respectively. In the second phase of growth CAMKIIβ, drebrin and α-actinin return to normal levels and stabilize the F-actin cytoskeleton. After this process, structural MAGUKs (PSD-95, Homer and SHANK) begin to increase in density, enabling more receptor expression.

LTD induction- During low-frequency stimulation all the same receptor systems are activated. LTD is defined by low-level currents of Calcium and as such the level of NMDAR activation is the key 'decider' in the outcome. It is generally accepted that low-level depolarisation and

short-term activity of CAMKII lead to LTD and high-level depolarisation and long-term activity of CAMKII lead to LTP. mGluR-dependent-LTD requires the activation of p38 and dephosphorylation of tyrosine kinases normally independent but sometimes dependent on NMDAR.

Based on this excellent preceding work it is clear how the structure indicates the function of dendritic spines. Most of this work has been performed using time-lapse confocal imaging. The recent development of high-speed AFM combined with inverted fluorescent confocal imaging offers a more detailed insight into the structural changes that occur in short periods. However, no measurement criteria have been developed for atomic force microscopic assessment of spines. It would be advantageous to develop these criteria and use them to investigate pharmacological effects on the structure, which can be used in future as a measure of the activity of dendritic spines.

1.8 Xenopus laevis

The African clawed frog (*Xenopus laevis*) is an ideal research animal. *X. laevis* has been at the forefront of developmental DNA and RNA investigations since 1958 when it was discovered that transplanting somatic nuclei into the egg can fully reprogram development (Gurdun, Elsdale and Fishberg, 1958; Gurdon and Uehlinger, 1966). Later *X. laevis* was key in finding evidence for mitochondrial DNA (Dawid, 1966) and was used to isolate the first eukaryotic genes (Birnsteil *et al.*, 1968; Brown, Wensink and Jordan, 1971). They can withstand invasive surgical manipulations and their cells can be cultured reasonably easily compared with more complex organisms because their cells can survive in rudimentary salt solutions (Peng, Baker and Chen, 1991; Harland and Grainger, 2011). The oocytes can be injected with gene transcripts, which are readily taken up and expressed with many studies expressing human receptors on their surface (Gurdon and Uehlinger, 1966). The genomes of *X. laevis* are highly conserved and have a high degree of genomic synteny with other mammals (Harland and Grainger, 2011). However, one of the negatives of *X. laevis* is its allotetraploid genome thought to be the result of two species merging (Session *et al.*, 2016). This means *X. laevis* has four sets of genes rather than two. Due to this, in the 1990s, researchers began looking at *Xenopus tropicalis. X. tropicalis* has a diploid genome and a shorter generation time, meaning it is better suited for studying genetic mutation over generations. The advantage of both *X. laevis* and *X. tropicalis* lies in the ease of access to oocytes to inject RNA transcripts and monitor changes in development (Gurdon and Uehlinger, 1966). Not limited to purely genetic studies, *X. laevis* oocytes were one of the first used to assess cloned acetylcholine receptors using electrophysiology (Kusano, Miledi and Stinnakre, 1977).

In recent years *X. laevis* tadpoles have become a key model in neuroscience, as *X. laevis* hatchling tadpoles have very simple behaviour until developmental stage 45. The tadpole only exhibits 2 behaviours: swimming in response to touch/ shadow detection via pineal eye or struggling when held around the neck. If left untouched these tadpoles will not move, although some spontaneous twitching and swimming may be observed. Alongside this simple behaviour, the spinal neurology of their swimming is relatively simple. Being an ectotherm means the *X. laevis* tadpole requires external energy (heat) to enable maturation. This means that a reduction in temperature below 23^{o}C can slow the development, maintaining the tadpole at certain stages for longer allowing more time for experimentation. Their spinal network's CPG has been well characterised through electrophysiological examination (Li, Roberts and Soffe, 2010; Roberts, Li and Soffe, 2010; Li and Moult, 2012; Moult, Cottrell and Li, 2013).

Fictive swimming electrophysiological preparations of *X. laevis* involve the immobilisation of the tadpole with α-bungarotoxin, pinning it in place with a tungsten needle through the notochord and removing the skin and myotomes while the tadpole is in physiological saline solution. This allows access to the motoneurons and spinal cord using glass suction electrodes. Motor activity is then stimulated by a glass suction electrode placed on the skin delivering a 1ms current pulse. Using this method the action potential patterns of the various neuron groups during swimming have been defined (Roberts, Li and Soffe, 2010; W.-C. Li, Roberts and Soffe, 2010; Li and Moult, 2012). This enables us to know the sequence of neuron firing and whether they produce inhibitory or excitatory signals.

1.8.1 CPG of Xenopus laevis controls frequency of swim-cycles through reciprocal inhibition and NMDA pacemakers

The *X. laevis* tadpole between stages 37-44 has a predictable and well-characterised reflex swimming response to touch or shadow detection via a pineal eye. This swimming response involves alternating contractions of swimming muscles spreading from head to tail along the tadpole's trunk. The alternation of the muscle contraction is achieved with a CPG network. Using paired cell recordings from three neurons the Rohon-beard (RB) sensory neuron, the dorsolateral commissural interneuron (dlc) and the motoneuron (mn) it was identified that a touch on one side of the tadpole stimulated a motoneuron to fire on the opposite side, a process mainly controlled by AMPARs. The RB neuron will amplify the signal stimulating many dlc interneurons to produce a full flexion away from the point of touch (Figure 1.8.1). It also stimulates dorsolateral ascending (dla) interneurons, which project axons to the hindbrain. This is the area with sufficient neurons identified to maintain swimming (Roberts, Li and Soffe, 2010).

Figure 1.8.1*- Example of initiation of swimming. Frame by frame example of stage 40-42 reaction to touch on the left side tail trunk. Touch at arrow. Recorded at 400fps. Sensory RB neurons stimulate dlc neurons to excite mn opposite side to touch which cause contraction away from touch.*

After the first full flexion, the signal has been amplified to the hindbrain where the descending interneurons (dINs) are located. These are excitatory interneurons, releasing glutamate and acetylcholine, which descend the spinal cord forming synapses with motoneurons, commissural interneurons (cIN) and ascending interneurons (aINs). Glutamate causes the motoneurons to become depolarised, firing action potentials and release acetylcholine onto the muscle causing contraction. The cINs release the inhibitory neurotransmitter glycine, that causes a hyperpolarising current (sometimes termed mid-cycle inhibitory release) in the dINs in the opposite half-centre. The aINs project back up the spinal cord releasing glycine to regulate timing of dIN firing and working with the cINs to create the smooth flow of muscle contraction down the tail of the tadpole. The dINs in the opposing half centre fire on rebound

after the hyperpolarising current has dissipated, stimulating the cINs, aINs and motoneurons repeating the process to control the frequency of tail contractions by reciprocal inhibition and rebound firing of dINs (Figure 1.8.2). Evidence has been provided that show the dINs in the hindbrain are connected via gap junctions. Gap junctions or electrically coupled synapses occur in excitatory neurons that wire together through these gap junctions. It has been shown that a hyperpolarising current to one dIN will stop the others nearby from firing an action potential in isolated *X. laevis* preparations (Li, Roberts and Soffe, 2009). This also provided evidence that in an isolated spinal cord with the half-centres of the spinal cord separated the dINs could generate a rhythm of action potentials similar to fictive swimming frequency regulated by the NMDAR pacemaker ability (Li, Roberts and Soffe, 2009). Although, it was demonstrated that stopping cIN release during fictive swimming stopped swimming and dIN action potentials (Moult, Cottrell and Li, 2013). Swimming will generally continue until the tadpole encounters a surface. The cement gland at the front of the tadpole produces a signal when it contacts a surface which releases GABA from axons that project from the trigeminal ganglia into the hindbrain and stop the NMDAR pacemaker activity (Li, Roberts and Soffe, 2010; Roberts, Li and Soffe, 2010; Li and Moult, 2012)

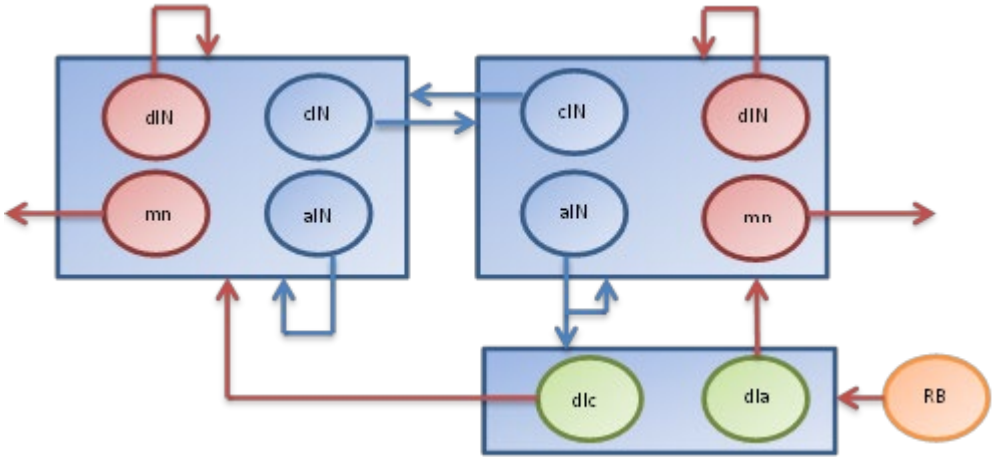

Figure 1.8.2*- Model of the neurons and connections in X. laevis tadpole spinal network central pattern generator. Red arrows indicate excitation, blue arrows indicate inhibition. Each box represents the two half-centres on the spinal cord. dINs stimulate all neurons in hemisphere (approx. 30-150 of each type) cINs produce inhibitory hyperpolarising currents in the dIN's on the other hemisphere which fire on rebound, the aINs produce inhibitory current within each hemisphere ascending to inhibit previous dINs and motoneurons to allow co-ordinate wave of muscle contraction. The dla's stimulate all fibres on side of touch whilst dlc produces initial reflex contraction. (Roberts, Li and Soffe, 2010; Moult, Cottrell and Li, 2013)*

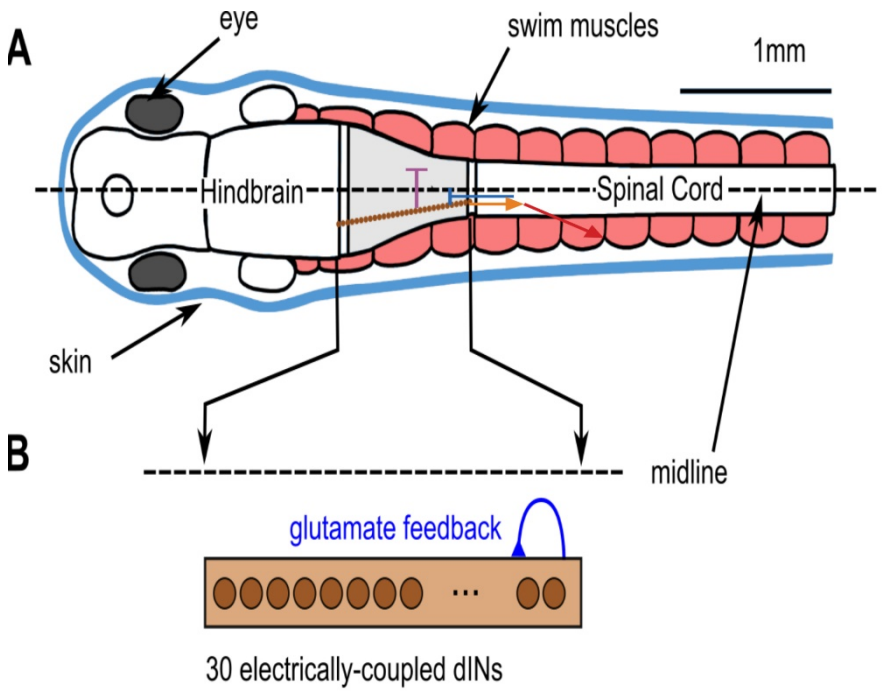

Figure 1.8.3*-Schematic showing X. laevis neuron layout. Electrically coupled dIN's in the hindbrain are stimulated to swim. They simultaneously excite (orange arrow) the motoneurons (red arrow), cINs (purple inhibitory line) and aINs (blue inhibitory line). The mns cause muscle contraction, the cINs release an inhibitory current hyperpolarising the opposing dINs and the aINs release modulatory ascending inhibitory current back up the spinal cord within one half-centre. Image modified from (Hull et al., 2016) using biorender.com*

The dINs release glutamate and acetylcholine, which stimulate, the mns, cINs and aINs. The dINs are electrically coupled (figure 1.8.3) and contain NMDAR, AMPAR nicotinic acetylcholine receptors (nAchRs). They also contain Glycine receptors (GlyRs) which are responsible for hyperpolarisation generation via glycine released from the cINs and aINs (Li, Roberts and Soffe, 2010; Roberts, Li and Soffe, 2010; Li and Moult, 2012; Moult, Cottrell and Li, 2013). The motoneurons also contain all these receptors on their postsynaptic densities and are proposed to contain group 1 mGluRs (Chapman and Sillar, 2007), although their exact location in the spinal cord of *X. laevis* is still to be confirmed. Similarly, the cINs and aINs are excited by glutamate and acetylcholine and inhibited by glycine. The location of group 1 mGluRs are not defined, but are expected to be present on most of the neurons in the spinal cord receptive to glutamate and previous experimental results would appear to confirm this. The location of CB1 in the spinal cord of the *X. laevis* tadpole are unknown, however locations in the adult *X. laevis* are and are discussed in a later section (1.8.4).

1.8.2 Group 1 mGluRs in locomotion and Xenopus laevis

The group 1 metabotropic glutamate receptors have previously been investigated in many locomotion models. In mice, it was shown that group 1 mGluRs increase the fire rate of motoneurons (Iwagaki and Miles, 2011). In fictive swimming of *X. laevis,* group 1 mGluRs increased locomotor network excitability through presynaptic inhibition of inhibitory interneuron release (Chapman, Issberner and Sillar, 2008). In fictive swimming of the isolated lamprey spinal cord, a similar result was achieved with group 1 mGluRs shown to be necessary to maintain the frequency of motoneuron output. However, both these experiments in *X. laevis* and lamprey highlighted a difference in the functions of the two group 1 mGluR sub-types. When $mGluR_1$ was inhibited a significant reduction in the frequency of motoneuron firing was observed, yet when $mGluR_5$ was inhibited, a significant increase in motoneuron output was observed. It was shown that $mGluR_1$ enhanced NMDAR depolarisation contributing a single calcium spike and reducing leak current, without which maintenance of normal excitatory depolarisation rate is reduced. This study also showed that DHPG would not induce depolarisation when neurons were held at resting potentials, but when held at slightly more depolarised potentials DHPG (group 1 mGluR agonist) increased depolarisation and rate of fire (Kettunen, Hess and Manira, 2003). This is evidence that group 1 mGluRs modulate rather than drive excitatory depolarisation. This study also provided evidence that $mGluR_5$, although not necessary for maintenance of depolarisation rate, was responsible for persistent calcium spikes released from the endoplasmic reticulum indicating it may have more of a function long-term. From their work in the isolated lamprey spinal cord they also found evidence that increases in locomotor frequency induced by group 1 mGluR activation involved a decrease in the mid-cycle inhibitory release similar to what was shown in *X. laevis* (Chapman, Issberner and Sillar, 2008). With work showing that DAG is a precursor to the cannabinoid receptor ligand 2-AG it was hypothesised that retrograde cannabinoid action was part of the process which increased excitation in the network.

The group 1 mGluRs have not been sequenced in *X. laevis*. However, the sequence has been predicted and it has been sequenced in *X. tropicalis.* The predicted sequence of $mGluR_1$ in *X. laevis* has an identity of 95.49% to *X. tropicalis,* 79.62% to humans, 79.17% to mouse and 79.32% to rat. The predicted sequence in *X. laevis* for $mGluR_5$ has an identity of 95.9% to *X. tropicalis,* 82.85% to humans, 84.28% to mouse and 83.22% to rat.

1.8.3 Cannabinoids in the CPG

Previous studies in the isolated lamprey spinal cord provided evidence that retrograde action of cannabinoids at inhibitory interneuron terminals was partly responsible for the increase in

motoneuron burst frequency produced by group 1 mGluR activation (El Manira *et al.*, 2002, 2008; Kettunen, Hess and Manira, 2003a; Kettunen *et al.*, 2005; Kyriakatos and El Manira, 2007). In these series of experiments, it was demonstrated that 5μM of synthetic CB1 agonist WIN-55 increased locomotor frequency by inhibiting cIN release. This effect was found to occlude the increase seen from group 1 mGluR activation. Antagonising the CB1 receptor with inverse agonist/antagonist AM-251 was also found to stop the DHPG induced increases. This was evidence that through group 1 mGluR activation endocannabinoids ensure normal locomotor frequency by regulating the timing and concentration of cIN inhibitory glycine release.

1.8.4 Cannabinoids in Xenopus laevis

The cannabinoid receptors have been shown to be present in the CNS of the adult *X. laevis* (Cottone *et al.*, 2003) and the functional receptor has been shown to be present in stage 41 of the developing tadpole (Beatrice *et al.*, 2006) with mRNA present from stage 26. Cottone *et al.*, (2003) showed that the nucleotide sequence identity between human and *X. laevis* was 73.9% with an amino acid sequence identity of 83.1%. To put this in context the two most studied organisms, rats and mice, have only marginally better sequence similarity. For rats, their nucleotide identity was 74.2% and amino acid identity was 83.5%, for mice it was 74.3% nucleotide identity and 83.1% amino acid identity. The distribution of CB1 in the spinal cord was at the highest intensity in the dorsal field and ventral field with high staining in large cell motor neurons alongside smaller adjacent cells, possibly interneurons. In particular staining in the dorsal field occurred in the Lissauer's tract (Salio *et al.*, 2002; Cottone *et al.*, 2003). In the brain very high staining was found in most areas of the hypothalamus, olfactory bulb, hippocampus, lateral pallium, medial amygdaloid nucleus and dorsal pallium (Cottone *et al.*, 2003).

1.9 Atomic Force Microscope (AFM)

The Atomic Force microscope was developed in 1986 (Binnig, Quate and Gerber, 1986). It was an improvement on the scanning tunnelling microscope, for which Binnig and Rohrer won the Nobel Prize. The AFM transformed our ability to visualise and analyse the nanoscale, reaching the amazing goal of viewing the structure of molecules (Gross *et al.*, 2009) confirming our theoretical calculations of natural carbon ring structures.

There are two key components that enable the AFM to exist, the quartz crystal piezo and the laser/photodiode detector system. The advances in precision with these two systems are what make the AFM a desirable tool for investigation into the nanoscale structure of the natural world. The laser is targeted to the back of the cantilever and tracks it as it scans the sample (Figure 1.9.1). The laser reflects into a photodetector that is calibrated during set up. Once calibrated the laser will try to stay in the centre. Variation from the centre in the lateral or vertical direction is recorded as lateral or vertical deflection in separate channels. The piezo is responsible for oscillating and moving the cantilever, with the oscillation controlled via a quartz crystal. In contact mode AFM, the cantilever scans backwards and forwards across the sample with the laser tracking the nanometre changes in topography. Non-contact mode AFM (mainly used for atomic structure investigations) operates by scanning over the sample without coming into contact, oscillating the cantilever near-resonant frequency, measuring the interaction of forces between sample and tip as it moves through the air. This is often performed in a vacuum in order to measure atomic forces such as the analysis of biomolecules (Gross *et al.*, 2009). In amplitude modulated (AC) mode (sometimes called tapping or intermittent contact mode) the piezo is tuned to the optimum oscillatory frequency for the cantilever type near-resonant frequency, it then oscillates the cantilever at this frequency as it scans the area selected. The laser measures the change in cantilever oscillation/amplitude. When the tip encounters a change in height or texture this will be shown in the height image or phase image respectively. This mode is advantageous to contact mode because it is less likely to damage the sample. For biological samples, which are large and very irregular in shape, this enables better resolution as the tip will not snag or catch on the membrane. AC, intermittent contact and tapping mode are used interchangeably as each hope to highlight a different aspect. AC mode refers to the amplitude of the tip, intermittent contact as the tip only ‘contacts’ the surface at the lowest point of oscillation and tapping mode is somewhat self-explanatory. It is now thought that AC mode or tapping mode is the most accurate descriptions as the tip is not really in contact with the sample, rather it is going through cycles of attraction and repulsion. If it does contact anything it is more likely a liquid bilayer on the

surface, which exerts attractive forces on the tip before it is repulsed and begins the oscillation again.

Phase imaging measures the tip-sample interaction. When the tip interacts with the sample it can either be slowed by the surface if it is viscous/attractive, or it can be repulsed pushing the tip further forward and shifting the amplitude wave of the cantilever ahead, represented in degrees of phase shift. Common analysis of phase images suggests large phase lag equals brighter pixels and smaller phase lag equals darker pixels. One problem with phase imaging is brighter pixels only tell you the degrees of phase shift and there are several factors which interact to cause a phase shift. There are two components measured in a phase image, the first is the combination of the piezo-cantilever-tip: the tip sharpness, driving amplitude frequency (this affects the force of interaction) and the cantilever spring constant. The second component is the sample properties; viscoelasticity, hydrophobicity, friction, adhesion and surface materials (in the case of biological samples this would include the substrate cells are grown or contained on).

The cantilever and tip are an important part of the AFM. The flexibility of the cantilever, termed the spring constant (*k*), is the force required to bend the cantilever. Different spring constants are required depending on type of sample and mode of scanning (contact, non-contact or AC). There are also different tip shapes. The thinner the tip at its end the higher resolution can be achieved. However, a very thin tip on a hard sample risks breaking the tip. Similarly, a very thin sharp tip on a soft sample, such as a biological membrane, risks tearing or puncturing the membrane. Recent force/Young's modulus measurements on neuronal membranes have used spheres on the tip to rectify this problem (Dimitriadis *et al.*, 2002, (Nikkhah *et al.*, 2011). Another factor is the material and reflective properties of that material used for the cantilever. A metal with higher reflective properties will be more accurate.

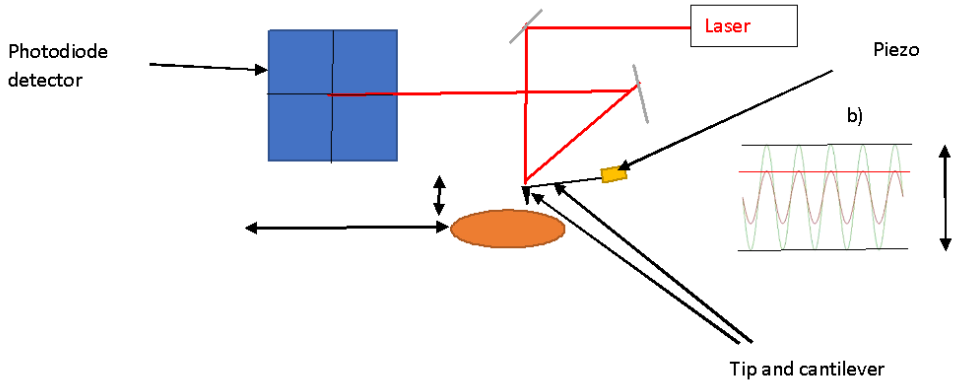

***Figure 1.9.1**- Schematics demonstrating the principle mechanisms of Atomic force microscopes b) example of wave tip forms while scanning in AC and non-contact modes.*

As seen in Figure 1.9.1, the AFM works with the laser targeted to the back of the cantilever via mirrors into the photodetector. The mirrors can be adjusted via screws on the AFM head (termed laser screws). In contact mode AFM the tip will only be moved in the lateral direction. In non-contact and AC mode AFM the tip will oscillate in the vertical direction while scanning in the lateral direction, forming a wave. The amplitude of this wave is set during tuning via the set point if the black lines (figure 2.4.2b) demonstrate an amplitude of 1V (in AFM the amplitude is represented in volts V) then the red lines represent the reduction in amplitude via the set-point. The program then maintains it at this amplitude as it scans, changes are detected by the laser feedback and result in height image topography, and phase image, vertical deflection and lateral deflection all presented as separate channels graphically via colour heat mapping.

1.9.1 Atomic Force Microscopy of Biological samples

Since its inception, AFM has been a vital tool in physics and material science. It has also been used in biological and chemical sciences, to analyse everything from pentacene (Gross *et al.*, 2009) to DNA (Hansma *et al.*, 1997) to red blood cells (Girasole *et al.*, 2007). Recently it has been used more and more in neuroscience with increased scanning speed and resolution enabling live cell measurements that give detail of dendritic spine development never seen before (Shibata *et al.*, 2015). For a detailed review of the possibilities of AFM in neuroscience see (Jembrek *et al.*, 2015). The attractive and repulsive forces of atomic interaction are measured in AC mode and non-contact mode AFM. In contact and non-contact mode, pN forces can be measured due to the tips extremely small size (5-50nm). This natural process can be enhanced in biological experiments by coating the tip in receptor ligands or antibodies and measuring the interaction forces while scanning the cell surface. Some experiments have taken this one step further attaching cells to the cantilever and measuring cell to cell adhesion (Benoit and Gaub, 2002). Topographic measurements can be used to assess cell health, for example, the average roughness of red blood cells (RBC) was taken as a measurement of RBC health (Girasole *et al.*, 2007).

Force spectroscopy measurements (Young's modulus) have been a widely used tool in biological science. This method pushes the tip into the sample with increasing force and measures the sample indentation vs force. This has been performed in live growth cones vs damaged growth cones (Martin *et al.*, 2013). In biological samples, elasticity, the readiness with which the membrane returns to normal after indentation, is also taken as a measure of healthiness. The viscoelastic properties of neurons and glial were compared (Lu *et al.*, 2006). The stiffness of the developing spinal cord of mice was investigated (Koser *et al.*, 2015) leading to a fascinating paper in which evidence was provided to show how mechanosensing receptor (piezo1) of developing growth cones effects branching and pathfinding, with variation in tissue stiffness causing aberrant axonal growth and pathfinding errors (Koser *et al.*, 2016). However, force spectroscopy measurements of membranes have their drawbacks. Under physiological conditions the membrane is prone to ripping or tearing and finding and measuring small structures such as dendritic spine membrane viscoelasticity has never been done.

1.9.2 Los tangent imaging

In an ideal scenario, we could have the precision of contact mode, the lack of damage caused by AC mode and the force measurements of force spectroscopy. Using AC mode there have been developments in quantifying the tip-sample interaction by combining the amplitude data

with the lock-in phase data to produce the loss tangent (Proksch *et al.*, 2016). The phase shift image has long been an image of frustration. It gives a great deal of detail, yet is specific to that image, making it difficult to use for anything other than individual qualitative image analysis. Loss tangent imaging takes the phase shift and quantifies it into a unitless ratio from 0-1, zero being a hard substance and one being a very viscous substance. The drive amplitude in AC mode determines the force the tip will interact with the surface and the phase image give details of the tip-sample interaction (Proksch *et al.*, 2016).

1.10 Primary tissue culture

Primary cell culture is a vital tool of analysis in all biological sciences. In neuroscience it allows us to strip away the complexity of inter-neuronal system communication and look directly at intrinsic signalling particularly in the synapse. The most common form of primary culture in neuroscience uses rats or mice. Being a mammal, the development of these neurons is much slower and more costly than *X. laevis*. In order to assess the structure of *X. laevis* neurons in culture we developed a primary neuron culture from stage 22-24 *X. laevis* embryos. This method has been developed over the years with the first publication in (Peng, Baker and Chen, 1991; Peng *et al.*, 2003) and a recent paper confirmed functional synapses within 24 hours tested by pre- and post-synaptic electrophysiological recordings (Yazejian *et al.*, 2013). Although enabling clear structural analysis and protein localisation, cell culture is not a perfect method. The obvious reason is that cells are not in the same environment and do not receive the same cues and guidance that they would if developing in the organism. This may mean their structure and rate of development are different from whole organism studies and this should be considered when analysing the results. This also has implications for pharmacological assessment. In an organism applying treatments will modulate the signalling that already exists. It is unclear how much signalling across synapses occurs in cell culture, however, recent electrophysiological recordings demonstrate they are functional (Yazejian *et al.*, 2013). Cell culture gives us the opportunity to scan the structure of dendritic spines which could not occur in the whole organism. It also offers the chance to visualise proteins tagged with fluorescent green fluorescent protein (GFP) or fixed and stained with fluorescent antibodies in immunohistochemistry techniques.

1.11 Immunohistochemistry

Immunohistochemistry stemmed from the discovery of serum antibodies in 1890. Quickly it was realised dyes could be attached to the antibodies to aid visualisation. The technique

developed until in 1941 Dr. Albert H. Coons produced the first fluorescent antibody labels. Fluorescent microscopes had been invented a few decades earlier in 1929 by Ellinger and Hirt with the epi-fluorescent microscope (the advancement being the ability to control which wavelengths of light reach the sample). Since the 1980s the development in this field has been rapid and the quality of fluorescent probes and the accuracy of microscopes, like confocal, enable us to visualise the inner workings and positioning of proteins of interest. This procedure is so endemic to biological sciences that it is almost impossible to think where we would be without it. The process of immunohistochemistry starts by first raising an antibody that will bind to a molecule of interest within the cell and the sequence must be unique in its expression. The cells must be permeabilised to allow antibodies into the cell. The antibody unique to the molecule of interest (termed primary antibody) is incubated with the permeabilised cells then unbound antibody is washed off and a secondary antibody specific to the primary antibody is added. The secondary antibody is attached to a fluorophore which can be excited by certain wavelengths of light. When the correct wavelength of light contacts the fluorophore, the interaction moves an electron in each atom up an energy level. The electron then moves back down an energy level releasing a photon that has less energy than one that first encountered the electron. This means the emission is always a larger (nm) wavelength of light than the excitation.

This method allows us to identify proteins of interest and since the improvement of microscopes to the confocal microscope it in now possible to localise proteins within cells. Further to this the massive improvements of genetic modification now allow us to tag proteins in live cells by adding the gene for GFP to proteins of interest and tracking and measuring them in live cells. We will apply immunohistochemistry techniques to try and measure the expression of PSD-95 in cell culture and in whole tadpole spinal cord. PSD-95 can be used as a marker for excitatory postsynaptic densities and also increases in more active synapses. This measure will elucidate whether the effect seen in the whole tadpole or in treatment of cell cultures has effects on the number of excitatory synapses present.

1.12 Aims and objectives

The overall aim of this study is to investigate the roles of group 1 mGluR and CB1 in the behaviour of *X. laevis* and how the structure of dendritic spines in primary culture may relate to this. We aim to focus our investigation on the dendritic spines first to demonstrate they are present in a primary spinal neuron culture, then to investigate their structural changes under pharmacological manipulation of CB1 and $mGluR_{1/5}$. To achieve these aims, the objective is to create a method of measurement for the CPG controlled swim-cycle speed of the *X. laevis* tadpole between stages 37-42. Using this method our objective was to investigate the effect of group 1 mGluRs on the frequency of swim-cycles of the *X. laevis* tadpole between stages 37-42. This has been investigated in fictive swimming electrophysiological preparations of *X. laevis* and other vertebrates. However, evidence of their effect in whole tadpole behaviour of *X. laevis* has not been observed. Following this, we wanted to examine if the CB1 receptor is involved in the control of this swim-cycle speed and if it is involved in group 1 mGluR induced changes. Evidence from fictive swimming electrophysiological recording in *X. laevis* and lamprey spinal cord suggest CB1 is responsible for regulating commissural interneuron inhibitory neurotransmitter release to dIN after group 1 mGluR activation. This measurement will be accompanied by an assessment of maximum flexion angle achieved during the swim-cycle speed measurement. This will assess if group 1 mGluRs and/or CB1 affect motoneuron/muscle output during swimming and if muscle flexion and frequency of swim-cycles are correlated (chapter 3).

Our next objective will be achieved using primary neuron cultures of *X. laevis* spinal neurons at 3 days in vitro (DIV). The neurons will be assessed for the presence of dendritic spines using atomic force microscopy and measurement criteria developed from previous literature. We will then test the treatments that caused changes in the behavioural assessment. The group 1 mGluRs and CB1R agonists and antagonists will be investigated for their effects on dendritic spine dimensions and membrane stiffness (loss tangent) assessed using atomic force microscopy (chapter 4).

Finally, 10µm thick microtome slices of whole tadpole spinal cord, treated in behavioural assessments, and the primary neuron cultures scanned in the AFM assessment, will be evaluated for changes in PSD-95 density using immunohistochemical staining measuring changes in fluorescence intensity, to assess if PSD-95 expression is correlated with behavioural and/or dendritic spine morphological changes. This will give an indication if the effects observed in behaviour or dendritic spine morphological analysis are short term ionic changes or due to changes in protein expression in excitatory dendritic spines (chapter 5).

2 Methods

2.1 Behavioural assessment of *Xenopus laevis* tadpole swimming response to touch

This section will outline the methods used to determine the length of time each swim-cycle takes during swimming, after it is initiated by touch to the tadpole trunk. By measuring the speed of the tadpoles swimming motion, we are assessing how pharmacological intervention of $mGluR_{1/5}$ and CB1 affects the output of the CPG. The combination of both: excitatory drive and inhibitory modulation, produces the overall output of the CPG. This output is measured by timing the muscle contractions. This will be compared with maximum muscle flexion during the swim-cycle assessment, to try and elucidate the pharmacological effects on muscle contraction.

2.1.1 Stages of X. laevis development

During its oocyte and tadpole development (stage 1-45 (Nieuwkoop and Faber, 1995)), the *X. laevis* tadpole grows from food stores inside cells contained in yok sacs. The tadpoles are staged on morphology. The development is very predictable, once fertilised the egg changes colour and shows a little dot, this is stage one. Stage two is determined when the eggs visibly divide into two cells (under low magnification 50x). Stages 2-6 are termed the cleavage stages, where the cells continue to divide. Stages 7-9 are the blastula stages, by the end of which identifying separate cells becomes difficult. By stage 20 the neural fields are fused and distinct, which can be seen as a ridge along the top that will develop into the spinal cord. After stages 21-25 they begin to elongate and break free of their jelly coat and vitelline membrane. Their first contractions of the tail begin to occur at stages 25-27. From stage 29 onwards they will swim briefly in response to touch and keep growing developing larger muscle columns (Nieuwkoop and Faber, 1995). As the tadpole develops past stage 45, the mouth opens, and the tadpole becomes self-feeding. At this stage they are classed as a sentient animal. Due to this all our tadpoles were anaesthetised by stage 44. They are an ectotherm, meaning the metabolism and development of the tadpoles (stage 1-45) can be staggered depending on temperature. At room temperature (23^{o}C) *X. laevis* will reach stage 45 in 4 days (96 hours) (Nieuwkoop and Faber, 1995) and reach full size (stage 66) in 58 days. It has a generation time of 1 year. To produce *X. laevis* embryos, the breeding pair of adult frogs are injected with human chorionic gonadotrophin (HCG) to stimulate the pair to mate. This can produce hundreds, sometimes thousands, of fertilised eggs each time, making this is a very cost-effective animal model.

2.1.2 Grouping

The concentrations of CB1 and group 1 mGluR, agonist and antagonist, used in the swimming assessment, were determined by literature review of previous experiments in *X. laevis*. Where none exist, such as CB1 receptor, experiments in similar models, like lamprey CPG, were used. For AM-251 application, a 5µM concentration was shown to have an effect in lamprey. We expanded the concentrations either side to 100nM, 2µM, 10µM and 50µM. Not only does this range exceed the EC50 for AEA and IC50 for AM-251 (Table 2.1.1), it also encompasses the concentration that DHPG will be used at (Table 2.1.2). AEA was selected for testing due to its endogenous activity at CB1 with lower affinity at CB2 (see Table 2.1.1), compared with 2-AG which is equally potent at both CB1 and CB2. This would make exogenous applications of 2-AG more likely to affect immune cells and tissue, compared to AEA. AEA also has a lower EC50 and higher affinity than 2-AG, which is thought to perform the majority of signalling in the CNS, as concentrations of 2-AG were 1000-fold higher than AEA.

The treatment conditions assessed using this method were: CB1 antagonism via AM-251 (50µM, 10µM, 2µM, 100nM), CB1 agonism via AEA (50µM, 10µM, 2µM, 100nM). All concentrations of AEA and AM-251 were assessed at two age group stages 37-39 and 40-42. Two age groups were chosen because previous reports suggested the presence of CB1 RNA at stage 26 but functional CB1 receptors from stage 41 (Beatrice *et al.*, 2006). By splitting the age groups, we expect differing levels of CB1 activity, with a larger effect in the stage 40-42 age group, due to increased receptor expression.

To investigate the functionality of both $mGluR_1$ and $mGluR_5$ in the control of swim-cycle frequency, we applied DHPG (group 1 mGluR agonist) (50µM). This dose was chosen because it has previously been shown to have effect in *X. laevis* (Chapman, Issberner and Sillar, 2008), and it is within the EC50 demonstrated in other studies (Table 2.1.1). To investigate the endogenous function and the constitutive activity of $mGluR_5$, MPEP ($mGluR_5$ non-competitive antagonist) (50µM) was applied. Similarly, to indicate the constitutive activity of $mGluR_1$ in the regulation of swim-cycle frequency, we applied LY367385 ($mGluR_1$ antagonist) (50µM). This aimed to differentiate the effect between the two subtypes that have previously shown to have different effects on swim cycle frequency (Chapman and Sillar, 2007; Chapman, Issberner and Sillar, 2008). Then, we antagonised both of group 1 mGluRs using MPEP (50µM) + LY367385 (50µM), to investigate the constitutive activity of both receptors. To test if this application had fully antagonised the group 1 mGluRs, we incubated the tadpole in MPEP (50µM) + LY367385 (50µM) (20 minutes incubation), followed by DHPG (50µM 10 minutes incubation).

To test the relationship between the CB1 receptor and the group 1 mGluRs, we antagonised CB1 with AM-251 (10µM, 20 minutes incubation), followed by incubation with group 1 mGluR agonist DHPG (50µM, 10 minutes incubation). We then assessed the effect of antagonism of all 3 receptors with: MPEP (50µM) + LY367385 (50µM) + AM-251 (10µM) for 20-minutes incubation. Then, we assessed if there were differential roles for $mGluR_1$ and $mGluR_5$ in the interaction with CB1 by applying LY367385 50µM + AM-251 10µM and then MPEP 50µM + AM-251 10µM, for 20-minutes incubation. All these conditions were performed on stage 40-42 tadpoles. All treatments were compared with vehicle control. DHPG, MPEP, LY367385 and AM-251 were compared with DMSO control. AEA was compared with Soya emulsion control. Pharmacological profiles of each of the chemicals applied are demonstrated below Tables 2.1.1 and 2.1.2.

Table 2.1.1*- Cannabinoid receptor agonist and antagonist pharmacological profile*

Drug applied	Mechanism of action	EC50 and Ki	Vehicle control
AEA (in Tocrisolve) Purchased from Tocris uk	CB1 agonist CB2 agonist TRVP1 agonist	EC50= 31nM, Kd =89nM EC50 = 27nM, Kd=371nM pKi = 5.68	Soya emulsion (tocrisolve)
Am-251 Purchased from Tocris uk	CB1 antagonist GPR55 agonist µ-opioid receptor antagonist	Ki=7.49nM, EC50= 39nM Ki=251nM	DMSO

Table 2.1.2*- Agonist and antagonists of group 1 metabotropic glutamate receptors pharmacological profile*

Drug applied	Mechanism of action	EC50/IC50	Vehicle control
DHPG Purchased from Tocris uk	$mGluR_1$ agonist $mGluR_5$ agonist	EC50=10-60µM	DMSO
MPEP Purchased from Tocris uk	$mGluR_5$ non-competitive antagonist	IC50= 36nM	DMSO
LY367385 Purchased from Tocris uk	$mGluR_1$ antagonist	IC50 = 8.8µM	DMSO

2.1.3 Applying treatments to tadpoles

The tadpole can absorb molecules through the skin, although the size of molecule and polarity can affect the uptake. To ensure substrate uptake a nick in the dorsal fin was made prior to treatment. To do this, the tadpoles were selected 1-2 stages before use (for stage 37-39

groups stage 36, and stage 40-42 stage 39 was used), the tadpole was anaesthetised in 0.1% MS222 by placing in for 20 seconds then removing to 10% saline (the tadpole was immobile for ~5 minutes). Then, using sharp forceps/ sharp wire scalpel, the small incision is made in the dorsal fin. The tadpole is placed is sterile saline and left to reach stage of analysis and recover from MS-222 (1-2 hours). Once at the right stage, the tadpoles were placed in a petri dish containing the appropriate treatment concentration and left to incubate for 20 minutes. After which, the tadpole was moved to a fresh petri dish, containing 10% saline, to begin filming. The tadpole was stimulated with a stroke of the tail by a pipette tip. The swimming response was filmed at 400 frames per second (fps), then the tadpole was left for two minutes to allow for cessation of ultra-slow after-hyperpolarisation, synapse reorganisation and neurotransmitter replenishment (Sillar et al personal communication,(Zhang and Sillar, 2012; Zhang *et al.*, 2015)). This was repeated 5 times for each tadpole, encompassing a 10-12-minute window, over which time the tadpole was filmed 5 times. After being removed from drug treatment, the tadpoles were fixed in 5% glutaraldehyde for 30 minutes, transferred to 10% saline and stored at 4^{o}C for microtome and immunohistochemical analysis (methods chapters 2.2 and 2.5, results chapter 5).

2.1.4 Analysis of frequency of swim-cycles

Using windows media player classic, the length of one swim-cycle was determined by counting the frames it took for the tail to return to the same spot. The frequency in hertz (Hz) was calculated by dividing 400 (number of frames per second recorded) by the frames counted for the swim cycles. To eliminate subjectivity the speed of swimming was taken over three swim-cycles, between the third and tenth cycle, and averaged.

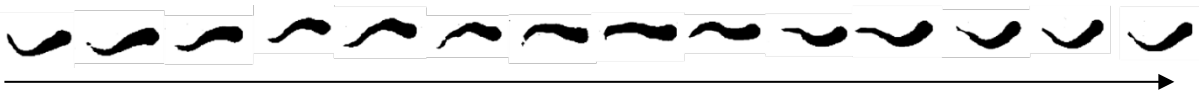

Figure 2.1.1*-Example of 1 complete swim-cycle by a stage 40-42 tadpole from control group (DMSO). Filmed at 400 fps; time between each frame= 2.5ms Images taken from video and converted to binary in Image J for presentation.*

2.1.4.1 Statistical analysis

The results were analysed in SPSS using a linear mixed model (LMM), with time point as a covariate and tadpole as a random factor, to assess if treatment (fixed factor) affected the frequency of swim-cycles. The assumptions for this model are normality of residuals, independence of residuals and linearity of the predicted vs residuals (presented in the appendix section 7.2). The test for normality used was Shapiro-Wilk, at a significance level of 0.05. Almost all analyses carried out passed this test for normality of residuals, though it is recognised some did not, the LMM is sufficiently robust test to withstand some deviation from the assumption of normality. Shapiro Wilk tests have some degree of fallibility. In cases where significance was achieved in Shapiro-Wilk the normality was reviewed with skewness and histograms. If this was not satisfying, the result was tested using a generalised linear mixed model (GLMM) in SPSS that does not have the normality assumption. The generalised linear mixed model has different link functions, which transform the data into an unbounded continuous scale. The gamma regression link function was chosen because it transforms data that is always positive, but non-normally distributed. The results of the GLMM with gamma regression link function, gave the same or similar p-values as the linear mixed model.

2.1.5 Angle of Flexion (AOF) measurement

As the frequency of swim-cycles was measured, three still images were taken of maximum flexions achieved during those swim-cycles. The flexion angle was measured in Image J using the angle function. This was repeated three times per image (Figure 2.1.2). This was necessary as there is some human subjectivity in this process as can be seen in Figure 2.1.2. From these three measurements an average was taken for each tadpole time point 2, 4, 6, 8 and 10 minutes. The results were analysed in SPSS using a linear mixed model, with time point as a covariate and tadpole as a random factor to assess if treatment affected the maximum angle achieved during swimming.

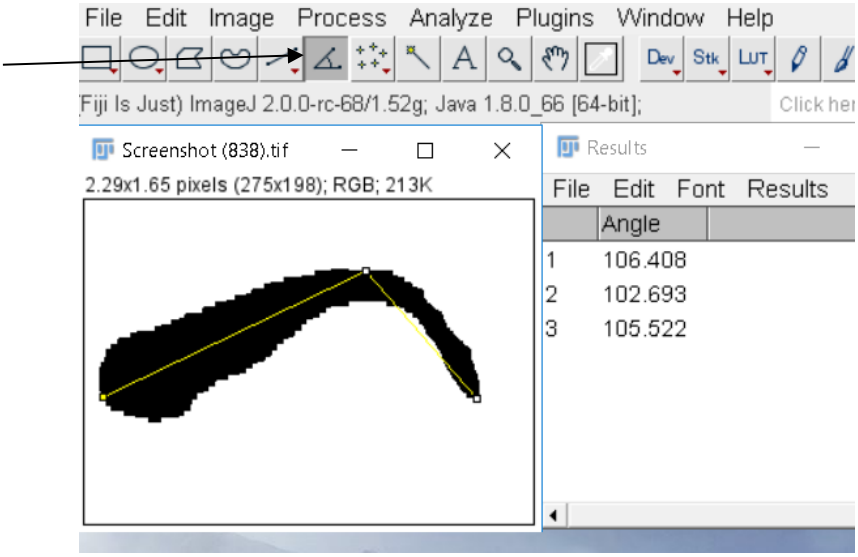

***Figure 2.1.2**- Angle of Flexion calculation example. Using the angle function (arrow) in Image J three points are selected; first the centre of the head at the pineal eye then straight back down the trunk to the edge then to the tail tip 3 measurements per image, 3 flexions per time point/video.*

2.2 Microtome of *Xenopus laevis* tadpole

Microtome is a process of dehydrating embedding and slicing tissue to a desired thickness before rehydrating to image. Prior to dehydration of the tadpole, the yolk sac was removed with thin wire scalpel. This was done to aid dehydration and the yok sac was extremely auto fluorescent. To begin dehydration of the tadpole, it was placed in 70% ethanol for one hour, changing tadpole to new ethanol every 20 minutes (two changes). After one hour, the tadpole was moved to 80% ethanol, with two changes. Then, the tadpole was moved into 90% ethanol for one hour with two changes. Then into 95% ethanol for one hour with two changes. Then, it was moved into 100% ethanol for one hour, with two changes. Finally, the tadpole was moved into Histoclear for one hour with two changes. During this time, paraffin wax was heated to 56-60^{o}C. When removed from the histoclear, the tadpole was placed in the mould and the mould was filled with the melted paraffin wax. The tadpole was moved to the middle of the wax mould before the wax cooled. The moulds were left to cool and harden overnight. When the moulds were fully hardened, they were trimmed to the right size and mounted onto a wooden block by heating the wax and fixing it in place and allowing to cool. The block was placed into the sample holder of the microtome (Figure 2.1.1) and the blade was then inserted into the microtome, selecting 10µm thickness for the slices. The sample was moved by turning the handle and when working well would give ribbons of tissue slices. These tissue slices were moved to a water bath, set at 50^{o}C for 5-10 minutes to get rid of the wrinkles. They were then picked up with a slide and placed on a heated drying rack, set at 45^{o}C and left for 2-4 hours. This not only dries the slide, but aids in fixing the sample to the slide. The samples were rehydrated by working in the reverse order to the dehydration steps. The slides with the samples on them were put in Histoclear for 15 minutes changing solution at 7.5 minutes. This was repeated with 100% ethanol for 15 minutes with one change, then 95% ethanol 15 minutes one change, 90% ethanol 15 minutes one change, 80% ethanol 15 minutes one change and finally 70% ethanol one change. After this the slide was gently washed with 10% saline. The integrity of the sample was assessed under the microscope (Figure 2.2.2). If intact, the sample was ready for immunostaining.

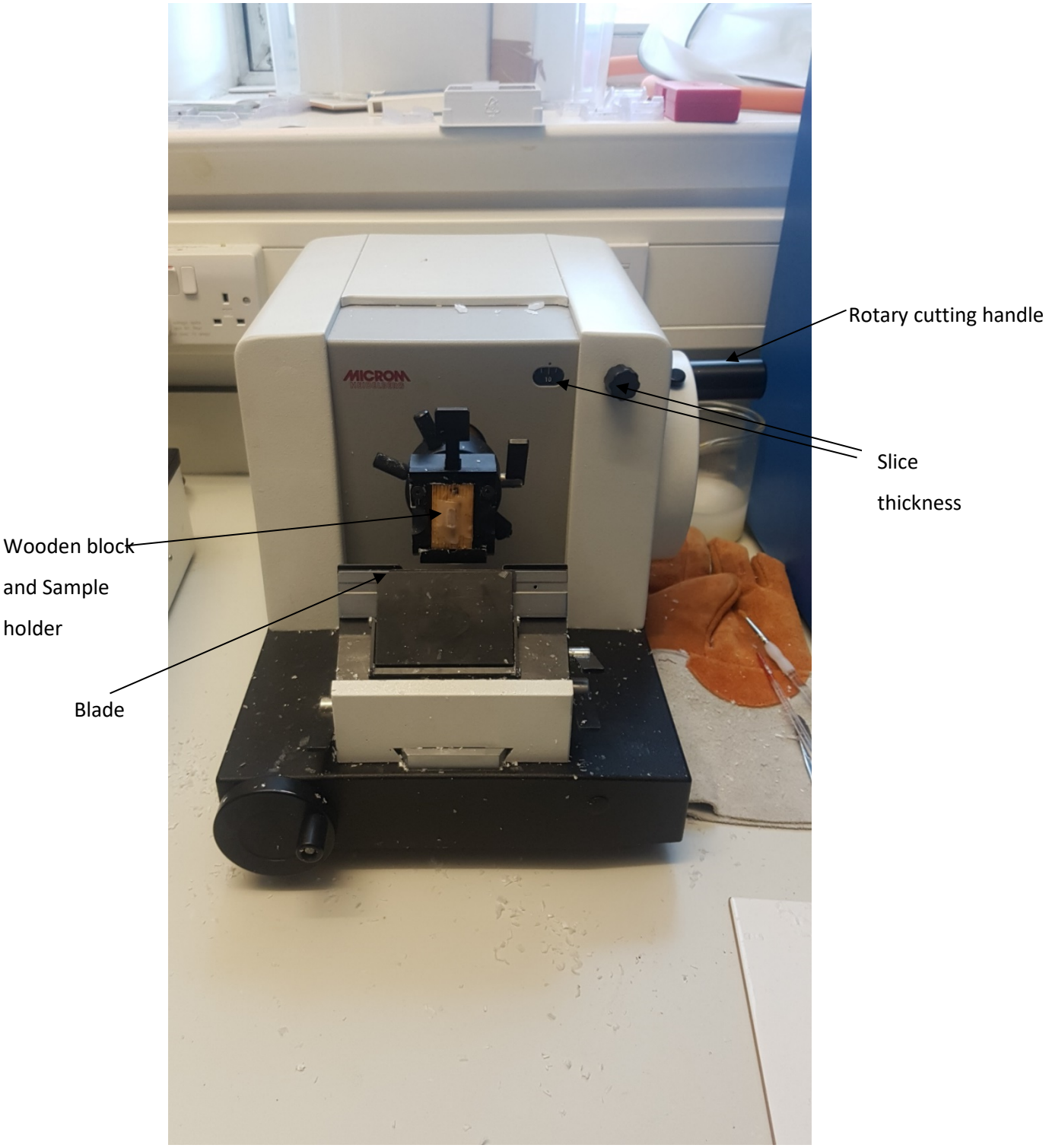

Figure 2.2.1*- Microm Heidelberg HM330 Rotary Microtome. Sample is attached to wooden block. Thickness of slice is selected (µm). Blade is put in last then sample is sliced by turning rotary cutting handle which moves the sample forward and down over the blade.*

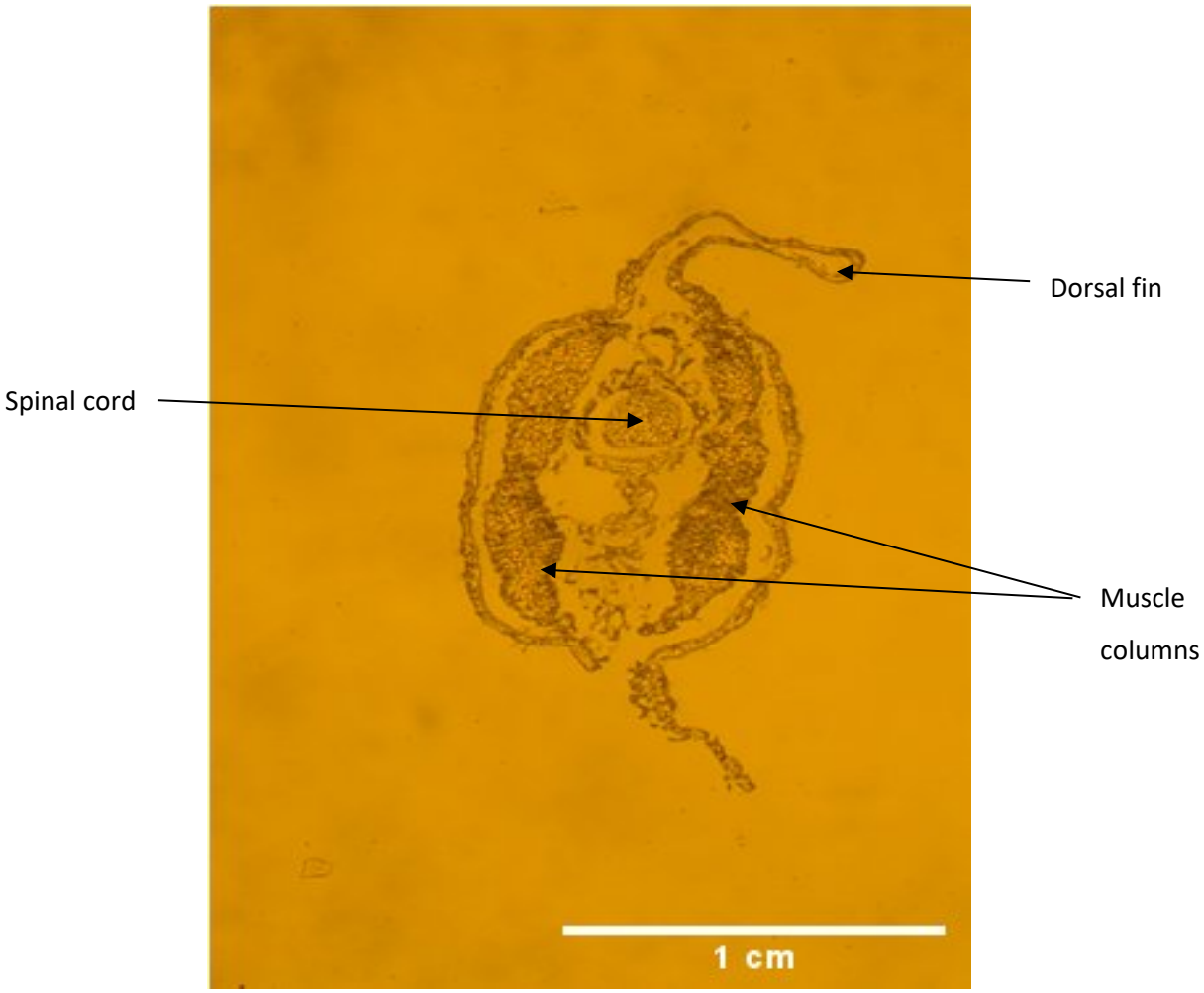

Figure 2.2.2*- Example of a transverse section of the tadpole stage 40-42 (10µm thick) obtained using the microtome. Can see intact spinal cord and muscle columns. Slight tear in the skin at the top on side yolk sac was removed.*

2.3 Primary neuron culture of stage 22-24 *Xenopus laevis* embryos

2.3.1 Method

The most difficult aspect of this tissue culture method was eliminating bacterial infection. To help with this, all stages of this method were carried out in a sterilised laminar flood hood using aseptic technique with the microscope and all areas around the hood wiped down with 70% ethanol. Healthy embryos at stage 22-24 (Figure 2.3.1) were selected, with five embryos used per coverslip. The culture media was made up as L-15 50% + Normal Frog ringer (NFR) 49% (per 1 litre: 116mM NaCl, 2mM KCl, 1.8mM $CaCl_2$, 5mM Na+-HEPES, pH 7.35.) + Insulin transferrin serilium (ITS) (thermofisher) 1% + Brain derived neurotrophic factor (BDNF (AbCam ab9794)) (3.5µg/ml 30µl stock diluted to final concentration in culture media of 17.5ng/ml) + antibiotic solution (Penicillin 1000U/ml, Amphotericin B 25µg/ml and Streptomycin 10mg/ml stock diluted by 1/1000 in culture media) in sterile conditions, then the media was sterile filtered. The coverslips were sterilised in an autoclave and/or incubated in ethanol prior to use. Sterile NFR washes were set up (5 washes per coverslip) and sterile Ca^{2+}/Mg^{2+} free solution (CMF) (per 1 litre 125mM NaCl, 2mM KCl, 1.2mM EDTA, 5mM Na^{+}-HEPES, pH 7.35.) washes set up (5 per coverslip). To ensure sterility, the NFR and CMF was sterile filtered into sterile culture dishes for dissection and washes. In sterile NFR and under the microscope, the outer jelly coat and inner vitelline membrane were removed with sharp forceps. The embryos were washed through three sterile NFR washes transferred with sterile disposable pipettes. Then, in sterile CMF, the spinal column was removed by cutting each end of the concave spinal column (cut along white lines in Figure 2.3.1). The removed spinal columns were washed through sterile CMF, then left in CMF for 10 minutes. After 10 minutes the skin peels off easily. Once the skin was removed, the remaining spinal tissue was washed through two sterile CMF washes and left for 2 hours at room temperature in sterile CMF, for cells to dissociate and form a pile. Once cells are dissociated, they are ready to plate. While the cells were dissociating, dry sterile coverslips were coated in 100µg/ml laminin (purchased from sigma) (diluted in sterile NFR) for at least 1 hour at room temperature, then washed in sterile NFR. Laminin coated coverslips were then placed in sterile culture dishes and 3ml of culture media was added to the dish. The dissociated cells were then carefully pipetted onto the coverslip trying to ensure even distribution. Once the cells were placed onto the coverslip, the dish was not moved for at least 12-24 hours, to ensure cells adhered to the coverslip. The culture media was replaced every 48 hours. This was done by removing old media with a sterile pipette (always ensuring cells never encounter air-liquid interface) and replacing with new media.

This method combines information from 3 publications (Peng, Baker and Chen, 1991; Peng *et al.*, 2003; Yazejian, *et al.*, 2013) and through a process of trial and error (testing different coating proteins and their concentration, antibiotics, BDNF concentration, plating technique and food source (ITS or FBS)) arrived at this method. Consistent with Peng *et al's.*, (2003) findings, keeping the neurons healthy past day 5 was difficult and is likely caused by the depletion of the yok sacs. We managed to keep cells healthy into week 2, however, this was irregular. With more development on the amount of additional nutrients and minerals needed to get the cultures past 7 days would enable these cultures to survive longer. However, for our purposes, we chose 3 DIV as our assessment. This time point was chosen because the neurons had developed multiple connections and the muscle cells were innervated and twitching, which is a sign of functioning synapses (Yazejian, *et al.*, 2013). The health of the culture was determined by a number of factors: general confluence of cells (approx. 4000 per slide), twitching innervated muscle, lack of bacterial infection observed, clear branching and growth of neurons, few undifferentiated cells, structure of cells consistent across multiple trials, an example of such a culture is demonstrated in Figure 2.3.2.

2.3.2 Drug treatment of Primary neuron culture for AFM and Immunohistochemical analysis

The culture media containing the appropriate concentrations of drug treatments was made. These were: DHPG 50µM, MPEP 50µM, AM-251 50µM, Control (DMSO) 50µM (1/1000), AEA 50µM and Control (soya emulsion) 50µM. The time point, 3 DIV was chosen for analysis, because dendrites had formed and muscle twitching was observed, indicating innervation (Yazejian, *et al.*, 2013). Before the addition of drug treatments, the cultures were assessed for their viability. The key factors for selection were healthy growth of axons and dendrites with lots of possible connections. As there were some muscle cells in this culture, twitching muscle cells were taken as a sign of healthy functioning cultures. And finally, general confluence of approx. 4000 cells per coverslip (13mm in diameter), too many cells made it hard to analyse, too few cells made it less likely to find dendritic spines, and for the cells to be communicating. Once selected, the media was changed for the one containing drug treatment by removing 90% of old media and replacing with media containing drug treatment, making sure not to expose the cells to air liquid interface, and left to incubate for 20 minutes. After incubation the media was removed and replaced with fixing agent, 5% glutaraldehyde in NFR, for 10 minutes. The glutaraldehyde was removed, and the cells were washed three times in NFR, and they were stored in NFR at 4^{o}C for future assessment with AFM (methods chapter 2.4 and

results chapters 4), then immunohistochemical staining (methods chapter 2.5 and results chapter 5).

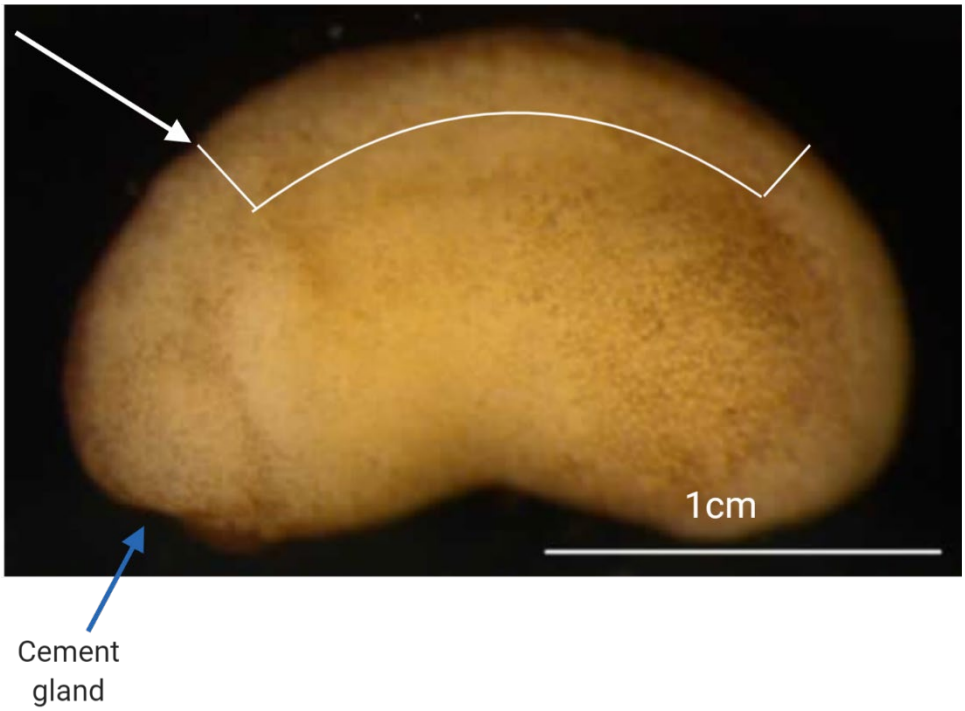

Figure 2.3.1*-Stage 24 embryo out of membrane shell. To remove spinal column, make incisions with thin wire at white arrows, then pick along curved white line until removed. Cement gland is an indented pigmented section on the head.*

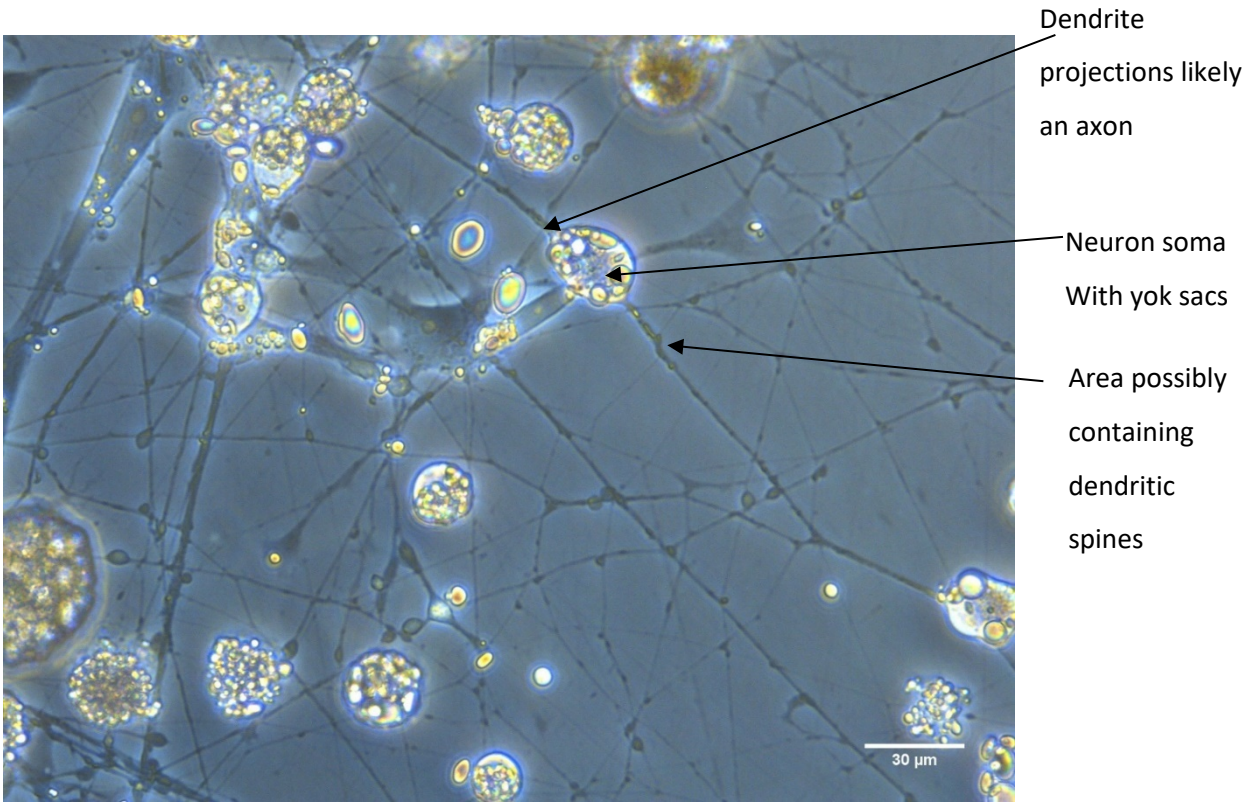

Figure 2.3.2*- Example image of X. laevis primary culture of stage 22-24 embryos. Image taken 3 DIV at 100x magnification with phase contrast microscope. The image demonstrates a good example of the neurons scanned with AFM. Axons are determined due to their thickness, straightness and lack of branching. Dendritic tree is identified by thinner projections with higher degree of branching. These areas were scanned for the possible detection of dendritic spines.*

2.4 Atomic force microscopy method

The AFM creates graphical heat maps representing the topography of a scanned area. As described in the introduction, a laser targeted to the back of a cantilever measures minute changes in surface topography as the tip scans across the surface. In AC mode the cantilever is oscillated at a set amplitude through the air, and the centre of the wave is maintained at a set-point distance from the surface. The tip interacts with the sample being scanned through Van der Waals forces and nuclear forces. As the tip approaches the sample it travels through a period of attraction, which accelerates the tip, then repulsion when it nears the sample as two atoms cannot "touch". Changes in the drive amplitude and set point change the speed with which the cantilever moves, and during set-up these factors are changed to ensure optimum oscillation for the cantilever. The resonance frequency of the cantilever is set by the tuning program, but the set-point can be changed dependent on the sample, to improve the image quality. The topographical scans give various channels. The two channels used in this study were the height channel, from which the 4 measurements of dimension were calculated, and the phase image which measures the tip-sample interaction and feeds into the loss tangent equation. Using the loss tangent equation, the phase image data can be normalised to a unitless ratio for comparison between samples.

The AFM will be used to scan for the presence of dendritic spines in the primary neuron culture set up in section 2.3.1. When possible dendritic spines were found, a measurement criteria was established (sections 2.4.3 & 2.4.4,) and the cultures treated in section 2.3.2 were scanned to investigate the effect of group 1 mGluRs and CB1 on dendritic spine plasticity. AFM gives nanoscopic scale measurements of dendritic spines. Given the recent development of combining high speed AFM with inverted fluorescent confocal microscopy (Shibata *et al.*, 2015), it is imperative an assessment criteria is developed so that this new technology can be utilised. This method does not use long-tip high speed AFM but the principles in measurement can be transferred.

2.4.1 Atomic Force Microscope Set up

The AFM head and cantilever were set up as explained in JPK user manual (JPK (2012) Nanowizard 3 user manual). Figure 2.4.1 shows the AFM head on the inverted microscope stage. The AFM head is movable and can be removed from the stage to fit cantilevers and put the sample on the stage. All the scans were performed in AC mode. Key set up points to get right are shown in Figure 2.4.2 and 2.4.3. The cantilever used was an aluminium reflex coated AC mode cantilever (Nanoworld technologies Non-contact / Tapping™ mode - Long Cantilever -

Reflex coating), with a resonance frequency of 190kHz, force constant 48N/m, length 225µm, mean width 38µm and thickness 7µm. The tip is shaped like a polygon-based pyramid with a typical height of 10 - 15 µm. Additionally, this probe has a typical tip radius of curvature of less than 8nm.

While the AFM head is off the microscope, the slide is prepared by dipping the culture coated coverslip in distilled water then leaving to air dry on a glass slide for 20 minutes. Once completely dry the slide was placed on the microscope stage. Distilled water was used because the sample was stored in NFR, when left to air-dry large salt crystals formed on the slide. The sample also deteriorated faster probably again due to salt crystal damage. The AFM head was carefully placed onto the stage, checking the sample is centred and under the cantilever, then the cantilever is tuned.

2.4.2 Cantilever tuning

Firstly, the laser screws were adjusted (shown in Figure 2.4.1) on the AFM head so that the laser is in the centre, or as close to 0.00 vertical deflection by 0.00 lateral deflection as possible (Figure 2.4.3). Then, in the cantilever-tuning window, the infinity symbol is selected to keep the tuning running. The initial window looked like Figure 2.4.3. The peak in Figure 2.4.3 is enhanced and if it looked like Figure 2.4.3c the phase and amplitude are in tune. If not, and it looked like Figure 2.4.3d, then the phase shift is changed by a range of -180 to 180 degrees until the crossover of lock-in phase (blue line) and lock-in amplitude (red line) look as they do in figure 2.4.3c. This is a process of trial and error. Once the crossover was at the correct point the cantilever was tuned to near its resonant frequency (the red amplitude peak). As shown in Figure 2.4.3c, the point selected is just below the peak resonant frequency. The horizontal line represents the set-point (distance the cantilever will be maintained from sample i.e. range of amplitude) and the vertical line represents oscillating frequency (kHz). Phase shift (blue line) is the result of the difference between the drive and the response. In the tuning stage this is caused by the tip/cantilever, so it is tuned to a specific point. When scanning the sample, further phase shift is caused by the sample and this is measured in the phase channel as degrees of phase shift.

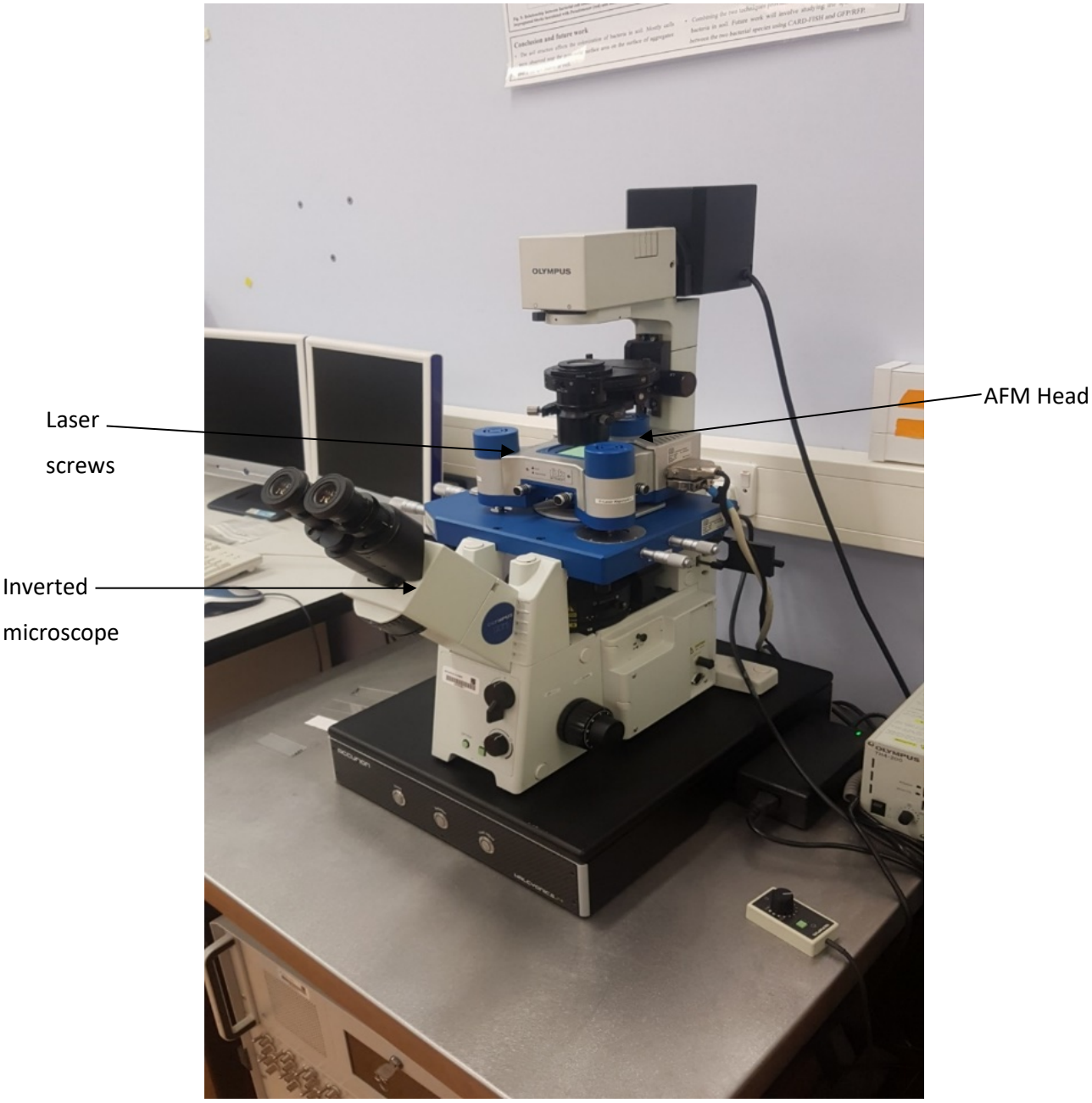

Figure 2.4.1*- Atomic Force Microscope setup. AFM head sits on top of inverted microscope stage and connects to computer where it is controlled, and output is recorded*

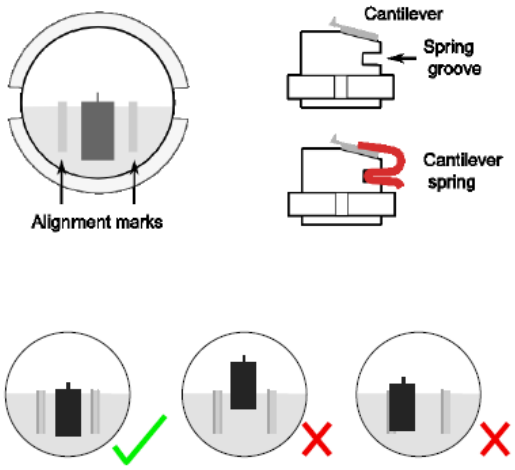

Figure 2.4.2*- Schematic demonstrating how to put the cantilever onto the glass block.*

a)

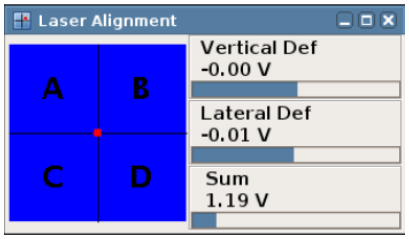

b)

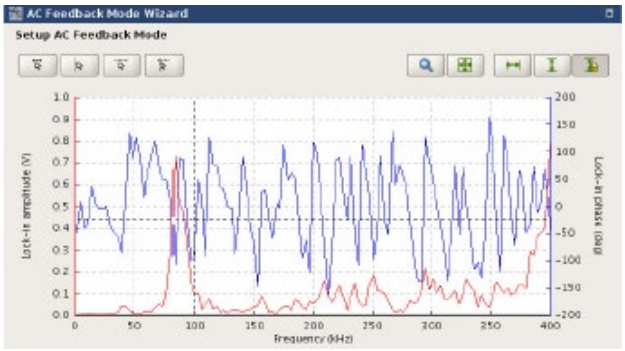

c)

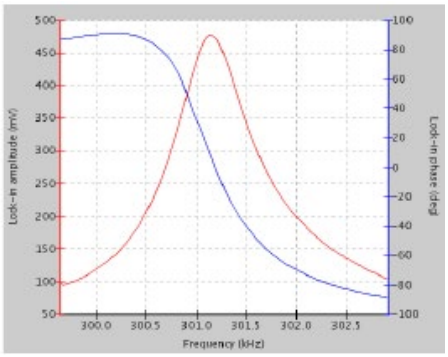

d)

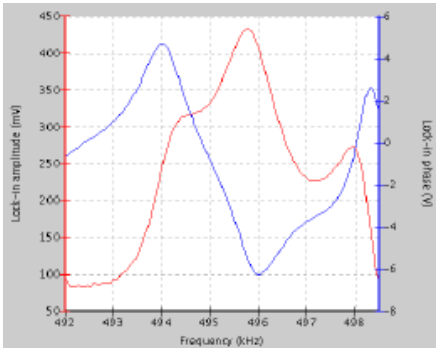

Figure 2.4.3*- Tuning the cantilever. A) laser alignment window. Laser screws are adjusted on the AFM head which move the laser in the lateral or vertical direction. B) in automatic cantilever tuning selection, the program will find the peak resonance. The red peak is enhanced to achieve (c) C) perfect lock-in phase (blue line) crossing peak amplitude resonance (red line). The vertical line represents frequency cantilever will oscillate at (x-axis) and horizontal line (thin arrow) represents the set point (left y-axis). (Phase shift degree are show on right y-axis) D) example of bad tuning*

2.4.3 Identification and scanning of dendrites

Using the inverted microscope, the sample was assessed for suitable areas which contained projections identified as dendrites, with the possibility of dendritic spines (such as demonstrated in Figure 2.3.2). The areas identified were usually between groups of neurons, where axons and dendrites meet. Some cell bodies were scanned successfully with one image appearing to show a developing dendritic tree. However, the large size of cell bodies made results irregular, due to large noise infarctions in the images. This may be due to the tip either falling too far from a cell body or getting stuck on the way back up. As shown in Figure 2.4.5, once an area was identified an exploratory 50µm x 50µm scan was performed and assessed for possible dendritic spines based on size (under 15µM in diameter), location (was it part of the dendritic tree or an axon, axons were much thicker and straighter and don't have dendritic spines, but occasionally have budding growth cones, these were larger and smoother than dendritic spines). Using the zoom and rescan function an area of the image containing dendritic spine-like structures were selected and rescanned (Figure 2.4.5a). In this example this produced a 9µm x 9µm scan (Figure 2.4.5b). An area was selected for rescan and this gave a more detailed 3.5µm x 3.5µm image (Figure 2.4.5c). All scans were performed at 0.5Hz. The set point changed occasionally when retuned but was kept at a range of 0.55V-0.65V, with an average of 0.635V. The drive amplitude was set automatically during tuning giving quite a large range 0.159V-0.837V, with an average of 0.379V. Some of the 'noisy' lines in the image were due to AFM settings in the feedback loop which move the cantilever slightly too fast. This setting was adjusted, and the dendritic spine rescanned (image shown in Figure 2.4.4). It would be desirable to eliminate all 'noise' from the images; however, this was simply not possible for two reasons. Firstly, the uneven and unexpected nature of the cell culture is difficult for the AFM to cope with. As discussed in the introduction during AC mode AFM the feedback loop reacts to the strength of Van der Waals forces (amongst others) during its downward motion. At peak point where attraction turns to repulsion the tip rebounds. This means the tip should never truly contact the sample. The problem with large uneven surfaces, however, comes from the need to maintain the cantilevers movement at the optimum amplitude, speed and set point. Secondly, as mentioned Van der Waals forces play a big role in AC mode AFM so the deeper the water layer on the surface of the sample the greater the disturbance to the tip motion. Although the cells were dry the membrane likely accumulated more moisture than would normally be expected from air precipitation. The increased water also increases capillary action and can wet the tip, which renders it unusable.

2.4.4 AFM height image analysis

All image analysis was performed using Gwyddion software. Using Gwyddion the line profile function was selected, and four cross sections of the dendritic spine were taken (Figure 2.4.5d). The cross-section lines were set to 50 pixels wide to encompass as much of the dendritic membrane as possible. Figure 2.4.5c and 2.4.5e show the output generated from this analysis method. Figure 2.4.5c shows all four line profiles compared on a graph. Figure 2.4.5e is the statistics window opened from the graph in figure 2.4.5c. From the output in Figure 2.4.5e, we recorded the: projected length, area under the curve, Ra and RMS (two measurements of roughness) and height was calculated by subtracting the minimum from maximum height of cross section. Once these figures were recorded for each line profile, the four values for each category were averaged and analysed using linear mixed model.

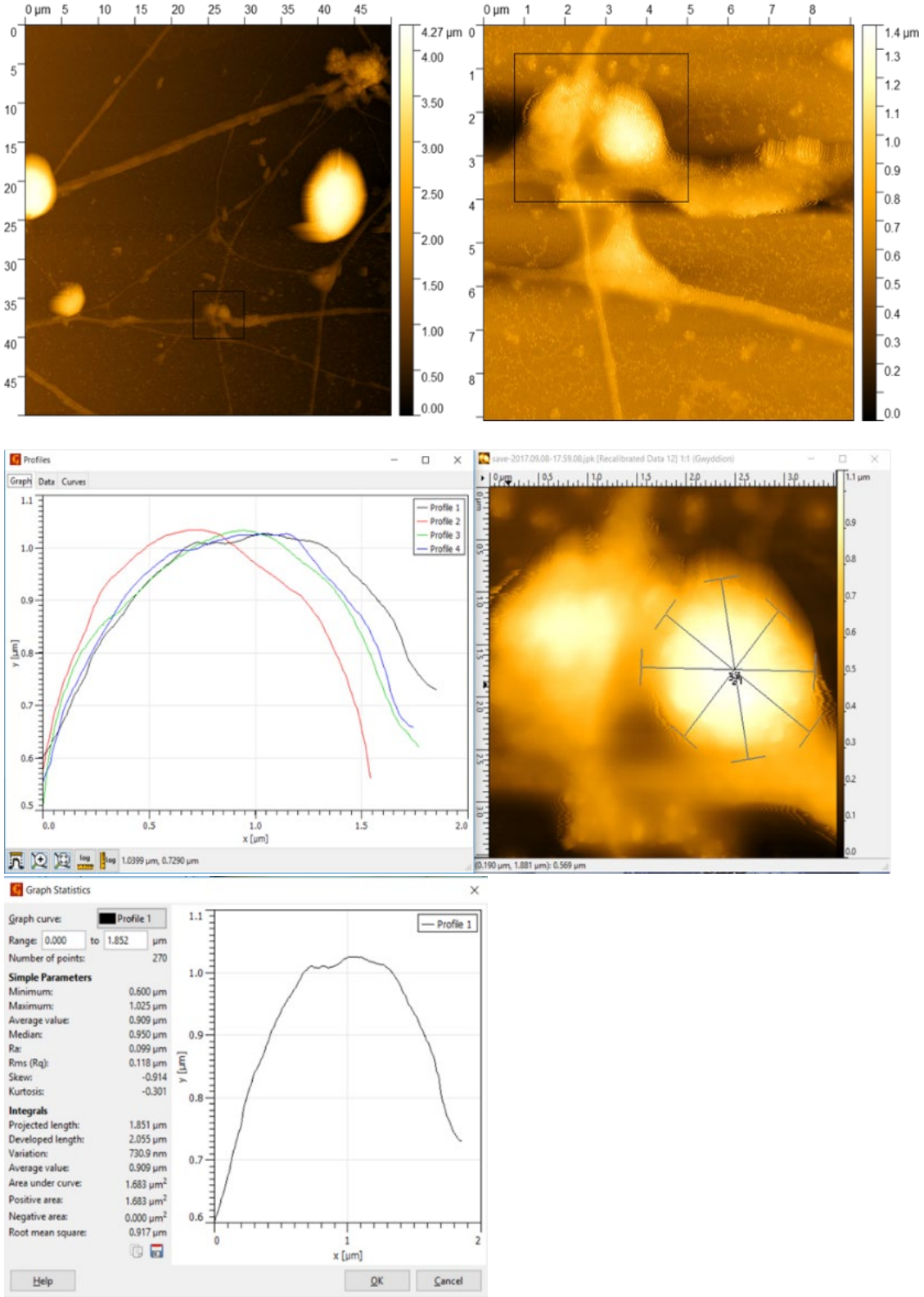

Figure 2.4.4*-Identification and analysis of possible dendrites. A) 50µm x 50µm exploratory scan, b) 9µm x9 µm rescan of possible dendrite, d) 3µm x 3µm scan of dendrite possibly a synapse with cross section analysis lines on dendrite. C) Cross section line graph output in Gwyddion. E) Line profile of 1 cross sectional line and corresponding statistical output*

2.4.5 *Los tangent imaging*

In an ideal scenario we could have the precision of contact mode, the lack of damage caused by AC mode and the force measurements of force spectroscopy. Using AC mode there have been developments in quantifying the tip-sample interaction by combining the amplitude data with the lock-in phase data to produce the loss tangent (Proksch *et al.*, 2016). The Phase shift image has long been an image of frustration. It gives a great deal of detail, yet, is specific to that image, making it difficult to use for anything other than individual qualitative image analysis. Loss tangent imaging takes the phase shift and quantifies it into a unitless ratio. The drive amplitude in AC mode determines the force the tip will interact with the surface and the phase image give details of the tip-sample interaction. These results are combined in the below equation, explained in (Proksch *et al.*, 2016).

$$\tan\delta = \frac{\langle F_{ts}\cdot\dot{z}\rangle}{\omega\langle F_{ts}\cdot z\rangle} = \frac{\dfrac{\omega}{\omega_{\text{free}}}\dfrac{V}{V_{\text{free}}} - \sin\phi}{Q\dfrac{V}{V_{\text{free}}}\left(1-\dfrac{\omega^2}{\omega_{\text{free}}^2}\right) - \cos\phi} = \frac{\Omega\alpha - \sin\phi}{Q\alpha(1-\Omega^2)-\cos\phi}. \quad (1)$$

In this expression, Fts is the tip-sample interaction force, z is the tip motion, ż is the tip velocity, ω is the angular frequency at which the cantilever is driven, Q is the quality factor of the resonance, V is the cantilever amplitude, the brackets ‹› represent a time average and *tan δ* represents the loss tangent. The parameter V_{free} is the "free" resonant amplitude of the first mode, measured at a reference position.

If we assume the cantilever operates at free resonant frequency (i.e. V/V_{free} =1 and Ω=1) then the equation simplifies to:

$$\tan\delta \approx \frac{\sin\phi - \alpha}{\cos\phi}. \quad (2)$$

Equation 2 can be viewed as an uncalibrated loss tangent calculation.

For our calculations of loss tangent, equation 2 was used with V/Vfree=1. This was because of large irregularities in the V/Vfree calculation leading to anomalous results.
Unlike previous publications (Proksch *et al.*, 2016), the software capable of producing loss tangent images was not available to us. This was also a factor in using the uncalibrated equation 2. We decided to take average measurements of the phase images, collecting data for the average phase-shift of the dendritic spine membrane and compare this with the average phase shift of the dendritic tree membrane (as shown in figure 2.4.6).

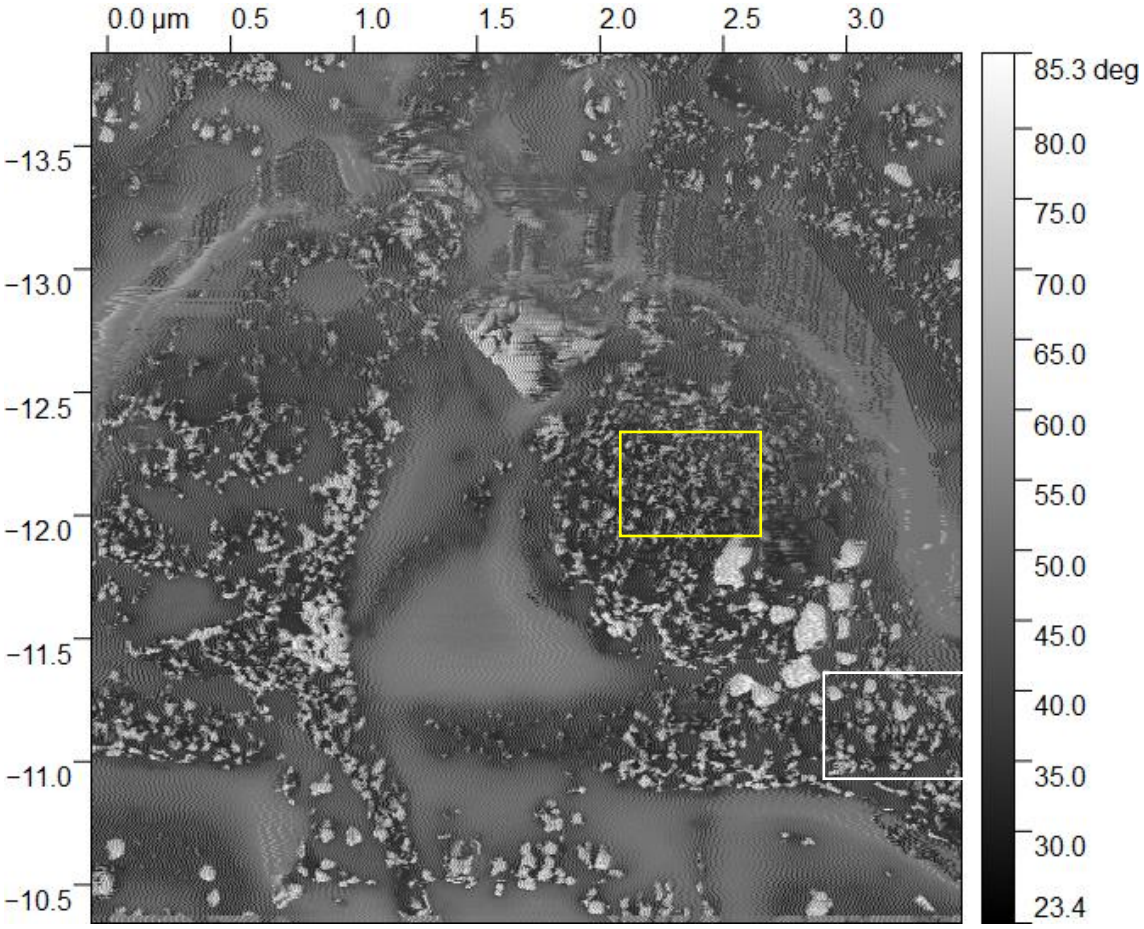

Figure 2.4.5*- Example of phase image analysis for loss tangent calculation. Yellow box indicates area of dendritic spine membrane sampled for analysis. White box indicates area of dendritic tree membrane sampled for analysis*

2.4.6 Study design and Statistical analysis

The design of this experiment was to scan 5 dendritic spines per slide treated with DHPG 50µM, MPEP 50µM, AM-251 50µM and AEA 50µM and compare these with vehicle control DMSO or soya emulsion. Due to time and financial constraints, two slides per treatment were scanned, meaning 6-11 different dendritic spines were scanned per treatment group, after the criteria for identifying dendritic spines was applied.

The statistical analysis method used was a linear mixed model carried out in SPSS. This was chosen because there is some variability between samples as the cantilever is lifted and retuned. The assumptions for this model are normality of residuals, independence of residuals and linearity of the predicted vs residuals (presented in the appendix section 7.3). The test for normality used was Shapiro-Wilk at significance level of 0.05. Almost all analyses carried out passed this test for normality of residuals, though it is recognised some did not, the LMM is sufficiently robust test to withstand some deviation from the assumption of normality. However, the assumption of linearity of residualsvs predicted value was questionable in some groups. This is most likely due to the small group size and large variation. More sampling would be required to see if this is a continued problem or just due to the small sample size. The independence of residuals was satisfied consistently across all treatment groups.

2.5 Immunohistochemistry

2.5.1 Method

The sample (culture slide, microtome section or whole tadpole) was removed from the fridge and allowed to come to room temperature. 0.1% Triton X was applied to sample for 10 minutes to permeabilise some of the cell membrane and allow diffusion of antibodies. After this, the sample was washed thoroughly with NFR. The excess sites were blocked with 5% BSA for 10 minutes, then the sample was washed in NFR. The primary antibody Anti PSD-95 (purchased from Abcam: ab18258) (1:1000) was added to the sample and left to incubate for 1 hour at room temperature. The sample was washed in NFR, then secondary antibody (Goat Anti-Rabbit IgG H&L (Alexa Fluor® 488 purchased from AbCam) (ab150077) (1:1000)) was added to the sample (carried out in reduced light to stop fluorophore damage). This was left to incubate for one hour at room temperature. The sample was washed with NFR, then imaged under a Lecia fluorescent microscope. The excitation wavelength for the fluorophore of 488 emits at 522 (red light). Controls were carried out to determine background fluorescence and unspecific binding. The two control groups were primary antibody only added to sample and secondary antibody only added to sample for one hour at room temperature and washed three times in NFR then assessed under microscope.

2.5.2 Fluorescence intensity calculation

The fluorescence intensity was calculated using Image J. The measurements set were: integrated density, mean grey value and area. An area of interest was selected and measured, then an area of darkness/relatively low fluorescence nearby is selected and measured. To calculate fluorescence intensity this equation was used:
corrected total cell fluorescence=Integrated density- (area selected x mean grey value of background readings). For whole tadpoles the spinal column was selected although this included many muscles (Figure 2.5.2). For microtome sections, only the spinal cord was selected (Figure 2.5.2). For cell culture areas that appeared to have high levels of neurite projections and neuron bodies were analysed. In many instances it was difficult to assess dendrites due to high background fluorescence with only cell bodies visible, so the neuron cell body was selected (figure 2.5.2).

Figure 2.5.1*- Lecia DMR fluorescent microscope. The Lecia DMR has 4 channels through which it excites a range of wavelengths. The excitation wavelength of the 4 channels are 1- 350-380nm 2-380-420nm, 3-420-450nm, 4- 450-500nm.*

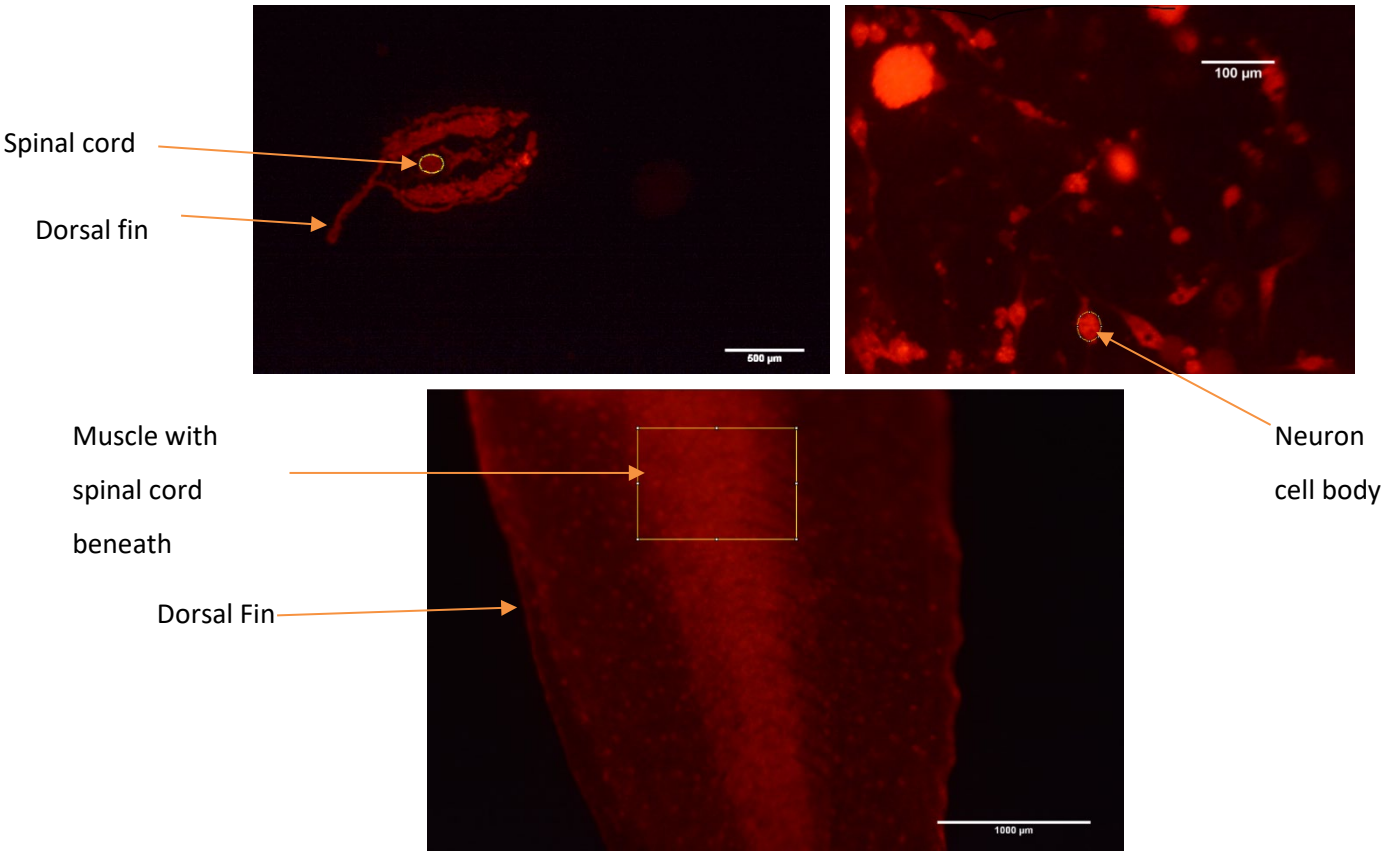

Figure 2.5.2*-Demonstration of the areas selected for fluorescence measurement top left- microtome slice 10µm thick cross section of tadpole tail, top right- primary neuron culture, bottom whole tadpole tail stage 40-42.*

3 Investigating the effect of CB1 and group 1 mGluRs on the central pattern generator regulation of *Xenopus laevis* swim-cycle speed

3.1 Introduction

Central pattern generators (CPG) are a common neural network that regulates rhythmic motor patterns such as: walking, mastication and respiration. Understanding their function and the receptors which populate them will aid recovery from injury and may have implication for other neurological disease. It is imperative that simple animal models, such as the *X. laevis* hatchling tadpole, are fully characterised and modes of assessment are cheap and simple. The *X. laevis* tadpole, until stage 45, is non self-feeding and has two simple behaviours: swimming in response to either touch to the skin/shadow detection by pineal eye, and struggling when held (Roberts, Li and Soffe, 2010). If left unstimulated the tadpole will rarely move simply growing from internal food stores. The spinal network of the *X. laevis* has been well documented and extensively investigated in fictive swimming electrophysiological measurements (Li, Roberts and Soffe, 2009; Roberts, Li and Soffe, 2010; Li and Moult, 2012). In this investigation we aim to assess the whole tadpole swimming behaviour, measuring the locomotor output using high speed video.

The swimming motion of the *X. laevis* tadpole is governed by a CPG. In the *X. laevis* hatchling tadpole, stage 28-44, the CPG regulates the left-right alternation of tail muscle contraction, as explained in the introduction. Briefly, rohon-beard sensory neurons are excited after skin stimulation. These neurons stimulate dorsolateral- commissural interneurons, which cause muscle contraction via motoneurons, while also stimulating excitatory electrically coupled descending interneurons (dINs). One half centre of the dIN population will excite motoneurons, ascending interneurons (aIN) and commissural interneurons (cINs) near simultaneously. The cINs inhibit the opposing sides dINs with a hyperpolarising current, the dINs on the opposing side then fire on rebound (Figure 1.8.2) (Li, Roberts and Soffe, 2009, 2010; Roberts, Li and Soffe, 2010; Li and Moult, 2012; Moult, Cottrell and Li, 2013). The frequency of alternation between the left and right is determined by the interplay between the size and speed of the hyperpolarising current received by the dINs (Li and Moult, 2012), and the underlying NMDAR pacemaker and gap junction excitation of dINs (Li, Roberts and Soffe, 2009, 2010). However, it is not possible for the tadpole to continue swimming without the hyperpolarising current of cINs (Moult, Cottrell and Li, 2013).

The two main neuronal signalling systems regulating this behaviour are: excitatory glutamate signalling and inhibitory glycine signalling. The group 1 mGluRs are postsynaptic GPCRs of the G_q type, and their activation via glutamate enacts second messenger signalling systems. The second messengers activated are PLC, PKC, IP3/DAG lipase, and adenylyl cyclase. The effect of this is increased calcium release from the endoplasmic reticulum enhancing depolarisation, CAMKII action, transcription of survival genes via NFkappaB, and the outcomes are survival and growth. In the short term the increased calcium/CAMKII enhances the potential for dendritic spine potentiation. However, $mGluR_{1/5}$ are also key players in the long-term depression of synapses, though this mainly happens in an NMDAR-independent manner. (Ito, Sakurai and Tongroach, 1982). Through PLC activation of DAG lipase, DAG is modified to the CB1 agonist 2-AG, which through retrograde action can inhibit future neurotransmission from the presynaptic terminal (DSI/E) via CB1.

The group 1 mGluRs have been investigated in the fictive swimming electrophysiological recordings of *X. laevis,* providing evidence for their intrinsic value in modulation of the CPG output (Chapman and Sillar, 2007; Chapman, Issberner and Sillar, 2008). It was shown in these experiments that $mGluR_1$ and $mGluR_5$ activation via DHPG increased locomotor frequency. Evidence was provided in these experiments that part of this increase was due to the reduction in the mid-cycle inhibition, regulated by glycinergic neurotransmission (the cINs) (Chapman, Issberner and Sillar, 2008). Work on fictive swimming of lamprey spinal CPG network provided similar evidence. First, it was shown that group 1 mGluRs enhanced locomotor frequency and were necessary in normal maintenance of frequency (El Manira *et al.*, 2002). Then evidence was provided that $mGluR_1$ and $mGluR_5$ performed different roles in maintenance of frequency (Kettunen, Hess and Manira, 2003) with $mGluR_1$ involved in mediating excitatory depolarisation. From these experiments, similar results and observations were drawn to the work in *X. laevis,* that the increase in frequency attributed to Group 1 mGluRs was in part, because of reduced inhibitory release during the mid-cycle (cIN hyperpolarisation of dIN). The same group performed a series of experiments defining the possible involvement of endocannabinoid signalling in the $mGluR_{1/5}$ mediated increase in locomotor output. In these experiments it was observed that, during fictive swimming electrophysiological recording, activation of $mGluR_1$ on postsynaptic motor neurons caused production of endocannabinoids and subsequent activation of the presynaptic CB1, suppressing the release of inhibitory neurotransmitters (Kettunen *et al.*, 2005; Kyriakatos and El Manira, 2007) (For review see El Manira and Kyriakatos, 2010). During normal swimming, glutamate activation of $mGluR_{1/5}$ causes short and long-term depression of the mid-cycle

inhibitory interneurons and causes long-term potentiation of the on-cycle motor neurons driving locomotion. This was confirmed by addition of DHPG ($mGluR_{1/5}$ agonist). It was found that inhibition with AM-251 (CB1 antagonist) had almost the opposite effect. It increased the effect of mid-cycle inhibitory neurons and decreased the on-cycle depolarisation. In normal swimming this would reduce the frequency of locomotor output. This provided strong evidence for the glutamate/endocannabinoid mediated long-term potentiation of excitatory synapses, and long-term depression of inhibitory interneurons, to enhance CPG mediated locomotion (El Manira *et al.*, 2002, 2008; Kyriakatos and El Manira, 2007; El Manira and Kyriakatos, 2010).

On review of this literature we set out to assess the frequency of left-right alternation in the swim-cycles of *X. laevis in vivo,* between stages 37-42, using high speed video analysis. Once we had established a reproducible assessment of swim-cycle frequency, we sought to confirm the effect of the group 1 mGluRs on the *X. laevis* tadpole's swimming behaviour in response to touch. The role of CB1 in the maintenance of swimming frequency has not been confirmed in *X. laevis* tadpole stage 37-42, so we then sought to investigate if this receptor was involved in *X. laevis* swim-cycle frequency. If there was a measurable effect of these receptors, we wanted to investigate if, like lamprey, the CB1 receptor and the group 1 mGluRs interact in the modulation of frequency and have intrinsic value in maintenance of locomotion frequency in whole tadpole swimming behaviour.

Due to the nature of bath application and reports of cannabinoid receptors present in motoneurons (Newman *et al.*, 2007; Sánchez-Pastor *et al.*, 2007) and muscle mitochondrial CB1 receptors (Mendizabal-Zubiaga *et al.*, 2016), the treatment groups were assessed for changes in the angle of flexion observed when measuring the frequency of swim-cycles. Still images were taken at 3 points of flexion during swimming, the angle was measured in Image J, and an average for each tadpole timepoint produced (as described in methods chapter 2.14). In isolated lamprey spinal cord it was reported that cannabinoid involvement in group 1 mGluR increases in frequency of swim-cycles, may have been cannabinoids produced from motoneuron dendritic spines, that inhibit cIN neurotransmitter release (Kettunen *et al.*, 2005; Kyriakatos and El Manira, 2007). If this is the case group 1 mGluR and/or CB1 agonism/antagonism may affect motoneuron output and thus the flexion of the muscle columns or simply effect the muscles themselves. However, it was also hypothesised that there is an optimum flexion: frequency ratio for efficient swimming. A fast swim-cycle with large flexion would by reason produce the fastest swim (i.e. shorter time to cover the same

distance). Similarly, however, there would be a point where a larger flexion might slow the CPG output or be due to reduced CPG swim-cycle frequency allowing larger tail flexions.

This method will be an accessible tool for future investigation into CPGs, and understanding how these two receptor systems influence the excitation: inhibition balance that underlies the output of the CPG has ramifications for many neurological systems, such as the hippocampus.

3.2 Method

As described in chapter 2.1, the receptors involvement in the swimming behaviour was assessed by 20-minute bath application of the agonist/antagonist, then 5 measurements, 2 minutes apart. The tadpole was stimulated to swim by touch to the tail and the swimming episode was recorded at 400 fps. The time taken for 1 swim-cycle was calculated by counting the frames for three consecutive sim-cycles, between the third and tenth cycle, and taking the mean (1 swim-cycle demonstrated in methods Figure 2.1.1). The flexion of the tail during swimming was measured to examine if there were effects on the motoneuron-muscle output by taking images of 3 flexions achieved during the measurement of frequency. The angles were measured in Image J and averages calculated for each tadpole timepoint. We hypothesised that changes in muscle contraction, without changes in flexion, or vice versa, would mean that the drug treatments are affecting either CPG or motoneuron/muscle contraction output independently. If both were affected, the effect at muscles may feedback to the CPG, indirectly affecting frequency of swim-cycles (Song *et al.*, 2015), or changes in CPG output affect the flexion of the tail during swimming. Before the treatment groups were analysed, the frequency and AOF was assessed for correlation. All control tadpoles, stage 40-42, showed there was no correlation between frequency and angle of flexion, this was concurred in stage 37-39. To assess if treatments influenced the angle of flexion the results were analysed in a linear mixed model with time point as a covariate and tadpole as a random factor. Time point had no effect in any treatment groups as a covariate. Increases in angle size indicate reduced maximum flexion, decreases in angle size are evidence of larger maximum flexions.

All treatments were compared with their respective vehicle control using a linear mixed model. Treatment was a fixed factor with timepoint as a covariate and tadpole was a random factor. Timepoint had no significant interactions with swim-cycle frequency in any of the treatment groups assessed.

3.3 Results -Group 1 mGluR activation increases the frequency of swim-cycles of stage 40-42 *Xenopus laevis* tadpoles

The group 1 metabotropic glutamate receptor agonist DHPG (50µM 10 minutes), significantly increased the frequency of swim-cycles (8.45±1.37%; Figure 3.3.1, Table 7.1.1). DHPG activates both sub-types of the group 1 mGluRs, $mGluR_1$ and $mGluR_5$, so it was investigated if either of the subtypes had any more value than the other in the maintenance of normal frequency of swim-cycles. Inhibition of $mGluR_1$ with LY367385 (50µM, 20 minutes) produced a significant decrease in frequency, with a change of -18.3±2.02% (Table 7.1.1, Figure 3.3.1), whereas inhibition of $mGluR_5$ with MPEP (50µM, 20 minutes) showed no significant change (-2.03±1.65% Table 7.1.1 Figure 3.3.1). When both subtypes were antagonised together (LY-367385 50µM + MPEP 50µM, 20 minutes) a significant decrease was observed, although it was only marginally larger than the decrease observed with just $mGluR_1$ inhibition, with a percentage change to EMM of -19.72± 1.959% (Figure 3.3.1, Table 7.1.1). It was investigated if both subtypes were fully antagonised by adding DHPG after the receptors were antagonised (LY365387 50µM + MPEP 50 µM (20 minutes) followed by DHPG 50 µM (10 minutes)). The decrease was still large and significant compared with DMSO control (-14.83±2.06% Figure 3.3.1 Table 7.1.1). Although it was 4.89% higher than without DHPG addition the result still confirms a high percentage of antagonism. We then investigated whether the selective inhibition of $mGluR_1$ and the addition of DHPG, effectively enhancing the activation of $mGluR_5$, would affect the frequency of swim-cycles. LY367385 50µM, (20 minutes) + DHPG 50 µM (10 minutes) caused no significant change (1.992±1.65% Figure 3.3.1). Next, the inhibition of $mGluR_5$ and addition of DHPG (MPEP 50µM 20 minutes followed by DHPG 50µM 10 minutes) was tested giving a significant decrease in frequency of swimming (-13.03 ±3.035%, Figure 3.3.1, Table 7.1.1).

All treatments were compared pairwise in a linear mixed model with timepoint as a covariate. Timepoint had no significant effect on the frequency of swim-cycles. DHPG 50µM was significantly different to all other treatments. MPEP 50µM was significantly different from; MPEP 50µM +DHPG 50µM, LY367385 50µM, LY367385 50µM + MPEP 50µM and LY367385 50µM + MPEP 50µM + DHPG 50µM. MPEP 50µM + DHPG 50µM was significantly different from all other treatments except LY367385 50µM + MPEP 50µM + DHPG 50µM. LY367385 50µM was significantly different from all treatments except LY367385 50µM + MPEP 50µM and LY367385 50µM + MPEP 50µM + DHPG 50µM. LY367385 50µM + DHPG 50µM was significantly different from LY367385 50µM + MPEP 50µM, LY367385 50µM +MPEP 50µM +DHPG 50µM. LY367385 50µM + MPEP 50µM was not significantly different from LY367385

50µM + MPEP 50µM + DHPG 50µM (Table 7.1.1, Figure 3.3.1). Since a group size of 5 tadpoles with replicates at 5 timepoints is a small sample size, a power analysis was performed using GLIMPSE program. The $mGluR_{1/5}$ groups were sufficiently powered (power=1.00, sample size=5).

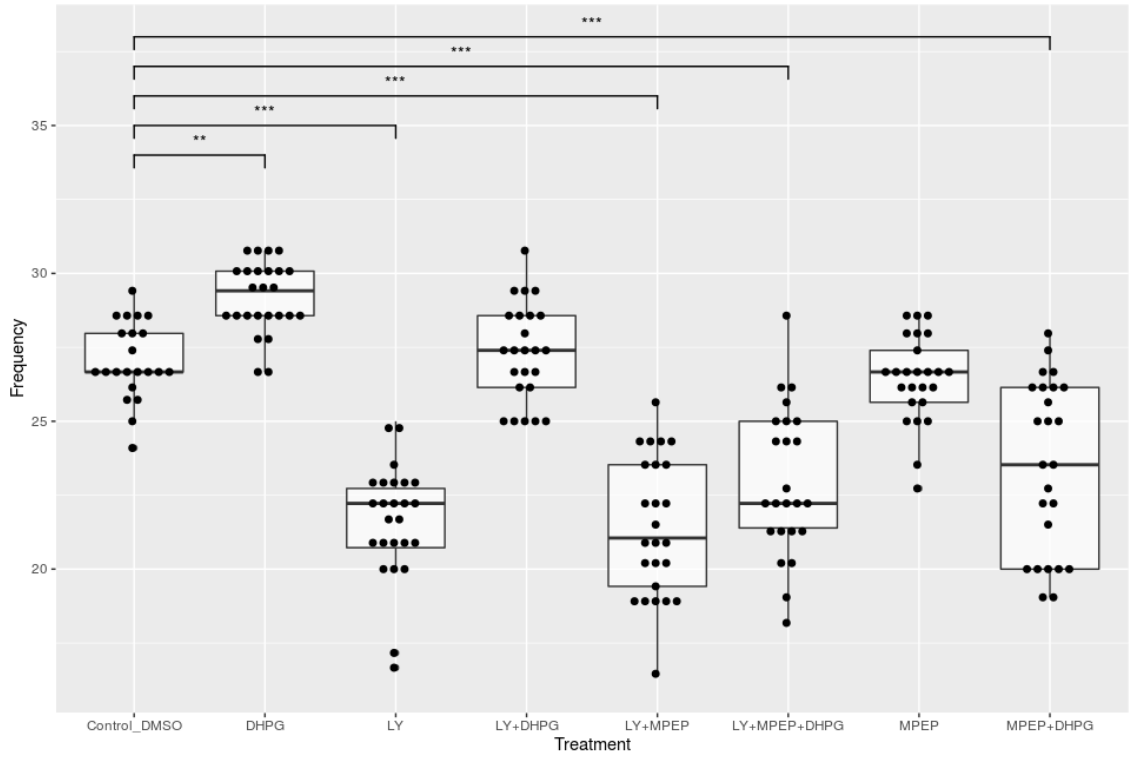

Figure 3.3.1*- The effect of group 1 metabotropic glutamate receptor activation (DHPG) or inhibition (LY367385 mGluR$_1$ antagonist, MPEP mGluR$_5$ antagonist) on the frequency of swim-cycle of the stage 40-42 X. laevis tadpole swimming behaviour. All treatments compared treatment with vehicle control (DMSO). Significance indicated by asterisk. (*=p<0.05, **=p<0.005, ***=p<0.001). n=5 tadpoles with 5 replicates over 10 minutes per tadpole*

3.4 CB1 receptor inhibition effects group 1 mGluR induced increase in frequency

We began by first inhibiting the CB1 receptor with AM-251 (10µM, 20 minutes). This produced a significant decrease in frequency of swimming (-9.47±1.56, Figure 3.4.1, Table 7.1.2). This was a slightly larger decrease than the increase seen in DHPG (8.45±1.37%), yet not so large a decrease as complete group 1 mGluR inhibition (-19.72±1.96%). Next, it was assessed if DHPG (50µM, 10 minutes) applied after CB1 antagonism (AM-251 10µM, 20 minutes) would still increase frequency. There was no significant change in frequency compared with control (-2.05±2.54 Figure 3.4.1, Table 7.1.2). The antagonism of all 3 receptors, $mGluR_1$, $mGluR_5$ and CB1 (Am-251 10 µM + LY367385 50µM + MPEP 50µM, 20 minutes) significantly decreased swim-cycle frequency, compared with control DMSO (-6.24±3.22% Figure 3.4.1, Table 7.1.2). The inhibition of $mGluR_1$ and CB1 (AM-251 10 µM + LY367385 50µM 20 minutes) was not a significant decrease (-3.58 ±3.09%, Figure 3.4.1., Table 7.1.2). When $mGluR_5$ and CB1 were antagonised (AM-251 10µM + MPEP 50µM, 20 minutes) the decrease was significant (-8.28±2.36%, Figure 3.4.1, Table 7.1.2). All treatments were compared pairwise in post-hoc analysis in the LMM. No other treatments were significantly different from each other (Table 7.1.2, Figure 3.4.1). Since a group size of 5 tadpoles with replicates at 5 timepoints per treatment is a small sample size, a power analysis was performed using GLIMPSE program. The CB1 antagonism with $mGluR_{1/5}$ groups were sufficiently powered (power=1.00, sample size=5).

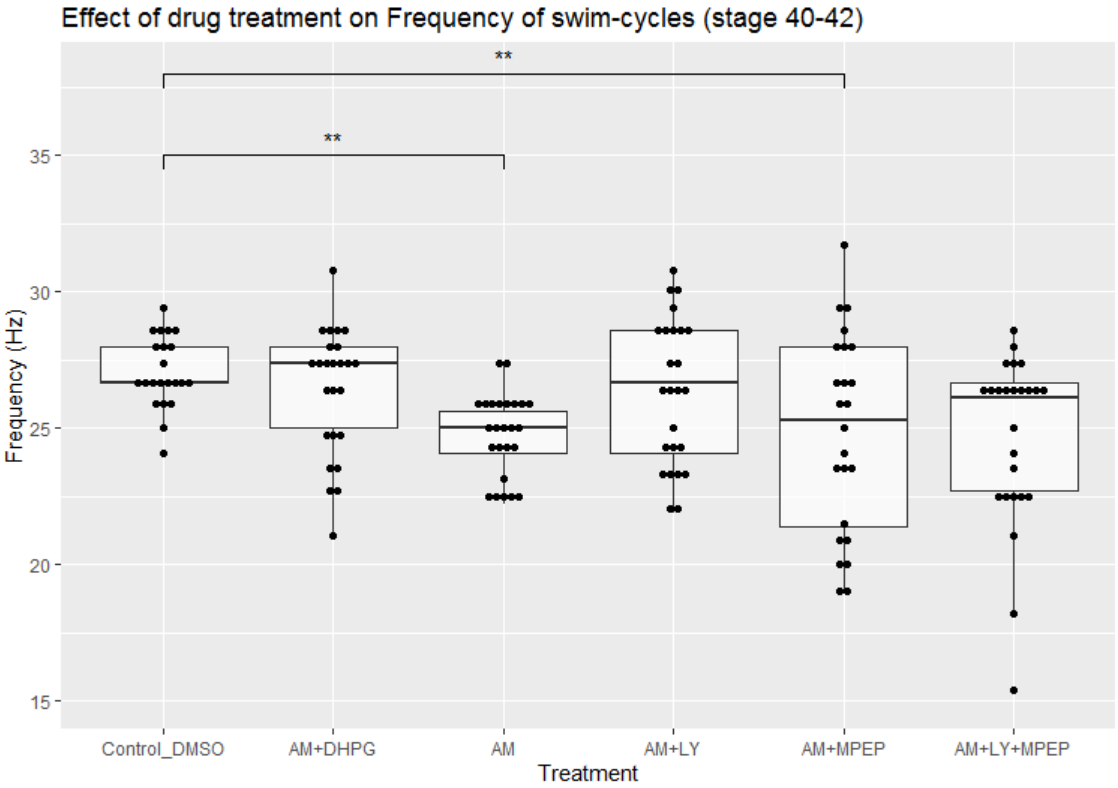

Figure 3.4.1*- The effect of CB1 antagonism with mGluR$_{1/5}$ antagonism or before mGluR$_{1/5}$ activation on the frequency of swim-cycles in the stage 40-42 X. laevis tadpole. All treatments compared treatment with vehicle control (DMSO). Significance indicated by asterisk. (*=p<0.05, **=p<0.005, ***=p<0.001). n=5 tadpoles with 5 replicates over 10 minutes per tadpole*

3.5 The endocannabinoid system contributes to the maintenance of frequency of swimming

As shown previously the CB1 receptor antagonist (AM-251 10µM, 20 minutes) significantly decreases frequency of swim-cycles in stage 40-42 *X. laevis* tadpoles. It is unclear from the results if this is related to group 1 mGluR activity or if it is affecting the regulation of neuron firing frequency separately. What is clear, it has a role in the maintenance of normal swimming frequency. Previous studies reported functional CB1 receptors at stage 41 and the presence of CB1 mRNA from stage 26 (Cottone *et al.*, 2003; Beatrice *et al.*, 2006) After our result with 10µM AM-251 (20 minutes) the experiment was repeated with a range of concentrations (0.1µM, 2µM, 10µM, 50µM), with both the endogenous agonist AEA and synthetic antagonist AM-251. This was done at two different stages of development: 40-42 and stage 37-39, as it was noticed in preliminary studies that the frequency of swimming becomes faster during development between stages 37-39 and 40-42. Also based on Beatrice et al (2006) the expression of CB1 will be different between the two age groups. Age was assessed as a covariate and it has a significant effect on frequency of swim-cycles ($F(1,396.139)=582.44$, $p=0.000$). We then assessed if age interacted with Treatment (treatment*age). This was a significant interaction ($F(15,192.860)=17.962$, $p<0.001$).

Table 3.5.1*- Results of linear mixed model analysis of increasing concentration of AM-251 on the frequency of swim-cycles in X. laevis tadpole at stage 40-42*

Comparison of AM-251 with control (DMSO) Stage 40-42	Mixed Model Result	Normality of Residuals	Independence of Residuals	Linearity of residuals v observed
0.1µM	F (1,8.055) =0.042; p=0.843	W (46) =0.969; p=0.258	Satisfied	Satisfied
2µM	F (1,11.869) =10.742; p=0.007	W (52) =0.962; p=0.098	Questionable	Satisfied
10µM	F (1,14.776) =39.172; p<0.001	W (48) =0.947; p=0.029	Satisfied	Satisfied
50µM	F (1,15.396) =21.828; p<0.001	W (89) =0.971; p=0.047	Questionable	Satisfied
AM-251 50µM + AEA 50µM	F (1,24.567) =51.792; p<0.001	W (65) =0.976; p=0.226	Satisfied	Satisfied

Starting with stages 40-42, the low dose antagonist (AM-251 0.1µM, 20 minutes) caused no significant change (0.83±2.83%). AM-251 2µM (20 minutes) caused a significant increase in frequency of swim-cycles (12.14±2.9%). AM-251 10µM (20 minutes) caused a significant decrease (-20.15± 3.15 %,). The maximum concentration, AM-251 50µM (20 minutes) had a significant decrease (-9.52±1.38%, Figure 3.5.1, Table 3.5.1).

***Table 3.5.2**- Results of linear mixed model analysis of increasing concentration of AM-251 on the frequency of swimming in X. laevis tadpole at stage 37-39*

Comparison of AM-251 with control (DMSO) stage 37-39	Mixed Model Result	Normality of Residuals	Independence of Residuals	Linearity of Predicted value vs observe d
0.1µM	F (1,11.491) =23.207; p<0.001	W (45) =0.974; p=0.387	Satisfied	Satisfied
2µM	F (1,16.468) =0.479; p=0.499	W (47) =0.988; p=0.921	Questionable	Satisfied
10µM	F (1,8.153) =6.497; p=0.029	W (48) =0.979; p=0.528	Satisfied	Satisfied
50µM	F (1,6.944) =32.263; p=0.001	W (44) =0.973; p=0.399	Questionable	Satisfied

As mentioned, the CB1 receptor was reported at stage 41 with mRNA reported at stage 26 so we explored the same concentrations at a younger age group (stage 37-39) to examine if the effects are the same. The overall trend was similar displaying a biphasic effect; however, the effect was not comparable between concentrations and age group. To begin with there was a significant decrease in frequency with 0.1µM AM-251 (20 minutes) (-11.04±1.63%, Table 3.5.2, Figure 3.5.1). AM-251 (2 µM, 20 minutes, and stage 37-39) had no significant change (2.47±2.66%) and in complete contrast to the stage 40-42 tadpoles AM-251 10µM increased frequency by 7.51±2.03% (Table 3.5.2). A significant decrease was observed with AM-251 50µM (-31.68±4.24%, Figure 3.5.2, Table 3.5.2).

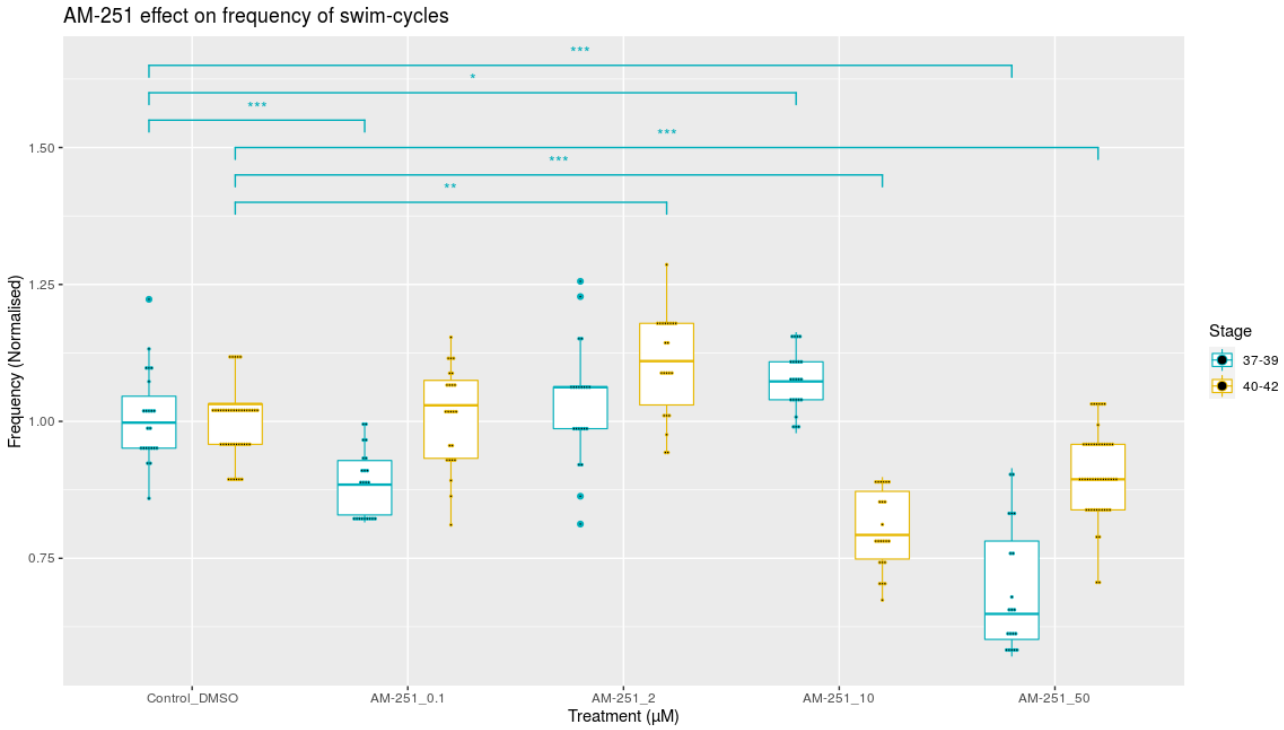

Figure 3.5.1*- The effect of CB1 receptor antagonist AM-251 on frequency of swim-cycles of the X. laevis tadpole in vivo. Frequency normalised to respective vehicle control mean. All treatments compared with vehicle control (DMSO) respective to concentration of vehicle used in treatment. Control shown is vehicle control for 50µM. Significance indicated by asterisk. (*=p<0.05, **=p<0.005, ***=p<0.001).n=5 tadpoles with 5 replicates over 10 minutes per tadpole*

Based on the work in isolated lamprey, that showed 5µM of synthetic CB1 agonist WIN-55 increased frequency of swimming by reducing mid-cycle inhibition (Kettunen *et al.*, 2005; Kyriakatos and El Manira, 2007), agonism of the CB1 receptor, with endogenous ligand AEA, was explored with increasing concentrations at both age groups (stage 40-42 and 37-39). In the stage 40-42 age group, the results illustrate that low dose AEA (0.1µM, 20 minutes) significantly decreased frequency of swim-cycles (-13.66±1.42%, Table 3.5.3, Figure 3.5.2). AEA 2µM (20 minutes), was also a significant decrease (-11.75±1.76%). AEA (10µM, 20 minutes) was a significant decrease (-12.11±2.72%, Table 3.5.3, Figure 3.5.2). However, 50µM showed no significant change (0.122±2.849%).

Table 3.5.3*- Results of linear mixed model analysis of increasing concentration of AEA on the frequency of swimming in X. laevis tadpole tails at stage 40-42*

Comparison of AEA with control (Soya) stage 40-42	Mixed Model Result	Normality of Residuals	Independence of Residuals	Linearity of residuals v observed
0.1µM	F (1,11.092) =154.163; p<0.001	W (45) =0.955; p=0.079	Satisfied	Satisfied
2µM	F (1,8.342) =19.466; p=0.002	W (51) =0.975; p=0.361	Questionable	Satisfied
10µM	F (1,20.77) =10.751; p=0.004	W (58) =0.985; p=0.683	Questionable	Satisfied
50µM	F (1,19.173) =0.905; p=0.353	W (77) =0.992; p=0.916	Satisfied	Satisfied

This trend was similar in the younger stage 37-39 age group. However, no concentration was significant compared with its respective vehicle control (Figure 3.5.2, Table 3.5.4).
Since a group size of 5 tadpoles, with replicates at 5 timepoints is a small sample size, a power analysis was performed using the GLIMPSE program. Each treatment was compared to its respective vehicle control. The sample size was 5 (5 tadpoles in treatment and 5 tadpoles in vehicle control). One significant result (AM-251 stage 37-39 10µM) was significant in the mixed model result but was slightly underpowered. The power analysis suggested 2 more tadpoles per group would have been a sufficient power for analysis (data presented in appendix tables 7.3.1-7.3.4).

Table 3.5.4 *- Results of linear mixed model analysis of increasing concentration of AEA on the frequency of swimming in X. laevis tadpole at stage 37-39*

Comparison of AEA with control (Soya) stage 37-39	Mixed Model Result	Normality of Residuals	Independence of Residuals	Linearity of residuals v observed
0.1µM	F (1,7.34) =0.277; p=0.138	W (49) =0.96; p=0.099	Satisfied	Satisfied
2µM	F (1,9.731) =2.781; p=0.127	W (46) =0.967; p=0.22	Satisfied	Satisfied
10µM	F (1,7.988) =0.579; p=0.469	W (50) =0.948; p=0.029	Satisfied	Satisfied
50µM	F (1,9.019) =2.908; p=0.122	W (54) =0.958; p=0.059	Questionable	Satisfied

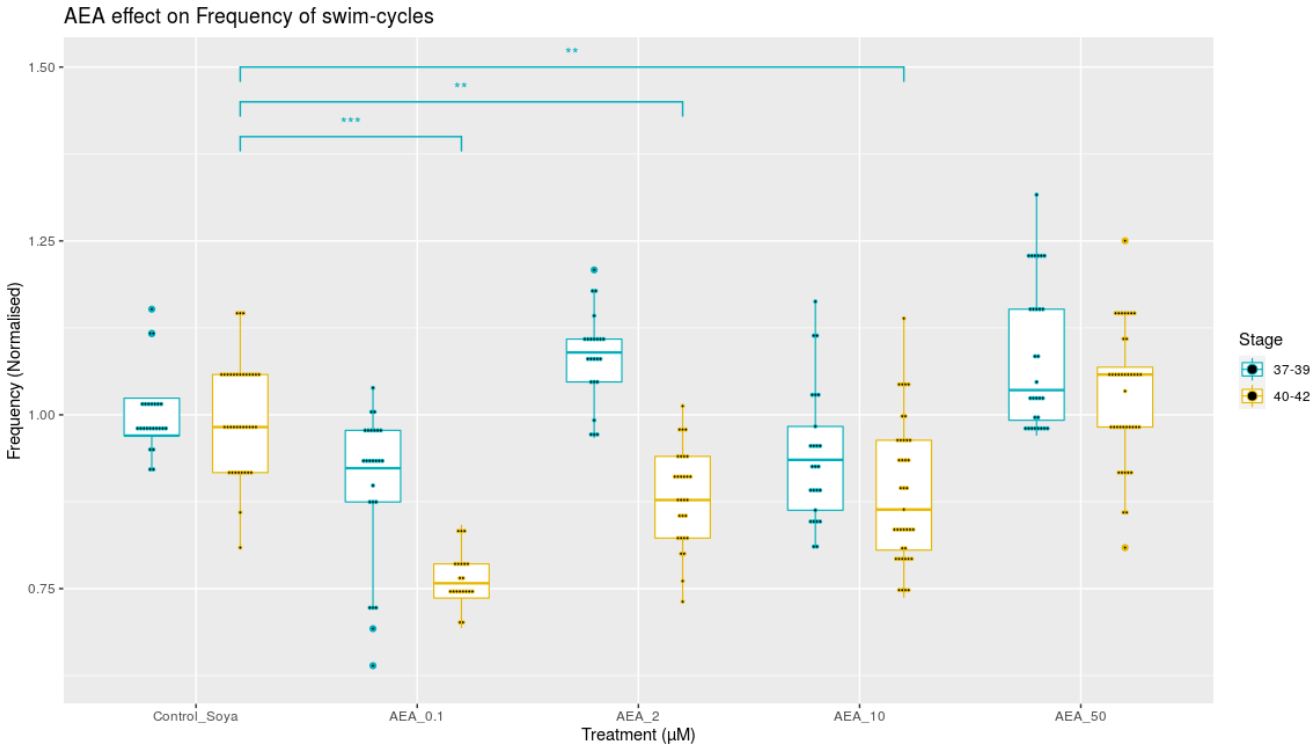

Figure 3.5.2*- The effect of CB1 receptor agonist AEA on frequency of swim-cycle of the X. laevis tadpole in vivo. Top) stage 40-42. Bottom) stage 37-39. Frequency normalised to respective vehicle control mean. All treatments compared with vehicle control (Soya) respective to concentration of vehicle. Control shown is vehicle control for 50µM. Significance indicated by asterisk. (*=p<0.05, **=p<0.005, ***=p<0.001).n=5 tadpoles with 5 replicates over 10 minutes per tadpole*

3.6 Assessment of the angle of tail flexion during swimming: a role for group 1 mGluRs and CB1 in maintenance of efficient muscle flexion during swimming

3.6.1 Group 1 mGluR effects on angle of tail flexion

As shown in Figure 3.6.1, MPEP 50µM (20 minutes) + DHPG 50µM (10 minutes) significantly increased angle size (12.35±2.11%, Figure 3.6.1, Table 7.2.1), as did MPEP 50µM + LY367385 50µM (20 minutes) + DHPG 50µM (10 minutes) (12.35±2.4%, Figure 3.6.1, Table 7.2.1). Treatment with MPEP (50µM, 20 minutes) caused a significant increase in angle size, though not as large a change from control (8.84±2.22%, Figure 3.6.1, Table 7.2.1) as MPEP + DHPG. There were no other significant changes observed in flexion angle with $mGluR_1$ inhibition or group 1 mGluR activation compared with control (Table 7.2.1, Figure 3.6.1). When the treatments were compared pairwise, DHPG was significantly different from LY367385 + MPEP + DHPG. MPEP 50µM was significantly different to LY367385 50µM. MPEP 50µM + DHPG 50µM was significantly different from DHPG 50µM and LY367385 50µM. LY367385 50µM was significantly different form LY367385 50µM + MPEP 50µM + DHPG 50µM (Table 7.2.1). Timepoint was not a significant effect on angle size. Since a group size of 5 tadpole with replicates at 5 timepoints is a small sample size a power analysis was performed using GLIMPSE program. The $mGluR_{1/5}$ groups were sufficiently powered (power=1.00 sample size=5).

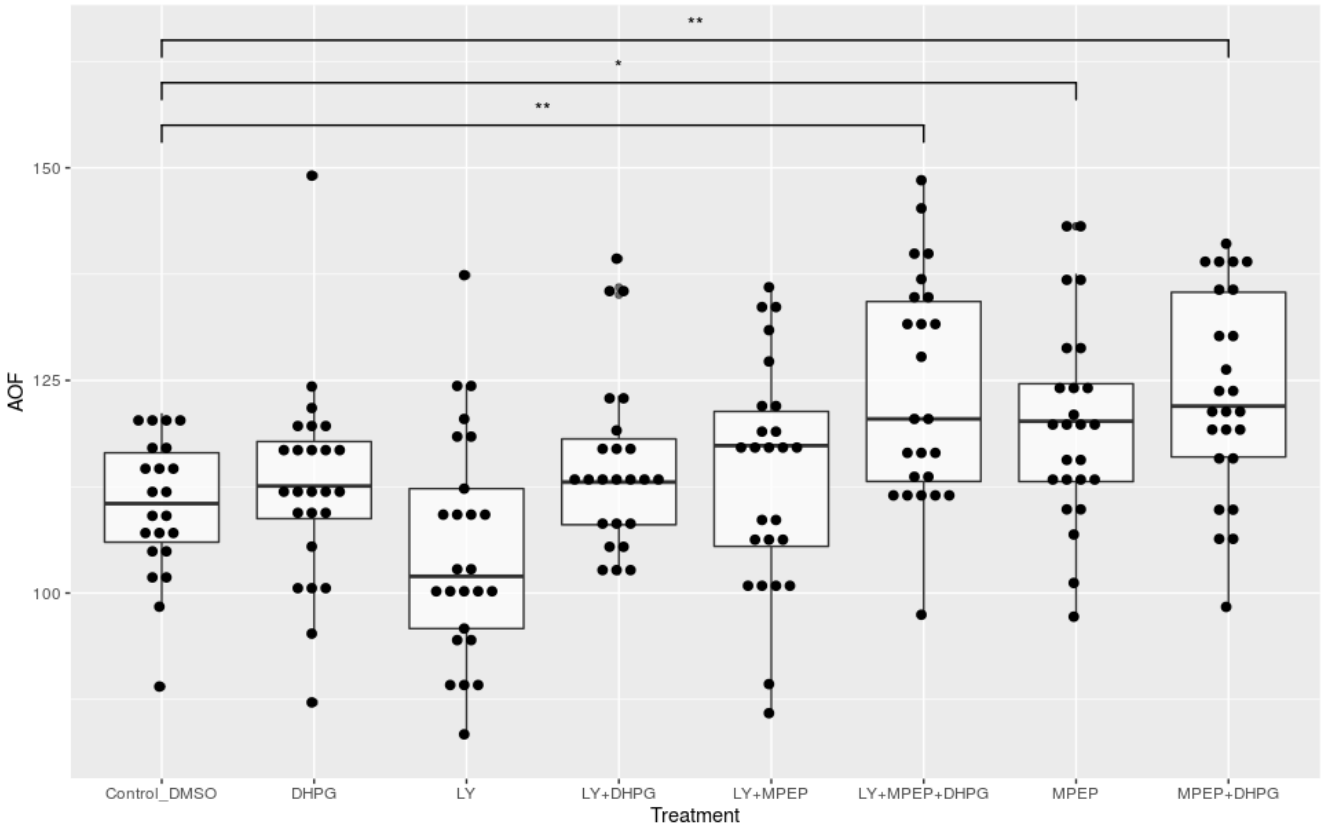

Figure 3.6.1*- The effect of mGluR$_{1/5}$ agonism and antagonism on the angle of flexion of the stage 40-42 X. laevis tadpole swimming behaviour in vivo. All groups compared to vehicle control (DMSO). Significance compared with vehicle control indicated by asterisk. (*=p<0.05, **=p<0.005, ***=p<0.001) n=5*

3.6.2 Gp1 mGluRs interact with CB1 in the maintenance of normal tail flexion

When antagonism of group 1 mGluRs was repeated with CB1 inhibition, a significant reduction in tail flexion was observed with $mGluR_5$ + CB1 antagonism (MPEP 50µM + AM-251 10µM, 20 minutes) (17.51±1.87%, Table7.2.2 Figure 3.6.2). AM-251 10µM (20 minutes), showed no significant change in flexion angle. $MGluR_1$ and CB1 inhibition (LY367385 50µM + AM-251 10µM, 20 minutes) significantly increased the size of flexion angle (12.17±1.66, Figure 3.6.2, Table 7.2.2), and complete inhibition of all three receptors (MPEP 50µM + LY367385 50 µM + AM-251 10µM, 20 minutes) significantly increased the size of flexion angle (8.21±1.66%, Table 7.2.2, Figure 3.6.2). When the treatments were compared with each other in a pairwise comparison, AM-251 + MPEP was significant against all other treatment except AM-251 + LY367385. And AM-251 + LY367385 was significant against all other treatments except AM-251 + LY + MPEP.

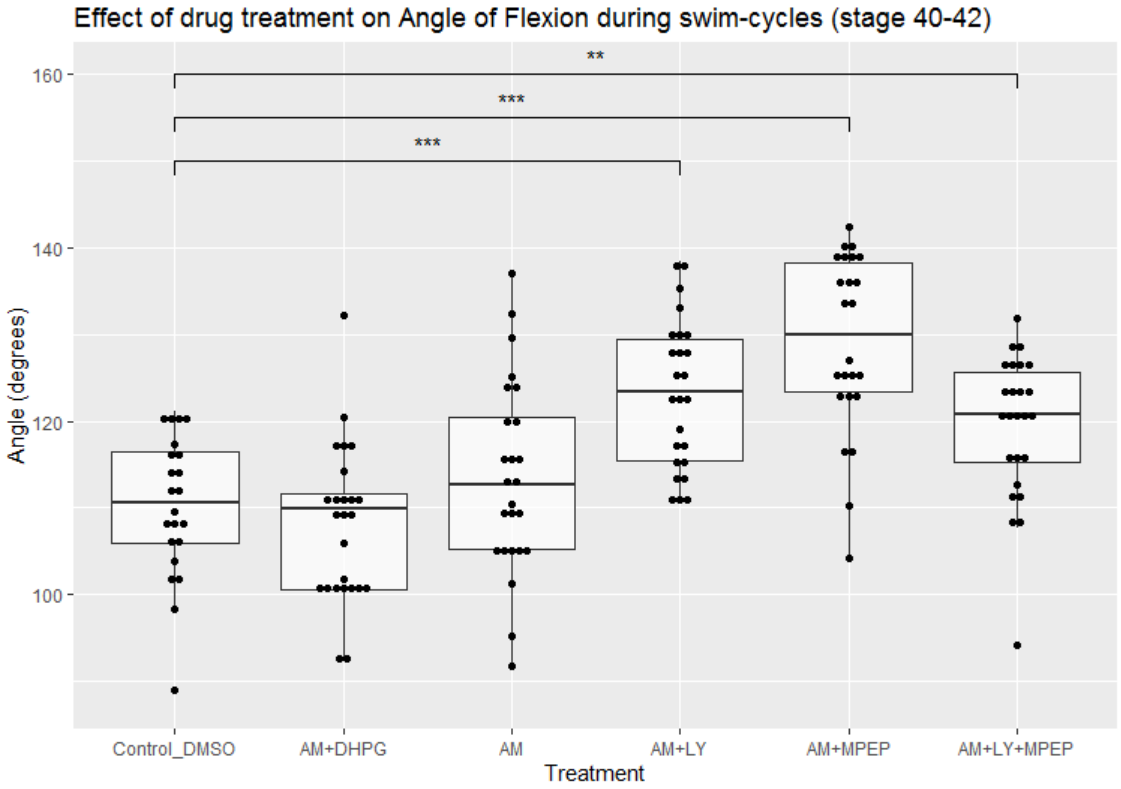

Figure 3.6.2*-The effect of CB1 inhibition before mGluR$_{1/5}$ activation/inhibition on the angle of flexion of the stage 40-42 X. laevis tadpole swimming behaviour in vivo. All treatments compared to vehicle control (DMSO), Significance indicated by asterisk. (*=p<0.05, **=p<0.005, ***=p<0.001) n=5 tadpoles with 5 replicates over 10 minutes*

3.6.3 CB1 effects on tail flexion

***Table 3.6.1**- Results of LMM analysis of AM-251 concentration on angle of flexion of stage 40-42 tadpoles*

Comparison of AM-251 with control (DMSO) Stage 40-42	Mixed Model Result	Normality of Residuals	Independence of Residuals	Linearity of residuals v Predicted value
0.1µM	F(1,38.39)=1.06; p=0.31	W(45)=0.985; p=0.809	Satisfied	Satisfied
2µM	F(1,17.155)=2.784; p=0.113	W(52)=0.987; p=0.838	Satisfied	Satisfied
10µM	F(1,13.089)=1.467; p=0.247	W(48)=0.972; p=0.314	Satisfied	Satisfied
50µM	F(1,29.812)=1.194; p=0.283	W(89)=0.988; p=0.608	Satisfied	Satisfied
AM-251 + AEA	F(1,21.907)=6.914; p=0.015	W(65)0.986; p=0.648	Satisfied	Satisfied

The interesting interaction, of CB1 antagonism with group 1 mGluR antagonism on the angle of flexion, suggests some role for CB1 in this effect. As such, increasing concentrations of CB1 agonist AEA and antagonist/inverse agonist AM-251, were assessed for changes in the angle of flexion. The effect of CB1 antagonism with AM-251, on angle of flexion, was not significant at any concentration in stage 40-42 tadpoles (Table 3.6.3, Figure 3.6.3). This was not the case for stage 37-39, where AM-251 2µM (20 minutes) significantly increased angle of flexion (13.31±2.21%, Table 3.6.4, Figure 3.6.3). This opposed the result for AM-251 50µM (20 minutes, stage 37-39) which significantly decreased size of angle of flexion (-9.73±3.15%, Table 3.6.4).

***Table 3.6.4**- results of linear mixed model analysis of AM-251 concentration on angle of flexion in stage 37-39 tadpoles*

Comparison of AM-251 with control (DMSO) stage 37-39	Mixed Model Result	Normality of Residuals	Independence of Residuals	Linearity of Predicted value vs observe red
0.1µM	F(1,17.75)=0.121; p=0.732	W(45)=0.974; p=0.388	Satisfied	Satisfied
2µM	F(1,15.096)=18.65; p=0.001	W(47)=0.98; p=0.573	Satisfied	Satisfied
10µM	F(1,46)=0.411; p=0.525	W(48)=0.986; p=0.848	Satisfied	Satisfied
50µM	F(1,18.277)=5.260; p=0.034	W(43)=0.983; p=0.77	Satisfied	Satisfied

The result with AM-251 50µM stage 37-39, is comparable with the endogenous CB1 agonist AEA 0.1µM stage 40-42, where the significant decrease in frequency is accompanied by a

significant decrease in angle of flexion (-9.66±1.74, Table 3.6.5, Figure 3.6.4). This is repeated in the treatment group AEA 10µM (stage 40-42), where the decrease in frequency is accompanied by a decrease in angle of flexion (-8.27±1.5%, Table 3.6.5, Figure 3.6.4). However, as with the two age groups treated with AM-251, this effect is not mirrored in the younger age group (stage 37-39) treated with increasing concentrations of AEA, where no concertation produced a change in angle of flexion (Table 3.6.5, Figure 3.6.4). Age was assessed as a covariate and has a significant effect on the angle of flexion of swim-cycles ($F(1,601.9)=5.457$, $p=0.02$). We then assessed if age interacted with Treatment (treatment*age). This was a significant interaction ($F(15,172.1)=4.01$, $p<0.001$).

***Table 3.6-5**- Results of linear mixed model analysis of AEA concentration on angle of flexion in stage 40-42 tadpoles*

Comparison of AEA with control (Soya) stage 40-42	Mixed Model Result	Normality of Residuals	Independence of Residuals	Linearity of residuals v Predicted value
0.1µM	$F(1,43)=16.994$; $p<0.001$	$W(45)=0.99$; $p=0.957$	Satisfied	Satisfied
2µM	$F(1,49)=4.2$; $p=0.046$	$W(51)=0.972$; $p=0.265$	Satisfied	Satisfied
10µM	$F(1,15.46)=9.749$; $p=0.007$	$W(58)=0.983$; $p=0.614$	Satisfied	Satisfied
50µM	$F(1,37.89)=0.000$; $p=0.984$	$W(77)=0.972$; $p=0.088$	Satisfied	Satisfied

***Table 3.6.6**- Results of linear mixed model analysis of AEA concentration on angle of flexion in stage 37-39 tadpoles*

Comparison of AEA with control (Soya) stage 37-39	Mixed Model Result	Normality of Residuals	Independence of Residuals	Linearity of residuals v Predicted value
0.1µM	$F(1,26.095)=0.553$; $p=0.464$	$W(49)=0.982$; $p=0.648$	Satisfied	Satisfied
2µM	$F(1,16.425)=0.916$; $p=0.352$	$W(46)=0.952$; $p=0.054$	Satisfied	Satisfied
10µM	$F(1,14.338)=0.72$; $p=0.41$	$W(50)=0.877$; $p=0.000$	Satisfied	Satisfied
50µM	$F(1,24.654)=0.375$; $p=0.546$	$W(54)=0.944$; $p=0.014$	Satisfied	Satisfied

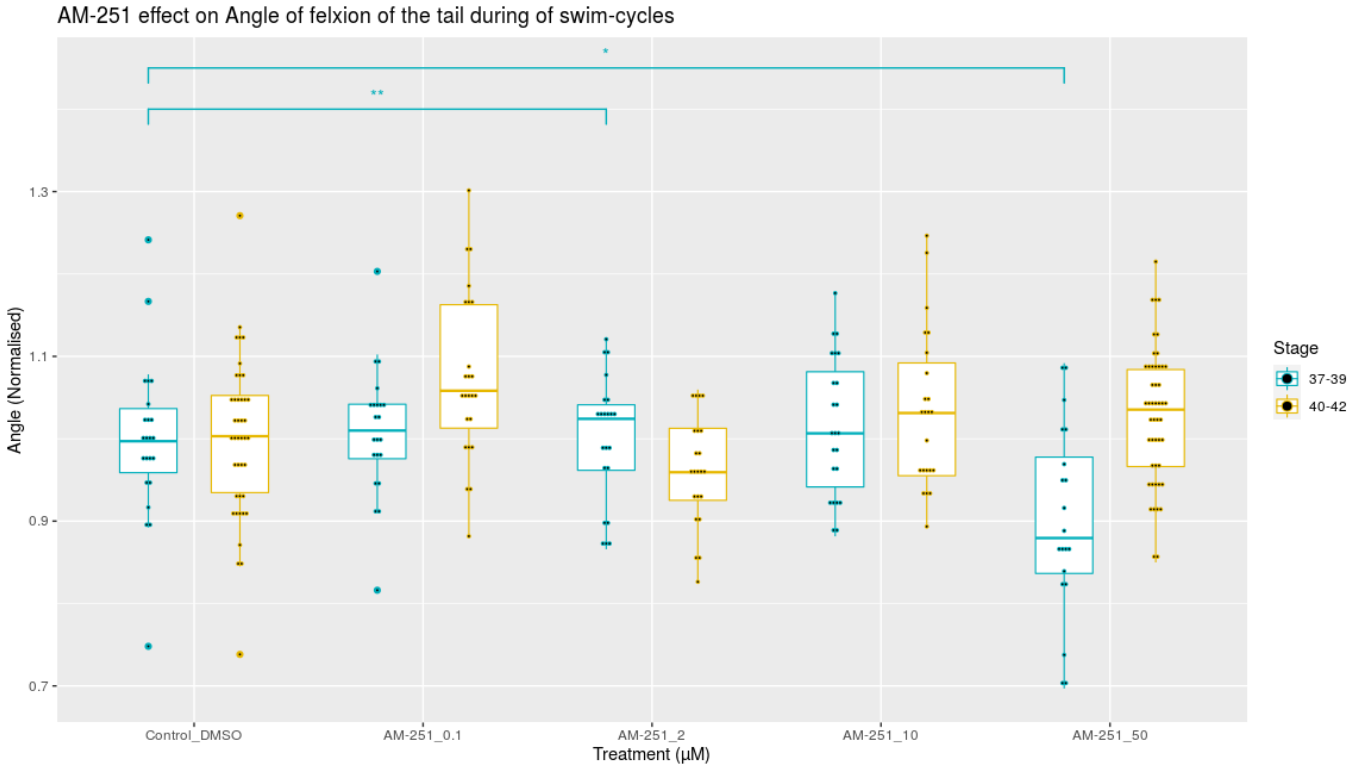

Figure 3.6.3*- The effect of CB1 receptor antagonist AM-251 on angle of flexion of the X. laevis tadpole in vivo. Angle normalised to respective vehicle control mean. All treatments compared with vehicle control (DMSO) respective to concentration of vehicle. Control shown is vehicle control for 50µM. Significance indicated by asterisk. (*=p<0.05, **=p<0.005, ***=p<0.001).n=5 tadpoles with 5 replicates over 10 minutes per tadpole*

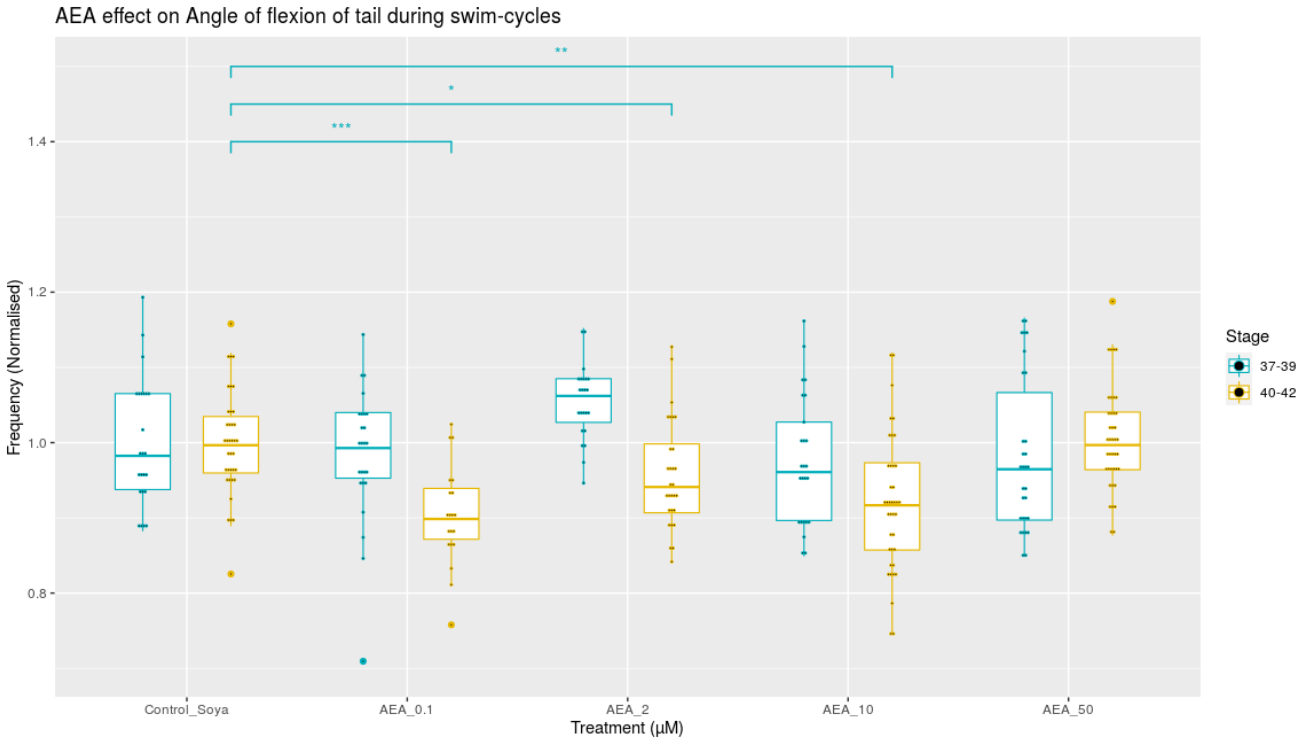

Figure 3.6.4*- CB1 receptor endogenous agonist AEA effects on angle of flexion of the X. laevis tadpole Frequency normalised to respective vehicle control mean. All treatments compared with vehicle control (Soya) respective to concentration of vehicle. Control shown is vehicle control for 50µM. Significance indicated by asterisk. (*=p<0.05, **=p<0.005, ***=p<0.001). n=5 tadpoles with 5 replicates over 10 minutes per tadpole*

3.7 Discussion

3.7.1 Group 1 metabotropic glutamate receptors effect frequency of swimming

Our results give the first whole tadpole evidence, that Group 1 mGluRs contribute to the maintenance of locomotor frequency in the *Xenopus laevis* tadpole. This concurs with previous fictive swimming electrophysiological experimentation of the immobilised *X. laevis* tadpole (Chapman and Sillar, 2007; Chapman, Issberner and Sillar, 2008) and lamprey (El Manira *et al.*, 2002; Kettunen *et al.*, 2005; Kyriakatos and El Manira, 2007; Nanou *et al.*, 2009). The group 1 mGluRs, activated by glutamate, can increase excitability of the network because of its g protein signalling. Once activated it increases intracellular calcium, inhibits inward rectifying K^+ currents and through activation of phospholipase Cβ (PLCβ) can produce the endocannabinoid 2-AG, which as described previously, acts as a retrograde messenger to inhibit future neurotransmitter release from inhibitory cINs in lamprey. With the evidence from previous literature demonstrating constitutive activity of cannabinoid receptors at inhibitory neurons (den Boon *et al.*, 2014), transporter proteins (Panlilio *et al.*, 2015) and intracellular regulatory proteins (Stauffer *et al.*, 2011; Guggenhuber *et al.*, 2016), the $mGluR_{1/5}$-CB1 interaction is most likely a very tightly controlled retrograde signalling mechanism used to potentiate excitatory signalling (Kyriakatos and El Manira, 2007) or protect from excessive excitatory signalling (Marsicano *et al.*, 2003; Stauffer *et al.*, 2011). Based on this information, group 1 mGluRs may increase excitability in PSDs through a 2-fold mechanism: the potentiation of NMDA receptors (Nanou *et al.*, 2009) and modulation of presynaptic inhibitory neurotransmitter release to enhance long and short-term potentiation of excitatory glutamate transmission (Kyriakatos and El Manira, 2007).

The experimentation with both antagonists of $mGluR_1$ (LY367385) + $mGluR_5$ (MPEP) showed a significant decrease which was not reversed via application of the agonist DHPG. This corroborated previous evidence that group 1 mGluRs are involved in the maintenance of normal swimming frequency in *X. laevis* (Chapman, Issberner and Sillar, 2008). One result, that is not in accordance with previous studies, was the inhibition of $mGluR_5$ via MPEP (50µM, 20 minutes) then addition of DHPH (50µM, 10 minutes). Previous results showed inhibition of $mGluR_5$ via MPEP increased frequency in isolated lamprey spinal cord (El Manira *et al.*, 2002). However, we observed no change with just MPEP application and a decrease in frequency after the addition of DHPG. This may indicate over-excitation of $mGluR_1$ reduces the locomotor output. The experimental setup used in the investigations in lamprey may lead to excessive activation of NMDAR and $mGluR_1$, due to the baseline frequency set by NMDA application (Kettunen, Hess and Manira, 2003b; Kyriakatos and El Manira, 2007). To make matters more

interesting when we inhibited $mGluR_1$ via LY367385 (50µM 20 minutes), there is a significant reduction in frequency, indicating its intrinsic value in the maintenance of swimming. When we inhibited $mGLuR_1$ and DHPG is added there is no change in frequency. This implies either: $mGluR_5$ can compensate for the absence of $mGluR_1$, but as previous result shows are not itself intrinsic to the maintenance of frequency, or the competitive antagonism of $mGluR_1$ by LY367385 is overcome by DHPG at this concentration, or there is some combination of the two. MPEP is a non-competitive antagonist. So the decrease in frequency when $mGluR_5$ is inhibited and DHPG is added may suggest over activation of $mGluR_1$ causes a decrease in frequency. The frequency of neuron firing in this swimming behaviour is one that, like all neuron systems, requires a homeostatic regulation of excitation via glutamate or acetylcholine and inhibition via glycine or GABA. This means that the modulatory effects of $mGluR_{1/5}$ and CB1 are going to be biphasic, dependent on level of receptor activation. To explore this relationship further dose response curves of LY367385, MPEP and DHPG need to be performed ideally in electrophysiological preparations and filmed swimming behaviour to elucidate the true concentration dependent changes in locomotor output caused by group 1mGluRs.

3.7.2 Group 1 mGLuR and CB1 antagonism decrease frequency of swim-cycles

The relationship between postsynaptic group 1 mGluRs and presynaptic CB1s has been investigated previously in fictive swimming electrophysiological preparations. Firstly, it was shown that the DHPG induced increases in fictive swimming frequency of swimming in the *X. laevis* tadpole was in part due to reduced glycine release (Chapman and Sillar, 2007; Chapman, Issberner and Sillar, 2008). In isolated lamprey spinal cord, this increased burst frequency and reduced glycine release, was attributed to cannabinoid production acting retrogradely on presynaptic CB1 receptors, inhibiting glycine release onto dINs (El Manira *et al.*, 2002; Kyriakatos and El Manira, 2007).

To assess the previous hypothesis that group 1 mGluRs increase frequency, partly through the production of endocannabinoids and activation of CB1, CB1 was inhibited in combination with group 1 mGluR activation and inhibition. Application of CB1 antagonist AM-251 decreased frequency. When AM-251 was applied (10µM) followed by DHPG (50µM) application, there was no significant change. If DHPG induced increase was solely through subsequent CB1 activation, then the initial decrease observed in AM-251 group should be retained after DHPG application. This not being the case may mean that DHPG is increasing frequency, in this animal model, independent of CB1. It could be that CB1 was not fully inhibited, although our results assessing increasing concentrations imply 10µM AM-251 had the maximum decrease on frequency. Interestingly, $mGluR_5$ inhibition (MPEP 50µM) + CB1 inhibition (AM-251 10µM) decreased frequency. However, the recorded decrease matches that of AM-251 alone. In conjunction with MPEP not decreasing frequency, indicates $mGluR_5$ is not vital in setting baseline frequency. On review of the videos it was evident that the MPEP groups were difficult to initiate swimming. The first 2-3 swim-cycle would occur as normal after touch, but the swimming was not maintained after this point. The sequence of neurons that initiate swimming are primarily independent of the CPG, until hindbrain neurons (dINs) are stimulated to begin the rhythmic CPG pattern. This was the case in all MPEP groups but was most significant in the MPEP 50µM + LY367385 50 µM + AM-251 10µM group. It is interesting that this was the case with MPEP alone which did not affect frequency. It should be noted that in MPEP 50µM once swimming was maintained past the third swim-cycle, frequency of CPG measured was not changed compared with control. This could highlight a role for $mGluR_5$ in the initial muscle contractions via the dlc, dla or rohon beard neurons. Given that frequency and flexion angle were not correlated in control groups it can be concluded that one does not predict the other. This would imply that although some treatments affected both the frequency of swim-cycles and the angle of flexion, their action might be occurring in two

places (CPG for frequency, muscle/motoneuron for flexion). However, it may also be hypothesised that muscle output is a measure of the CPG, as this is responsible for motoneuron depolarisation. If CPG signalling was impeded (by $mGluR_{1/5}$ antagonism) all glutamate signalling could be affected, particularly this may affect dIN→motoneuron signalling. Similarly, the difficulty in maintaining swimming could be attributed to inhibited glutamate excitation of dINs by the rohon-beard neurons.

When $mGluR_1$ is inhibited and DHPG applied, there is no longer a decrease in frequency observed with $mGluR_1$ inhibition alone. If we combine this information with the subsequent analysis of tail flexion it may be that $mGluR_5$, present at motoneurons, can enhance frequency through eCB production, which inhibits cIN -glycine release. However, if this change was due to cannabinoid production why then does antagonism of $mGluR_1$ (LY367385 50µM) + CB1 antagonism (AM-251 10µM) not decrease frequency? Considering LY367385 alone decreased frequency and AM-251 alone decreased frequency it seems surprising that combined there was no significant change. If the mechanism by which $mGluR_5$ maintains frequency is via CB1, the inhibition of $mGluR_1$ and CB1 should maintain this decease. We have shown that $mGluR_1$ antagonism followed by DHPG addition causes no significant change, implying that increased $mGluR_5$ activation is enough to mitigate decreased $mGluR_1$ availability. This is similar to the original *in vitro* studies in lamprey (El Manira *et al.*, 2002), that showed $mGluR_1$ inhibition decreased frequency and $mGluR_5$ inhibition increased frequency. It is possible that AM-251 + LY367385 does not affect frequency compared with control because more glutamate released from presynaptic axon terminals, due to AM-251, activates more NMDARs and $mGluR_5$ almost replicating the effect seen with LY367385 + DHPG which also did not change frequency of swim-cycles.

To then explain why MPEP + DHPG would decrease frequency, we must consider that inhibition of one subtype receptor with addition of DHPG may excessively activate the other subtype and cause opposing or negative effects. As discussed previously, DHPG at 100µM can cause LTD in hippocampal slices (Palmer *et al.*, 1997), yet 10-50µM has resulted in potentiation of certain neural connections, such as the dIN of lamprey (Kyriakatos and El Manira, 2007). As such, the receptor systems themselves do not determine the fate of the synapse but the location specific conditions modulate the signalling of the group 1 mGluR -eCB system which could be better thought of as a tuning and homeostasis regulator of excitatory synapses.

3.7.3 Cannabinoids affect the frequency of swim-cycles

We have presented the first evidence that exogenously applied cannabinoids affect the frequency of swim-cycles of the *X. laevis* hatchling tadpole, stages 37-42. Our data suggests

that AM-251, the CB1 antagonist, biphasically affects frequency in a concentration dependent manner in both age groups. Rather interestingly, we have also shown that the endogenous CB1 agonist AEA, decreases frequency at low concentrations, the decrease becoming less pronounced as the concentration increases, until no change was observed at 50µM. As mentioned in the methods, it was also observed that stage 40-42 tadpoles had a faster swim-cycle frequency than stage 37-39 tadpoles. When assessed as a covariate in the LMM it confirmed that the differences were significant between the two age groups. The fact that age had a significant interaction with treatment, also highlights that CB1 is most likely expressed differently in the two age groups.

AEA is a complex molecule in terms of the array of affects attributed to it. As mentioned previously, it is an endogenous CB1 ligand with a higher affinity than 2-AG (k_i=89 and 472nM respectively), and a greater potency than 2-AG (EC50 =31 and 519nM respectively). However, it is 2-AG that is found in the brain at concentrations up to 1000-fold higher than AEA (Buczynski and Parsons, 2010). Given AEA's more complex synthetic pathways and more complex degradation pathway (covered in introduction section 1.5), it is thought that 2-AG performs the majority of the signalling. If synthetic agonist WIN-55 increased frequency of locomotor output in fictive swimming in lamprey, why has there been no increases observed with AEA in *X. laevis*? The answer to this conundrum may lie in the constitutive activity of the endocannabinoid system. If the normal function of the endocannabinoid system is to enhance excitatory signalling and reduce IPSPs in such a manner as to enhance frequency of swim cycles, it stands to reason that many of the cIN-CB1 receptors would be active during swimming. So exogenous application of AEA would not find an active site at the cIN-CB1 or not change the already active state of it. However, there are also CB1 receptors presents at glutamatergic terminals (Glu-CB1) in other organisms so it may be the case in *X. laevis*. It is possible that the low concentration of exogenous cannabinoid has only found its target on open Glu-CB1s, with 2-AG occupying its normal position on Glycinergic-CB1 receptors (Gly-CB1). Evidence has been presented previously which provides some substance to this argument. Mice were generated lacking CB1 at either GABAergic axon terminals (GABA-CB1-KO) or glutamatergic axon terminal (Glu-CB1-KO). From this the constitutive activity was calculated to be 30-40% for GABA-CB1, but only 5-7% at Glu-CB1 (Steindel *et al.*, 2013). If the function of CB1 is to enhance excitatory signalling in the CPG, it could be expected that the activity profile would be very similar, if not larger in difference. However, if we follow this train of thought, would 50µM AEA not just produce a massive reduction as it reaches maximum saturation and activates CB1 receptors on both excitatory axon terminals and inhibitory axon

terminals. The answer may lie in the distribution of CB1 and in the distribution of neuron populations. The expression of CB1 is thought to be higher at inhibitory terminals according to previous studies. This might mean that the low concentrations produce a decrease because they initially take the easy path, activating free Glu-CB1s and reducing excitation, but as the concentration increases they outcompete 2-AG for Gly-CB1s, causing a larger decrease in glycine release compared to glutamate release and begin to readdress the balance in excitation: inhibition ratio (den Boon *et al.*, 2014).

The biphasic interplay of inhibitory and excitatory signalling, in relation to exogenous cannabinoid application, has been evidenced in: voluntary movement (Sulcova, 1998; Sañudo-Peña *et al.*, 2000; Bruijnzeel *et al.*, 2016), reward seeking and locomotion (Katsidoni, Kastellakis and Panagis, 2013; Polissidis *et al.*, 2013), anxiety (Viveros, Marco and File, 2005; Rubino *et al.*, 2008; Rey *et al.*, 2012), hippocampal acetylcholine release (Tzavara, Wade and Nomikos, 2003; Steindel *et al.*, 2013) and feeding behaviour (Wiley *et al.*, 2005; Bellocchio *et al.*, 2010). The consensus is cannabinoids effect different neuron populations in time and dose dependent manner. As the concentration increases, more CB1s in different neuron groups are activated/inhibited and the effects become opposing. This effect means that application of an antagonist, with much higher affinity than the endogenous ligands, such as AM-251, would increase GABA/glycine release more so than glutamate release. However, this effect would be time and dose dependent. Therefore, a low dose antagonist would have an easier time finding a free Glu-CB1 than a GABA-CB1, initially increasing glutamate release. As this concentration increases, the balance is redressed eventually becoming biphasic.

As discussed in the introduction, Li and Moult, 2012; Moult, Cottrell and Li, 2013 demonstrated the role of the cINs in maintaining and regulating frequency of left-right tail contractions. Through hyperpolarising current injection and optogenetic hyperpolarisation, testing the parameter of hyperpolarisation rebound firing, indicated weak hyperpolarisation (below -43.3mV) produced slower rebound firing and above -43.3mV there was no change. One explanation of the results could be that AEA reduced cIN release so as to delay threshold hyperpolarisation potential attainment and reduce frequency. However, as discussed above, also decreased background depolarisation which can also effect frequency (Li and Moult, 2012). I propose that although a large decrease in cIN-glycine release can slow frequency by not initiating hyperpolarisation rebound firing, increasing glycine release via AM-251 inhibition of CB1R, reduces frequency because the hyperpolarisation is large and sustained, delaying rebound firing. It can be thought of as having an optimum hyperpolarisation range if the release of glycine is too little of too slow rebound firing is delayed, if the glycine release is

sustained and too large rebound firing is delayed. This could be one explanation for the biphasic results presented in this work. Particularly, it may affect the cannabinoid regulated potentiation of glutamate signalling previously proposed (Kyriakatos and El Manira, 2007). Some evidence has been presented that might substantiate the theory that high dose AM-251 generates such a large IPSP at the dIN that rebound firing is delayed. Li and Moult (2012), showed large chlorine injections slowed frequency.

Cannabinoids, in the context of the CPG, have been investigated in the fictive swimming of lamprey (Kettunen *et al.*, 2005; Kyriakatos and El Manira, 2007; El Manira *et al.*, 2008; Song, Kyriakatos and El Manira, 2012). The short conclusion from these studies was that cIN-CB1 inhibition increased the IPSP at dINs and decreased the frequency of MN bursts. Further experiments showed cannabinoid ligands, particularly 2-AG or synthetic cannabinoid WIN 55, potentiated the excitatory transmission by decreasing glycine release from adjacent synapses, particularly cINs. When considering these conclusions, in the context of our AEA application results, it seems surprising that more increases in frequency were not observed. It is highly likely that the cIN-CB1s are tightly regulated, activated by 2-AG and the effect of exogenous AEA is more likely to affect background depolarisation. So only at specific concentrations, it will modulate the network in such a manner as to increase frequency. Although slightly different results were obtained in lamprey, the conclusions the group drew are consistent with the literature even producing a biphasic sine plot to explain how cannabinoids shift the relationship between excitation and inhibition (for review of lamprey cannabinoids and group 1 mGuRs studies see El Manira & Kyriakatos 2010). Recent work has produced measurements of different brain regions with cannabinoid application and the results show a shift in inhibition: excitation ratio from 90:10 to 70:30 (den Boon *et al.*, 2014). When discussing AEA we must also consider its limitations as an exogenous cannabinoid. There are conflicting reports on the affinity and efficacy of AEA compared with 2-AG. The previously mentioned Kd and EC50 for AEA and 2-AG were from the supplier (Tocris). However, AEA has been described as a partial agonist compared with 2-AG which is a full agonist (Console-Bram, Marcu and Abood, 2012). Often affinity and efficacy experiments are tissue and cell type dependent, and CB1 effects have not been characterised in the neural system of *X. laevis.* It is possible that the lower EC50 value for AEA is because it has a lower maximum response than 2-AG, making it a partial agonist. With a higher affinity this would mean AEA is acting almost like an antagonist at low concentrations, occupying the receptor and causing less of a response. In this context it is possible that low concentrations outcompete 2-AG for the active site at cIN-CB1, but do not reduce glycine release to the same extent. As the concentration

increases, the effect caused is similar to 2-AG's endogenous effect and frequency of swim-cycles are not changed. This would fit with our data in the stage 40-42 group, where low doses decreased frequency and as the AEA concentration increased this effect became lessened, until at 50µM no change was observed. AEA can also activate TRVP1 cation channels, which can allow calcium into the PSD (Starowicz, Nigam and Di Marzo, 2007; Tóth, Blumberg and Boczán, 2009). If TRVP1 was present on cINs, this would increase their rate of depolarisation, possibly increasing glycine release rate. If TRVP1 was present on dINs it may increase the rate of dIN depolarisation and increase frequency. AEA application has also been reported to inhibit the production of 2-AG and lessen the effect of DHPG (Maccarrone *et al.*, 2008).

Noting our slightly different results to previous *in vitro* lamprey experimentation, we must comment on the difference in methodology. Our drugs were bath applied, possibly increasing off target effects, and were only applied for 20 minutes prior to recording, as opposed to experiments in lamprey which had 1-2 hours perfusion of the spinal cord. Although the CPG of *X. laevis* operates with little to no input from higher brain regions, the trigeminal ganglia that stop swimming, are activated in response cement gland touch, and release GABA onto hindbrain to stop dIN pacemaker firing. It was noted in our preliminary experiments that AEA treated tadpoles swam for longer periods, but there were too many variables such as frequency of cement gland touch and our camera only recorded for short timeframes leading to incomplete datasets. This is something that could be looked at in more detail in the future. Cannabinoids also affect metabolism and there is a body of work beginning to provide evidence for mitochondrial cannabinoid receptors (Bénard *et al.*, 2012; Hebert-Chatelain *et al.*, 2014; Ma *et al.*, 2015), which may mean a reduced energy availability. In the lamprey the baseline frequency was set by NMDA bath application (Kyriakatos and El Manira, 2007), as opposed to our work were control frequency is set purely based on CPG function and initiated by touch to the trunk. There is also the *in vitro* vs *in vivo* debate to be had, especially considering the neuroprotective properties displayed by endocannabinoids (Marsicano *et al.*, 2003). Surgical preparations can evoke cannabinoid signalling (Arevalo-Martin *et al.*, 2012), which may affect the level of constitutive activity of CB1 before treatment application.

From this work in neuroprotection an interesting family of proteins, the cannabinoid receptor interacting protein (CRIP) 1a, was identified to modulate the activity of the CB1R (Stauffer *et al.*, 2011; Ahmed *et al.*, 2014; Blume *et al.*, 2014; More and Choi, 2015; Guggenhuber *et al.*, 2016). Current consensus is this protein interacts with the intracellular domain but does not contribute to desensitisation. It would appear that CRIP1a interacts in such a manner as to change/enhance preference for certain G-protein signalling, in some cases

sequestering stimulatory alpha g- protein as opposed to inhibitory alpha g-protein that CB1 normally activates (Blume *et al.*, 2014). In one study it even reversed the effect of an antagonist to an agonist (Stauffer *et al.*, 2011). This could mean the biphasic effect of cannabinoids is due simply to this protein becoming active in order to stop erroneous cannabinoid signalling, severely changing the range of neurotransmission past a certain point and may be why fatalities are not seen with cannabinoid abuse. If this protein is present in *X. laevis*, its activation may change the neurotransmitter release probability and explain the biphasic response. Particularly in AM-251 as the neural systems try to balance the dysregulation in excitatory signalling CRIP1a could become active to effectively change the g-protein signalling and thus the effect on ion channels where necessary to maintain signalling within a range and allow swimming to continue. This is essentially an evolutionary fail safe that would mean, if for example an animal ate a cannabinoid plant, it could still maintain neuronal signalling without completely reducing neurotransmitter release to the point of shutting down key functions such as movement and homeostatic regulation.

Finally, I would like to highlight a study into spike timing dependent plasticity involving the endocannabinoid system and group 1 mGluRs (Cui *et al.*, 2015). This study explored standard LTD and LTP spike timing dependent protocols in corticostriatal neurons. The fascinating outcome was a bidirectional role of endocannabinoids in the induction of either LTD or LTP. The evidence shows that cannabinoids are involved in both LTP and LTD the defining factor was the induction protocol. A small number of paired stimulations (5-10 pre and postsynaptic spikes) induced LTP and this was dependent on both TRVP1 and CB1 activation. In the same neuron groups, paired stimulation was increased (50x pre and postsynaptic spike) and the LTP was reversed to a LTD. Then increasing this to 100 pre and post stimulations induced LTP again. This is further evidence in a short term setting that cannabinoids are not solely responsible for increases or decreases themselves, they modulate synaptic activity based on complex activity dependent signalling systems that are neuron population dependent.

3.7.4 Angle of tail flexion affected by mGluR$_{1/5}$ and CB1

If angle of flexion is affected and not frequency, it is assumed the treatments have affected motorneuron depolarisation rate/ muscle cell contraction. If frequency is affected it has likely affected the balance of cIN-dIN hyperpolarisation and dIN pacemaker activity.The results of the tail flexion measurement demonstrate that the two measurements are independent as the groups that reduced or increased frequency were not the same as ones which altered tail flexion. However, some groups did affect both frequency and flexion, such as MPEP + DHPG

and LY367385 + MPEP + DHPG. This is an interesting result, and hard to explain why the addition of DHPG to these groups would affect tail flexion, when LY367385 + MPEP did not significantly affect flexion. When CB1 antagonism was combined with these groups tail flexion was once again affected significantly. By far the largest increase in angle size (reduction in tail flexion) was seen in the MPEP + AM-251 group. However, LY367385 + MPEP + AM-251 also significantly reduced tail flexion. Although it is unclear how the DHPG/ increased glutamate (via AM-251 application) would reduce the tail flexion, unless excessive activation of a particular receptor causes negative effects on muscle contraction.

Although the control groups displayed no correlation between frequency of swim-cycles and angle of flexion, many groups which display significant decreases in frequency also had reduced tail flexions, but not all of them. For example, LY367385 application significantly reduced swim-cycle frequency but tail flexion was not altered significantly. This sequence of results may indicate that $mGluR_5$ is present on motorneurons whereas $mGluR_1$ is present on dINs. If we compare this with the result of measured change in frequency of swim-cycles, we can see that the increased tail flexion of 50µM AM-251 was accompanied by a very large decrease in frequency of swim-cycles. If CB1 receptors are present at cIN axon terminals it is possible that motoneuron depolarisation produces cannabinoids which inhibit adjacent cIN neurotransmitter release. In the antagonism of CB1, this process is decreased effectively increasing inhibitory neurotransmission and slowing frequency. It might also be the case that larger muscle contractions slow the frequency of swim-cycles, if larger depolarisations/ increased group 1 mGluR activation produced more cannabinoids. If the CPG frequency slowed but the motoneuron output is the same this might enable larger flexions as there is longer between alternating contractions, simply allowing the tail to travel slightly further before the other side pulls it back.

AM-251 (2µM, 20 minutes) did not affect frequency of swim-cycles in stage 37-39 tadpoles, but it did affect the angle of flexion. This is different to the trend seen in $mGluR_{1/5}$ + CB1 inhibition, where the frequency of swim-cycles decreased, and the tail flexion decreased. As the two variables are not correlated it can be deemed that two separate effects are being measured, unless, $mGluR_{1/5}$ and CB1, present at motoneuron PSD/dIN axon terminal respectively, modulate motor output (angle of flexion) in such a manner as to affect and feedback to modulate CPG output (frequency of swim-cycles) through cannabinoid modulation of CPG neurotransmitter release.

3.7.5 Assessment of method as a viable measure of swimming output in Xenopus laevis tadpoles

The methods used to assess the motor output of the *X. laevis* tadpole are novel and as such are imperfect. The power analysis highlights that where results are significant in all but one case the study was sufficiently powered. Where there are not significant differences in the data, the studies are generally underpowered (results in appendix Tables: 7.1.1-7.1.4). However, there are a couple of groups where they only appear marginally underpowered suggesting in some cases 4-14 more tadpoles in the sample would ensure a sufficiently powered study. The small sample size and imperfect method of data collection has led to some variability in the standard deviation and large variations in this were usually a predictor for an underpowered study. The possible issues identified that may have led to increased variability are: tadpole staging, drug penetration/application, subjectivity in swim-cycle selection, subjectivity in angle of flexion selection.

3.7.5.1 Staging

Firstly, the staging of the tadpoles was performed according to Nieuwkoop and Faber (1995). Although there is a clear progression of stages at room temperature, we staggered the development by placing the tadpoles in coolers at 12^{o}C. This meant that the timeframe no longer applied. The reduction in temperature slows the metabolism and thus development of the tadpole. Experiments were performed to assess the differences in stage 37-39 compared with stage 40-42 defined by stage, with significant differences in swim-cycle frequency between the two age groups. Tadpoles which had their development staggered by cooling showed no significant changes to their developmental stages when they were compared. However, it is possible that over the course of the experiments when treatment was applied that slight misjudgements in the stages could have caused variability in the controls. A good example of this would be the controls for AEA in the stage 37-39 group, which varied more than the means of the treatment did with each other. When a post-hoc test was performed comparing all groups including controls with each other, the control groups had statistical significance from one another and treatment groups did not. It was difficult to differentiate between a stage 37 tadpole and stage 39 so they were classed as one group. If a situation arose where one control was predominantly stage 39 and the other stage 37 it would be likely those two means would be significantly different from one another. This would need to be explored further to identify this as the source of variability as we do not know if stage 39 swims significantly faster than stage 37. This again could be a problem in the stage 40-42 groups. However, there is a much clearer developmental change that happens at stage 40 and

again at stage 42 so this group is easier to differentiate and can be more confidently asserted that all tadpoles tested were in fact stage 40 or stage 41. By stage 42 there is a clear change in the yolk sac mass and the shape of the proctodueum becoming conical. There is also a colour change in the skin as pigment becomes more pronounced. Although not entirely related, the staging problems also relate to how the drug was applied. The tadpole was anaesthetised in MS-222 and a small nick was made in the dorsal fin. The tadpole was allowed to recover for longer than 1 hour. This recovery time was not always exact as the nick was done in batches and thus some tadpoles may have healed more than others by the end of a treatment group. This would then have inter-treatment differences dependent on the size and polarity of the molecule. The unknown factor of this may have led to some increase in random variation between tadpoles and treatments.

3.7.5.2 Selection of swim-cycles

The subjectivity in the selection of the data may have caused variation. Although this method was carried out methodically and without bias the swim-cycles that were measured had to be ones where the tadpole swam at the best angle to be filmed. Sometimes the tadpole would swim on its side for some of the video meaning those swim-cycles could not be measured. The method used always measured swim-cycles between the 3rd and 10th cycle. However, what is not known is if there is variation in these cycles. Also, it is unlikely that two people analysing the same video would get exactly the same results. To improve this, two things should happen in the future: the sample sizes could be increased, this would increase the power where it is underpowered, but would also allow for ruthless elimination of swimming bouts that did not produce measurable swim-cycles between the 3rd and 6th cycle. To improve this further all swim-cycles would be measured and recorded with no average taken. There are video analysis programs, such as worm tracker for Image J, which could measure the frequency of all the tail movements so the analysis would be much more in depth giving a clear picture of the variability in swim-cycle speed across the entire swimming bout. The use of worm tracker was investigated during the project, however, the video format we used was not compatible with this program. In future studies this would need to be considered. The frame rate could be increased to improve accuracy. One frame represents 2.5 milliseconds in our current set up. The average swim-cycle for the control groups for all stage 40-42 tadpoles in the cannabinoid receptor assessment was 33.137 milliseconds (30.177Hz with SD=2.7Hz). This allowed for significant interaction to be determined when they are very large but possibly not when they are small, as indicated by the power analysis.

One way to eliminate many of these problems would be to use spinalised tadpoles. The tadpole can be decapitated above the brainstem and survive in an appropriate saline solution. This would remove drug accessibility issues, remove possible off target effects in the brain and allow electrophysiological recording from the 3 main neuron groups (dIN, cIN and motoneurons) that produce and regulate swim-cycle frequency. Corroborating these results in this way would ensure that the effect seen in whole tadpole swimming under these drug treatments is caused by neuron specific interaction in the CPG of the spinal cord.

3.7.5.3 Statistical analysis and power analysis

The sample size was low and as such the power analysis indicates that some groups were underpowered. On assessment of the assumptions it is clear this is not an ideal dataset and the linear mixed model used was not the best fit to get the most accurate assessment of the data. In many of the residual vs predicted value plots (appendix 7.2) clear patterning and unequal distribution/ non-linearity can be seen, particularly in the cannabinoid groups which due to being compared with individual concentrations of vehicle control (i.e. 0.1uM AEA to equivalent volume of soya emulsion AEA was dissolved in) had very low numbers per model (10 values). However, there is also some patterning in the mGluR and CB1 + mGluR data, which had larger model numbers. To address this a generalised linear mixed model was attempted with the different link functions offered by SPSS. Link functions transform the data so that it can be modelled linearly. This is particularly relevant to our frequency data. Since timepoint did not significantly change frequency across treatment groups it meant we had lots of values around the same frequency for each tadpole. It may be this factor combined with the averaging of the 3 swim-cycles, compounded the error and made the data badly grouped and not continuous. However, when link functions such as loglinear and binomial were attempted the model excluded lots of data points sometime up to 90% of them. This would need to be examined further to understand what can be done to improve the analysis of this method.

3.8 Summary of proposed effects at each key synapse

Figure 3.8.1 is a simple schematic showing the effect the different drug treatment would theoretically have on each key synapses in the CPG. The location of the receptors in this system has not been confirmed to these exact locations so we have assumed they are present at all synapses in the most commonly located positions (i.e. CB1 located on axon terminals and group 1 mGluRs located on PSDs). If we assume a 1:1 ratio of each neuron type, then AM-251 would increase glutamate released by dIN to the cIN and the motoneuron. This would increase the rate of summation for action potential generation at the motoneuron and cIN. However, it

would also increase the amount of glycine released by the cIN to dIN possibly increasing the length of time of hyperpolarisation of the opposing side dINs. This would have a concentration dependent result on the frequency of dIN rebound firing as shown in (Li and Moult, 2012). In that study weak IPSP from the cINs, smaller than -43.2mV, slowed the rate of dIN rebound firing. Above this threshold the speed of dIN rebound firing was not changed. However, large chlorine injections slowed frequency of dIN rebound firing. This would indicate that large hyperpolarisation is needed to maintain normal frequency of swimming, whereas reduction in the glycine induced hyperpolarisation of the dIN (below -43.2mV) from the cIN would reduce frequency. This would suggest there is an optimum level of hyperpolarisation, and either side of that level it will decrease frequency. This might mean that 2µM AM-251 stage 40-42 is in that optimum range, where it has increased glutamate and glycine release just the right amount to increase frequency. Concentrations above this (10µM and 50µM) significantly decrease frequency by releasing so much glycine that it causes a longer hyperpolarisation decreasing frequency. Similarly, if we look at AEA it would theoretically decrease glutamate released by the dIN to the cINs and motoneurons, decreasing the rate of action potential generation, while simultaneously decreasing the glycine released by the cIN to dIN. The effect of this would expect a decrease in frequency of swim-cycles. Particularly a decrease in the size of hyperpolarisation, below that previously discussed threshold would slow the rate of rebound firing. However, again we only see a significant decrease in the stage 40-42 group with AEA applied at 100nM, 2µM and 10µM and no significant change at 50µM. A possible explanation for the unexpected results with AEA and AM-251 lie in the work of previous experiments documenting the distribution and constitutive activity of CB1 in various brain regions. As discussed previously CB1 was shown to be constitutively active at GABAergic terminal 30-40% of the time while only constitutively active at glutamatergic terminal 5-7% of the time. This would mean the active site is occupied more often on inhibitory neurotransmitter releasing terminals, such as glycine releasing cINs, and make exogenous application more likely to affect glutamatergic-CB1 first. Functional selectivity experiments would also indicate that these receptors at inhibitory terminals may be more receptive to particular ligands than others, and different ligands cause different effects possibly through the action of CRIP1a, further confusing the elucidation of results for whole organism application.

Using the same theory for group 1 mGluRs, activation of either receptor subtype via DHPG is likely to increase the rate of dIN, motoneuron and cIN depolarisation and action potential generation. This is corroborated by what our results show, a significant increase in

frequency by 8.45± 1.37%. It would then be expected that inhibition of either group 1 mGluR subtype would significantly decrease frequency. However, this is only the case with $mGluR_1$ antagonism via LY367385 and not $mGluR_5$ antagonism via MPEP. This result may highlight the different locations of $mGluR_5$ compared with $mGluR_1$. Previous studies in *X. laevis* and lamprey also highlight a different effect of the two receptors on frequency. From our studies it would appear that $mGluR_1$ is located on the dIN, as increased rate of depolarisation and rebound firing helped by increased internal calcium release is the most probable explanation of increases in frequency. If $mGluR_5$ is not present on the dIN PSD or dIN –dIN gap junctions, then it makes sense that it is not vital in the maintenance of normal swimming frequency. The interesting and unexplained results for $mGluR_5$, come when DHPG is added after inhibition via MPEP reducing frequency of swim-cycles. This may indicate that over activation of $mGluR_1$ is detrimental and may be akin to the DHPG induced LTD protocol. Similarly, antagonism of $mGluR_1$ and application of DHPG had no effect on frequency. When just $mGluR_1$ was inhibited frequency was significantly reduced. This indicates either $mGluR_5$ can substitute for the loss of $mGluR_1$ or the competitive inhibition of $mGluR_1$ by LY367385 is washed out/ out competed by the subsequent application of DHPG.

The picture becomes more complicated when we try to assess the combination of CB1 and group 1 mGluRs. Evidence from the literature suggests group 1 mGluRs potentiate glutamate signalling by producing endocannabinoids which retrogradely inhibit neurotransmitter release from adjacent inhibitory neurotransmitter releasing terminals. If we go back to Figure 3.8.1 and imagine the dINs are in larger groups than 1 neuron which electrically couple through gap junctions, the rate at which they fire is the interplay between the hyperpolarising current and rate of rebound firing and the underlying excitation generated by glutamate at NMDARs. To enhance this excitation group 1 mGluRs may produce endocannabinoids which reduce cIN glycine release to enhance depolarisation and rate of action potentials. This would be a tightly controlled mechanism which if unregulated would lead to large variations in frequency of dIN action potentials. This might explain the results of AM-251 application and the result that AM-251 then DHPG application cause no significant change as part of the increase seen with DHPG application comes from the reduction in rate/amount of glycine released from the cIN. The theory would suggest that DHPG application after AM-251 would lead to increased post-synaptic rate of depolarisation via group 1 mGluR and increased neurotransmitter releases from all axon terminals. This would increase the amount of glycine released to the dIN, possibly counteracting the increased depolarisation of the dIN via DHPG. If as previous studies suggested all hyperpolarisation above -43.2mV had no

effect on rate of rebound firing then this AM-251 + DHPG treatment would increase frequency. However, this is not the case in our results here. It must be that very large releases of glycine, unregulated because of CB1 antagonism, delays the rate of dIN firing action potentials and thus slow frequency of swim-cycles.

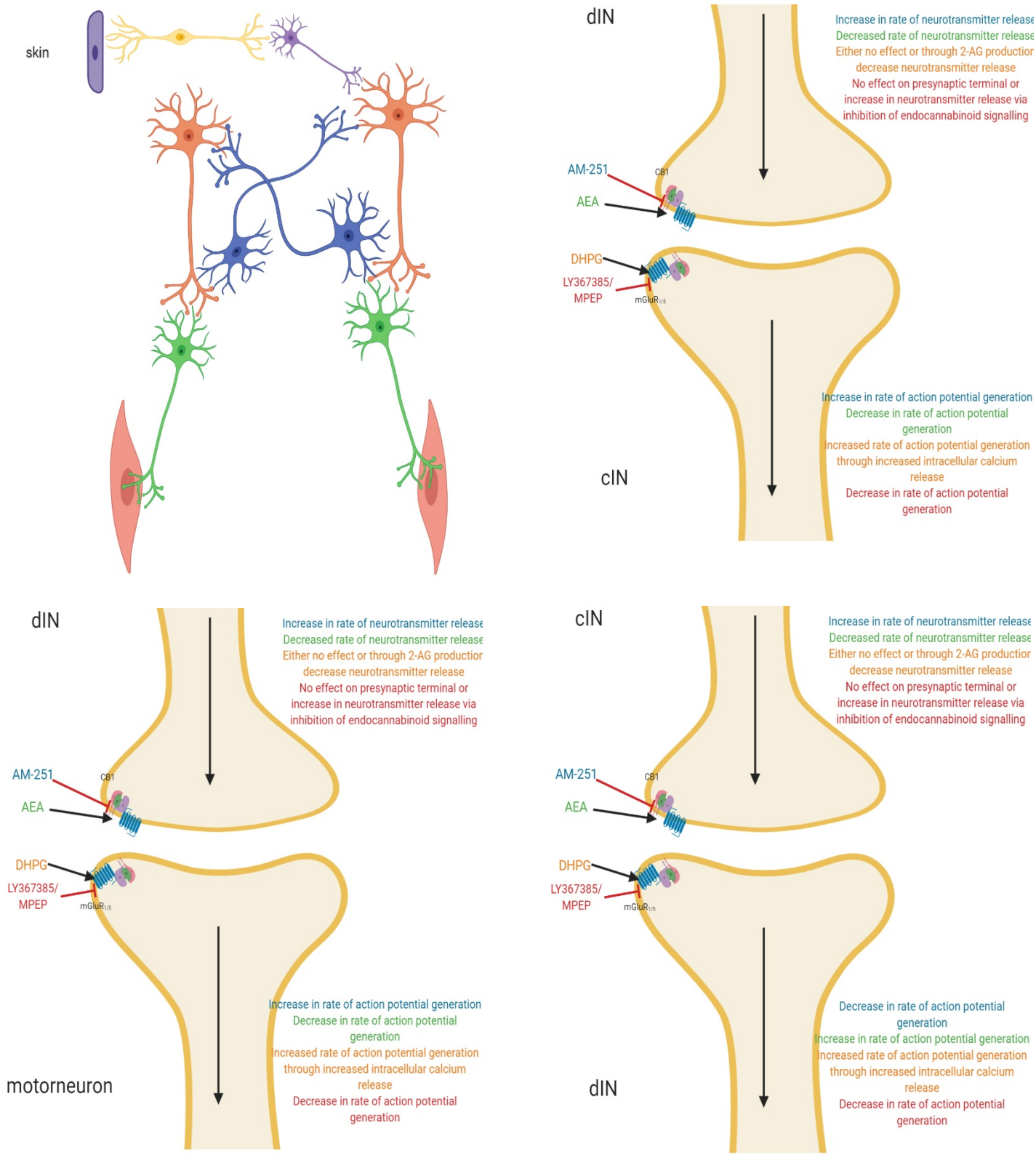

Figure 3.8.1*-Schematic of the effect of drug treatment at each of the important synapses in the CPG. Top left- simple schematic of the CPG (yellow-RB, purple-DLC, orange-dIN, Blue- cIN, green-motoneuron. Top right- a schematic of dIN-cIN synapse, bottom left dIN motoneurons synapse, bottom right- cIN-dIN synapse (Blue -AM-2521, Green -AEA, orange -DHPG and Red- LY367385 or MPEP). Theoretically describes in simple terms whether drug treat will increase/decrease rate of neurotransmitter release and increase/decrease rate of action potential generation at specific synapses*

3.9 Conclusion

This series of experiments has presented further evidence for the involvement of the group 1 mGluRs, and new evidence for the CB1R, in the CPG mediated regulation of left-right muscle contraction frequency during swimming of the *X. laevis* tadpole, from stage 37-42. Group 1 mGluRs, when activated via DHPG, increase the frequency of swim-cycles. $MGluR_1$ is revealed to be intrinsic in this maintenance of normal swimming frequency, whereas $mGluR_5$ is not. Although the data suggests $mGluR_5$ may compensate for $mGluR_1$ when it is antagonised. We provide the first evidence that CB1 contributes to swim-cycle frequency in *X. laevis*. Although, the extent of its intrinsic effect is unclear, due to a biphasic dose-dependent response to antagonism via AM-251. In future it would be advised to use a neutral antagonist which simply occupies the active site and induces no inverse agonism and of target effects that AM-251 is marred with. Similarly, the picture with endogenous agonist AEA is unclear. However, its application does affect frequency of swim-cycles. Again, in future synthetic agonists need to be applied and electrophysiological recordings made to confirm the extent of CB1's action and the location that it affects. This method offers a cheap and accessible way of measuring the effect of pharmacological intervention on the output of the CPG of *X. laevis*, which can be used in future studies alongside electrophysiological measurement.

4 Assessment of dendritic spines in primary *Xenopus laevis* neuron culture with AFM

4.1 Introduction

In the previous results chapter, we presented evidence of pharmacologically induced changes in the swimming output of the CPG, which reduced or enhanced the frequency of swim-cycles in the swimming behaviour of the *X. laevis* tadpole stages 37-42. To exert these changes in the frequency of swim-cycles the treatments are most likely activating their corresponding GPCR and causing an effect through changes in ion channel conductance and neuron excitability. When the GPCR ($mGluR_{1/5}$ or CB1) is activated, the g-proteins affect second messenger systems that lead to changes in the transcription of RNA. The products of transcription can change the shape, enhance or reduce the size of the PSD and change the receptor expression density. Over a continued period of time these changes result in long-term potentiation (LTP) or long-term depression (LTD) of synapse transmission.

One of the key constituents of excitatory synapses are dendritic spines. Dendritic spines are tiny protrusions that receive the excitatory signal released from the axon terminal. They are generally split into four categories: mushroom, filipodia, thin and thick (Sala and Segal, 2014). Dendritic spines have been examined in primary culture of *X. laevis* granule cells (Zhang, Huang and Hu, 2016), but not yet in the culture of spinal neurons. The development and maintenance of dendritic spines is fluid. Recent high-speed AFM imaging, on living cultured hippocampal neurons, provided evidence of dendritic spines developing in 20 minutes (Shibata *et al.*, 2015). The evidence on dendritic spines *in vivo* indicates they increase in number and size during the day and decrease during sleep. Current theory suggests the strength of the synapse and stability of the dendritic spine at point of sleep determines if the synapse will be consolidated or pruned (Tononi and Cirelli, 2014, 2016). Currently the measurements of dendritic spines *in vitro* rely on confocal imaging, documenting the stability of spines over time or sectioning organisms and monitoring spines position and size (Bosch, Martínez, Masachs, C. M. Teixeira, *et al.*, 2015). Recent developments have been made combining confocal spine imaging with algorithms of machine learning (Shi, Huang and Hong, 2014). Improvements on this method have recently been presented (Basu *et al.*, 2018). From these studies the key measurements of dendritic spines were volume, shape/morphology and length.

Alongside size and number, there are key components of dendritic spines that are used as determinants of strength. The primary measure is AMPAR expression (Matsuzaki *et al.*,

2001, 2004). The most abundant excitatory glutamate receptor, increased AMPAR expression increases the conductance of the spine and is accompanied by phosphorylation events that enhance potentiation (Barria *et al.*, 1997; Ehlers, 2000; Lee *et al.*, 2000; Huganir and Nicoll, 2013). The current theory on AMPAR potentiation suggests the receptors are trafficked in laterally where they are tagged to the PSD if the dendritic spine is potentiated. If it is not, the receptor continues to the extra-synaptic location where it is degraded or cycled back into the synapse (Barria *et al.*, 1997; Redondo and Morris, 2011; Huganir and Nicoll, 2013). Other key measures of the potentiation state of dendritic spines are the phosphorylation states of CAMKII and GSK3β (Lee *et al.*, 2009). CAMKII is activated when Ca^{2+} increases in the spine. When the threshold is reached the Ca^{2+}/calmodulin auto-phosphorylates CAMKII. Once activated it sets off a series of phosphorylation events that strengthen the actin cytoskeleton, binding newly created F-actin to the PSD-95 and Homer domains, enabling large AMPA receptor rafts to be in optimal position for enhanced synaptic signalling. It is also involved in LTD where it phosphorylates AMPAR at S567, a site known to reduce synaptic GluA1 localization (Lee *et al.*, 2009; Okamoto, Bosch and Hayashi, 2009; Bosch *et al.*, 2014). The difference appears to be the rate of CAMKII phosphorylation, which fits with the knowledge that high frequency stimulation results in LTP and low frequency stimulation results in LTD.

Using the AFM, we sought to identify dendritic spines in the primary neuron culture of developing *X. laevis* spinal neurons. Once possible dendritic spines were identified, a measurement criteria was determined, analysing the volume, radius, cross-sectional area and the roughness of the membrane. The roughness (RMS) of a surface is the root means square (RMS) of the surface's peaks and valleys. AFM assessment of red blood cell membrane roughness was used as a measure of health (Girasole *et al.*, 2007). Recently the roughness of a neuronal cell calculated using non-interferometric wide-field optical profilometry (NIWOP) (Lee *et al.*, 2016) and proposed as a measure of health. It could be hypothesised that a rough/folded membrane would be a sign of poor transmission and connectivity, as it is accepted that mushroom shape spine, with the PSD located in prime position for signalling, is preferential. Volume and radius changes are the standard measurements of dendritic spines, and changes in these parameters might indicate spines that are undergoing plasticity. We also developed a method of quantifying the visco-elasticity of the membrane by using the loss tangent equation (Proksch *et al.*, 2016). It was hypothesised that spines undergoing plasticity, whether to decrease surface area and become depressed or increase surface area and become potentiated, would change the tension in their membrane.

We then set out to test if the drug treatments used in the previous chapter significantly affected these measurements. It may be expected that group 1 mGluR agonist (DHPG) or antagonist (MPEP) are more likely to induce plasticity changes in dendritic spines compared with CB1 agonist and antagonist, as they are located on the PSD. The CB1 receptor is a presynaptic receptor so any changes in dimensions of dendritic spines would have to be caused by either: affecting neurotransmitter release from axon terminals, which in turn modulates the dendritic spine; activating off-target sites such as TRVP1 or possibly effecting mitochondrial CB1 receptors if they are present in *X. laevis*. It has been shown that neurons have functional synapses from 24 hours (Yazejian, Rita M Yazejian, *et al.*, 2013) and the twitching muscle observed in cultures indicates spontaneous signalling. The cannabinoid agonist AEA and antagonist/inverse agonist AM-251 both caused measurable changes in the output of the CPG of the swimming tadpole (results chapter 3).

4.1.1 Method

Primary *X. laevis* neuron cultures were generated, then treated for 20 minutes with DHPG 50µM, MPEP 50µM, AM-251 50 µM or AEA 50 µM and fixed in 5% glutaraldehyde (as described in the methods 2.3.2). Cultures were scanned with the atomic force microscope in air using AC mode (described in detail in section 2.4).

4.2 Identification of dendritic spines

The criteria for identifying dendritic spines was formulated upon review of confocal assessment of spines in culture (Bosch *et al.*, 2014; Basu *et al.*, 2018). Previous work, in multiple animal model cultures, shows spines vary in length and volume depending on cell type and organism (Bosch *et al.*, 2014; Huang *et al.*, 2015; Zhang, Huang and Hu, 2016). *X. laevis* spinal neurons are relatively large and we expected them to have far fewer dendritic spines than a neuron culture from the brain, such as the granule cells assessed previously (Zhang, Huang and Hu, 2016). As a result of this, we investigated protrusions from areas identified as dendritic trees due to morphology. Dendritic trees are thinner with more branching than axons. These projections were identified with an inverted microscope and scanned with the AFM. Protrusions from the dendritic trees were determined as dendritic spines if they were less than 7µm in length. We further assessed the likelihood they were dendritic spines by morphological analysis. We deemed it unlikely for a spine to be completely spheroid with no clear branching from the dendrite, and should resemble previous images and models of dendritic spines (Harris, Jensen and Tsao, 1992; Hering and Sheng, 2001; Mancuso *et*

al., 2013). Figure 4.2.1 presents 3 examples of dendritic spines that were scanned and used (Figure 4.2.1a, c, e), compared with 3 protrusions that were scanned and excluded (Figure 4.2.1b, d, f). Figures 4.2.1b and f were excluded for similar reasons; both were too large, they were quite near the soma and were part of what appears to be the axon, based on its thickness, smoothness and straightness coming from the soma. Figure 4.2.1d was excluded due to lack of membrane integrity. Although fragments can be seen in Figure 4.2.1c, the membrane was deemed of good enough quality for analysis. These images (Figure 4.2.1 a, c and e) represent the first instance of dendritic spines identified in the spinal neurons of *X. laevis*.

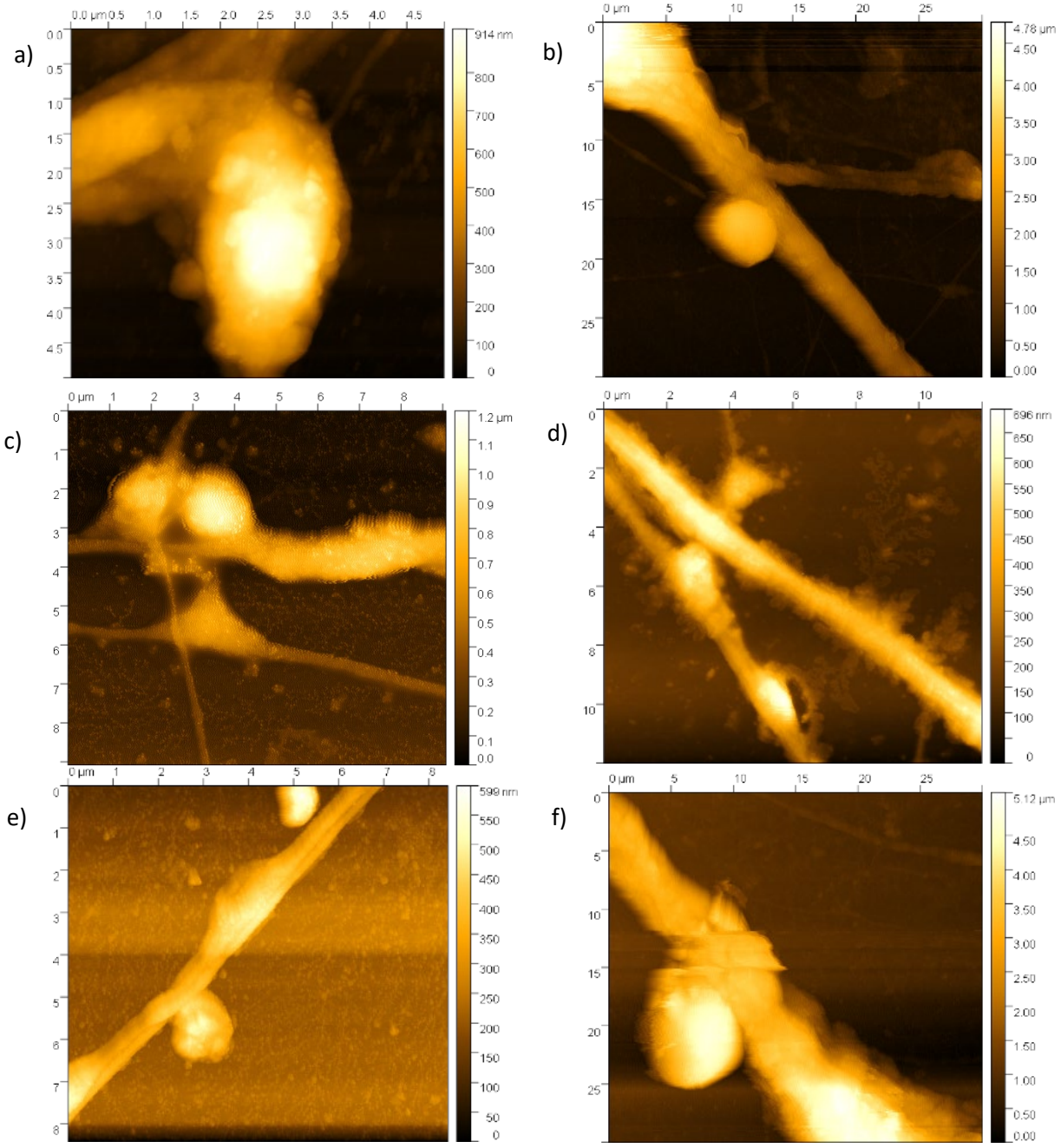

Figure 4.2.1*- Identification of dendritic spines. Left- dendritic spines accepted for analysis. Right- rejected as dendritic spines based on size and morphology and integrity. As described in methods, exploratory 50µm x50µm scans were performed on areas recognised to be dendrites. Then areas were selected for possible dendritic spines and rescanned to produce images like these.*

4.3 Changes in dendritic spine dimensions

More than just identifying dendritic spines in a spinal neuron culture of *X. laevis,* we wanted to produce reliable measurements of structural plasticity. Could we detect changes in dendritic spine radius, volume, cross sectional area, membrane roughness and membrane viscoelasticity (loss tangent), when treated with DHPG 50µM (20 minutes) (group 1mGluR agonist), MPEP 50µM (20 minutes) ($mGlUR_5$ antagonist), AM-251 50µM (20 minutes) (CB1 antagonist/inverse agonist) or AEA 50µM (20 minutes) (endogenous CB1 agonist). All these treatments produced measurable changes in behavioural output (chapter 3). There were two neuron culture slides (containing cells from five *X. laevis* embryos (stage 20-22) per slide) per drug treatment, with five different dendritic spines sampled per slide. The total number of dendritic spines identified and included in the analysis was 53.

The scans with the AFM produce different channels depending on what is being measured. The height channel produces the topographic images, represented graphically in a heat map. These images were evaluated using Gwyddion software line profile analysis. Using 4-line profiles of each dendritic spine, the mean value of four parameters were investigated: mean dendritic spine radius, mean dendritic spine volume, mean dendritic spine area of cross section and mean roughness (RMS) of dendritic spine membrane. A linear mixed model (LMM) was performed to compare each drug treatment with its respective control. In the LMM, slide was a random factor and dendritic spines were the participant nested within the slide. We also ran an independent t-test to test if there were differences within groups between the two slides, the results of which indicated there were no significant differences between slides within treatments (results presented in appendix 7.5).

4.3.1 Results- Group 1 mGluRs influence dendritic spine dimensions

The results of the LMM demonstrate significant changes in mean dendritic spine radius when treated with either DHPG (50µM, 20 minutes, n=10) (Figure 4.3.1, Table 4.3.1) or MPEP (50uM, 20 minutes, n=10) (Figure 4.3.1, Table 4.3.1). Both had an increased radius compared with control (DMSO, 50µM, 20 minutes, n=6) (control estimated marginal mean (EMM) 0.736µm vs DHPG 1.208µm and MPEP 1.353µm).

Table 4.3.1- *The results of linear mixed model comparing the effect of group 1 mGluRs on EMM radius of dendritic spine*

Comparison	Mixed Model Result	Normality of Residuals	Independence of Residuals	Linearity of observed v residuals
DHPG 50µM vs Control	F(1,13)=10.061; p=0.007	W(15)=0.842; p=0.013	Satisfied	Satisfied

MPEP 50µM vs Control	F(1,12)=5.648; p=0.035	W(14)=0.954; p=0.632	Satisfied	Satisfied

Both DHPG 50µM and MPEP 50µM (Figure 4.3.1) increased the mean volume of the dendritic spine compared with control, although neither were significantly different. Compared with control it was the MPEP treatment which had the greatest increase (control DMSO EMM 6.461µm^3 vs MPEP 25.01µm^3 (Figure 4.3.1, Table 4.3.2)).

Table 4.3.2*- Results of linear mixed model comparing the effect drug treatment has on volume of dendritic spines*

Comparison	Mixed Model Result	Normality of Residuals	Independence of Residuals	Linearity of observed v residuals
DHPG 50µM vs Control	F(1,13)=4.2; p=0.061	W(15)=0.974; p=0.910	Satisfied	Satisfied
MPEP 50µM vs Control	F(1,12)=4.344; p=0.059	W(14)=0.924; p=0.247	Satisfied	Satisfied

The effect of DHPG and MPEP on the mean cross-sectional area of the dendritic spine obtained from line profile analysis was analysed with an LMM. This, similar to the volume analysis, highlighted the result of treatment with MPEP increasing the size of the dendritic spine. In this measurement parameter MPEP 50µM (Figure 4.3.2) was significant compared with control (Table 4.3.3). DHPG 50 µM (Figure 4.3.2) was not significant and as with the volume measurement it was slightly behind the increase seen in MPEP treatment (EMM MPEP 15.937µM^2, DHPG 12.822µM^2 compared with DMSO control 8.169µM^2 (Figure 4.3.2).

Table 4.3.3*- The results of linear mixed model comparing the effect of drug treatment has on cross-sectional area of dendritic spines*

Comparison	Mixed Model Result	Normality of Residuals	Independence of Residuals	Linearity of observed v residuals
DHPG 50µM vs Control	F(1,14)=2.465; p=0.139	W(16)=0.966; p=0.777	Satisfied	Satisfied
MPEP 50µM vs Control	F(1,13)=5.03; p=0.043	W(15)=0.96; p=0.698	Satisfied	Satisfied

The last parameter of the height image analysis to be evaluated was roughness (RMS). There were no significant changes in average roughness when treatment groups were compared to respective controls (Table 4.3.4 Figure 4.3.2).

Table 4.3.4*- Results of linear mixed model comparing the effect of drug treatment on EMM Roughness (RMS) of dendritic spine*

Comparison	Mixed Model Result	Normality of Residuals	Independence of Residuals	Linearity of observed v residuals
DHPG 50µM vs Control	F(1,13)=3.292; p=0.093	W(15)=0.944; p=0.433	Satisfied	Satisfied
MPEP 50µM vs Control	F(1,12)=1.621; p=0.227	W(14)=0.826; p=0.011	Satisfied	Satisfied

4.3.2 CB1 did not affect dendrite dimensions

Table 4.3.5*- The results of linear mixed model comparing the effect of drug treatment on EMM radius of dendritic spine*

Comparison	Mixed Model Result	Normality of Residuals	Independence of Residuals	Linearity of observed v residuals
AM-251 50µM vs Control	F(1,13)1.250; p=0.284	W(15)=0.969; p=0.843	Satisfied	Satisfied
AEA 50µM vs Control	F(1,17)=0.114; p=0.739	W(19)=0.961; p=0.598	Satisfied	Satisfied

In all measures of dendritic spines scanned with AC mode AFM, AEA 50µM (n=10) or AM-251 50µM (n=11, 20 minutes) caused no significant changes in radius (Table 4.3.5 and Figure 4.3.1), dendrite volume (Table 4.3.6 and Figure 4.3.1), dendrite cross sectional area (Table 4.3.7 and Figure 4.3.2) and dendrite membrane roughness (RMS) (Table 4.3.8 and Figure 4.3.2).

The number of dendritic spines sampled were small and only two slides containing cells from five embryos per slide were scanned. To assess this a power analysis was performed using GLIMPSE sample size software. The low sample number was expected to be an issue for the non-normal distribution of residuals. However, when the data was put into glimpse the power of the study was 0.951. This would imply that, despite large standard deviation for some measurements (particularly volume), the study was sufficiently powered.

Table 4.3.6*- Results of linear mixed model comparing the effect of drug treatment on EMM volume of dendritic spine*

Comparison	Mixed Model Result	Normality of Residuals	Independence of Residuals	Linearity of observed v residuals
AM-251 50µM vs Control	F(1,13)=0.332; p=0.574	W(15)=0.954; p=0.584	Satisfied	Satisfied
AEA 50µM vs Control	F(1,17)=0.230; p=0.637	W(19)=0.91; p=0.075	Satisfied	Satisfied

Table 4.3.7*- Results of linear mixed model comparing the effect of drug treatment on EMM area of cross section of dendritic spine*

Comparison	Mixed Model Result	Normality of Residuals	Independence of Residuals	Linearity of observed v residuals
AM-251 50µM vs Control	F(1,14)=4.44; p=0.54	W(16)=0.895; p=0.068	Satisfied	Satisfied
AEA 50µM vs Control	F(1,17)=1.278; p=0.274	W(19)=0.954; p=0.464	Satisfied	Satisfied

Table 4.3.8*- Results of linear mixed model comparing the effect of drug treatment on EMM Roughness (RMS) of dendritic spine*

Comparison	Mixed Model Result	Normality of Residuals	Independence of Residuals	Linearity of observed v residuals
AM-251 50µM vs Control	F(1,13)=1.824; p=0.199	W(15)=0.942; p=0.409	Satisfied	Satisfied
AEA 50µM vs Control	F(1,17)=0.159; p=0.695	W(19)=0.9; p=0.048	Satisfied	Satisfied

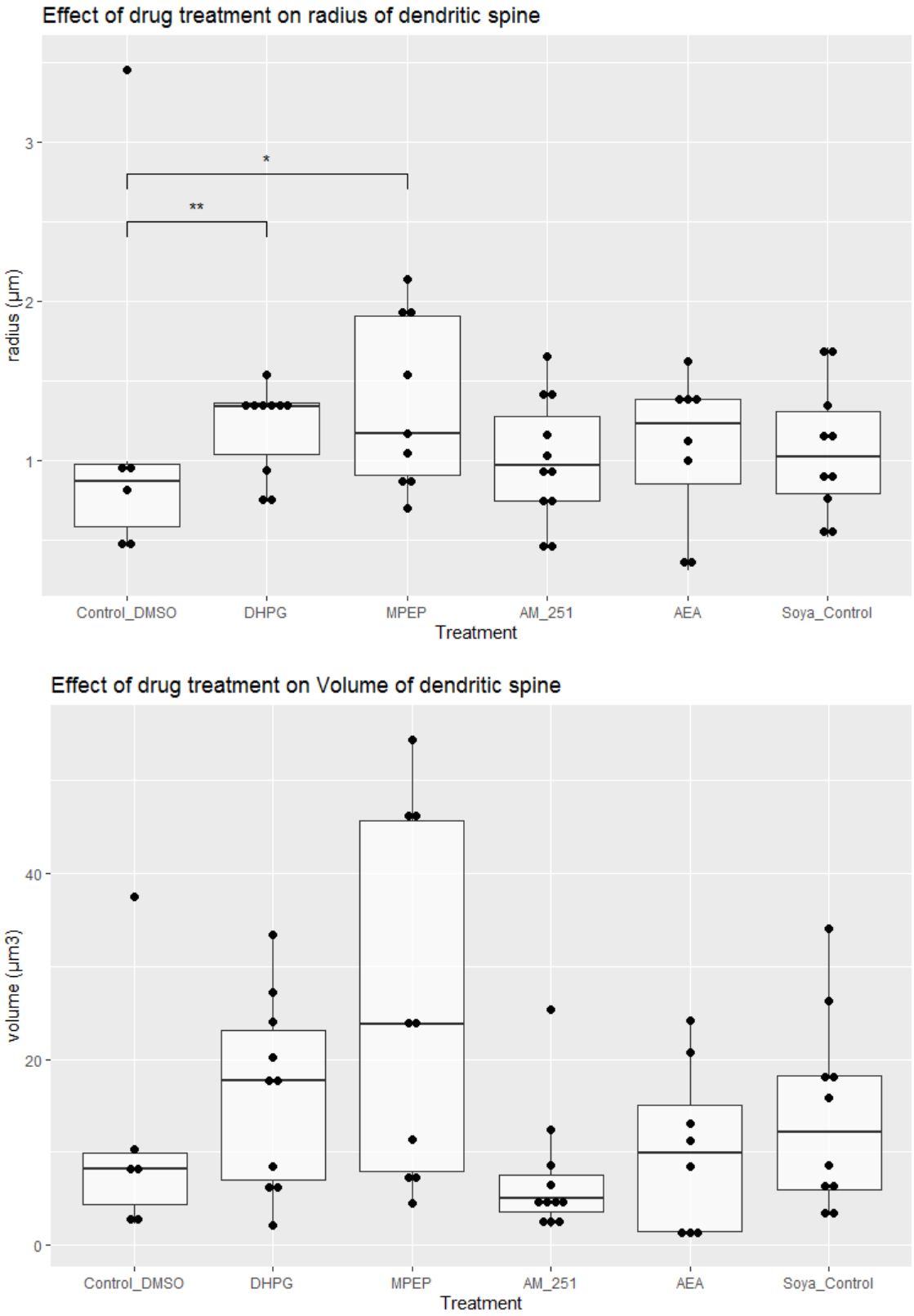

Figure 4.3.1*- Boxplots of the radius (Top) and volume (bottom) of dendritic spines in each treatment group. Significance compared to vehicle control indicated by asterisk (*=p<0.05, **=p<0.005, ***=p<0.001). n=6-11 dendritic spines*

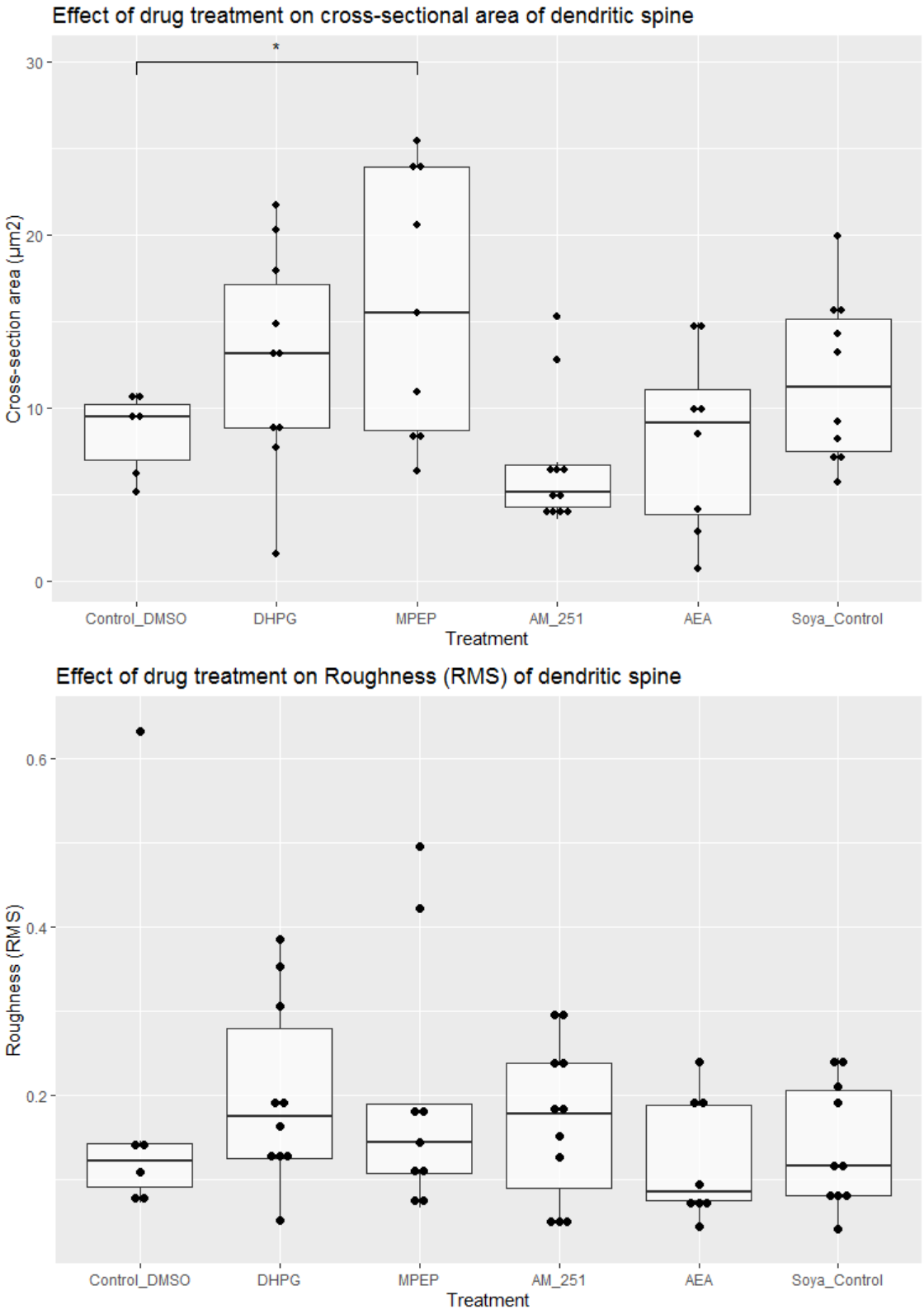

Figure 4.3.2*-Boxplots of the mean cross-sectional area (top) and mean roughness (bottom) of dendritic spines in each treatment group. Significance compared to vehicle control indicated by asterisk (*=p<0.05, **=p<0.005, ***=p<0.001). n=6-11 dendritic spines*

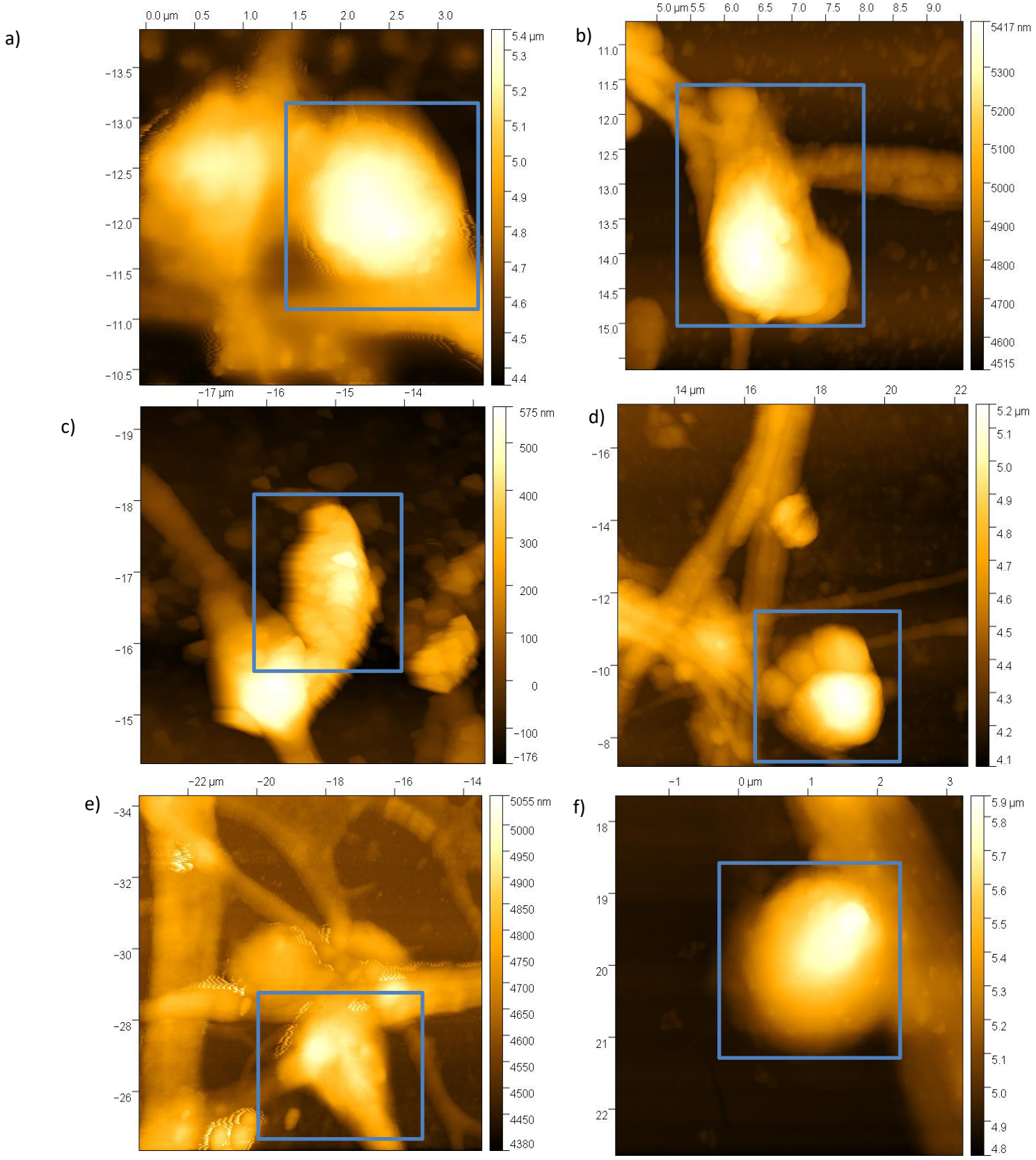

Figure 4.3.3- *A figure of representative dendritic spines (blue box) in each group. a) Control (DMSO), b) DHPG 50µM, c) MPEP 50µM, d) AM-251 50µM, e) AEA 50µM, f) Control (Soya)*

4.4 Loss tangent analysis of dendritic spine membranes

Treatment with DHPG 50µM (20 minutes), significantly altered the loss tangent (Figure 4.4.1 and Table 4.4.1). MPEP 50µM (20minutes) also significantly affected the loss tangent (Figure 4.4.1 and Table 4.4.1). When looking at the original measurements, both DHPG (mean loss tangent of dendritic spine 0.44) and MPEP (mean loss tangent of dendritic spine 0.42) had considerably lower loss tangents than the control DMSO (0.84), suggesting the membranes were harder and more repulsive than control. AM-251 and AEA had no significant effect on loss tangent.

Table 4.4.1*- Results of linear mixed model comparing the effect of drug treatment on the loss tangent measurement of dendritic spines*

Comparison	Mixed Model Result	Normality of Residuals	Independence of Residuals	Linearity of observed v residuals
DHPG 50µM vs Control	F(1,13) = 5.844; p= 0.031	W(15) = 0.883; p=0.052	Satisfied	Satisfied
MPEP 50µM vs Control	F(1,12) = 14.758; p= 0.002	W(14)=0.922; p=0.236	Satisfied	Satisfied
AM-251 50µM vs Control	F(1,14)=3.140; p=0.098	W(16)=0.903; p=0.091	Satisfied	Satisfied
AEA 50µM vs Control	F(1,17)=1.738; p=0.205	W(19)=0.978; p=0.912	Satisfied	Satisfied

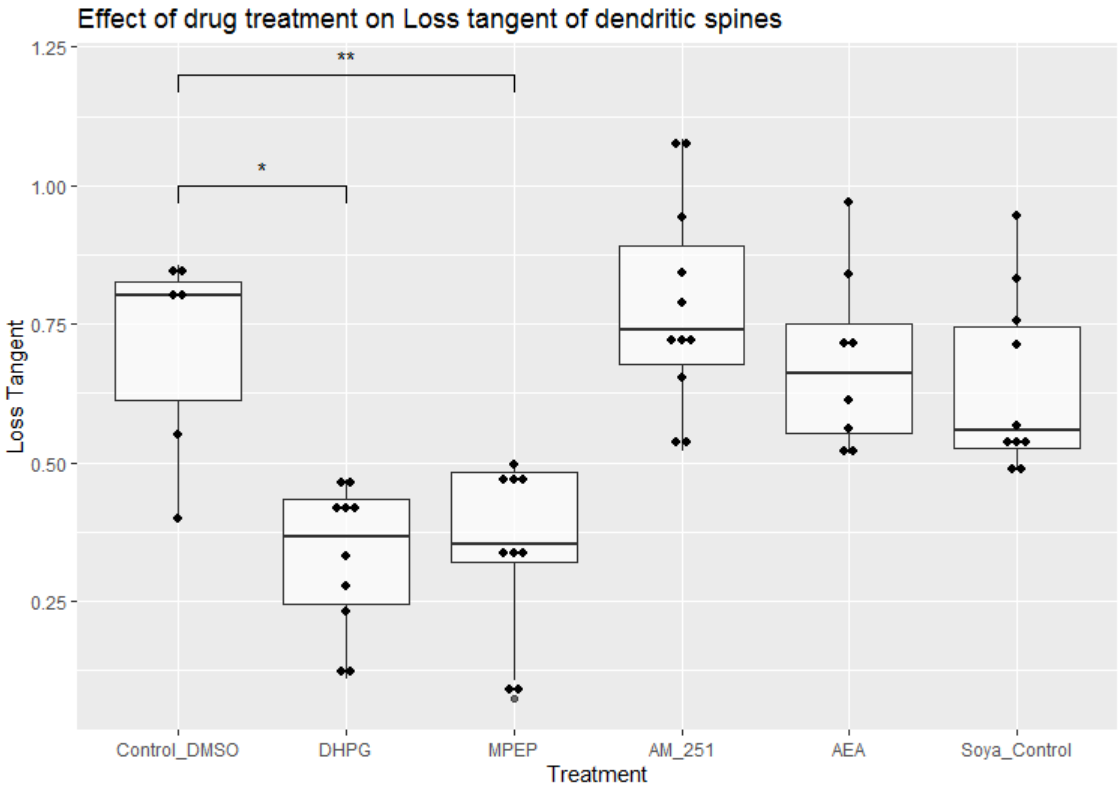

Figure 4.4.1*-Boxplot of the loss tangent measurement of dendritic spine membrane compared with vehicle control. (*=p<0.05, **=p<0.005, ***=p<0.001) n=6-11 dendritic spines*

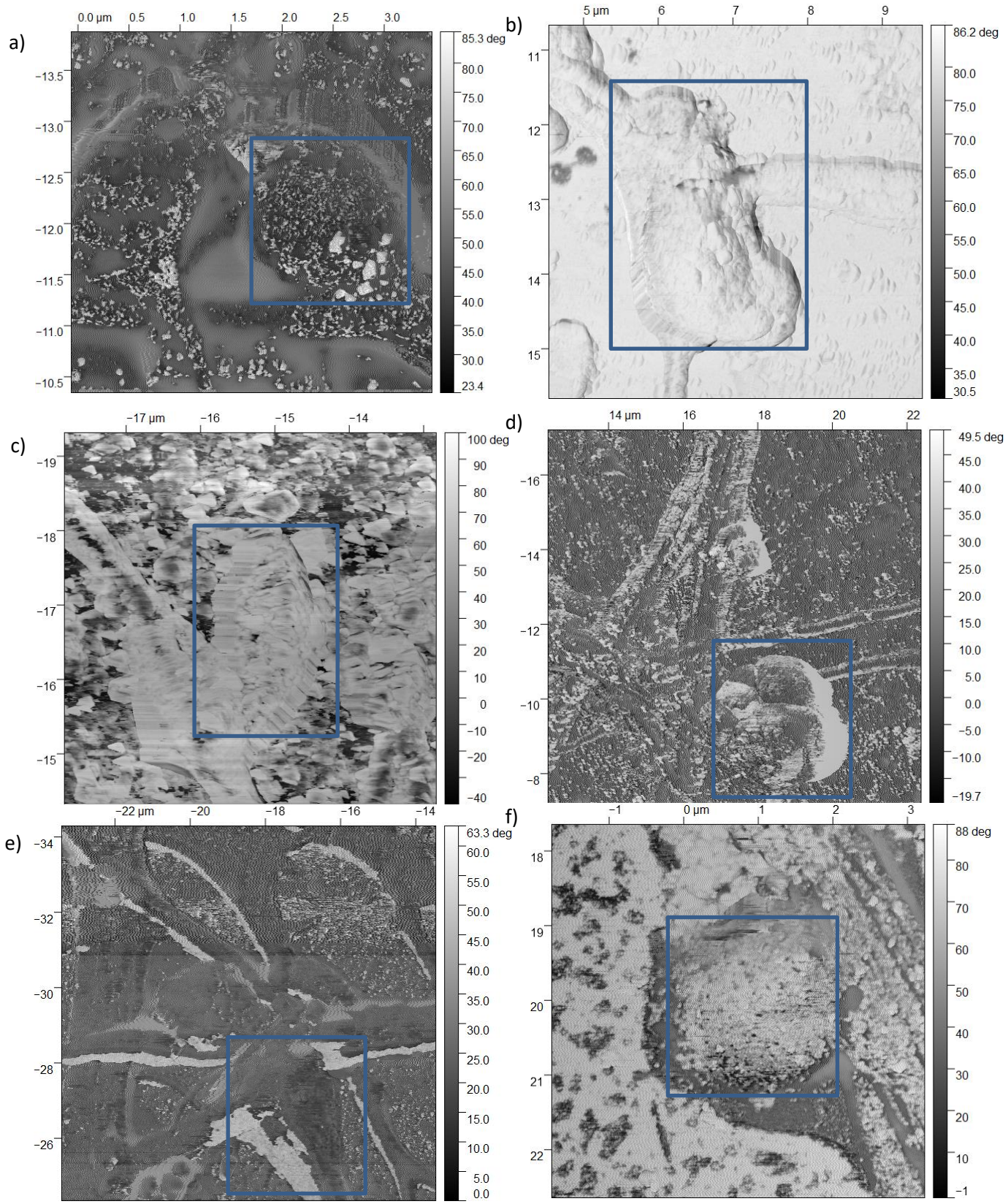

Figure 4.4.2*- Demonstration of the phase images of one dendritic spine from each group the same spine demonstrated in figure 4.3.3. a) Control (DMSO), b) DHPG 50µM, c) MPEP 50µM, d) AM-251 50µM, e) AEA 50µM, f) Control Soya 50µM*

4.5 Discussion

4.5.1 Dendritic spines identified with AFM in primary culture of spinal neurons

This is the first evidence that dendritic spines exist in the spinal neurons of *X. laevis* tadpoles. Using the AFM and an inverted microscope it was possible to scan dendritic spines with a high resolution and minimal technical noise, in a primary spinal cord culture at 3 DIV. Dendritic spines have been scanned with AFM before. However, a measurement criterion has not been adopted. Using previous literature of confocal z-stack images of dendritic spines in culture, the measurement criteria of length and volume was applied to AFM scanned spines in our study. Dendritic spines were identified and quantified based on previous observation, analysis and modelling (Matsuzaki *et al.*, 2004; Bosch *et al.*, 2014; Bosch, Martínez, Masachs, C. M. Teixeira, *et al.*, 2015; On *et al.*, 2017; Basu *et al.*, 2018). Examples of the dendritic spines measured in each group are presented in Figure 4.3.3.

4.5.2 Group 1 mGluRs increased dendritic spine dimensions

As shown in chapter 3, DHPG increases the frequency of swim-cycles and based on the action of the group 1 mGluRs in previous studies in *X. laevis* (Chapman and Sillar, 2007; Chapman, Issberner and Sillar, 2008) and in other animal organisms (Kettunen *et al.*, 2002, 2005; Kettunen, Hess and Manira, 2003;), may be expected to increase the excitability of the excitatory interneurons and grow dendritic spines through the increase in Ca^{2+}, activation of kinases such as CAMKII, the regulation of transcription factors and the subsequent increase in protein transcription. However, it is well recognised that 100µM DHPG application for 10 minutes in the hippocampus will induce LTD (Palmer *et al.*, 1997). It is worth noting that CAMKII activation is not a prerequisite for potentiation and it is involved in LTD and LTP, the defining factor is rate of activation. Constitutively activated CAMKII will continue to grow dendritic spines but CAMKII activated for less than 1 minute at a time can lead to phosphorylation events that promote depression (Lee *et al.*, 2009). Further investigation in the hippocampus revealed that 100µM application of DHPG (10-30minutes) resulted in dendrite elongation (Vanderklish and Edelman, 2002). In that study it was shown that Ca^{2+} increase was key to this elongation. The fact we observed an increase in radius with DHPG at 50µM, might suggest that it is the excessive activation of group 1 mGluRs with 50µM- 100µM that elongates the dendritic spine, and this may be a sign of LTD-like changes in spine morphology. It was noted that elongation in the hippocampus was not accompanied by increase in volume, so it may be that DHPG-induced LTD in the hippocampus results in elongated dendritic spines whereas potentiated dendritic spines increase in volume in the *X. laevis* spinal cord, or that

DHPG enhance the spinal cord CPG by depressing adjacent synapses so on average dendritic spines are elongated and depressed allowing excitatory gap junctions to enhance dIN depolarisation rate. It would be interesting to examine the effects at particular neuron groups *in vivo* to assess dendritic spine changes at dIN compared with other neuron groups, such as cINs and aINs.

The rather surprising result is the bigger average increase seen when cultures were treated with MPEP 50µM. It was expected that antagonism of the $mGluR_5$ for such a short time (20 minutes) would not affect dendritic spines. $MGluR_1$ and $mGluR_5$ can have several splice variants and their locations can differ, meaning there is a great deal of variability in their action. However, it is generally accepted that activation of $mGluR_1$ and $mGluR_5$ leads to phospholipase C γ (PLCγ) activation and IP3 induced release of Ca^{2+} from stores in the endoplasmic reticulum that can enhance activation of CAMKII. Also, the activation of PI3K and PDK1 can stimulate mtor and NFkappaB transcription of survival and growth genes, and AKT phosphorylation can inhibit apoptosis (Willard and Koochekpour, 2013). MPEP inhibits $mGluR_5$ but it may also antagonise NMDA receptors (O'Leary *et al.*, 2000) and be an positive allosteric modulator of $mGluR_4$ (Mathiesen *et al.*, 2003). The antagonism of NMDA receptors could be helping promote LTD for which elongation may be a measure (results presented in Table 4.3.1 and Figure 4.3.1).

Evidence for the increase in volume of dendritic spines with constitutively active CAMKII demonstrates the role CAMKII plays in the potentiation and growth of the dendritic spine. This process is blocked by NMDAR antagonism (Lee *et al.*, 2009). Activation of the group 1 mGluRs has long been a model for LTD in the hippocampus, and elongation of dendritic spines was observed under LTD inducing conditions (100µM DHPG + LFS, 10 minutes) (Vanderklish and Edelman, 2002; Cruz-Martín, Crespo and Portera-Cailliau, 2012). We provide further evidence for the elongation of dendritic spines with the treatment of DHPG. Since we did not observe a significant increase in volume this might indicate reduced signalling in the dendritic spines measured. However, this then asks the question what is happening in the MPEP treated dendritic spines? In all categories of size; radius, volume and cross-sectional area MPEP had a greater effect than DHPG. It seems impossible that this is a result of potentiation. MPEP is an interesting molecule and has been shown to be a positive allosteric modulator of $mGluR_4$ (a presynaptic metabotropic glutamate receptor responsible adenylyl cyclase inhibition) and a mild antagonist of NMDAR (O'Leary *et al.*, 2000). In a whole organism the inhibition during a behaviour decreases the excitability of the neuron, inhibiting existing signalling that would have taken place. In the primary culture the level of signalling will not be

as strong and is likely to be very different from *in vivo.* As demonstrated in previous studies, from 24 hours onwards the neurons in primary *X. laevis* cultures have functional synapses (Yazejian, *et al.*, 2013), and as discussed earlier twitching muscle cells were observed throughout the cultures, indicating spontaneous signalling. It is possible that the interference with normal signalling, caused by $mGluR_5$ antagonism and mild NMDAR antagonism, combine to change the dendritic spine structurally especially given the developing nature of the culture. Another avenue that should be explored is the inactivation of the RNA binding protein FMRP. Activation of $mGluR_5$ initiates a number of signalling cascades that can lead to growth of dendritic spines. However, it also activates FMRP, which binds RNA and can stop local protein synthesis. The abnormality in this gene is thought to be responsible for fragile X syndrome. Evidence has shown that during development, *in vivo* and *in vitro,* glutamate elongates dendritic spines through $mGluR_5$. This elongation was not observed in FMRP knockout or with MPEP application (Cruz-Martín, Crespo and Portera-Cailliau, 2012). This was performed in cortical pyramidal neurons of immature mice, so there is likely to be differences compared with our study. This data would confirm the effects of DHPG. To explain why MPEP may have increased dendritic spine size, we must consider the conditions of the culture. BDNF was added to the culture media to stimulate growth through TrkB receptor activation. BDNF is a neurotrophic factor thought to be essential in the developing CNS. Combined with the possibility that neurons are releasing glutamate and the observed rapid growth and development over the first 48 hours, the cultures are in a high state of growth. BDNF through the TrkB receptor initiates many of the same excitatory signalling cascades as glutamate, such as PI3K, IP3, PLC, NFkB and Erk1/2 (Gupta *et al.*, 2013). There is evidence showing that BDNF interacts with FMRP (Louhivuori *et al.*, 2011). In FMRP knockout mice BDNF's effects lead to abnormal dendritic spine development. It was noted in this study that there were large differences between cortical neurons and hippocampal neurons, as such it would be difficult to draw conclusion across species and neuron groups, but based on the signalling cascade they are involved in, there is a high probability of an interaction between them. This interaction in our study might be that $mGluR_5$ antagonism via MPEP has attenuated the negative regulation of FMRP on BDNF development of dendritic spines. This combination of BDNF and MPEP leads to a fragile X autism like developmental culture.

Next, a rather interesting study showed that FMRP has effects beyond transcription, through interaction with Bk channels (voltage activated potassium channels) it has a role in regulating neurotransmitter release, by modulating action potential duration. FMRP knockout leads to excessive action potential broadening, enhanced presynaptic Ca^{+} influx and elevated

neurotransmitter release (Deng *et al.*, 2013). This combination of BDNF and FMRP inactivity (due to MPEP antagonism of $mGluR_5$) may have contributed to an increase in dendritic spine size. It would be interesting to test this culture without BDNF in the culture media, to assess if this is the interaction causing these results or it is simply that antagonism of $mGluR_5$ has blocked FMRP activation in this developing culture. If this is the case, we would need to assess how regularly and how much glutamate is released during spontaneous signalling in this culture setting. If very little glutamate is released spontaneously it would be questionable that $mGluR_5$ antagonism should change the morphology of dendritic spines. If lots of glutamate is released during development, then it is reasonable that MPEP has these effects.

Given that DHPG did not significantly affect volume, we would suggest that on average the dendritic spines in this group followed previously reported results demonstrating a role for group 1 mGluRs in dendritic spine elongation in developing cultures (Cruz-Martín, Crespo and Portera-Cailliau, 2012). The two treatments which activate/inhibit post-synaptic receptors ($mGluR_{1/5}$) present in dendritic spines, both caused measurable changes in dendritic spine size and membrane loss tangent. The results are supported by the fact that the CB1 agonism/antagonism did not cause any measurable changes in dendritic spine size or membrane loss tangent. This could be expected given its presynaptic location.

4.5.3 CB1 receptor did not affect dendritic spine dimension

The agonism (AEA 50µM) or antagonism (AM-251 50µM) of the presynaptic CB1 receptor produced no measurable changes in the dimensions of dendritic spines. The CB1 receptor has been linked to synapse depression and one of its key functions in the short term is to inhibit neurotransmitter release. Beyond this it inhibits adenylyl cyclase, which is often thought to decrease growth through decreased CREB transcription of growth factor activation, although CREB transcription is a broad and often cell-type dependent transcriptions factor. For the activation or inhibition of CB1 receptor to affect dendritic spines it would have to be through secondary effects. If for example the CB1 had inhibited neurotransmitter release to such an extent as to stop glutamate exciting and growing dendritic spines, then some change in dendritic spine dimensions may have occurred. As it did not, we can assume the effect of reduced neurotransmitter release had minimal if any structural effects on the dendritic spines. In the future it would be pertinent to examine the dendritic spines during and after high frequency stimulation induced-LTP (HFS-LTP) with cannabinoid application which has been shown to have a bidirectional role in LTP or LTD of a synapse (Cui *et al.*, 2015). This, alongside treatment with $mGluR_{1/5}$ agonist/antagonist application, could help elucidate this relationship.

$MGluR_{1/5}$ has been studied extensively in LTP and LTD protocols, but its relationship with CB1 is still undetermined, particularly in the hippocampus.

4.5.4 Group 1 mGluR treated dendritic spines have harder membranes measured through loss tangent

During structural changes in the dendritic spine, the tension or viscosity of the membrane is likely to change as the actin cytoskeleton is remodelled. Young's modulus assessment (described in the introduction) of cell membranes has been used extensively. However, there are limitations to this method. One of the limitations lies within the size of dendritic spines. Locating them and performing force measurements is challenging in live neurons. Also, there are other disadvantages, such as tearing or puncturing the cell membrane. AC mode AFM protects the sample, the tip having very limited contact. AC mode also produces phase images. These are graphical heat maps depicting the degrees of phase shift the cantilever/tip has undergone due to the sample, compared with the expected path of the tip based on the set-point, drive amplitude and frequency. As such, the phase measurement is said to represent the tip-sample interaction. General assessment of these images suggests that low-negative phase degrees measurements represent an attractive interaction, with high degrees shift representing repulsion/hard materials. The problem with phase imaging in the past is the result is not comparable between images due to changes in drive amplitude, set-point, frequency and scan rate altering the force of tip-sample interaction. Recent developments in the algebra of this problem have lead researchers to the loss tangent (Proksch *et al.*, 2016). This calibrates the phase shift by tying it to changes in the amplitude through trigonometry (equations provided in methods section 2.4.4). The outcome of this equation is to produce a unit less ratio where 0 represents a hard surface and 1 would be a very viscous surface.

Both group 1 mGluR activation and $mGluR_5$ inhibition caused significant changes in the stiffness of the membrane measured by loss tangent (Proksch *et al.*, 2016). As discussed in the introduction, changes in dendritic spine signalling are accompanied by structural changes which enhance/reduce the size of the PSD and result in enhanced/reduced receptor expression and positioning. In our cultures they were treated with the drug then fixed in glutaraldehyde. The glutaraldehyde fixation works by crosslinking the cytoskeleton. If there was an increase of F-actin within the 20 minutes, then fixation, it is possible that this would make the membrane stiffer, due to a higher degree of cross-linking internally. Also, receptors would register as harder than the membrane so increased receptor expression would be expected to give a lower loss tangent value. The combination of the two events may suggest that we should have observed harder membranes for potentiated spines and softer

membranes for depressed spines. The lack in volume increase with elongation may suggest the opposite. It is possible that under these conditions, dendritic spine remodelling; whether it be to enhance the dendritic spine or depress the dendritic spine; will give harder membrane measurements when fixed regardless of which direction the synapse is heading as there is increased protein activity and actin remodelling required for any change in spine morphology. This may mean that in a fixed culture loss tangent will only tell us if the spine or cell was undergoing some transition. If this was used in living cells with new high-speed AFM scanning and the software to produce the loss tangent channel, we could obtain almost real time information on the changes in loss tangent at cell membranes. This would be much more relevant as it may allow us to detect immediate changes in viscosity during LTP and LTD conditions which could then be used as a template for further investigations in pharmacology and neuroscience.

4.5.5 Assessment of method

While the results are extremely interesting, and the method used to collect them was robust, this was a process of development and could be improved upon. The most important improvement would be increased sampling per slide. At set out it was expected that at least five different dendritic spines would be scanned on each of the slides treated per group with at least three slides scanned. However, due to unforeseen circumstances and significant time delays this was not achieved, meaning our total sample size was 53 dendritic spines, 6-11 per treatment group and only 2 slides scanned. In hindsight, with the variability in spine size and morphology evident in Figure 4.3.3, five per slide seems too little. The power analysis performed on GLIMPSE indicated the study was sufficiently powered. However, I would still question whether 10 dendritic spines per group is a large enough sample size, given the variability in measurements of the control groups. If we look at Figure 4.3.3 the variation in spine morphology is clear to see. One factor that might have been worth assessing, but was not in this method, was whether the dendritic spines were forming or close to forming a synapse. This figure demonstrates that there was variation in this respect. On a review of the images the majority of the spines identified were not forming a synapse. This was generally a practical reason as it was easier to scan the small protrusions on their own. As one can see in Figure 4.3.3a and e, there is more technical noise than the other images and these were the good scans of synapses. There were many synapses identified that simply could not be scanned. It is also evident in Shibata et al's (2015) paper that some noise and disruption at the synapse has not been resolved, but given the speed of their scan and the number of images generated in a short space of time, this noise can be overcome. Our scans took up to 40

minutes depending on size of the scan area and sometimes the image produced was not good enough quality for analysis. As can be seen in Figure 4.4.2 there is a great deal of variation is the degrees measurement between images. This initially meant phase images were only assessed qualitatively. The development of the loss tangent equation by Proksch et al has changed this dramatically. By considering the variation in the scans it normalises the data into a unitless ratio enabling comparison between scans and between treatments.

Repeatability is an issue in this study. For two observers to get the same result they would have to scan the entire slide to find the same dendritic spines I found in the cultures. Once dendritic spines are identified the method of measurement criteria can be followed to achieve the same results. The loss tangent measurement I used was subjective as I selected an area of the membrane then took an average of phase to put into the loss tangent equation. Programs have been developed which give the loss tangent as an output channel, meaning the entire phase image is converted into loss tangent and each pixel can be measured for its hardness. This would offer a much more detailed examination of the changes in membrane tension than the method I carried out.

It would be desirable to induce LTP using stimulatory protocols (High frequency stimulation) and chemical protocols (NMDA 100µM, Mg^{2+} free solution) and LTD protocols (low frequency stimulation + DHPG 100µM or chemical LTD DHPG 100µM + high Mg^{2+} solution). This way any ambiguity in the direction of change could be tested against known parameters. The next issue was all samples were fixed and air-dried. This would significantly affect the integrity, stiffness and viscoelasticity of the membrane. This also made problems for AFM scans as varying degrees of moisture affect the tip-sample interaction (phase shift). If the experiment was repeated in a fluid cell the cells could be live and the measurement of changes in membrane viscosity would be much more relevant. Although these conditions are not desirable it was the same for all treatments and the controls they were compared with. Compared with confocal z-stack, this method offers more detail ,although interpreting that detail is tricky. Also scanning dendritic spines with AFM only measures one half of the spine. As can be seen from the images they are far from uniform in shape and size so losing the underside of the spine means measurements are only ever an estimation.

There were dendritic spines in the culture, but they were sparse meaning lots of tips were lost scanning objects that turned out not to be dendritic spines. If we were to continue trying to develop methods measuring structural plasticity of dendritic spines with AFM, it would be recommended to use a model such as the granule cells previously mentioned (Zhang, Huang and Hu, 2016) or the classical neurons studied for dendritic spines, pyramidal neurons

of the hippocampus. This way large group sizes would be made more achievable. It would also be interesting to compare the differential effects treatment have on dendritic spines of immature cultures vs mature cultures as this may help tease apart the effect of group 1 mGluRs. One of the main issues with this study comes from idrentifying what type of neuron is being scanned and the affect the drug treatment has had on a particular dendritic spine. It would be much more valuable to scan a spine, apply the drug then scan the same spine again. If this was combined with electrophysiological recording, identifying the electrochemical and neurotransmitter properties of the synapse, we could understand how drug treatments are truly interacting in spine remodelling.

4.5.6 Future directions

We have shown that the use of AFM to study dendritic spines is a viable tool. The recent showcasing of long-tip high-speed AFM combined with inverted fluorescent confocal microscopy opens possibilities for dendritic spine structural investigations in near real time. If high-speed long tip AFM is combined with loss tangent calculations, this could give details of immediate changes in membrane viscoelasticity. The value of combining fluorescent confocal with high speed AFM could help eliminate the pitfalls of the two methods and by doing it in real-time, the pharmacologically induced changes could be viewed and measured in close to real-time ((Shibata *et al.*, 2015) scanned a 5µmx5µm sample in 5 seconds). This would enable us to view the movement and estimate concentration of proteins, while measuring the structural changes of the membrane occurring. As we look to the current very exciting work, which demonstrates the relationship between mechanical forces and chemical signals in the development and guidance of neuron growth (Koser *et al.*, 2016), understanding and defining the structural and mechanical properties of neurons in health and disease could provide the key to neuron regrowth and repair. It is in these experiments, using live cells to assess receptors such as piezo 1, that the loss tangent could be an excellent tool in understanding the mechanical properties of the membrane as conditions change, and how this interacts to guide the neurons growth. Live cells also come with drawbacks, such as puncturing. However, the recent developments in high-speed AFM appear to have progressed this to a more viable method of investigation.

*4.5.7 **Conclusions***

Dendritic spines exist in the primary culture of stage 22-24 *X. laevis* spinal neurons at 3 DIV and they can be observed by scanning with AFM. The structural dimensions appear to be significantly changed when group 1 mGluRs are activated or $mGluR_5$ is inhibited and in both these conditions the loss tangent measurements indicate the membrane became harder.

5 Fluorescent immunohistochemistry of PSD-95 in *X. laevis*

5.1 Introduction

In the previous result chapters, evidence was provided that manipulation of group 1 mGluRs and CB1 receptors induce changes in the output of the CPG and muscle flexion. Then, possible events of plasticity at dendritic spines were investigated *in vitro,* using a primary neuron culture, scanned with AFM and assessed for changes in structure. Changes in the activity of $mGluR_{1/5}$ affected the dimensions of the dendritic spines, and resulted in a harder membrane measurement via loss tangent. The literature, mostly produced in mature hippocampal slices and cultures, suggests that dendritic spines grow and stabilize before increases in PSD proteins (such as Homer and SHANK) occur. The timescale of dendritic spines undergoing potentiation was suggested to be: 1-7 minutes- increases in actin accumulation and polymerisation to F-actin; 7-60 minutes- stabilisation of newly polymerised actin cytoskeleton via G2 proteins (such as CAMKIIβ, α-actinin and drebrin); 60+ minutes- increases in structural MAGUKS (Homer and SHANK)(Bosch *et al.*, 2014). These results were obtained using quantitative fluorescence and confocal assessment of dendritic spines undergoing LTP protocols and suggest that increases in proteins, such as PSD-95, can take up to an hour. There is other evidence that PSD-95 can be inserted into dendritic spines via microtubules initiated by BDNF (Hu *et al.*, 2011) and that this occurred over the course of 20 minutes. In Hu *et al's* study, it was shown that BDNF increases the length of time microtubules invade dendritic spines and not how many spines are invaded, and it is this increased window that enhanced PSD-95 density. Another study into the dynamics of PSD-95, demonstrated that the density of PSD-95 is fluid, changing rapidly in 20min-1hour. Evidence was provided which indicates PSD-95 is exchanged with neighbouring spines by diffusion and that larger spines accumulated more PSD-95 and retained it for longer. When the mice underwent sensory deprivation, PSD-95 retention and density decreased dramatically (Gray *et al.*, 2006). The conclusions from that work suggests dendritic spines compete for PSD-95 based on their activity, and there is something that 'tags' PSD-95 to larger PSDs where it is needed.

PSD-95 is a key structural protein of dendritic spines. It is responsible for tethering AMPA receptor rafts and can be used as a measure of functional dendritic spines. It has roles in stabilisation of dendritic spines, and increases in PSD-95 density at dendritic spines have been associated with increased signalling efficiency (Ehrlich *et al.*, 2007; Cane *et al.*, 2014; Henley and Wilkinson, 2016). The slot hypothesis would suggest that increases in PSD-95

correlate with increased AMPAR expression or at least increases the probability of increased AMPAR expression on dendritic spine surface.

Since this evidence suggests that PSD-95 is in effect a determining factor if an excitatory synapse is functional, the aim was to investigate if PSD-95 expression changed as a result of the activation/inhibition of group 1 mGluRs and/or the CB1receptors *in vivo* and *in vitro*. Increases in PSD-95 expression may indicate increased level of excitatory synapses, an increase in active synapses or an increase in the ability of the synapses present to tether more AMPARs making it more efficient and increasing the probability of potentiation.

5.2 Methods

As described in section 2.5, the whole tadpoles were fixed in 5% glutaraldehyde for 10 minutes, then they were permeabilised in 0.1% triton X for 15 minutes, and were either incubated with: primary antibody goat-anti-PSD-95 (1:1000, 1 hour, room temp.); secondary antibody (anti-goat fluoro488, 1:1000, 1-hour room temp.); primary antibody (1 hour room temperature) + secondary antibody (1 hour room temperature), or control (no antibodies). The spinal cords/muscle columns were assessed in Image J, selecting and area away from the yok sac and ensuring the area selected was the same section for each group. This was repeated in microtome sections of the tadpole as described in methods section 2.2 and 2.5. The same experiment was also repeated in the cell cultures, first to see if the cells without any antibodies would be fluorescent individually, then to see if areas with high neurite concentration would increase in fluorescence with the correct addition of primary antibody (1:1000, 1-hour room temp) + secondary antibody (1:1000, 1-hour room temp).

5.3 Results

5.3.1 Developing Xenopus laevis tadpoles when fixed with glutaraldehyde are auto fluorescent

The results (Figure 5.2.1a) analysed in SPSSS using a one-way ANOVA with Bonferroni post-hoc analysis showed there was no significant difference between any of the groups (n=3; p=1 for all groups). This was repeated in microtome sections where the spinal cord can be more accurately assessed without fluorescence from other tissues (shown in methods 2.5). The result for this was the same as whole tadpole, with no significant changes in fluorescence intensity between any of the groups (Figure 5.2.2). The results of cell culture assessment

(Figure 5.2.3) demonstrate that no statistically significant changes were seen in the cultures between any groups.

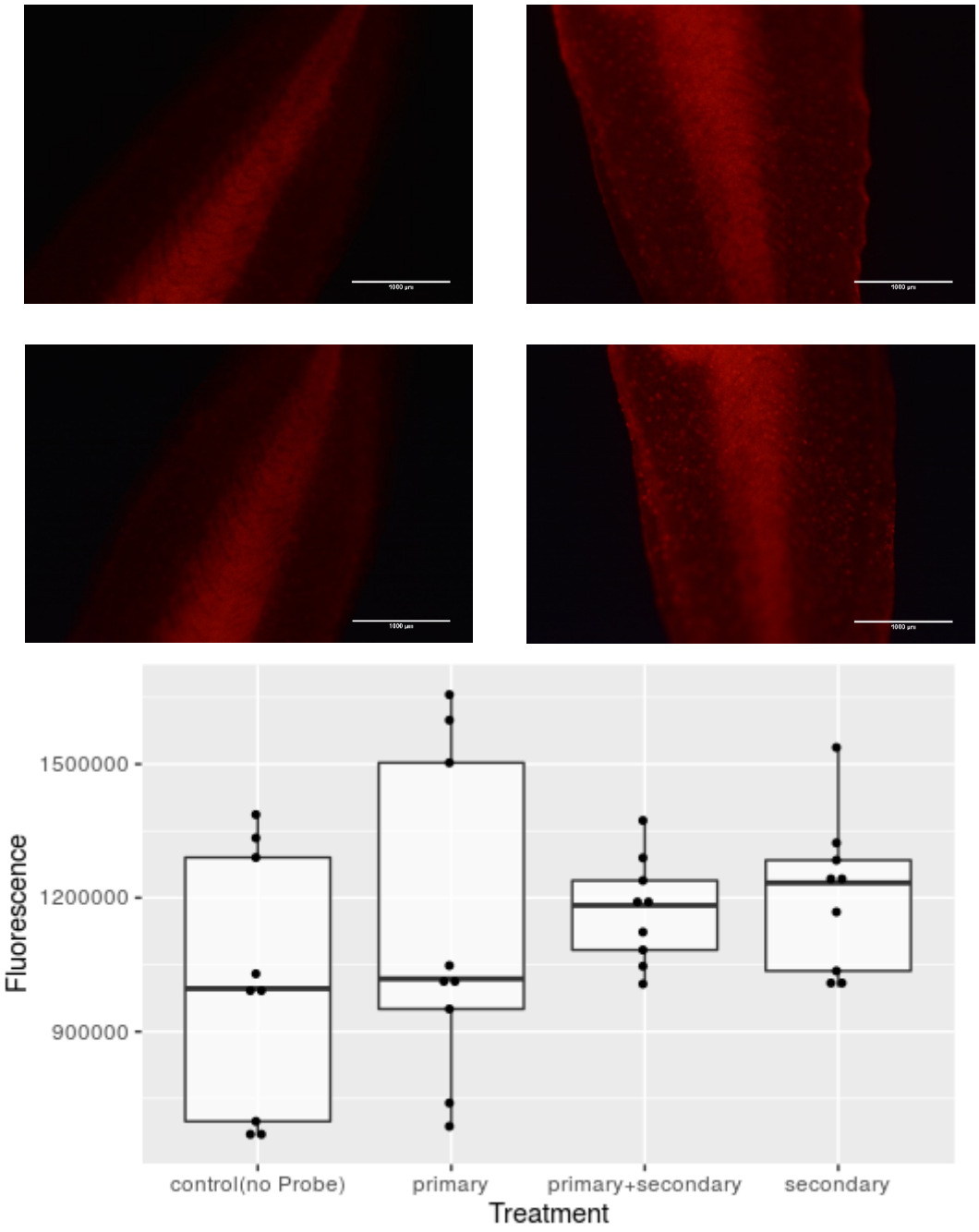

Figure 5.3.1*-Comparing the change in fluorescence of with no antibodies (control), primary antibody only, secondary antibody only and primary then secondary treated tadpoles. Excitation wavelength 470-520nm; n=9. Top- example images of whole tadpole tail fluorescence a) secondary antibody only, b) primary antibody only, c) primary and secondary antibody, d) control no antibodies. Bottom Boxplot of the fluorescence for each Treatment*

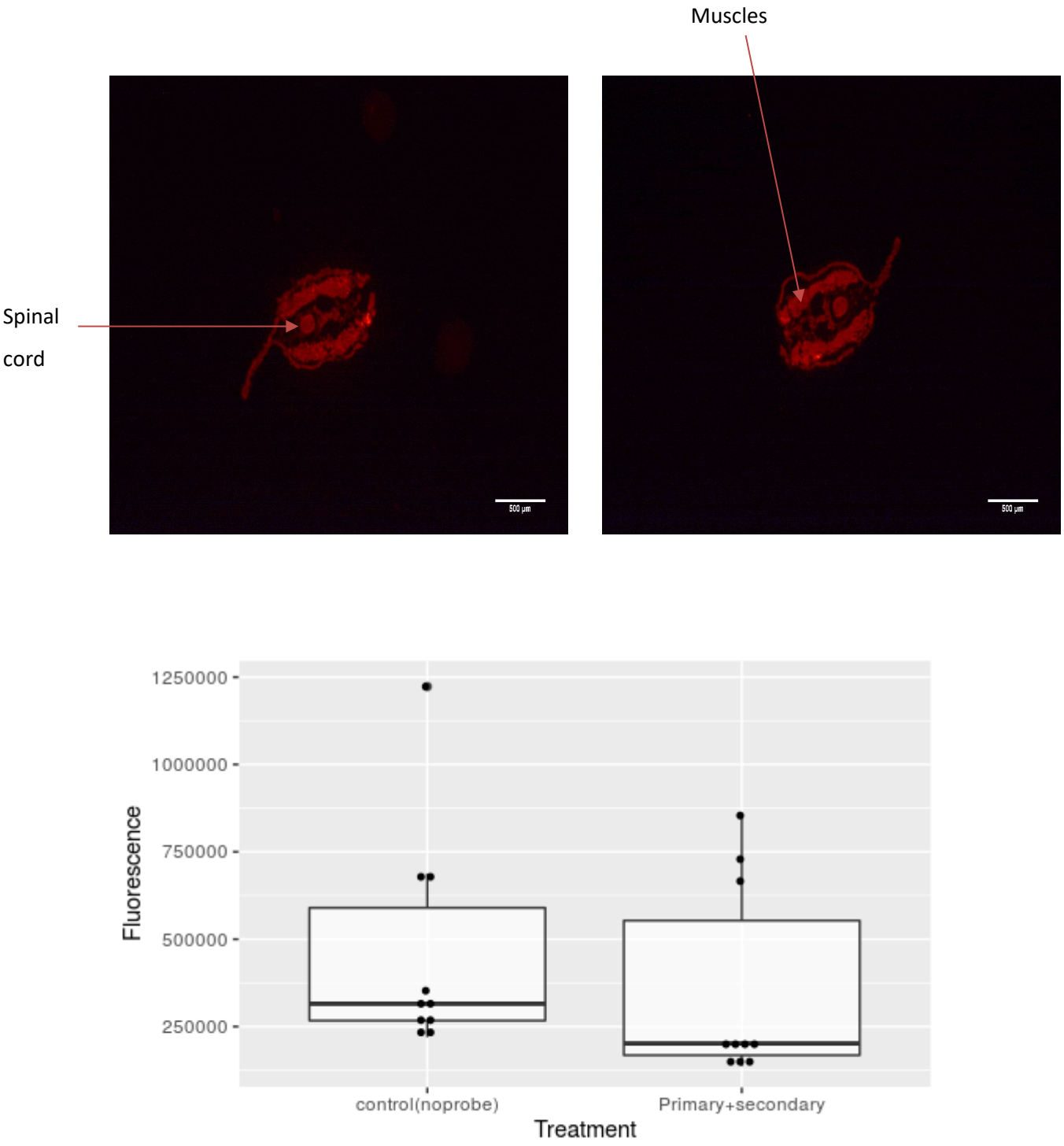

Figure 5.3.2*- microtome slices of stage 40-42 tadpoles. Top- a) example of slice treated with no antibodies b) example slices treated with both primary and secondary. Bottom Boxplot representing change in fluorescence intensity n=10*

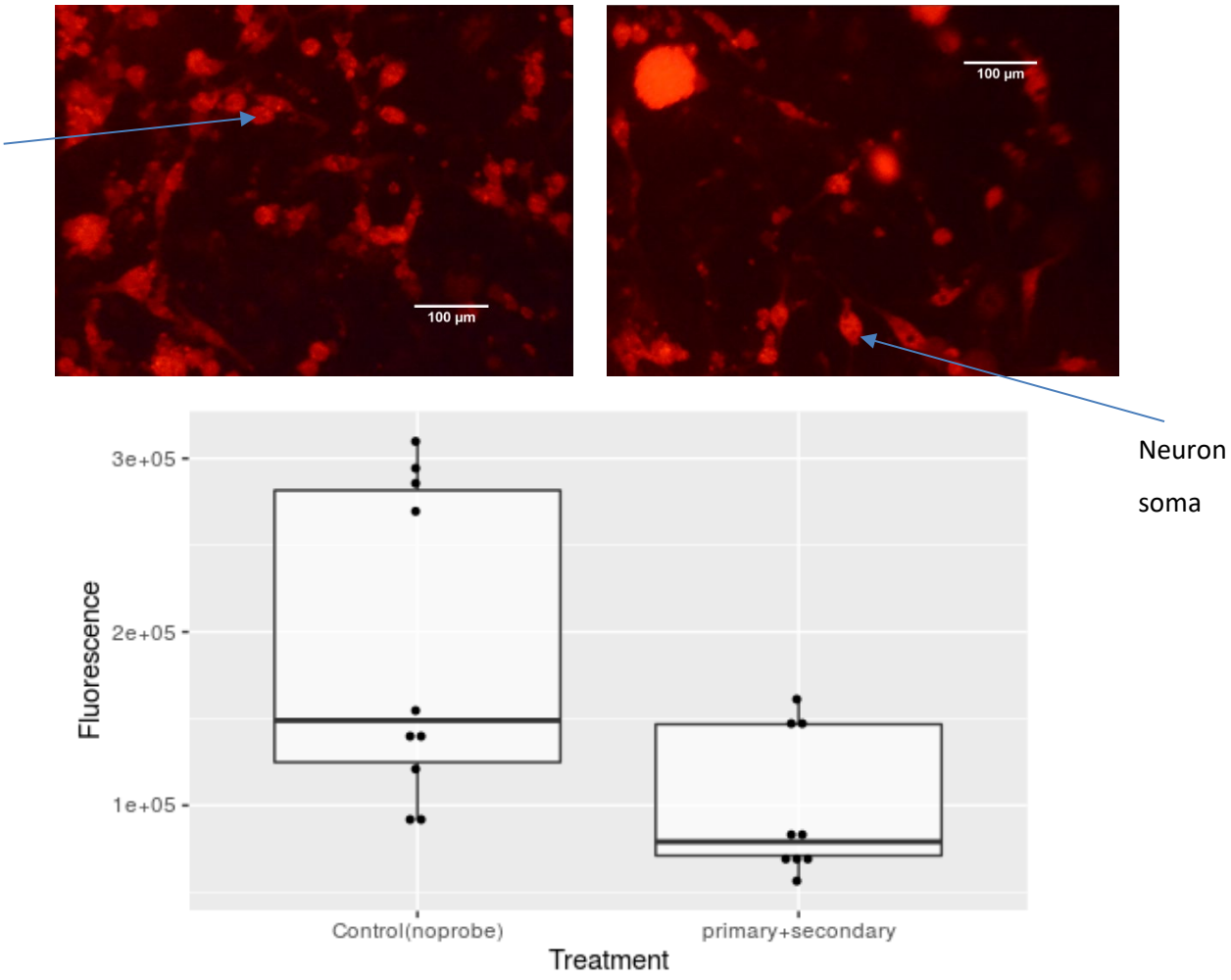

Figure 5.3.3*-Boxplot comparing the fluorescence of neuron cell bodies in culture without antibody application compared with neuron cell bodies with immunohistochemical antibody staining(n=9). Above- example images of the neurons measured left) control with no antibodies added, right) culture with both primary then secondary added, arrows indicate neuron cell body*

5.3.2 Cures for glutaraldehyde induced autofluorescence

There are a few methodological publications which suggest cures for glutaraldehyde, or just aldehyde fluorescence. The most common proposed are: sodium borohydride (Beisker, Dolbeare and Gray, 1987; Wessendorf, 2004) glycine quenching and H_2O_2 bleaching (personal communication). Glycine and hydrogen peroxide 0.3% were methods consistently mentioned on research forums as solutions to autofluorescence, they are also readily available in most labs, so these were tried first. Glycine is hypothesised to work by binding to glutaraldehyde's free amine groups thought to be primarily responsible for high degrees of fluorescence.

5.3.2.1 Result of autofluorescence quenching techniques

After fixation and permeabilization tadpoles were incubated in 50mM glycine for three hours. There was a slight, but not significant decrease compared with the fixed tadpole control. When Primary + secondary antibody was added to the same glycine quenched tadpoles there was still no significant change (Figure 5.2.5). This was the same conclusion for hydrogen peroxide bleaching, which besides probably damaging the tissue, was ineffective at reducing fluorescence compared with control, and once antibodies were added no significant change was observed (Figure 5.2.5).

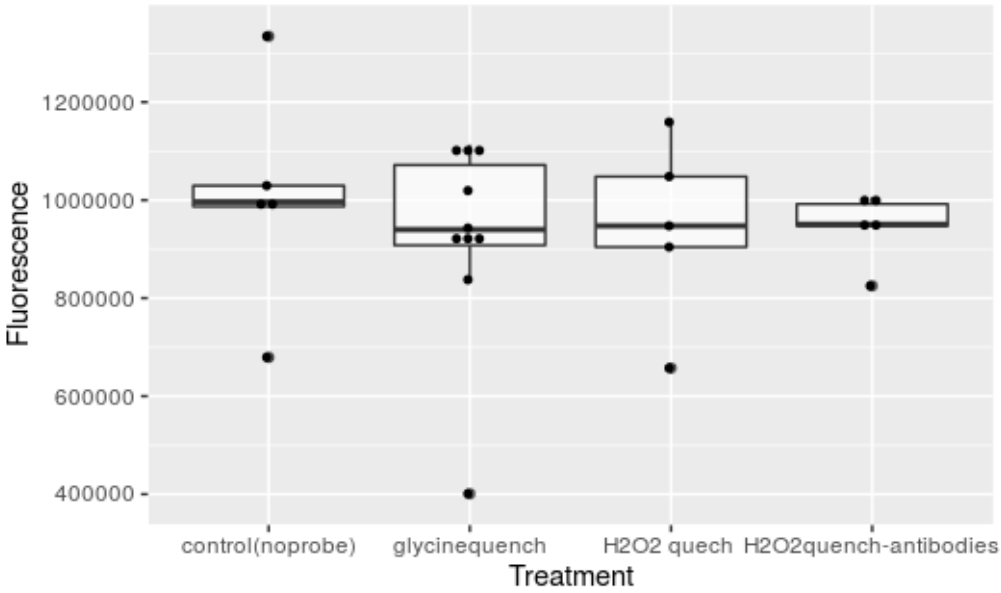

Figure 5.3.4*- Boxplot comparing fluorescence of whole tadpole after methods to decrease autofluorescence were attempted. (n=5-10)*

5.4 Discussion

No clear result was obtained that signified the antibody staining was successful. These results suggest that either: the antibody used is not specific to PSD-95 in *X. laevis* tadpoles, the secondary or primary antibody are binding to unspecific sites in *X. laevis* tadpoles or that the background fluorescence is 'drowning out' the fluorescent signal of the fluorophore.
The pictures of whole tadpoles where only the secondary antibody was added appear remarkably similar to images of both primary and secondary antibody application, with clear areas of increased fluorescence, and although neither group were significantly different to control, both groups showed increased fluorescence intensity. This may indicate unspecific binding of secondary antibodies. However, the microtome section showed very few puncta in any group assessed and all groups were even more similar to control groups with no antibodies added. It was also noticed that the general level of fluorescence in microtome slices was reduced per μm^2 compared with whole tadpole (although this doesn't consider that the tadpole is deeper than the 10µm slice). Similarly, the results obtained in cell culture produced no discernible differences between no antibody and antibody treated groups.

5.4.1 Assessment of method

Although controls were applied that demonstrated either unspecific binding or tissue autofluorescence drowning out the signal, other positive and negative control should possibly have been carried out to ensure the validity of the results. Areas of pure central nervous system should have been separated and compared with negative control, such as an area of tissue with known non-existence of PSD-95 such as adipose or connective tissue. This extra level of certainty in the positive and negative controls would have ensured the validity of the results. However, despite a full complement of antibody assessment we can still ascertain that our experimental procedure using 5% glutaraldehyde, lead to increased autofluorescence. In future it would be recommended that *X. laevis* are fixed in paraformaldehyde, as other groups have done and achieved positive staining using immunohistochemical means for PSD-95 (Liu, Tari and Haas, 2009). Another method which would ensure specificity of PSD-95 in *X. laevis* to these antibodies would be to perform a western blot. This would definitively confirm the presence of PSD-95, if a positive control of a known PSD-95 sample was used alongside. It would also be of interest if in subsequent analysis of bound proteins from *X. laevis* sample that protein other than PSD-95 were binding to the primary or secondary antibody to help eliminate the possibility of unspecific binding. Another method would be to genetically

manipulate the tadpole to express PSD-95 with a GFP tag. We did experiment with acquiring some tadpoles with a MAP-2 GFP tag which were excellent to image live. However, when fixed the tadpole became autofluorescent. If the cells were not necessary to be fixed and the AFM could be performed in a fluid cell allowing the analysis to be performed in live cells in real time, such as in (Shibata *et al.*, 2015), GFP tagged proteins could feasibly be used without detrimental autofluorescence.

The possibility of unspecific binding meant that an alignment analysis of the protein sequence was performed. Firstly, it is worth mentioning that the sequence for PSD-95 in *X. laevis* has not been sequenced, but predicted by computational model. The genome of *X. tropicalis* has been fully sequenced and data exists for the protein sequence in *X. tropicalis*. Although very similar organisms, there is quite a difference in genetic organisation mainly that *X. laevis* has four sets of chromosomes compared with X. tropicalis which has two, like most other vertebrates. To begin our alignment using NCBI gene and protein database a BLAST (basic local alignment search tool) query was run on the predicted sequence of *X. laevis* PSD-95 encoded by the gene dlgh4 (disks large homolog 4 isoform X1), which identifies proteins with similar sequences in other organisms or different isoforms in the same organism. The results of this search show that PSD-95 is highly conserved across species. However, there were differences. To investigate further a CLUSTAL omega alignment was performed using the FASTA sequences for *X. laevis*, *X. tropicalis*, zebrafish, human, mouse and rat. The sequence identity of *X. laevis* was: 86.96% to *X. tropicalis*, 87.01% to human, 78.93% to zebrafish, 85.15% to mouse and 86.29% to rat. This is fairly high level of conservation between species, although it is clearly not 100% across species. If we compare human PSD-95 to rat the sequence identity is 98.85%. Although there are clearly some differences in sequence of the protein, the antibody has been reported to work in zebrafish, human, mouse and rat. It then seems unlikely that the one area of difference in *X. laevis* has caused the antibodies not to bind, especially if we compared zebrafish to human which has a sequence identity of 83.36%. There are also publications which have successfully identified a signal from PSD-95 in *X. laevis*. To investigate this further it would be beneficial to have the sequence of the active site of the antibody. Maybe then a more in-depth analysis would clarify if the differences in sequence lie in areas of antibody binding or not.

5.4.2 Autofluorescence

The fluorescence of biological molecules has been well categorised, and in fact fluorescent microscopes were invented before fluorescent antibodies. Fluorescence occurs by aiming a known wavelength of light at a sample, this light (photon) is absorbed into the electron cloud

of the molecule and briefly increases the energy level of the outer electrons. When the electrons move back to their original energy level, they emit a photon now at an increased wavelength. For example, a molecule may absorb/be excited by light of a wavelength at 450nm and emit the photon at 520nm. This occurs in almost all molecules to some extent, but certain biological molecules have a higher probability of excitation and emission. Review of the literature shows that the most fluorescent biomolecules categorised are: flavins, NADPH, lipofuscins, collagen and elastins (Billinton and Knight, 2001). Tadpole spinal cords and the majority of their tail structure at this age are extremely high in collagen which is fluorescent at the wavelength used for assessment. Flavins are also a ubiquitous biomolecule that we can assume are in high quantities in *X. laevis,* given their high energy demand for metamorphosis and are very fluorescent excited by 488nm, the same excitation wavelength as the secondary antibody used in our experiments. Flavins have been studied in *X. laevis* (Weber *et al.*, 2002), and riboflavin is classed as an essential biomolecule for the existence of life. Lipofuscins are molecules which are documented to fluoresce a red-orange colour when excited at 460-490nm, although there are reports of excitation from 345nm (Yin, Yuan and Brunk, 1995). The literature states that lipofuscins are accumulated in aging, through continual oxidative stress the lipofuscin complexes form. This makes it an unlikely candidate for 3-day old *X. laevis* tadpoles. However, the orange-red fluorescence is similar to what was regularly observed particularly from the yok sac. Lipofuscins are essentially lipids, proteins and carbohydrates, which through failure of the cells recycling system, form large heterogenous cross-linking fluorescent complexes. Although they may not exist in *X. laevis* cells there are a great deal of vesicles within their cells at this age which are full of carbohydrates, lipids and proteins. The process of glutaraldehyde fixation cross links carbon molecules inside the cell, probably cross linking the vesicles forming similar complexes to lipofuscins.

Glutaraldehyde on its own has been reported to have a very weak blue fluorescence, and this was attributed to possible impurities (Lee *et al.*, 2013). The same study showed that glutaraldehyde linked most biomolecules and once linked produced fluorescence of varying wavelengths dependent on the biomolecule attached. The fluorescence of glutaraldehyde was attributed to a free ethylenediamine and a secondary amine (Lee *et al.*, 2013). Given the developing nature of the primary cultures and the tadpoles themselves the combination of lipids, proteins, flavins, amino acids all cross-linked with glutaraldehyde may result in high

autofluorescence as shown in Figure 5.4.1, comparing a live tadpole imaged in methylcellulose and the same tadpole after 30-minute fixation in 5% glutaraldehyde.

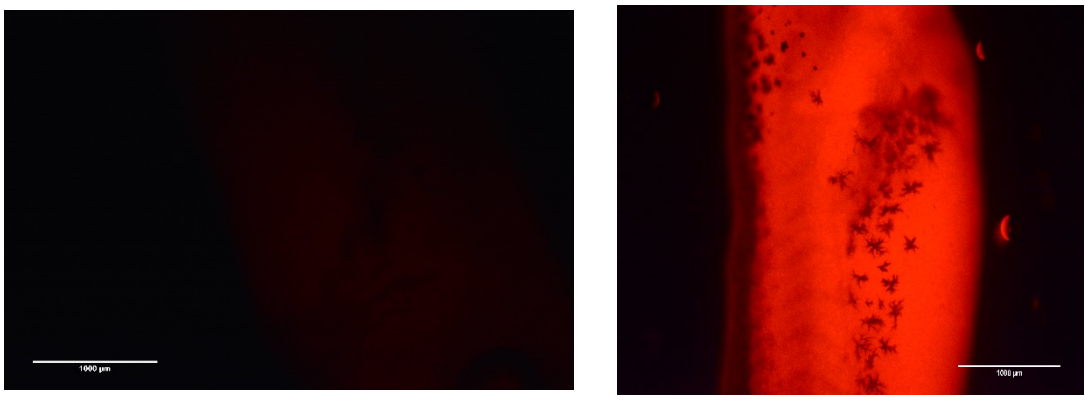

Figure 5.4.1*-Example of fluorescence in live tadpole imaged in methylcellulose (left) and the same tadpole after 30-minute fixation in 5% glutaraldehyde (right).*

5.4.3 Exploration of our hypotheses

Our hypothesis for this experiment was that drug treatment which increased the swim-cycle frequency and altered dendritic spine dimensions, such as DHPG, would increase the expression of PSD-95, a key protein in the enhancement of excitatory signalling. Similarly, drug treatments which depress synaptic excitatory signalling, such as cannabinoid agonists, CB1 antagonists at specific concentrations *in vivo* (through enhanced glycine signalling depressing future glutamate releasing neurons) and group 1 mGluR antagonists MPEP and LY367385, may all decrease PSD-95 expression. The likely hood of $mGluR_{1/5}$ antagonists to decrease PSD-95 expression is questionable and may be concentration dependent, as we would also expect DHPG to be concentration dependent. Group 1 mGluR induced LTD requires very high concentrations of DHPG (Fitzjohn *et al.*, 1999), this may have been sufficient in our culture model where 50µM DHPG was applied without significant stimulation protocols which may have led to an LTD-like dendritic spine morphology possibly observed in the AFM assessment. The result in culture may have discriminated between DHPG and MPEP, both of which showed similar results in the AFM analysis of dendritic spine dimensions and loss tangent. Or if the result was the same expression levels of PSD-95 it may have indicated that in this culture system MPEP and DHPG have inadvertently had the same effect on dendritic spines overall. As I have mentioned DHPG can cause LTD like phenotypes. In the live tadpole swimming motion DHPG may have potentiated excitatory synapses and depressed adjacent inhibitory synapses. This would have happened because the excitatory synapses were undergoing high frequency signalling during the swimming bouts. This would mean large amounts of glutamate release and consequently AMPAR and NMDAR excitation. DHPG on top of this already highly active

system may increase output of the dIN and reduce rebound firing through inhibition of glycine release. However, in the culture system, the frequency and strength of signalling is likely to be reduced. In these circumstances, large amounts of DHPG lead to depressed synapses and an LTD-like phenotype of dendritic spines. For this chapter it might have meant we saw an increase in PSD-95 in the fixed tadpoles treated with DHPG and a decrease in PSD-95 in the cultures. Similarly, the CB1 antagonist AM-251 may well have decreased PSD-95 expression in whole tadpoles. Large concentrations of AM-251 significantly decreased frequency and this is likely because high amounts of glycine were released onto the dINs. This may have depressed signalling and effected the growth of adjacent dendritic spines, possibly decreasing the expression of PSD-95.However, in culture AM-251 and AEA are unlikely to have effected PSD-95 expression as their effect on signalling and growth of dendritic spines may have been negligible. In future, it would be interesting to investigate if the axon structure was affected by CB1 in culture and see if this correlated with reduced axon protein expression such as SNAP-25 (synaptic associated protein-25, a vesicle release protein) or tau/ MAP-2 (structural neurite proteins). These may be affected due to the inhibitory g-protein signalling effected by CB1 activation.

The most interesting results in this section would have come from the microtome sections of hindbrain/rostral spinal cord of $mGluR_{1/5}$ manipulated tadpoles, as this would have determined if increases in swim-cycle frequency seen from treatment of DHPG were transient or related to increases in protein expression.

5.5 Conclusion

There is evidence in previous studies that PSD-95 is present in *X. laevis* at this stage and that it can be detected and visualised using immunohistochemical methods (Liu, Tari and Haas, 2009). In our study we observed high levels of autofluorescence when the tadpoles and cultures were fixed in 5% glutaraldehyde. Although no positive and negative control were carried out which are recommended in the previous section, there would appear to be sufficient evidence that autofluorescence meant the signal, if there was any, could not be detected. Previous studies which have successfully used immunohistochemistry to identify, visualise and quantify PSD-95 and other synaptic proteins, have done so via paraformaldehyde fixation (Liu, Tari and Haas, 2009). It would be recommended that this be used in future IHC experiments using *X. laevis*, although it would be interesting to test if this affected structural integrity for AFM assessment. It would also be recommended that these antibodies be tested using western blot for the specificity to PSD-95 in *X. laevis,* compared with known samples of PSD-95 from other organisms and using tissue from the brain known to contain PSD-95. This could ensure the specificity and accuracy for future experimentation.

With the success of genetic manipulation in recent years and the possibility of live cell AFM analysis in the future GFP tagged PSD-95 could be used so that AFM assessment of dendritic spine morphology and evolution under drug treatment conditions could be explored. However, genetic addition of GFP to key proteins in the synapse may come with its own set of problems that affect development and correct expression. This may not solve the issue of localising PSD-95 in microtome sections as we observed “bleeding” of the fluorescence into other tissue after fixation. This may again be a glutaraldehyde problem and would need to be explored further.

6 General Discussion

6.1 Behavioural results

In this thesis we set out to determine if an *in vivo* measurement of *X. laevis* tadpoles swimming, at stage 37-42, with high-speed video, could determine changes in the swim-cycle frequency, regulated by a well characterised CPG network, when group 1 mGluR and CB1 receptors are manipulated. The results of this experiment, outlined in chapter 3, demonstrate that in agreement with previous studies (Chapman and Sillar, 2007; Chapman, Issberner and Sillar, 2008), activation of group 1 mGluRs increases swim-cycle frequency *in vivo*. Also, in corroboration with those previous electrophysiological investigations in *X. laevis,* were the findings that antagonism of $mGluR_{1,}$ and not $mGluR_{5,}$ reduced the frequency of swim-cycles, indicating an intrinsic role for $mGluR_1$ in the maintenance of normal swim-cycle frequency. *In vitro* studies suggest (Chapman, Issberner and Sillar, 2008) an intrinsic role of $mGluR_1$ in the maintenance of swim-cycle frequency and the increases seen with DHPG may be due to decreased inhibitory glycine release from cIN to dIN. Previous studies in lamprey CPG had observed similar results and went further attributing this decrease in glycine release to the presence of CB1 receptors (Kettunen, Hess and Manira, 2003a; Kyriakatos and El Manira, 2007). CB1's endogenous function when activated is to reduce neurotransmitter release from axon terminals. We hypothesised that this mechanism was similar in *X. laevis* and the CB1 receptor may be present and interact in the swim-cycle frequency. To test this, we first used our *in vivo* high-speed video method of swim-cycle assessment to see if CB1 agonism or antagonism affected frequency of swim-cycles. The results from this experiment were difficult to attribute directly to cIN-CB1 presence, and produced some interesting biphasic results. First, to address agonism of CB1 we applied endogenous cannabinoid ligand AEA and we observed an interesting result where low doses (0.1μM) significantly decreased frequency. As this dose increased the decrease in swim-cycle frequency compared with vehicle control became less pronounced, until at highest concentration (50μM) no significant changes were observed. We have attributed this effect to two possible explanations. First, it may simply be that the endogenous ligand constitutively active at this receptor is the cannabinoid 2-AG, a ligand produced in response to $mGluR_{1/5}$ activation. AEA has a lower EC50 value and Kd, but lower maximal response than 2-AG in some experiments (Reggio, 2010), meaning it is possibly a partial agonist with a higher affinity. This may mean that at low concentrations AEA almost behaves like an antagonist, occupying the receptor while causing a lower response. This would mean less axon terminals are inhibited from releasing neurotransmitter, this would increase

the level of inhibition in the CPG if CB1 is located on more glycine axon terminals. As the concentration increases it begins to have similar effects to 2-AG eventually reaching normal cannabinoid effect and normal swim-cycle frequency. Another explanation may lie in the distribution and constitutive activity of CB1. Experiments in mice and rat brains demonstrate that CB1 is more constitutively active on inhibitory GABAergic terminals (the main inhibitory neurotransmitter releasing neurons in the brain) and although CB1 is present on glutamatergic axon terminals, glutamatergic-CB1 is only active 5-7% of the time (Steindel *et al.*, 2013; den Boon *et al.*, 2014). If this pattern of expression and activity was consistent in the *X. laevis* tadpole spinal cord, it may be that low doses of AEA would initially reduce neurotransmitter release from glutamatergic axons first, such as the dINs. If this was the case it would be reasonable that low concentration would first decrease excitatory release, then as the concentration of AEA increases more glycinergic CB1s are activated reducing inhibition and readdressing the excitation-inhibition balance (den Boon *et al.*, 2014). It is noted that neither of these explanations take into account that other experiments have shown that reducing cIN glycine release only effects frequency of swim-cycles to a certain point (reducing hyperpolarising current below -43.2mV decreased frequency of motoneuron firing but any hyperpolarisation greater than -43.2mV had no significant effects) (Li and Moult, 2012). This would mean that significant reduction in glycine release by CB1 activation would slow frequency and not increase it as other studies previously stated in *X. laevis* and lamprey (Kettunen *et al.*, 2005; Chapman, Issberner and Sillar, 2008). As the effect of cannabinoids in the *X. laevis* CPG have not previously been determined, it would be recommended that these experiments are repeated using electrophysiological recordings to clarify if the effect on swim-cycle frequency is due to cIN-dIN CB1 or dIN-motoneuron/dIN-cIN CB1. If time to summation in the cIN was decreased this may reduce the frequency of swim-cycles as hyperpolarisation is needed at the opposing side for rebound firing.

Our results with CB1 antagonism via AM-251 gave a complicated biphasic result at stages 40-42. Low concentration of AM-251 (0.1µM) decreased frequency, 2µM increased frequency significantly and 10µM and 50µM significantly decreased frequency. This biphasic concentration dependent pattern has been observed in mice during voluntary locomotion studies and may be due to the previously discussed shift in excitation: inhibition balance (den boon et al 2014). Our explanation of this result pattern relies on the variation in antagonism of cIN-CB1 or dIN-CB1. The concentration dependent shift in the excitation: inhibition balance which is at the heart of what determines swim-cycle frequency in the CPG, means that either glycine release is increased by such a large amount that it delays dIN rebound firing reducing

frequency or increased glutamate release and increased glycine release, but not so much as to delay rebound, can increase frequency as seen at 2µM. Previous results using AM-251 in lamprey suggested that increased glycine release is responsible for decreases in frequency. However, a significant range of concentrations was not used (Kettunen *et al.*, 2005). Those studies had also set the baseline frequency with bath application of NMDA.

From the literature research a protein of interest identified was CRIP1a. This protein, activated through coincidence detection of internal neuron environment, can sequester opposing g-proteins, meaning an agonist which would normally activate inhibitory alpha g-protein can activate stimulatory alpha g-proteins (Stauffer *et al.*, 2011). In this vein it is noted that AM-251 is often considered an inverse agonist rather than a neutral antagonist which means at certain concentrations it may activate stimulatory alpha g-protein, but this effect may be concentration dependent. This complicated picture would need clarification via electrophysiological recording, but also confirmation of CB1 receptor location using fluorescent confocal imaging. Also, it would be beneficial to determine if the CRIP1 protein is present and active in *X. laevis* at this stage.

This complicated picture makes determining the explanation results obtained when CB1 was antagonised (via AM-251) and group 1 mGluRs were activated (via DHPG) or antagonised (via MPEP or LY367385), more difficult. Although AM-251 10µM application occluded the increase of DHPG 50µM, it is difficult to say this is directly related to blocking 2-AG action at CB1 on cINs after $mGluR_{1/5}$ activation from DHPG. It was previously suggested that this reduction in glycine release, via CB1 present at cIN terminals, was responsible for some of the increases in swim-cycle frequency seen with DHPG application, which is also thought to increase dIN depolarisation rate. Again, this should be confirmed with electrophysiological recording. Also as previously mentioned confirming the location of CB1 at this stage would make understanding the results easier.

We also hypothesised that if cannabinoid and $mGluR_{1/5}$ receptors were present in dIN-motoneuron synapses, reduction in the excitation of motoneurons may result in reduced maximum tail flexion achieved during swimming. The results from this analysis aroused some interesting possibilities. In the case of $mGluR_5$ inhibition with MPEP significantly increased angle size (decreased tail flexion). Then, when MPEP inhibited $mGluR_5$ followed by DHPG application or both subtypes were inhibited (MPEP + LY367385) and DHPG added, there was a larger significant decrease in the amount of tail flexion. This may indicate that $mGluR_5$ and not $mGluR_1$ is present on motoneurons. However, it does not explain what DHPG is activating to increase this effect given MPEP is a non-competitive antagonist. Since there is no clear

explanation for the results it is worth considering that the variability in the method led to false significance. As these measurements are taken from high-speed video frames there is 2.5 milliseconds between each frame that the camera does not pick up. Also, to compound this error the tadpole did not swim perfectly upright in every video and even the measurement criteria using Image J was imperfect, meaning three measurements of the same image produce three slightly different angles. It might also be that, as discussed in chapter 3 hypothesis for this experiment, there is an interplay between speed and angle of tail-flexion. This might mean that tail flexion is not itself a good measure of swimming functionality and should be combined with a speed over distance measurement to see if the tadpoles swim faster or slower with larger or smaller tail flexions. For these reasons it is difficult to prescribe any significance to the effect of treatment on tail flexion angle.

6.2 AFM scanning of dendritic spines

The results obtained using AFM to scan for and assess dendritic spines, presented in chapter 4, indicate that changes in dendritic spine morphology take place within the 20-minute incubation period. Particularly, activation of $mGluR_{1/5}$ with DHPG or antagonism of $mGluR_5$ with MPEP significantly affect the radius and membrane stiffness of dendritic spines identified. The significant increase in radius, seen with both DHPG and MPEP, indicate a possible elongation of dendritic spines, which is consistent with previous literature (Vanderklish and Edelman, 2002; Cruz-Martín, Crespo and Portera-Cailliau, 2012). We hypothesise that application of DHPG in this culture set up may produce a LTD-like response, as previous literature has shown that group 1 mGluR activation without high frequency stimulation or NMDAR activation can elongate and depress synapse signalling (Vanderklish and Edelman, 2002). We hoped in chapter 4 to a) see if identification of dendritic spines in this culture was possible and an assessment criterion could be generated and b) test if treatments that changed frequency of swim-cycles or tail flexion effected dendritic spine dimension in culture. As this culture is not behaving in the same way as the whole tadpole it may be unlikely that DHPG is elongating dendritic spines in the whole tadpole as, if $mGluR_{1/5}$ is effective on dINs and motoneurons there is likely to be high frequency stimulation during swimming bouts. For this experiment to be developed it would be beneficial to assess dendritic spines under LTP and LTD protocols as the results could be clearly compared to existing literature.

6.3 Immunohistochemistry

This is not dissimilar to what we had hoped to achieve by measuring the fluorescence intensity of PSD-95 in culture and in whole tadpole in chapter 5. Had it worked we may have teased

apart some of the relationship between dendritic spine morphology, tadpole swim-cycle frequency and PSD-95 expression. However, this final experiment to quantify PSD-95 fluorescence intensity failed to obtain any signal which we could be certain was of antibodies attached to PSD-95. Particularly of disappointment, it may have offered some clarity on the difference between DHPG and MPEP application as both increased radius and had harder membrane measurements. If PSD-95 had been increased with DHPG application, for example, it may have indicated these dendritic spines were enlarging for more efficient synaptic transmission. Unfortunately, the only result we can offer from this chapter is that 5% glutaraldehyde fixation significantly increases the auto fluorescence of the tadpole compared with a live tadpole.

6.4 Future implications

Many neurological diseases such as fragile X, autism, neurodegeneration and stroke, have problems which are compounded by erroneous glutamate signalling and abnormal neuron morphology. One of the main issues with targeting glutamate signalling is it's vital and ubiquitous nature in the CNS. For example, inhibiting or reducing NMDAR function (NMDAR hypofunction) can lead to psychosis as seen in 'angel dust' (Phencyclidine (PCP)) consumption, but also to lesser extent in cannabis abuse, particularly in youth. Understanding how modulatory GPCRs such as $mGluR_{1/5}$ and CB1 can alter glutamate signalling in particular neuron systems may hold the key to treating or at least managing certain diseases without extreme negative effects. An obvious application of cannabinoids, for example, would be to severely reduce glutamate release after stroke or injury to stop or slow the runaway effects of excitotoxity. It is imperative that we fully characterise and utilise accessible, yet relevant model systems such as *X. laevis*. Our work developing behavioural methods can be used in future alongside electrophysiology to test the pharmacological implications of receptor systems in a CPG, which is representative of how inhibitory and excitatory signalling regulate each other to produce output, a commonality in neural systems.

The AFM methods can be improved and used in understanding the dynamics of membranes in the development of dendritic spines and their changes in mature samples. During the development of this method, experiments were published which combined confocal imaging with high-speed AFM scanning, meaning near real-time assessment of dendritic spines in culture could be performed (Shibata *et al.*, 2015). The future of this field could apply this set-up under aforementioned LTP/D protocols and not only measure radius, volume and membrane stiffness changes in real time, it could also, via fluorescent confocal imaging, track and measure internal protein changes. The measurement of loss tangent could

vastly improve our understanding of membrane dynamics in developing neurons as recent studies show the importance of physical cues in the growth of neurons (Koser *et al.*, 2016). This measurement may also enable us to visualise and understand how membrane tension during these events changes and be enhanced to enable neuron recovery from injury. The ability of the loss tangent to measure stiffness while obtaining other information about the dimensions means that, in the setup of high speed AFM scanning with inverted fluorescent confocal in the future, we can measure the movement and quantity of proteins of interest, measure the dimensions of dendritic spines by combining z-stack from confocal and AFM height images and measure the fluid movements and viscoelasticity of the membrane.

7 Appendices

7.1 Frequency of swim cycles results tables

Table 7.1.1*-Results of linear mixed model comparing the effect agonism/antagonism of the group 1 metabotropic glutamate receptor has on the swim-cycle frequency of X. laevis tadpole, stage 40-42, all results compared pairwise*

Treatment	Mixed Model Result	Normality of residuals in treatment group	Independence of Residuals	Linearity of residuals v observed
Control (DMSO) vs DHPG 50µM	p=0.009	p=0.252	Satisfied	Satisfied
Control (DMSO) vs MPEP 50µM	p=1.000	p=0.197	Satisfied	Satisfied
Control (DMSO) vs MPEP 50µM + DHPG 50µM	p=0.000	p=0.039	Satisfied	Satisfied
Control (DMSO) vs LY 50µM	p=0.000	p=0.197	Satisfied	Satisfied
Control (DMSO) vs LY 50µM +DHPG 50µM	p=1.000	p=0.475	Satisfied	Satisfied
Control (DMSO) vs LY 50µM + MPEP 50µM	p=0.000	p=0.376	Satisfied	Satisfied
Control (DMSO) vs LY + MPEP 50µM+ DHPG 50µM	p=0.000	p=0.937	Satisfied	Satisfied
DHPG 50µM vs MPEP 50µM	p=0.000			
DHPG vs MPEP+DHPG	p=0.000			
DHPG vs LY	p=0.000			
DHPG vs LY+DHPG	p=0.035			
DHPG vs LY+MPEP	p=0.000			
DHPG vs LY+MPEP+DHPG	p=0.000			
MPEP vs MPEP+DHPG	p=0.000			
MPEP vs LY	p=0.000			
MPEP vs LY+DHPG	p=1.000			
MPEP vs LY+MPEP	p=0.000			
MPEP vs LY+ MPEP+ DHPG	p=0.000			
MPEP+DHPG vs LY	p=0.031			
MPEP+DHPG vs LY+DHPG	p=0.000			
MPEP+DHPG vs LY+MPEP	p=0.008			
MPEP+DHPG vs LY+MPEP+DHPG	p=1.000			
LY vs LY+DHPG	p=0.000			
LY vs LY+MPEP	p=1.000			
LY vs LY+MPEP+DHPG	p=0.652			
LY+DHPG vs LY+MPEP	p=0.000			
LY+DHPG vs LY+MPEP+DHPG	p=.000			
LY+MPEP vs LY+MPEP+DHPG	p=0.231			

***Table 7.1.2**-Results of linear mixed model comparing the effect selective antagonism of CB1 effects $mGluR_{1/5}$ induced increase in frequency of swimming of X. laevis tadpole tail at stage 40-42*

Treatment	Mixed Model Result	Normality of residuals	Independence of Residuals	Linearity of residuals v observed
Control (DMSO) vs AM-251 10µM	p=0.013	W (47) =0.978; p=0.522	Satisfied	Satisfied
Control (DMSO) vs AM-251 10µM +DHPG 50µM	p=1.000	W (47) =0.94; p=0.018	Satisfied	Satisfied
Control (DMSO) vs AM-251 10µM + LY 50µM	p=1.000	W (47) =0.956; p=0.078	Satisfied	Satisfied
Control (DMSO) vs AM-251 10µM + MPEP 50µM	p=0.019	W (46) =0.976; p=0.436	Satisfied	Satisfied
Control (DMSO) vs AM-251 10µM+ LY 50µM + MPEP 50µM	p=0.007	W (47) =0.988; p=0.905	Satisfied	Satisfied
AM-251 10µM vs AM-251 10µM +DHPG 50µM	p=.105			
AM-251 10µM vs AM-251 10µM + LY 50µM	p=.111			
AM-251 10µM vs AM-251 10µM + MPEP 50µM	p=1.000			
AM-251 10µM vs AM-251 10µM +LY 50µM + MPEP 50µM	p=1.000			
AM-251 10µM +DHPG 50µM vs AM-251 10µM + LY 50µM	p=1.000			
AM-251 10µM +DHPG 50µM vs AM-251 10µM + MPEP 50µM	p=0.156			
AM-251 10µM +DHPG 50µM vs AM-251 10µM +LY 50µM + MPEP 50µM	p=0.064			
AM-251 10µM + LY 50µM vs AM-251 10µM + MPEP 50µM	p=0.165			
AM-251 10µM + LY 50µM vs AM-251 10µM +LY 50µM + MPEP 50µM	p=0.068			
AM-251 10µM + MPEP 50µM vs AM-251 10µM +LY 50µM + MPEP 50µM	p=1.000			

7.2 Angle of Flexion results tables

***Table 7.2.1**- Results of AOF analysis in LMM with group 1 mGluR manipulations*

Treatment	Mixed Model Result	Normality of residuals in treatment group	Independence of Residuals	Linearity of observed v Predicted value
Control (DMSO) vs DHPG 50µM	p=1.000	p=0.153	Satisfied	Satisfied
Control (DMSO) vs MPEP 50µM	p=0.037	p=0.809	Satisfied	Satisfied
Control (DMSO) vs MPEP 50µM +DHPG 50µM	p=0.005	p=0.406	Satisfied	Satisfied
Control (DMSO) vs LY 50µM	p=1.000	p=0.752	Satisfied	Satisfied
Control (DMSO) vs LY 50µM + DHPG 50µM	p=1.000	p=0.023	Satisfied	Satisfied
Control (DMSO) vs LY 50µM + MPEP 50µM	p=1.000	p=0.751	Satisfied	Satisfied
Control (DMSO) vs LY + MPEP 50µM+ DHPG 50µM	p=0.003	p=0.239	Satisfied	Satisfied
DHPG 50µM vs MPEP 50µM	p=0.823			
DHPG vs MPEP+DHPG	p=0.041			
DHPG vs LY	p=0.827			
DHPG vs LY+DHPG	p=1.000			
DHPG vs LY+MPEP	p=1.000			
DHPG vs LY+MPEP+DHPG	p=.024			
MPEP vs MPEP+DHPG	p=1.000			
MPEP vs LY	p=0.001			
MPEP vs LY+DHPG	p=1.000			
MPEP vs LY+MPEP	p=1.000			
MPEP vs LY+ MPEP+ DHPG	p=1.000			
MPEP+DHPG vs LY	p=0.000			
MPEP+DHPG vs LY+DHPG	p=0.410			
MPEP+DHPG vs LY+MPEP	p=0.118			
MPEP+DHPG vs LY+MPEP+DHPG	p=1.000			
LY vs LY+DHPG	p=0.115			
LY vs LY+MPEP	p=0.345			
LY vs LY+MPEP+DHPG	p=0.000			
LY+DHPG vs LY+MPEP	p=1.000			
LY+DHPG vs LY+MPEP+DHPG	p=0.264			
LY+MPEP vs LY+MPEP+DHPG	p=.073			

Table 7.2.2- Results of LMM analysis of AOF when CB1 antagonism combined with mGluR1/5 agonism/antagonism

Treatment	Mixed Model Result	Normality of residuals	Independence of Residuals	Linearity of residuals v Predicted value
Control (DMSO) vs DHPG 50µM	p=1.000	W(47)=0.946; p=0.031	Satisfied	Satisfied
Control (DMSO) vs AM-251 10µM	p=1.000	W(47)=0.985; p=0.789	Satisfied	Satisfied
Control (DMSO) vs AM-251 10µM +DHPG 50µM	p=1.000	W(47)=0.974; p=0.369	Satisfied	Satisfied
Control (DMSO) vs AM-251 10µM + LY 50µM	p=0.000	W(47)=0.982; p=0.687	Satisfied	Satisfied
Control (DMSO) vs AM-251 10µM + MPEP 50µM	p=0.000	W(47)=0.957; p=0.086	Satisfied	Satisfied
Control (DMSO) vs AM-251 10µM+ LY 50µM + MPEP 50µM	p=0.030	W(47)=0.943; p=0.024	Satisfied	Satisfied
DHPG 50µM vs AM-251 10µM	p=1.000			
DHPG 50µM vs AM-251 10µM +DHPG 50µM	p=1.000			
DHPG 50µM vs AM-251 10µM + LY 50µM	p=0.004			
DHPG 50µM vs AM-251 10µM + MPEP 50µM	p=0.000			
DHPG 50µM vs AM-251 10µM+ LY 50µM + MPEP 50µM	p=0.338			
AM-251 10µM vs AM-251 10µM +DHPG 50µM	p=0.963			
AM-251 10µM vs AM-251 10µM + LY 50µM	p=0.011			
AM-251 10µM vs AM-251 10µM + MPEP 50µM	p=0.000			
AM-251 10µM vs AM-251 10µM +LY 50µM + MPEP 50µM	p=0.667			
AM-251 10µM +DHPG 50µM vs AM-251 10µM + LY 50µM	p=0.000			
AM-251 10µM +DHPG 50µM vs AM-251 10µM + MPEP 50µM	p=0.000			
AM-251 10µM +DHPG 50µM vs AM-251 10µM +LY 50µM + MPEP 50µM	p=0.001			
AM-251 10µM + LY 50µM vs AM-251 10µM + MPEP 50µM	p=0.768			

AM-251 10µM + LY 50µM vs AM-251 10µM +LY 50µM + MPEP 50µM	p=1.000
AM-251 10µM + MPEP 50µM vs AM-251 10µM +LY 50µM + MPEP 50µM	p=0.014

7.3 Power analysis of Cannabinoid data

A power analysis was performed on frequency of swim-cycle measurements to determine if sufficient sample sizes were achieved. In the table below sufficient power is designated at >0.95, results below this are deemed to be underpowered and required total sample size is calculated. All power analysis were performed on GLIMPSE software and were done for each treatment compared with its respective vehicle control. Where initial analysis of data with LMM showed no significant interaction and null hypothesis is accepted a power analysis is not applicable.

***Table 7.3.1**- Power analysis for AM-251 stage 40-42*

concentration	power	Sample size needed for power of 0.95
0.1µM	n/a	n/a
2µM	0.98	n/a
10µM	0.99	n/a
50µM	1.00	n/a

***Table 7.3.2**- Power analysis for AM-251 stage 37-39*

concentration	power	Sample size needed for power of 0.95
0.1µM	1.00	n/a
2µM	n/a	n/a
10µM	0.833	14 (n=7)
50µM	1.00	n/a

***Table 7.3.3-** Power analysis for AEA stage 40-42*

concentration	power	Sample size needed for power of 0.95
0.1µM	0.959	n/a
2µM	1.00	n/a
10µM	1.00	n/a
50µM	n/a	n/a

***Table 7.3.4-** Power analysis for AEA stage 37-39*

concentration	power	Sample size needed for power of 0.95
0.1µM	n/a	n/a
2µM	n/a	n/a

10µM	n/a	n/a
50µM	n/a	n/a

7.4 Frequency appendix

All residual vs predicted plots for the assumption of linearity and independence of residuals obtained for frequency of swim-cycles. Plots indicate the model may not be a good fit if there is clear patterning and grouping rather than an equal distribution of errors.

Stage 40-42

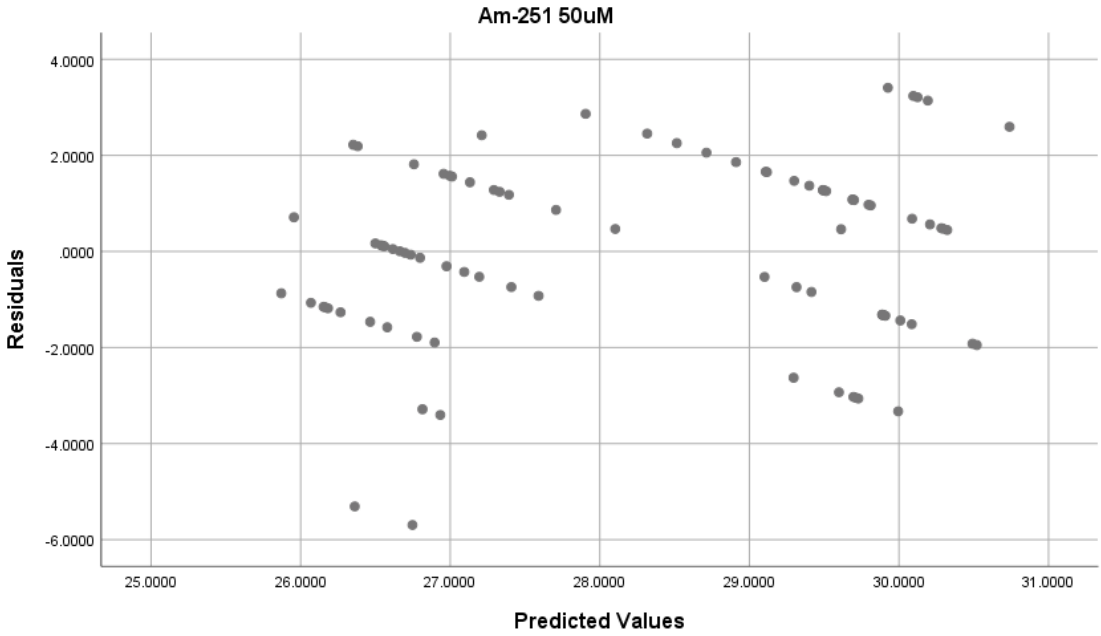

***Figure 7.4.1**- Residuals from LMM for AM-251 50µM compared with control (DMSO) vs predicted values. Stage 40-42*

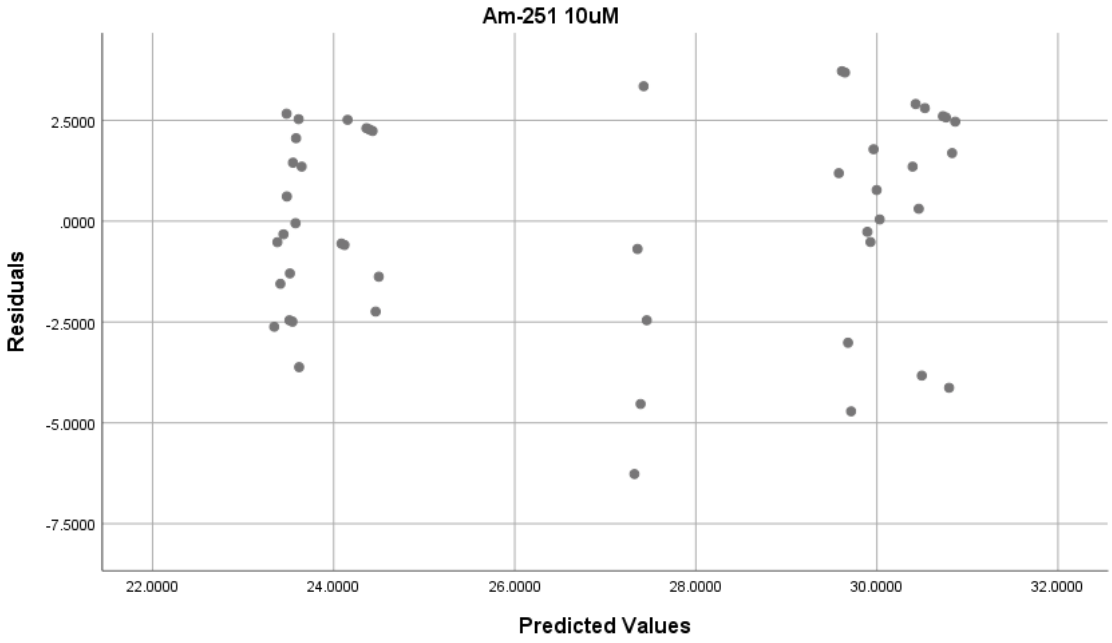

Figure 7.4.2*- Residuals from LMM for AM-251 10µM compared with control (DMSO) vs predicted values. Stage 40-42*

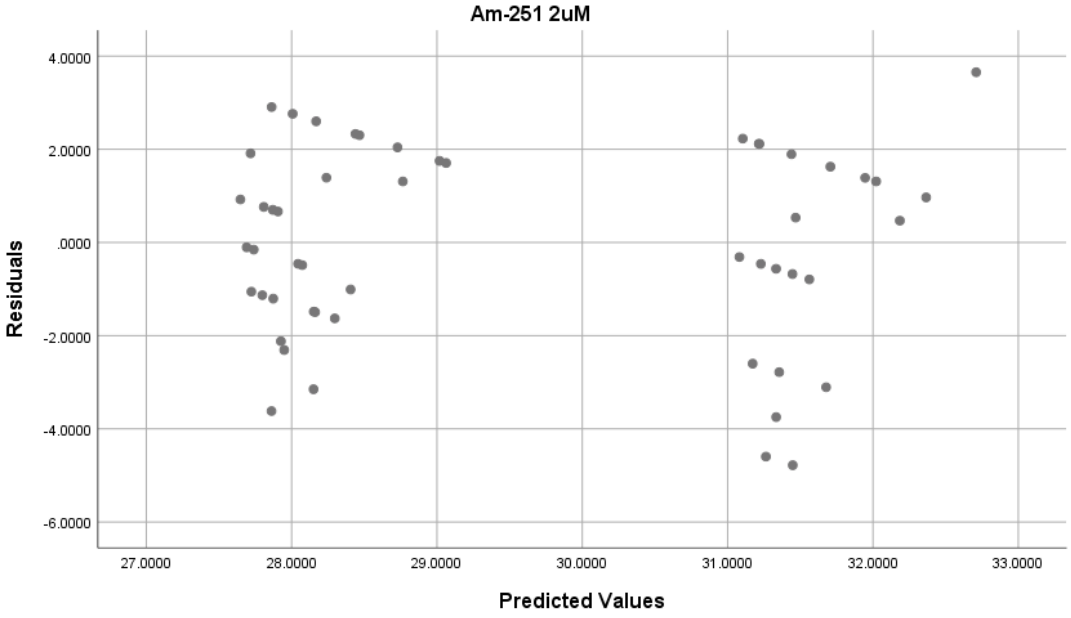

Figure 7.4.3*- Residuals from LMM for AM-251 2µM compared with control (DMSO) vs predicted values. Stage 40-42*

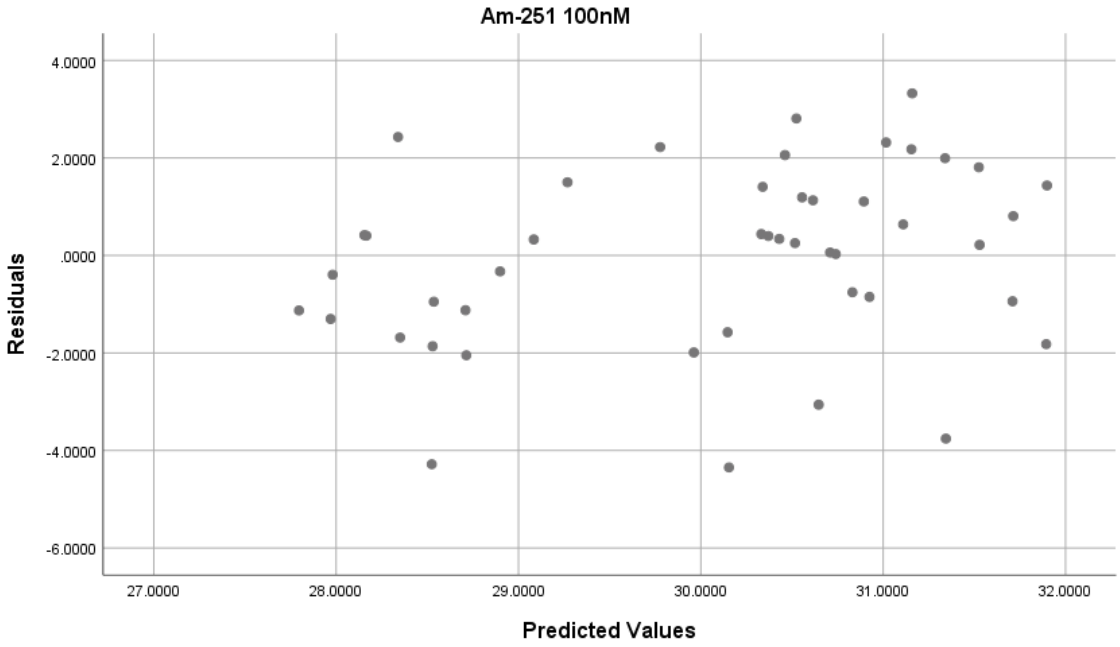

Figure 7.4.4*- Residuals from LMM for AM-251 0.1µM compared with control (DMSO) vs predicted values. Stage 40-42*

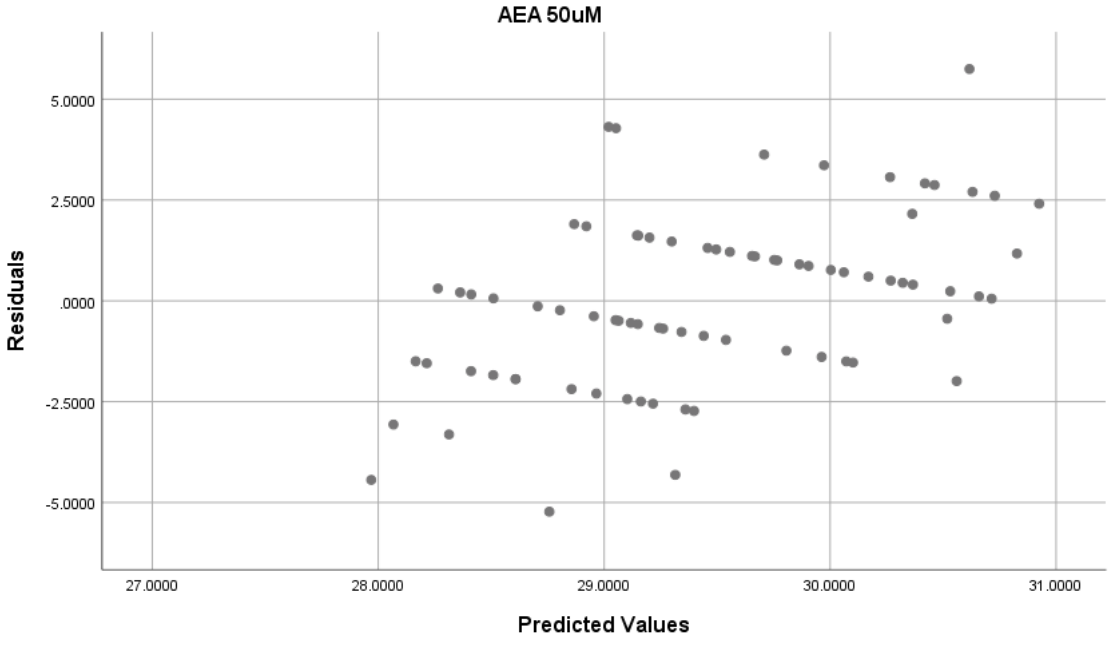

Figure 7.4.5*- Residuals from LMM for AEA 50µM compared with control (Soya) vs predicted values. Stage 40-42*

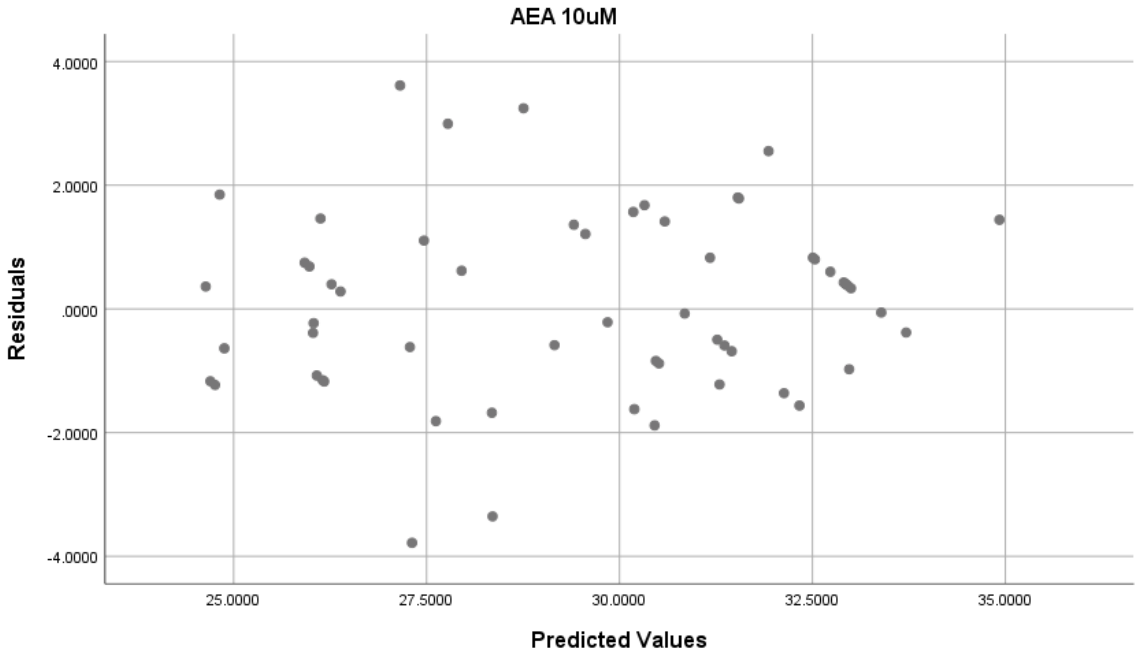

Figure 7.4.6*- Residuals from LMM for AEA 10µM compared with control (Soya) vs predicted values. Stage 40-42*

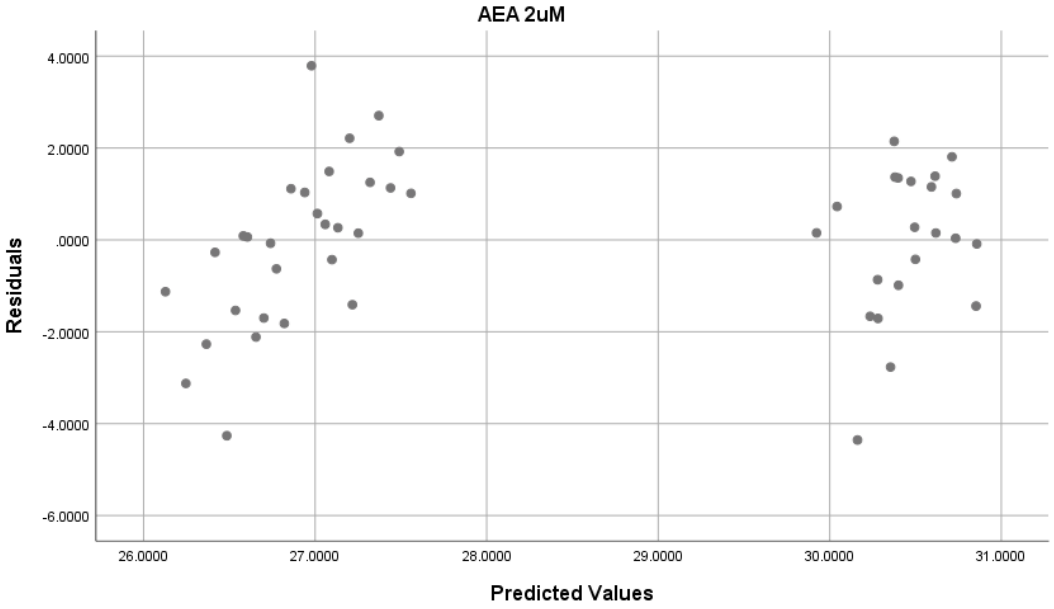

Figure 7.4.7 *-Residuals from LMM for AEA 2µM compared with control (Soya) vs predicted values. Stage 40-42*

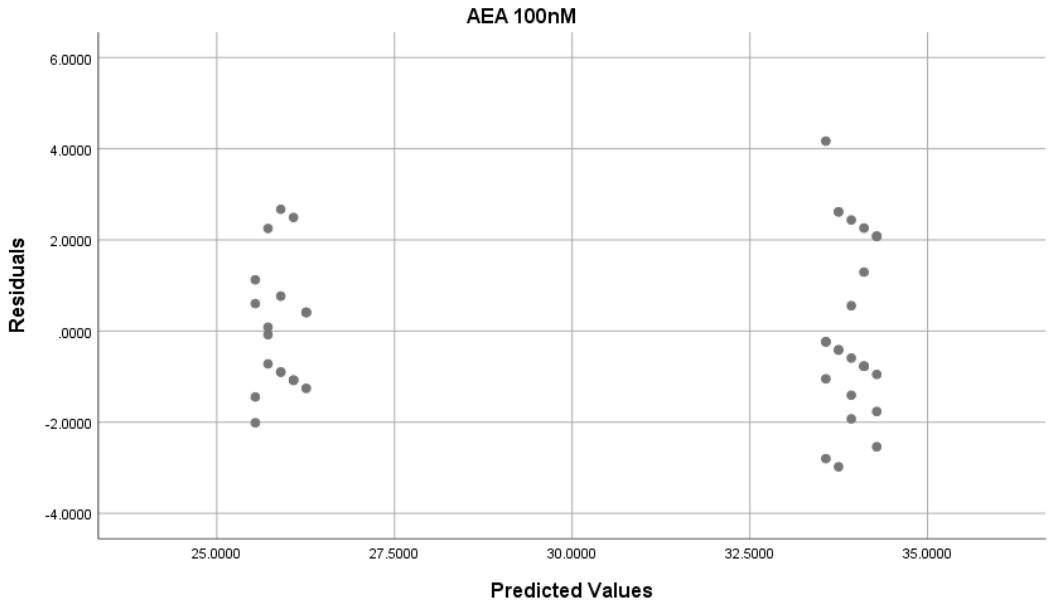

Figure 7.4.8*- Residuals from LMM for AEA 0.1µM compared with control (Soya) vs predicted values. Stage 40-42*

Stage 37-39

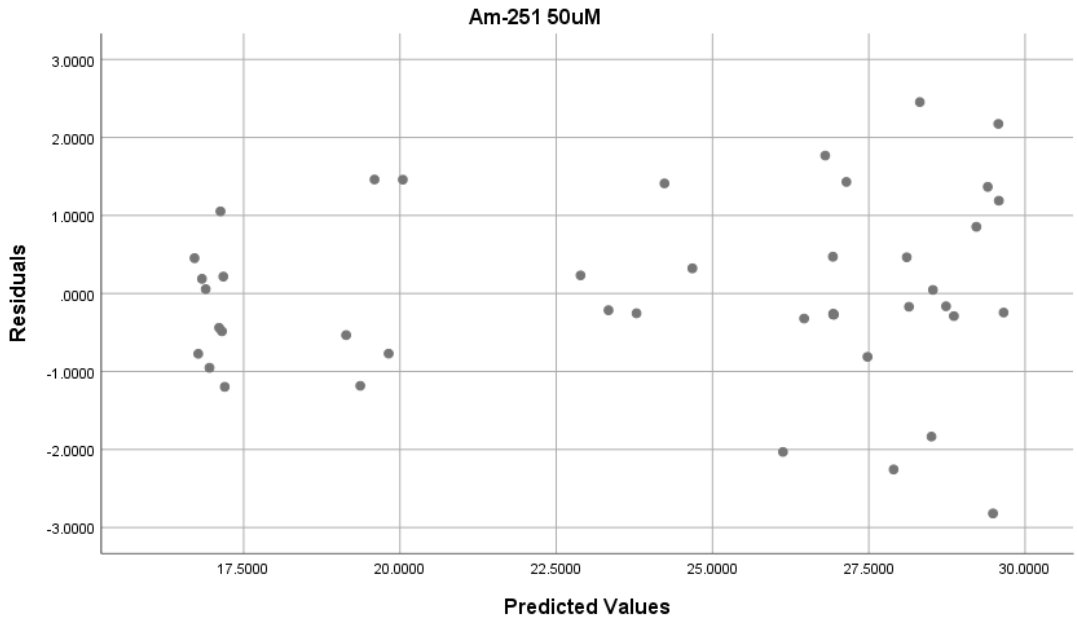

Figure 7.4.9*- Residuals from LMM for AM-251 50µM compared with control (DMSO) vs predicted values. Stage 37-39*

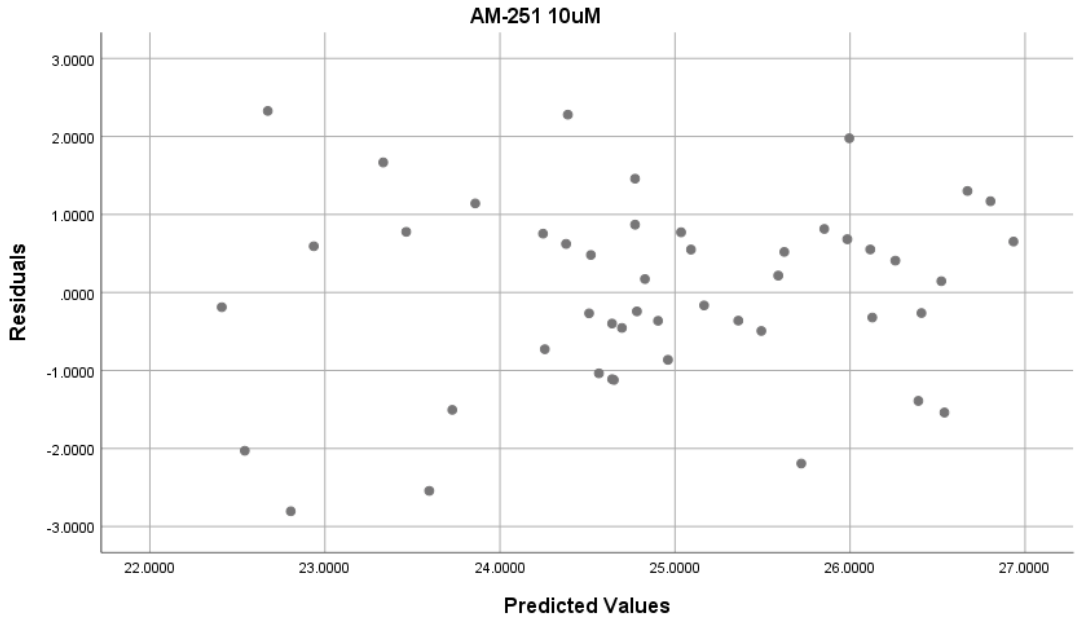

Figure 7.4.10*- Residuals from LMM for AM-251 10µM compared with control (DMSO) vs predicted values. Stage 37-39*

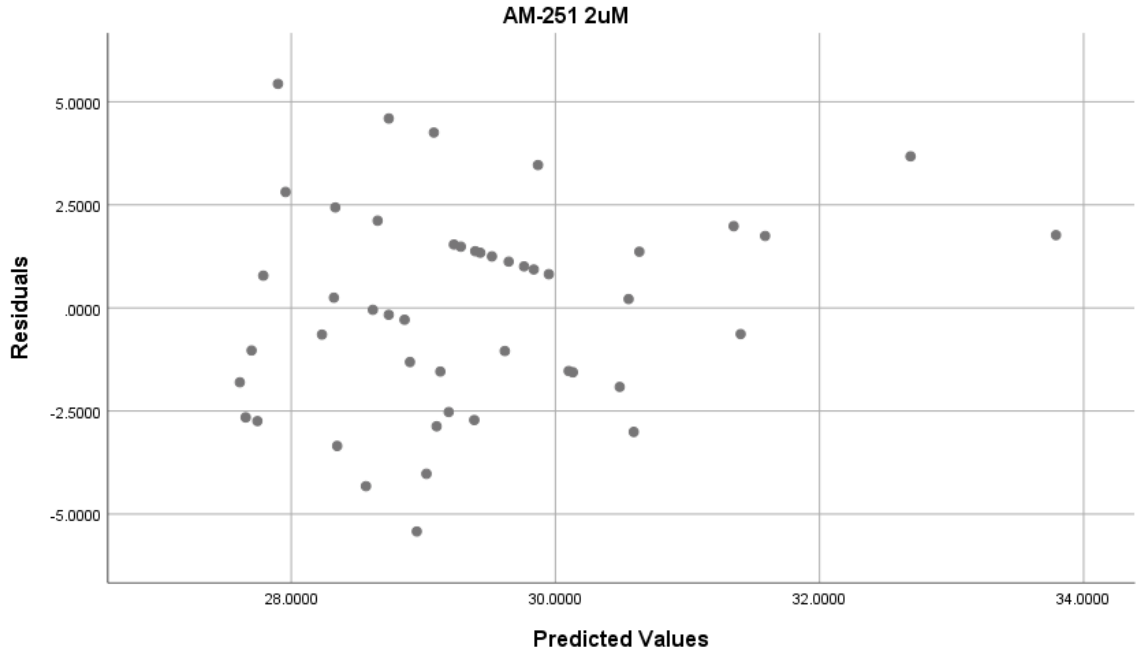

Figure 7.4.11*- Residuals from LMM for AM-251 2µM compared with control (DMSO) vs predicted values. Stage 37-39*

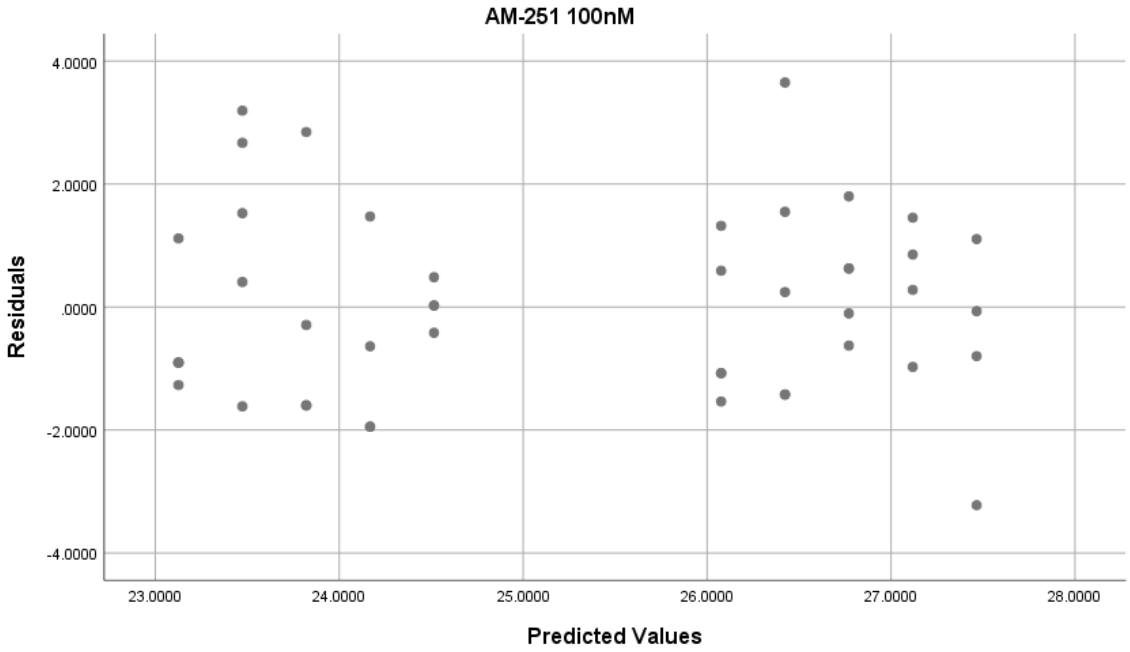

Figure 7.4.12*- Residuals from LMM for AM-251 0.1µM compared with control (DMSO) vs predicted values. Stage 37-39*

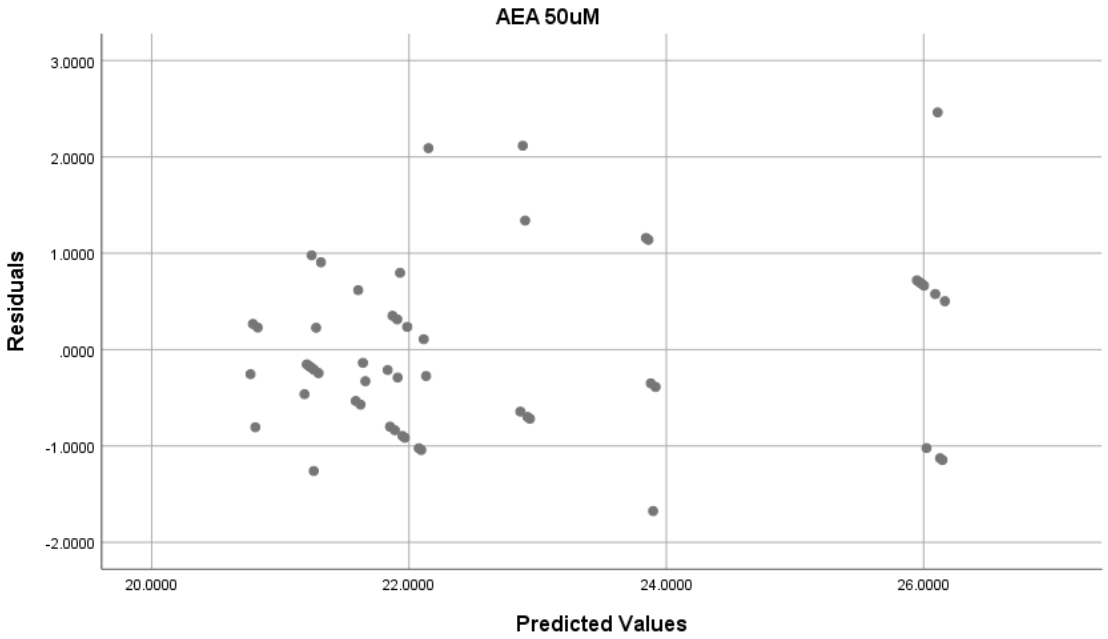

Figure 7.4.13*- Residuals from LMM for AEA 50µM compared with control (Soya) vs predicted values. Stage 37-39*

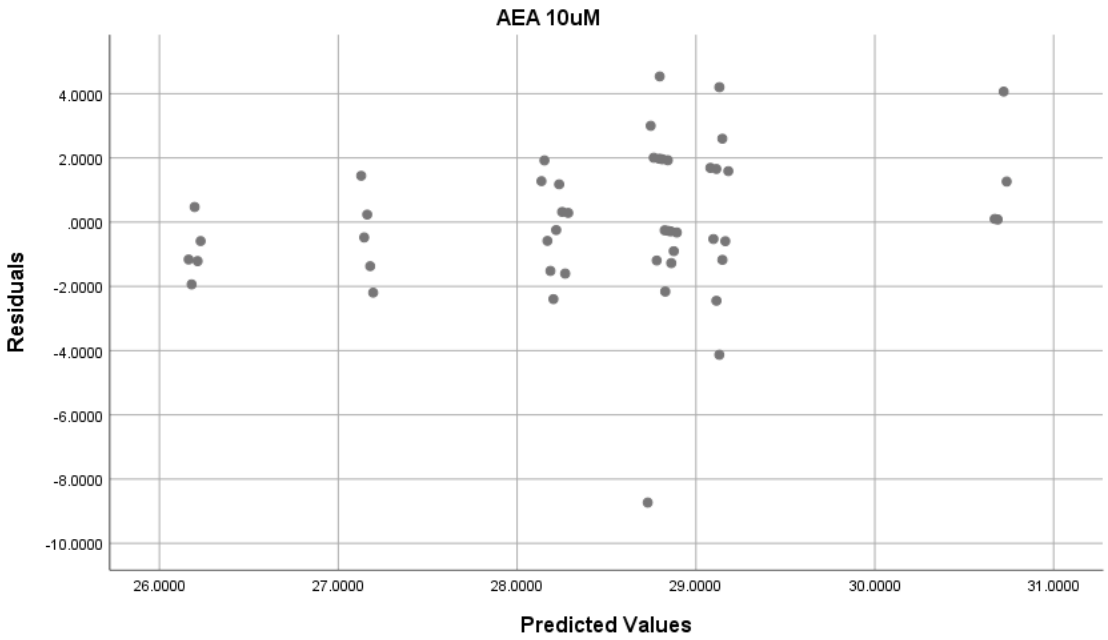

Figure 7.4.14*- Residuals from LMM for AEA 10µM compared with control (Soya) vs predicted values. Stage 37-39*

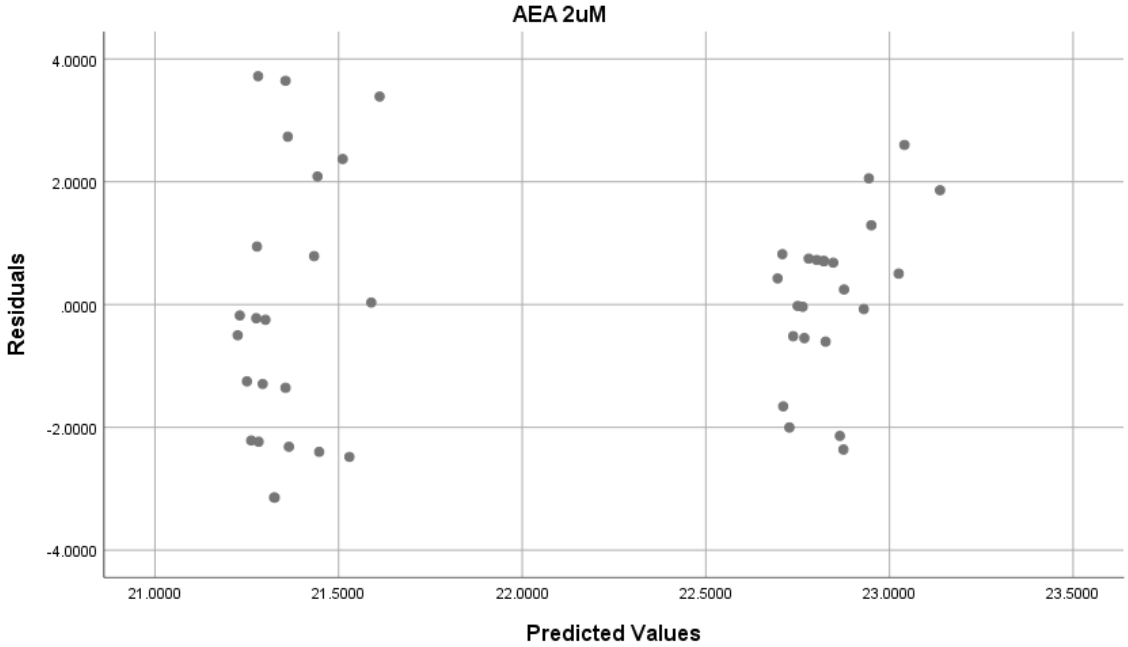

Figure 7.4.15*- Residuals from LMM for AEA 2µM compared with control (Soya) vs predicted values. Stage 37-39*

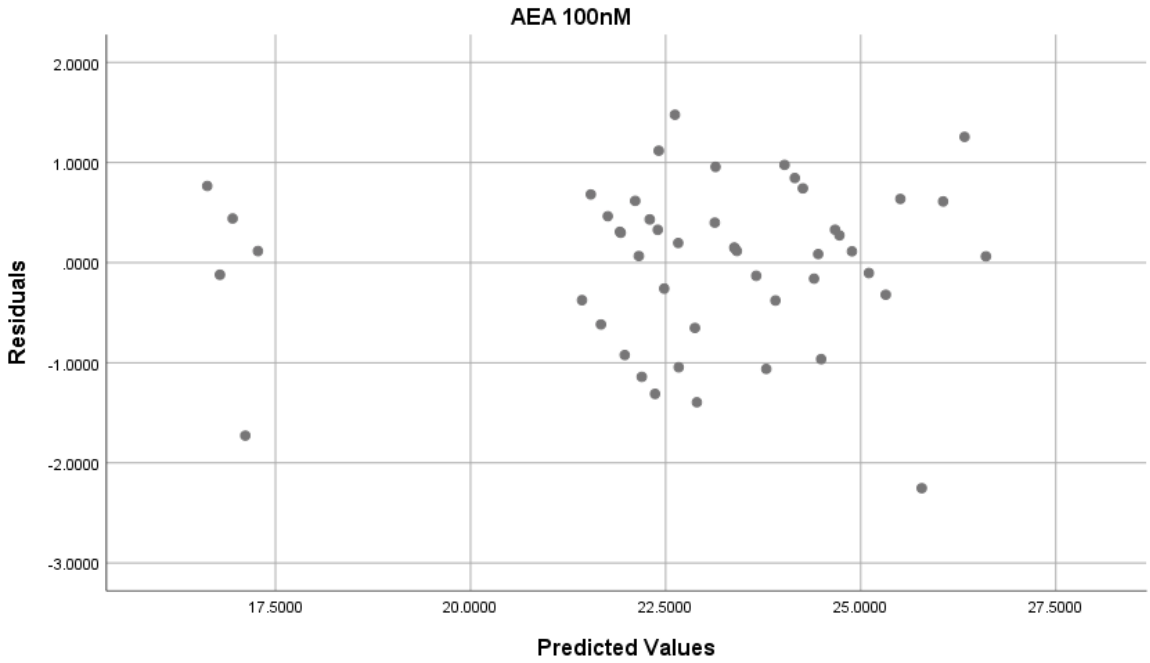

Figure 7.4.16*- Residuals from LMM for AEA 0.1µM compared with control (Soya) vs predicted values. Stage 37-39*

mGluR1/5

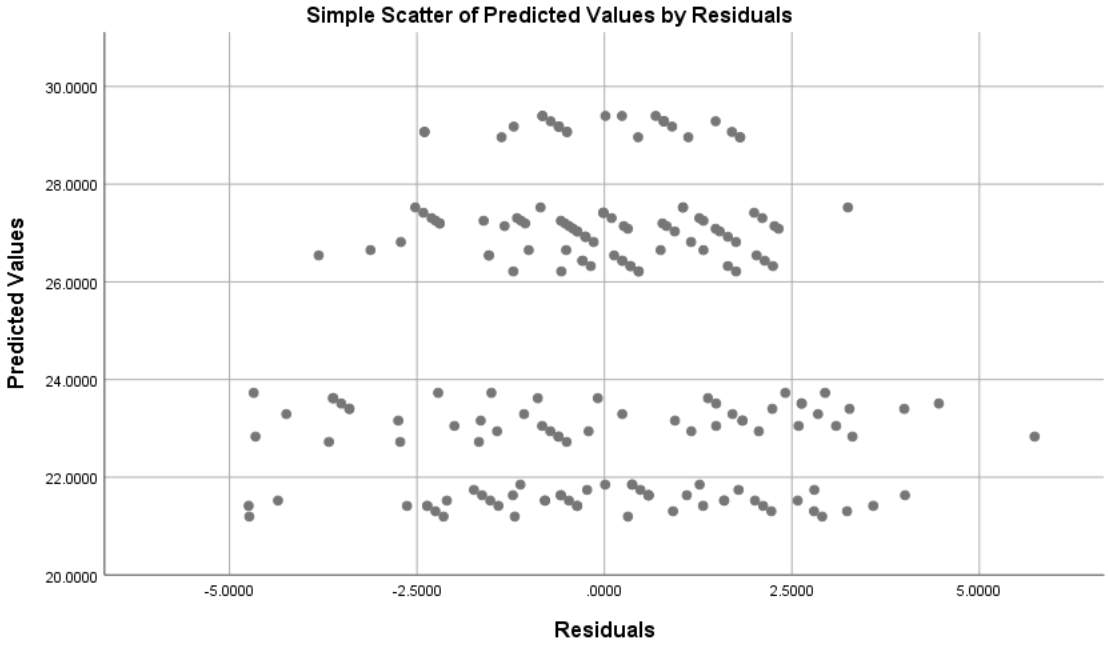

Figure 7.4.17*- Residuals from LMM for mGluR$_{1/5}$ manipulations compared with control (DMSO) vs predicted values. Stage 40-42*

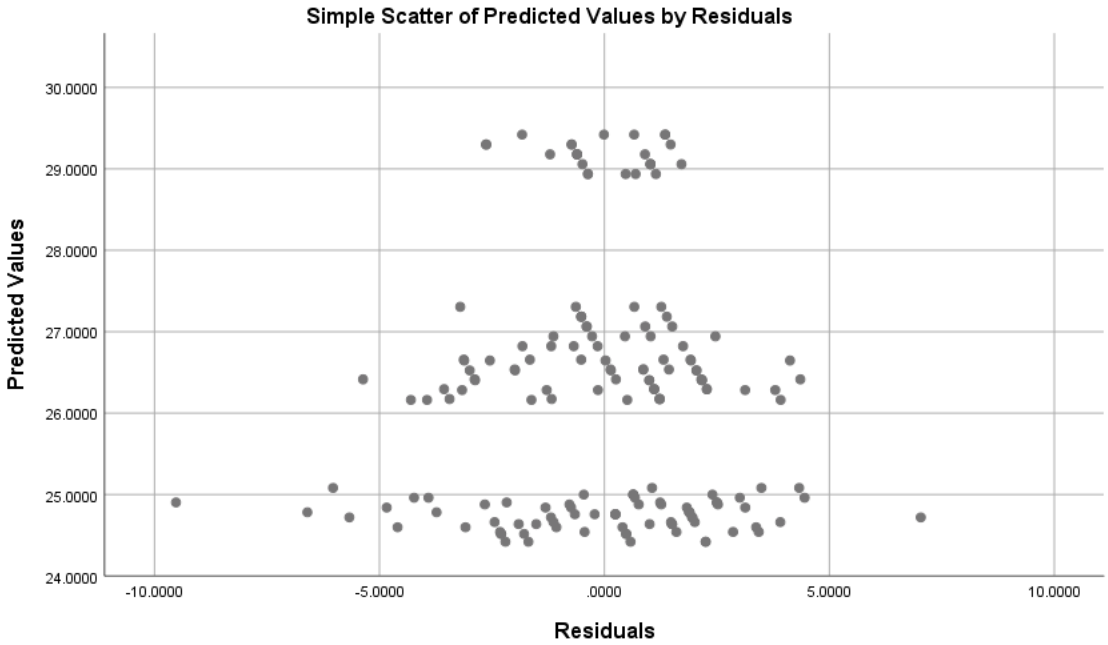

Figure 7.4.18*- Residuals from LMM for Cb1 antagonism +mGluR$_{1/5}$ manipulation compared with control (DMSO) vs predicted values. Stage 40-42*

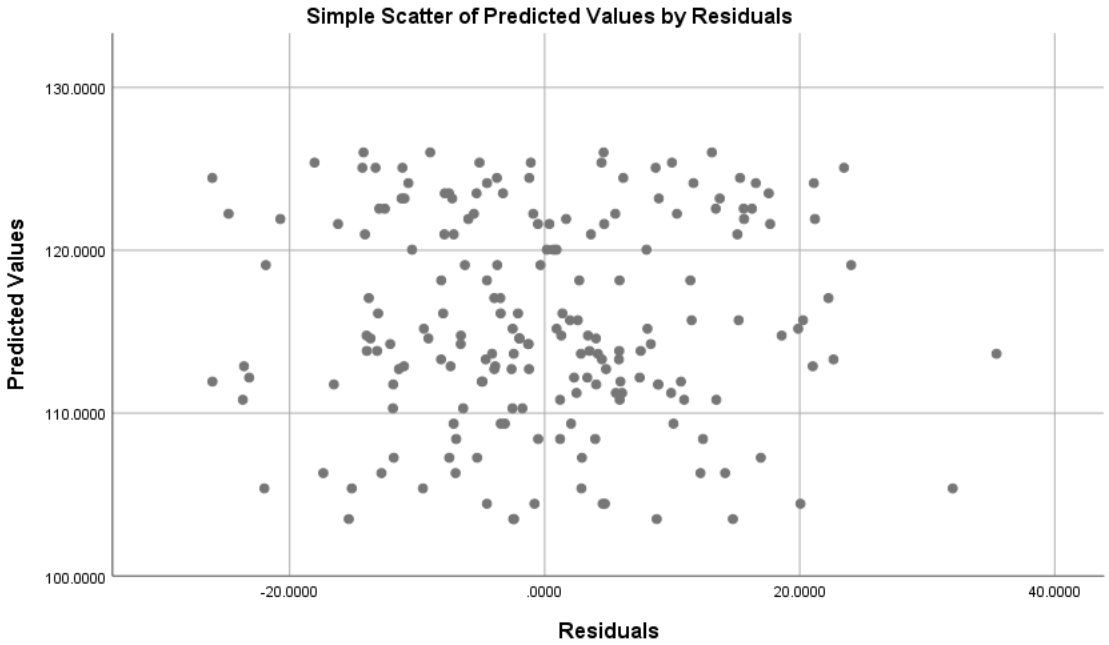

***Figure 7.4.19**- residual vs predicted plot for angle of flexion measurement mGluR$_{1/5}$ vs control DMSO dataset*

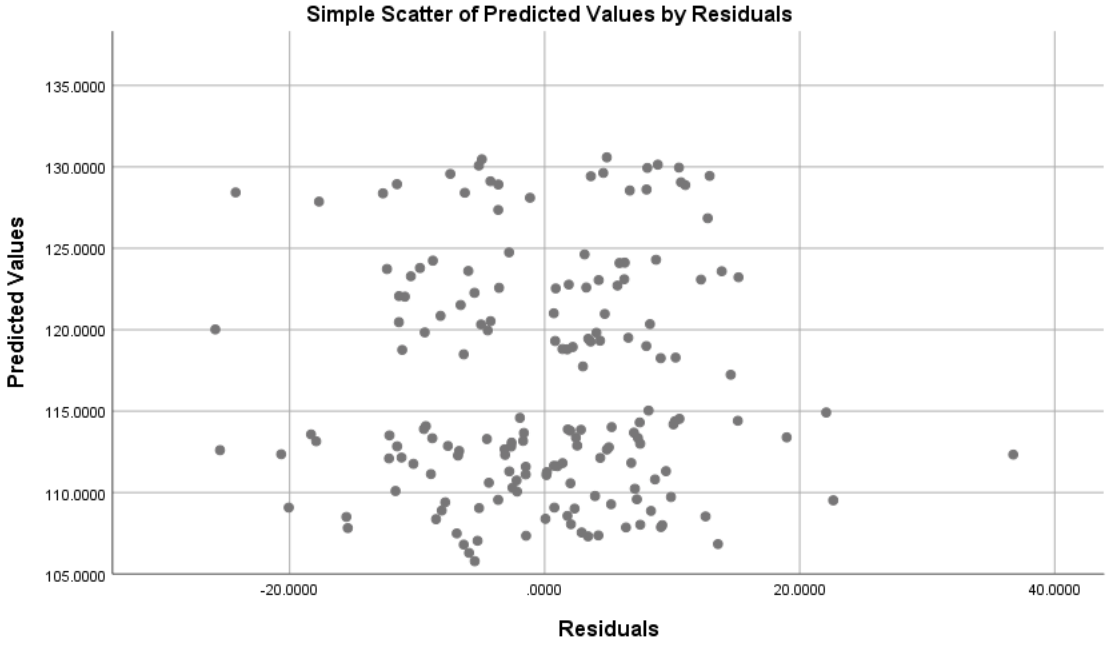

***Figure 7.4.20**- residual vs predicted plot for angle of flexion measurement CB1 +mGluR$_{1/5}$ vs control DMSO dataset*

7.5 AFM appendix

Table 7.5.1*- table of p-values investigating if slide had effects within groups. Slide 1 was tested against slide 2 for each treatment in an independent t-test in SPSSS*

Treatment	radius	Volume	Cross-section	Roughness	Loss tangent
Control (DMSO)	0.486	0.563	0.614	0.255	0.109
DHPG	0.515	0.436	0.218	0.055	0.061
MPEP	0.163	0.183	0.108	0.373	0.082
AM-251	0.783	0.253	0.140	0.083	0.894
AEA	0.279	0.219	0.170	0.419	0.708
Control (Soya)	0.253	0.210	0.116	0.327	0.085

Although no slides within groups were significantly different to one another there are some areas of interest and enough of a difference for slide to be included as a random factor in the LMM.

Loss tangent linear mixed model assumption predicted vs residuals

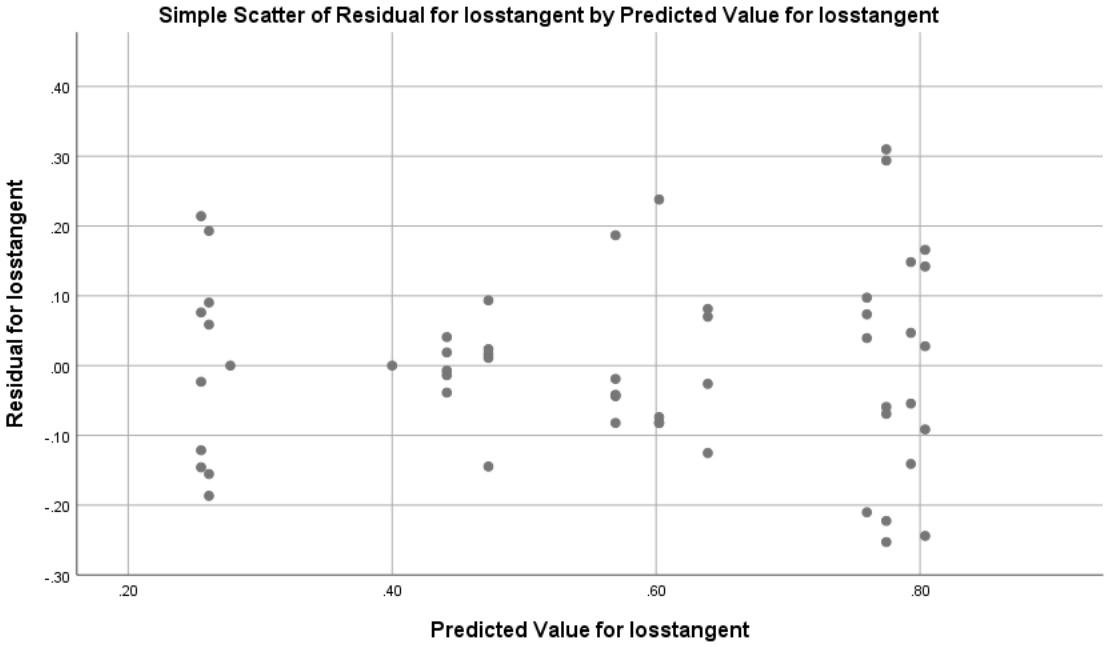

Figure 7.5.1*- loss tangent residuals v predicted*

Height image parameter analysis

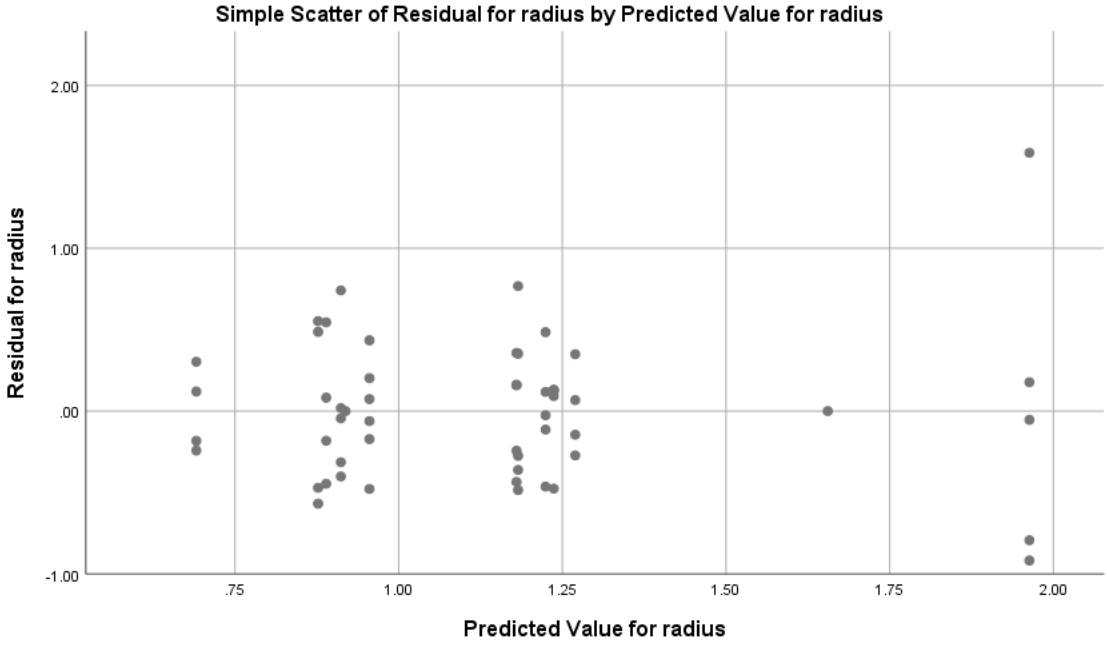

Figure 7.5.2*- Radius residuals of dendritic spine v predicted values*

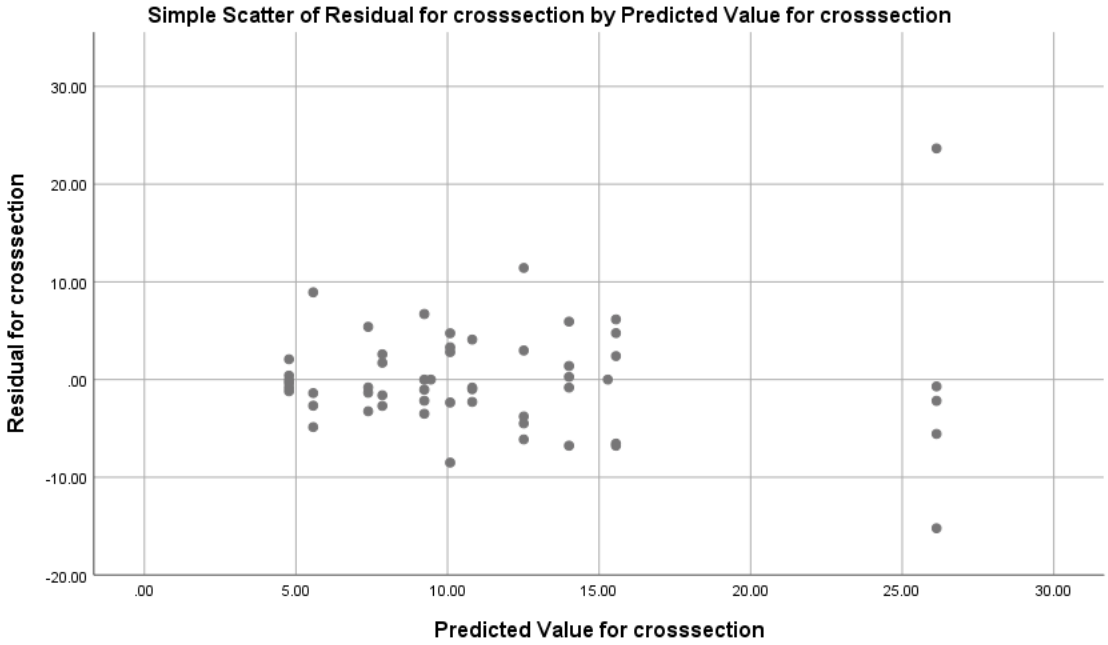

Figure 7.5.3*- cross-section residuals v predicted values*

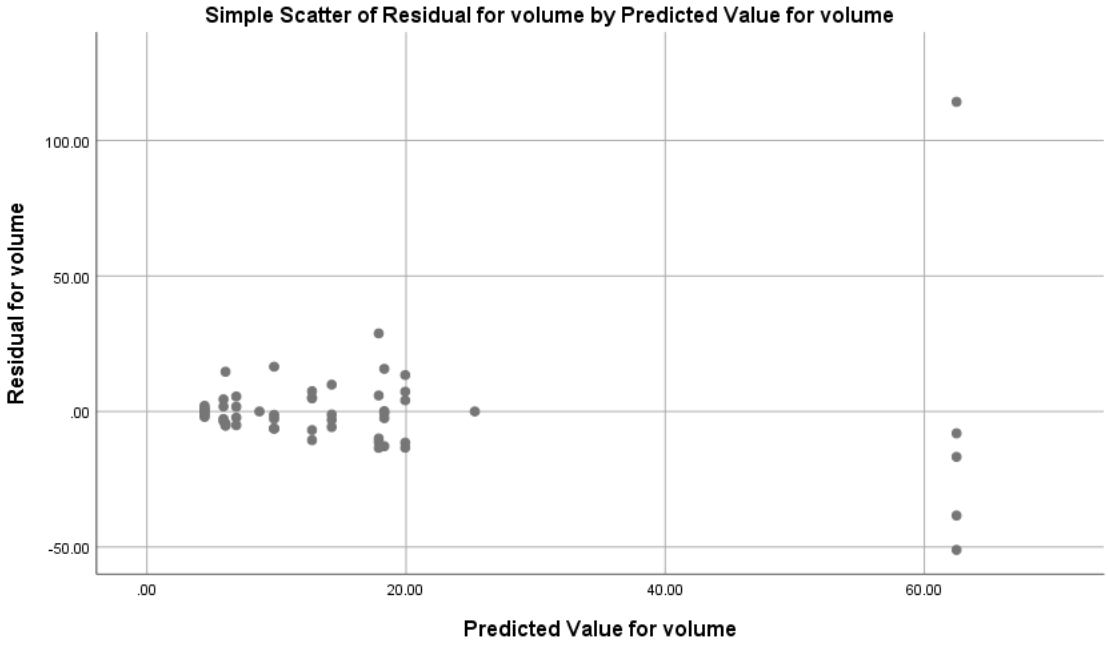

Figure 7.5.4*- Volume residuals v predicted values*

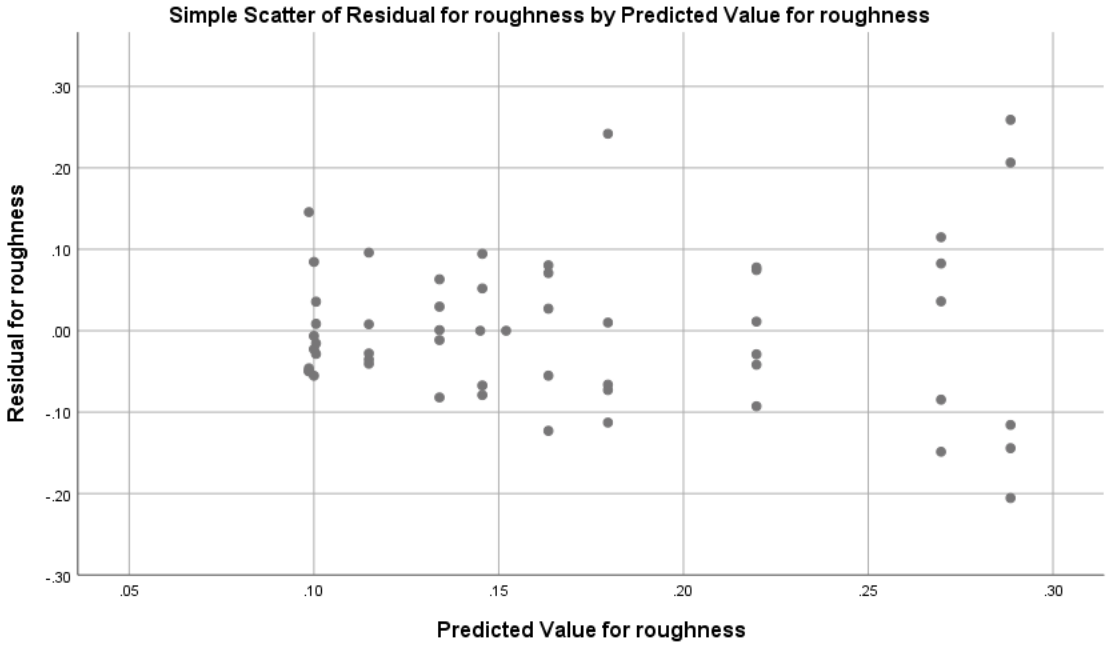

Figure 7.5.5- *Roughness residuals v predicted values*

8 References

Ahmed, M. H. *et al.* (2014) 'Predicting the molecular interactions of CRIP1a-cannabinoid 1 receptor with integrated molecular modeling approaches.', *Bioorganic & medicinal chemistry letters*, 24(4), pp. 1158–65. doi: 10.1016/j.bmcl.2013.12.119.

Arevalo-Martin, A. *et al.* (2012) 'Early endogenous activation of CB1 and CB2 receptors after spinal cord injury is a protective response involved in spontaneous recovery.', *PloS one*, 7(11), p. e49057. doi: 10.1371/journal.pone.0049057.

Augustine, G. J. (2001) 'How does calcium trigger neurotransmitter release?', *Current Opinion in Neurobiology*, pp. 320–326. doi: 10.1016/S0959-4388(00)00214-2.

Barria, A. *et al.* (1997) 'Regulatory phosphorylation of AMPA-type glutamate receptors by CaM-KII during long-term potentiation.', *Science (New York, N.Y.)*. American Association for the Advancement of Science, 276(5321), pp. 2042–5. doi: 10.1126/SCIENCE.276.5321.2042.

Basu, S. *et al.* (2018) 'Quantitative 3-D morphometric analysis of individual dendritic spines.', *Scientific reports*. Nature Publishing Group, 8(1), p. 3545. doi: 10.1038/s41598-018-21753-8.

Beatrice, M. *et al.* (2006) 'Endocannabinoid system in Xenopus laevis development: CB1 receptor dynamics', *FEBS letters*, 580(8), pp. 1941–1945. doi: 10.1016/j.febslet.2006.02.057.

Beattie, E. C. *et al.* (2000) 'Regulation of AMPA receptor endocytosis by a signaling mechanism shared with LTD', *Nature Neuroscience*, 3(12), pp. 1291–1300. doi: 10.1038/81823.

Beisker, W., Dolbeare, F. and Gray, J. W. (1987) 'An improved immunocytochemical procedure for high-sensitivity detection of incorporated bromodeoxyuridine', *Cytometry*, 8(2), pp. 235–239. doi: 10.1002/cyto.990080218.

Bellocchio, L. *et al.* (2010) 'Bimodal control of stimulated food intake by the endocannabinoid system.', *Nature neuroscience*. Nature Publishing Group, 13(3), pp. 281–283. doi: 10.1038/nn.2494.

Bénard, G. *et al.* (2012) 'Mitochondrial CB_1 receptors regulate neuronal energy metabolism.',

Nature neuroscience. Nature Publishing Group, a division of Macmillan Publishers Limited. All Rights Reserved., 15(4), pp. 558–64. doi: 10.1038/nn.3053.

Benoit, M. and Gaub, H. E. (2002) 'Measuring Cell Adhesion Forces with the Atomic Force Microscope at the Molecular Level', *Cells Tissues Organs*, 172(3), pp. 174–189. doi: 10.1159/000066964.

Bessis, A. S. *et al.* (2002) 'Closure of the Venus flytrap module of mGlu8 receptor and the activation process: Insights from mutations converting antagonists into agonists.', *undefined*.

Billinton, N. and Knight, A. W. (2001) 'Seeing the wood through the trees: a review of techniques for distinguishing green fluorescent protein from endogenous autofluorescence.', *Analytical biochemistry*, 291(2), pp. 175–97. doi: 10.1006/abio.2000.5006.

Binnig, G., Quate, C. F. and Gerber, C. (1986) 'Atomic Force Microscope', *Physical Review Letters*. American Physical Society, 56(9), pp. 930–933. doi: 10.1103/PhysRevLett.56.930.

Birnsteil, M. *et al.* (1968) 'Properties and Composition of the Isolated Ribosomal DNA Satellite of Xenopus laevis', *Nature*. Nature Publishing Group, 219(5153), pp. 454–463. doi: 10.1038/219454a0.

Bisogno, T. *et al.* (2003) 'Cloning of the first sn1-DAG lipases points to the spatial and temporal regulation of endocannabinoid signaling in the brain', *Journal of Cell Biology*, 163(3), pp. 463–468. doi: 10.1083/jcb.200305129.

Blume, L. C. *et al.* (2014) 'Cannabinoid receptor interacting protein (CRIP1a) attenuates CB1R signaling in neuronal cells.', *Cellular signalling*, 27(3), pp. 716–726. doi: 10.1016/j.cellsig.2014.11.006.

den Boon, F. S. *et al.* (2014) 'Activation of type-1 cannabinoid receptor shifts the balance between excitation and inhibition towards excitation in layer II/III pyramidal neurons of the rat prelimbic cortex.', *Pflugers Archiv : European journal of physiology*. doi: 10.1007/s00424-014-1586-z.

Bosch, C., Martínez, A., Masachs, N., Teixeira, C. M., *et al.* (2015) 'FIB/SEM technology and high-throughput 3D reconstruction of dendritic spines and synapses in GFP-labeled adult-generated neurons.', *Frontiers in neuroanatomy*, 9(May), p. 60. doi: 10.3389/fnana.2015.00060.

Bosch, C., Martínez, A., Masachs, N., Teixeira, C. M. C. M., *et al.* (2015) 'FIB/SEM technology and high-throughput 3D reconstruction of dendritic spines and synapses in GFP-labeled adult-generated neurons', *Frontiers in neuroanatomy*. Frontiers, 9(May), p. 60. doi: 10.3389/fnana.2015.00060.

Bosch, M. *et al.* (2014) 'Structural and molecular remodeling of dendritic spine substructures during long-term potentiation.', *Neuron*. NIH Public Access, 82(2), pp. 444–59. doi: 10.1016/j.neuron.2014.03.021.

Bosch, M. and Hayashi, Y. (2012) 'Structural plasticity of dendritic spines.', *Current opinion in neurobiology*. NIH Public Access, 22(3), pp. 383–8. doi: 10.1016/j.conb.2011.09.002.

Brown, A. J. (2007) 'Novel cannabinoid receptors.', *British journal of pharmacology*, 152, pp. 567–575. doi: 10.1038/sj.bjp.0707481.

Brown, D. D., Wensink, P. C. and Jordan, E. (1971) 'Purification and some characteristics of 5S DNA from Xenopus laevis.', *Proceedings of the National Academy of Sciences of the United States of America*. National Academy of Sciences, 68(12), pp. 3175–9. doi: 10.1073/PNAS.68.12.3175.

Bruijnzeel, A. W. *et al.* (2016) 'Behavioral Characterization of the Effects of Cannabis Smoke and Anandamide in Rats', *PLOS ONE*. Edited by J. M. Dominguez, 11(4), p. e0153327. doi: 10.1371/journal.pone.0153327.

Buczynski, M. W. and Parsons, L. H. (2010) 'Quantification of brain endocannabinoid levels: methods, interpretations and pitfalls.', *British journal of pharmacology*. Wiley-Blackwell, 160(3), pp. 423–42. doi: 10.1111/j.1476-5381.2010.00787.x.

Calabrese, B., Wilson, M. S. and Halpain, S. (2006) 'Development and Regulation of Dendritic

Spine Synapses', *Physiology*, 21(1), pp. 38–47. doi: 10.1152/physiol.00042.2005.

Cane, M. *et al.* (2014) 'The relationship between PSD-95 clustering and spine stability in vivo.', *The Journal of neuroscience : the official journal of the Society for Neuroscience*. Society for Neuroscience, 34(6), pp. 2075–86. doi: 10.1523/JNEUROSCI.3353-13.2014.

Castillo, P. E. *et al.* (2012) 'Endocannabinoid Signaling and Synaptic Function', *Neuron*, 76(1), pp. 70–81. doi: 10.1016/j.neuron.2012.09.020.

Chaouloff, F. *et al.* (2011) 'Endocannabinoids and motor behavior: CB1 receptors also control running activity.', *Physiology (Bethesda, Md.)*, 26(2), pp. 76–7; author reply 78. doi: 10.1152/physiol.00050.2010.

Chapman, R. J., Issberner, J. P. and Sillar, K. T. (2008) 'Group I mGluRs increase locomotor network excitability in Xenopus tadpoles via presynaptic inhibition of glycinergic neurotransmission', *European Journal of Neuroscience*, 28(5), pp. 903–913. doi: 10.1111/j.1460-9568.2008.06391.x.

Chapman, R. J. and Sillar, K. T. (2007) 'Modulation of a spinal locomotor network by metabotropic glutamate receptors', *European Journal of Neuroscience*, 26(8), pp. 2257–2268. doi: 10.1111/j.1460-9568.2007.05817.x.

Chen, J. L. *et al.* (2012) 'Clustered dynamics of inhibitory synapses and dendritic spines in the adult neocortex.', *Neuron*. NIH Public Access, 74(2), pp. 361–73. doi: 10.1016/j.neuron.2012.02.030.

Cho, K. *et al.* (2000) 'A new form of long-term depression in the perirhinal cortex', *Nature Neuroscience*. Nature Publishing Group, 3(2), pp. 150–156. doi: 10.1038/72093.

Console-Bram, L., Marcu, J. and Abood, M. E. (2012) 'Cannabinoid receptors: nomenclature and pharmacological principles.', *Progress in neuro-psychopharmacology & biological psychiatry*. Elsevier Inc., 38(1), pp. 4–15. doi: 10.1016/j.pnpbp.2012.02.009.

Cottone, E. *et al.* (2003) 'Xenopus laevis CB1 cannabinoid receptor: molecular cloning and

mRNA distribution in the central nervous system.', *The Journal of comparative neurology*, 464, pp. 487–496. doi: 10.1002/cne.10808.

Cruz-Martín, A., Crespo, M. and Portera-Cailliau, C. (2012) 'Glutamate induces the elongation of early dendritic protrusions via mGluRs in wild type mice, but not in fragile X mice.', *PloS one*. Public Library of Science, 7(2), p. e32446. doi: 10.1371/journal.pone.0032446.

Cui, Y. *et al.* (2015) 'Endocannabinoids mediate bidirectional striatal spike-timing-dependent plasticity', 13, pp. 2833–2849. doi: 10.1113/JP270324.

Dawid, I. B. (1966) 'Evidence for the mitochondrial origin of frog egg cytoplasmic DNA.', *Proceedings of the National Academy of Sciences of the United States of America*. National Academy of Sciences, 56(1), pp. 269–76. doi: 10.1073/PNAS.56.1.269.

Deng, P.-Y. *et al.* (2013) 'FMRP regulates neurotransmitter release and synaptic information transmission by modulating action potential duration via BK channels.', *Neuron*. NIH Public Access, 77(4), pp. 696–711. doi: 10.1016/j.neuron.2012.12.018.

Devane, W. A. *et al.* (1988) 'Determination and characterization of a cannabinoid receptor in rat brain.', *Molecular pharmacology*, 34(5), pp. 605–13.

Devane, W. a *et al.* (1992) 'Isolation and Structure of a Brain Constituent That Binds to the Cannabinoid Receptor', *Science*, 258(10), pp. 1946–1949.

Diana, M. A. and Marty, A. (2003) 'Characterization of depolarization-induced suppression of inhibition using paired interneuron--Purkinje cell recordings.', *The Journal of neuroscience : the official journal of the Society for Neuroscience*, 23, pp. 5906–5918.

Dimitriadis, E. K. *et al.* (2002) 'Determination of elastic moduli of thin layers of soft material using the atomic force microscope.', *Biophysical journal*. The Biophysical Society, 82(5), pp. 2798–810. doi: 10.1016/S0006-3495(02)75620-8.

DiPatrizio, N. V. and Piomelli, D. (2012) 'The thrifty lipids: Endocannabinoids and the neural control of energy conservation', *Trends in Neurosciences*, pp. 403–411. doi:

10.1016/j.tins.2012.04.006.

Dudek, S. M. and Bear, M. F. (1993) 'Bidirectional long-term modification of synaptic effectiveness in the adult and immature hippocampus.', *The Journal of neuroscience : the official journal of the Society for Neuroscience*. Society for Neuroscience, 13(7), pp. 2910–8. doi: 10.1523/JNEUROSCI.13-07-02910.1993.

Ehlers, M. D. (2000) 'Reinsertion or Degradation of AMPA Receptors Determined by Activity-Dependent Endocytic Sorting', *Neuron*. Cell Press, 28(2), pp. 511–525. doi: 10.1016/S0896-6273(00)00129-X.

Ehrlich, I. *et al.* (2007) 'PSD-95 is required for activity-driven synapse stabilization.', *Proceedings of the National Academy of Sciences of the United States of America*. National Academy of Sciences, 104(10), pp. 4176–4181. doi: 10.1073/pnas.0609307104.

Fitzjohn, S. M. *et al.* (1999) 'DHPG-induced LTD in area CA1 of juvenile rat hippocampus; characterisation and sensitivity to novel mGlu receptor antagonists', *Neuropharmacology*, 38(10), pp. 1577–1583. doi: 10.1016/S0028-3908(99)00123-9.

Gao, Y. *et al.* (2010) 'Loss of Retrograde Endocannabinoid Signaling and Reduced Adult Neurogenesis in Diacylglycerol Lipase Knock-out Mice', *Journal of Neuroscience*, 30(6), pp. 2017–2024. doi: 10.1523/JNEUROSCI.5693-09.2010.

García-López, P., García-Marín, V. and Freire, M. (2007) 'The discovery of dendritic spines by Cajal in 1888 and its relevance in the present neuroscience', *Progress in Neurobiology*. Pergamon, 83(2), pp. 110–130. doi: 10.1016/J.PNEUROBIO.2007.06.002.

Girasole, M. *et al.* (2007) 'Roughness of the plasma membrane as an independent morphological parameter to study RBCs: A quantitative atomic force microscopy investigation', *Biochimica et Biophysica Acta (BBA) - Biomembranes*. Elsevier, 1768(5), pp. 1268–1276. doi: 10.1016/J.BBAMEM.2007.01.014.

Godlewski, G. *et al.* (2009) 'Receptors for acylethanolamides-GPR55 and GPR119', *Prostaglandins and Other Lipid Mediators*, pp. 105–111. doi:

10.1016/j.prostaglandins.2009.07.001.

Gray, N. W. *et al.* (2006) 'Rapid redistribution of synaptic PSD-95 in the neocortex in vivo.', *PLoS biology*. Public Library of Science, 4(11), p. e370. doi: 10.1371/journal.pbio.0040370.

Gross, L. *et al.* (2009) 'The Chemical Structure of a Molecule Resolved by Atomic Force Microscopy', *Science*, 325(5944), pp. 1110–1114. doi: 10.1126/science.1176210.

Guggenhuber, S. *et al.* (2016) 'Cannabinoid receptor-interacting protein Crip1a modulates CB1 receptor signaling in mouse hippocampus', *Brain Structure and Function*, 221(4), pp. 2061–2074. doi: 10.1007/s00429-015-1027-6.

Gulyas, A. I. *et al.* (2004) 'Segregation of two endocannabinoid-hydrolyzing enzymes into pre- and postsynaptic compartments in the rat hippocampus, cerebellum and amygdala', *European Journal of Neuroscience*, 20, pp. 441–458. doi: 10.1111/j.1460-9568.2004.03428.x.

Gupta, V. K. *et al.* (2013) 'TrkB receptor signalling: implications in neurodegenerative, psychiatric and proliferative disorders.', *International journal of molecular sciences*. Multidisciplinary Digital Publishing Institute (MDPI), 14(5), pp. 10122–42. doi: 10.3390/ijms140510122.

Gurdon, J. B. and Uehlinger, V. (1966) '"Fertile" intestine nuclei.', *Nature*, 210(5042), pp. 1240–1.

Gurdun, J. B., Elsdale, T. R. and Fishberg, M. (1958) 'Sexually Mature Individuals of Xenopus laevis from the Transplantation of Single Somatic Nuclei', *Nature*. Nature Publishing Group, 182(4627), pp. 64–65. doi: 10.1038/182064a0.

Hansma, H. G. *et al.* (1997) 'Properties of Biomolecules Measured from Atomic Force Microscope Images: A Review', *Journal of Structural Biology*. Academic Press, 119(2), pp. 99–108. doi: 10.1006/JSBI.1997.3855.

Hanus, L. *et al.* (2001) '2-arachidonyl glyceryl ether, an endogenous agonist of the cannabinoid CB1 receptor.', *Proceedings of the National Academy of Sciences of the United States of*

America, 98, pp. 3662–3665. doi: 10.1073/pnas.061029898.

Harland, R. M. and Grainger, R. M. (2011) 'Xenopus research: Metamorphosed by genetics and genomics', *Trends in Genetics*. Elsevier Ltd, 27(12), pp. 507–515. doi: 10.1016/j.tig.2011.08.003.

Harris, K. M., Jensen, F. E. and Tsao, B. (1992) 'Three-dimensional structure of dendritic spines and synapses in rat hippocampus (CA1) at postnatal day 15 and adult ages: implications for the maturation of synaptic physiology and long-term potentiation.', *The Journal of neuroscience : the official journal of the Society for Neuroscience*. Society for Neuroscience, 12(7), pp. 2685–705. doi: 10.1523/JNEUROSCI.12-07-02685.1992.

Hebb, D. (1949) 'The organization of behavior: A neuropsychological theory.', *Science Education*. Wiley-Blackwell, 34(5), pp. 336–337. doi: 10.1002/sce.37303405110.

Hebert-Chatelain, E. *et al.* (2014) 'Cannabinoid control of brain bioenergetics: Exploring the subcellular localization of the CB1 receptor.', *Molecular metabolism*. Elsevier, 3(4), pp. 495–504. doi: 10.1016/j.molmet.2014.03.007.

Henley, J. M. and Wilkinson, K. A. (2016) 'Synaptic AMPA receptor composition in development, plasticity and disease', *Nature Reviews Neuroscience*. Nature Publishing Group. doi: 10.1038/nrn.2016.37.

Henry, D. J. and Chavkin, C. (1995) 'Activation of inwardly rectifying potassium channels (GIRK1) by co-expressed rat brain cannabinoid receptors in Xenopus oocytes', *Neuroscience Letters*. Elsevier, 186(2–3), pp. 91–94. doi: 10.1016/0304-3940(95)11289-9.

Hering, H. and Sheng, M. (2001) 'Dentritic spines : structure, dynamics and regulation', *Nature Reviews Neuroscience*. Nature Publishing Group, 2(12), pp. 880–888. doi: 10.1038/35104061.

Hermans, E. and Challiss, R. A. (2001) 'Structural, signalling and regulatory properties of the group I metabotropic glutamate receptors: prototypic family C G-protein-coupled receptors.', *The Biochemical journal*, 359(Pt 3), pp. 465–84.

Howlett, A. C., Blume, L. C. and Dalton, G. D. (2010) 'CB(1) cannabinoid receptors and their associated proteins.', *Current medicinal chemistry*, 17(14), pp. 1382–93.

Hu, X. *et al.* (2011) 'BDNF-induced increase of PSD-95 in dendritic spines requires dynamic microtubule invasions.', *The Journal of neuroscience : the official journal of the Society for Neuroscience*. NIH Public Access, 31(43), pp. 15597–603. doi: 10.1523/JNEUROSCI.2445-11.2011.

Huang, S. M. *et al.* (2002) 'An endogenous capsaicin-like substance with high potency at recombinant and native vanilloid VR1 receptors.', *Proceedings of the National Academy of Sciences of the United States of America*, 99, pp. 8400–8405. doi: 10.1073/pnas.122196999.

Huang, W.-J., Chen, W.-W. and Zhang, X. (2016) 'Endocannabinoid system: Role in depression, reward and pain control (Review).', *Molecular medicine reports*. Spandidos Publications, 14(4), pp. 2899–903. doi: 10.3892/mmr.2016.5585.

Huang, Y.-B. *et al.* (2015) 'In Vivo Study of Dynamics and Stability of Dendritic Spines on Olfactory Bulb Interneurons in Xenopus laevis Tadpoles', *PLOS ONE*. Edited by X. Zha. Public Library of Science, 10(10), p. e0140752. doi: 10.1371/journal.pone.0140752.

Huganir, R. L. and Nicoll, R. A. (2013) 'AMPARs and synaptic plasticity: the last 25 years.', *Neuron*, 80(3), pp. 704–17. doi: 10.1016/j.neuron.2013.10.025.

Hull, M. J. *et al.* (2016) 'Modelling Feedback Excitation, Pacemaker Properties and Sensory Switching of Electrically Coupled Brainstem Neurons Controlling Rhythmic Activity', *PLoS Computational Biology*. Public Library of Science, 12(1), p. e1004702. doi: 10.1371/journal.pcbi.1004702.

Hunt, D. L. and Castillo, P. E. (2012) 'Synaptic plasticity of NMDA receptors: mechanisms and functional implications.', *Current opinion in neurobiology*, 22(3), pp. 496–508. doi: 10.1016/j.conb.2012.01.007.

Iacovelli, L. *et al.* (2002) 'Native group-III metabotropic glutamate receptors are coupled to the mitogen-activated protein kinase/phosphatidylinositol-3-kinase pathways.', *Journal of*

neurochemistry, 82(2), pp. 216–23.

Ijspeert, A. J. (2008) 'Central pattern generators for locomotion control in animals and robots: A review', *Neural Networks*. Pergamon, 21(4), pp. 642–653. doi: 10.1016/J.NEUNET.2008.03.014.

Ito, M., Sakurai, M. and Tongroach, P. (1982) 'Climbing fibre induced depression of both mossy fibre responsiveness and glutamate sensitivity of cerebellar Purkinje cells.', *The Journal of physiology*, 324, pp. 113–34.

Iwagaki, N. and Miles, G. B. (2011) 'Activation of group I metabotropic glutamate receptors modulates locomotor-related motoneuron output in mice.', *Journal of neurophysiology*. American Physiological Society, 105(5), pp. 2108–20. doi: 10.1152/jn.01037.2010.

Jembrek, M. J. *et al.* (2015) 'Atomic force microscopy as an advanced tool in neuroscience.', *Translational neuroscience*. De Gruyter Open, 6(1), pp. 117–130. doi: 10.1515/tnsci-2015-0011.

Katsidoni, V., Kastellakis, A. and Panagis, G. (2013) 'Biphasic effects of Δ9-tetrahydrocannabinol on brain stimulation reward and motor activity.', *The international journal of neuropsychopharmacology / official scientific journal of the Collegium Internationale Neuropsychopharmacologicum (CINP)*. The Oxford University Press, 16(10), pp. 2273–84. doi: 10.1017/S1461145713000709.

Kettunen, P. *et al.* (2002) 'Signaling mechanisms of metabotropic glutamate receptor 5 subtype and its endogenous role in a locomotor network.', *The Journal of neuroscience : the official journal of the Society for Neuroscience*, 22(5), pp. 1868–73.

Kettunen, P. *et al.* (2005) 'Neuromodulation via conditional release of endocannabinoids in the spinal locomotor network.', *Neuron*, 45(1), pp. 95–104. doi: 10.1016/j.neuron.2004.12.022.

Kettunen, P., Hess, D. and Manira, A. El (2003a) 'mGluR1, But Not mGluR5, Mediates Depolarization of Spinal Cord Neurons by Blocking a Leak Current', *Journal of Neurophysiology*. American Physiological Society, 90(4), pp. 2341–2348. doi: 10.1152/jn.01132.2002.

Kettunen, P., Hess, D. and Manira, A. El (2003b) 'mGluR1, But Not mGluR5, Mediates Depolarization of Spinal Cord Neurons by Blocking a Leak Current', *Journal of Neurophysiology*. American Physiological Society, 90(4), pp. 2341–2348. doi: 10.1152/jn.01132.2002.

Koser, D. E. *et al.* (2015) 'CNS cell distribution and axon orientation determine local spinal cord mechanical properties.', *Biophysical journal*. The Biophysical Society, 108(9), pp. 2137–47.

Koser, D. E. *et al.* (2016) 'Mechanosensing is critical for axon growth in the developing brain', *Nature Neuroscience*, 19(September), pp. 1592–1598. doi: 10.1038/nn.4394.

Kunishima, N. *et al.* (2000) 'Structural basis of glutamate recognition by a dimeric metabotropic glutamate receptor', *Nature*, 407(6807), pp. 971–977. doi: 10.1038/35039564.

Kusano, K., Miledi, R. and Stinnakre, J. (1977) 'Acetylcholine receptors in the oocyte membrane', *Nature*. Nature Publishing Group, 270(5639), pp. 739–741. doi: 10.1038/270739a0.

Kyriakatos, A. and El Manira, A. (2007) 'Long-term plasticity of the spinal locomotor circuitry mediated by endocannabinoid and nitric oxide signaling.', *The Journal of neuroscience : the official journal of the Society for Neuroscience*, 27, pp. 12664–12674. doi: 10.1523/JNEUROSCI.3174-07.2007.

Lee, C.-W. *et al.* (2016) 'Membrane roughness as a sensitive parameter reflecting the status of neuronal cells in response to chemical and nanoparticle treatments', *Journal of Nanobiotechnology*. BioMed Central, 14(1), p. 9. doi: 10.1186/s12951-016-0161-5.

Lee, H.-K. *et al.* (2000) 'Regulation of distinct AMPA receptor phosphorylation sites during bidirectional synaptic plasticity', *Nature*. Nature Publishing Group, 405(6789), pp. 955–959. doi: 10.1038/35016089.

Lee, K. *et al.* (2013) 'Autofluorescence generation and elimination: A lesson from glutaraldehyde', *Chemical Communications*, 49(29), pp. 3028–3030. doi: 10.1039/c3cc40799c.

Lee, S.-J. R. *et al.* (2009) 'Activation of CaMKII in single dendritic spines during long-term

potentiation.', *Nature*. NIH Public Access, 458(7236), pp. 299–304. doi: 10.1038/nature07842.

Lee, S. H., Simonetta, A. and Sheng, M. (2004) 'Subunit Rules Governing the Sorting of Internalized AMPA Receptors in Hippocampal Neurons', *Neuron*, 43(2), pp. 221–236. doi: 10.1016/j.neuron.2004.06.015.

Leung, D. *et al.* (2006) 'Inactivation of N-Acyl phosphatidylethanolamine phospholipase D reveals multiple mechanisms for the biosynthesis of endocannabinoids', *Biochemistry*, 45, pp. 4720–4726. doi: 10.1021/bi060163l.

Leung, K. *et al.* (2013) 'Role of FAAH-like anandamide transporter in anandamide inactivation', *PLoS ONE*, 8. doi: 10.1371/journal.pone.0079355.

Li, W.-C. and Moult, P. R. (2012) 'The control of locomotor frequency by excitation and inhibition.', *The Journal of neuroscience : the official journal of the Society for Neuroscience*, 32(18), pp. 6220–30. doi: 10.1523/JNEUROSCI.6289-11.2012.

Li, W.-C., Roberts, A. and Soffe, S. R. (2009) 'Locomotor rhythm maintenance: electrical coupling among premotor excitatory interneurons in the brainstem and spinal cord of young Xenopus tadpoles.', *The Journal of physiology*, 587(Pt 8), pp. 1677–93. doi: 10.1113/jphysiol.2008.166942.

Li, W.-C. W.-C., Roberts, A. and Soffe, S. R. (2010) 'Specific brainstem neurons switch each other into pacemaker mode to drive movement by activating NMDA receptors.', *The Journal of neuroscience : the official journal of the Society for Neuroscience*, 30(49), pp. 16609–16620. doi: 10.1523/JNEUROSCI.3695-10.2010.

Li, X.-M. *et al.* (2007) 'JNK1 contributes to metabotropic glutamate receptor-dependent long-term depression and short-term synaptic plasticity in the mice area hippocampal CA1', *European Journal of Neuroscience*, 25(2), pp. 391–396. doi: 10.1111/j.1460-9568.2006.05300.x.

Liu, J. *et al.* (2006) 'A biosynthetic pathway for anandamide.', *Proceedings of the National Academy of Sciences of the United States of America*, 103, pp. 13345–13350. doi:

10.1073/pnas.0601832103.

Liu, X. F., Tari, P. K. and Haas, K. (2009) 'PKM zeta restricts dendritic arbor growth by filopodial and branch stabilization within the intact and awake developing brain.', *The Journal of neuroscience : the official journal of the Society for Neuroscience*, 29(39), pp. 12229–35. doi: 10.1523/JNEUROSCI.2842-09.2009.

Louhivuori, V. *et al.* (2011) 'BDNF and TrkB in neuronal differentiation of Fmr1-knockout mouse', *Neurobiology of Disease*, 41(2), pp. 469–480. doi: 10.1016/j.nbd.2010.10.018.

Lu, Y.-B. *et al.* (2006) 'Viscoelastic properties of individual glial cells and neurons in the CNS.', *Proceedings of the National Academy of Sciences of the United States of America*, 103(47), pp. 17759–64. doi: 10.1073/pnas.0606150103.

Lynch, G. S., Dunwiddie, T. and Gribkoff, V. (1977) 'Heterosynaptic depression: a postsynaptic correlate of long-term potentiation', *Nature*. Nature Publishing Group, 266(5604), pp. 737–739. doi: 10.1038/266737a0.

Ma, L. *et al.* (2015) 'Mitochondrial CB1 receptor is involved in ACEA-induced protective effects on neurons and mitochondrial functions.', *Scientific reports*, 5, p. 12440. doi: 10.1038/srep12440.

Maccarrone, M. *et al.* (2008) 'Anandamide inhibits metabolism and physiological actions of 2-arachidonoylglycerol in the striatum', *Nature Neuroscience*, 11(2), pp. 152–159. doi: 10.1038/nn2042.

Madabhushi, R. *et al.* (2015) 'Activity-Induced DNA Breaks Govern the Expression of Neuronal Early-Response Genes', *Cell*. Elsevier, 161(7), pp. 1592–605. doi: 10.1016/j.cell.2015.05.032.

Mallet, P. E. and Beninger, R. J. (1998) 'The cannabinoid CB 1 receptor antagonist SR141716A attenuates the memory impairment produced by ? 9 -tetrahydrocannabinol or anandamide', *Psychopharmacology*. Springer-Verlag, 140(1), pp. 11–19. doi: 10.1007/s002130050733.

Mancuso, J. J. *et al.* (2013) 'Methods of dendritic spine detection: from Golgi to high-resolution

optical imaging.', *Neuroscience*. NIH Public Access, 251, pp. 129–40. doi: 10.1016/j.neuroscience.2012.04.010.

El Manira, A. *et al.* (2002) 'Metabotropic glutamate receptors provide intrinsic modulation of the lamprey locomotor network', *Brain Research Reviews*, pp. 9–18. doi: 10.1016/S0165-0173(02)00184-4.

El Manira, A. *et al.* (2008) 'Endocannabinoid signaling in the spinal locomotor circuitry', *Brain Research Reviews*. Elsevier, 57(1), pp. 29–36. doi: 10.1016/j.brainresrev.2007.06.020.

El Manira, A. and Kyriakatos, A. (2010) 'The role of endocannabinoid signaling in motor control.', *Physiology (Bethesda, Md.)*, 25, pp. 230–238. doi: 10.1152/physiol.00007.2010.

Marder, E. and Bucher, D. (2001) 'Central pattern generators and the control of rhythmic movements', *Current Biology*. Cell Press, 11(23), pp. R986–R996. doi: 10.1016/S0960-9822(01)00581-4.

Marsicano, G. *et al.* (2003) 'CB1 cannabinoid receptors and on-demand defense against excitotoxicity.', *Science (New York, N.Y.)*, 302(5642), pp. 84–8. doi: 10.1126/science.1088208.

Marsicano, G. and Lafenêtre, P. (2009) 'Roles of the Endocannabinoid system in learning and memory', *Current Topics in Behavioral Neurosciences*, pp. 201–230. doi: 10.1007/978-3-540-88955-7_8.

Martin, M. *et al.* (2013) 'Morphology and nanomechanics of sensory neurons growth cones following peripheral nerve injury.' Edited by I. Sokolov. Public Library of Science, 8(2), p. e56286. doi: 10.1371/journal.pone.0056286.

Mathiesen, J. M. *et al.* (2003) 'Positive allosteric modulation of the human metabotropic glutamate receptor 4 (hmGluR4) by SIB-1893 and MPEP.', *British journal of pharmacology*. Wiley-Blackwell, 138(6), pp. 1026–30. doi: 10.1038/sj.bjp.0705159.

Matsuzaki, M. *et al.* (2001) 'Dendritic spine geometry is critical for AMPA receptor expression in hippocampal CA1 pyramidal neurons', *Nature Neuroscience*. NIH Public Access, 4(11), pp.

1086–1092. doi: 10.1038/nn736.

Matsuzaki, M. *et al.* (2004) 'Structural basis of long-term potentiation in single dendritic spines', *Nature*, 429(6993), pp. 761–766. doi: 10.1038/nature02617.

Mechoulam, R. *et al.* (1995) 'Identification of an endogenous 2-monoglyceride, present in canine gut, that binds to cannabinoid receptors.', *Biochemical pharmacology*, 50(1), pp. 83–90.

Mendizabal-Zubiaga, J. *et al.* (2016) 'Cannabinoid CB1 Receptors Are Localized in Striated Muscle Mitochondria and Regulate Mitochondrial Respiration.', *Frontiers in physiology*. Frontiers Media SA, 7, p. 476. doi: 10.3389/fphys.2016.00476.

More, S. V. and Choi, D.-K. (2015) 'Promising cannabinoid-based therapies for Parkinson's disease: motor symptoms to neuroprotection.', *Molecular neurodegeneration*, 10, p. 17. doi: 10.1186/s13024-015-0012-0.

Morgan, N. H., Stanford, I. M. and Woodhall, G. L. (2009) 'Functional CB2 type cannabinoid receptors at CNS synapses.', *Neuropharmacology*, 57(4), pp. 356–68. doi: 10.1016/j.neuropharm.2009.07.017.

Moult, P. R. *et al.* (2008) 'Co-activation of p38 mitogen-activated protein kinase and protein tyrosine phosphatase underlies metabotropic glutamate receptor-dependent long-term depression', *The Journal of Physiology*, 586(10), pp. 2499–2510. doi: 10.1113/jphysiol.2008.153122.

Moult, P. R., Cottrell, G. A. and Li, W.-C. C. (2013) 'Fast silencing reveals a lost role for reciprocal inhibition in locomotion.', *Neuron*, 77(1), pp. 129–40. doi: 10.1016/j.neuron.2012.10.040.

Nanou, E. *et al.* (2009) 'Separate signalling mechanisms underlie mGluR1 modulation of leak channels and NMDA receptors in the network underlying locomotion', *The Journal of physiology*. Wiley-Blackwell, 587(Pt 12), pp. 3001–8. doi: 10.1113/jphysiol.2009.172452.

Newman, Z. *et al.* (2007) 'Endocannabinoids mediate muscarine-induced synaptic depression

at the vertebrate neuromuscular junction.', *The European journal of neuroscience*. Wiley-Blackwell, 25(6), pp. 1619–30. doi: 10.1111/j.1460-9568.2007.05422.x.

Nieuwkoop, P. D. and Faber, J. (1995) 'Normal table of Xenopus laevis (Daudin)', *Trends in Genetics*. Elsevier, 11(10), p. 418. doi: 10.1016/S0168-9525(00)89129-5.

Nikkhah, M. *et al.* (2011) 'Evaluation of the influence of growth medium composition on cell elasticity', *Journal of Biomechanics*, 44(4), pp. 762–766. doi: 10.1016/j.jbiomech.2010.11.002.

Niswender, C. M. and Conn, P. J. (2010) 'Metabotropic glutamate receptors: physiology, pharmacology, and disease.', *Annual review of pharmacology and toxicology*. NIH Public Access, 50, pp. 295–322. doi: 10.1146/annurev.pharmtox.011008.145533.

O'Leary, D. M. *et al.* (2000) 'Selective mGluR5 antagonists MPEP and SIB-1893 decrease NMDA or glutamate-mediated neuronal toxicity through actions that reflect NMDA receptor antagonism.', *British journal of pharmacology*. Wiley-Blackwell, 131(7), pp. 1429–37. doi: 10.1038/sj.bjp.0703715.

Okamoto, K., Bosch, M. and Hayashi, Y. (2009) 'The Roles of CaMKII and F-Actin in the Structural Plasticity of Dendritic Spines: A Potential Molecular Identity of a Synaptic Tag?', *Physiology*, 24(6), pp. 357–366. doi: 10.1152/physiol.00029.2009.

Okamoto, Y. *et al.* (2004) 'Molecular Characterization of a Phospholipase D Generating Anandamide and Its Congeners', *Journal of Biological Chemistry*, 279(7), pp. 5298–5305. doi: 10.1074/jbc.M306642200.

On, V. *et al.* (2017) 'Automated spatio-temporal analysis of dendritic spines and related protein dynamics', *PLOS ONE*. Edited by L. Mei. Public Library of Science, 12(8), p. e0182958. doi: 10.1371/journal.pone.0182958.

Page, G. *et al.* (2006) 'Group I metabotropic glutamate receptors activate the p70S6 kinase via both mammalian target of rapamycin (mTOR) and extracellular signal-regulated kinase (ERK 1/2) signaling pathways in rat striatal and hippocampal synaptoneurosomes', *Neurochemistry International*, 49(4), pp. 413–421. doi: 10.1016/j.neuint.2006.01.020.

Palmer, M. J. *et al.* (1997) 'The group I mGlu receptor agonist DHPG induces a novel form of LTD in the CA1 region of the hippocampus.', *Neuropharmacology*, 36(11–12), pp. 1517–32.

Panlilio, L. V. *et al.* (2015) 'Effects of fatty acid amide hydrolase (FAAH) inhibitors on working memory in rats', *Psychopharmacology*. doi: 10.1007/s00213-015-4140-6.

Peng, H. B. *et al.* (2003) 'Differential effects of neurotrophins and schwann cell-derived signals on neuronal survival/growth and synaptogenesis.', *The Journal of neuroscience : the official journal of the Society for Neuroscience*, 23(12), pp. 5050–5060. doi: 23/12/5050 [pii].

Peng, H. B., Baker, L. P. and Chen, Q. (1991) 'Chapter 26 Tissue Culture of Xenopus Neurons and Muscle Cells as a Model for Studying Synaptic Induction', *Methods in Cell Biology*. Academic Press, 36, pp. 511–526. doi: 10.1016/S0091-679X(08)60294-0.

Pitler, T. A. and Alger, B. E. (1992) 'Postsynaptic spike firing reduces synaptic GABAA responses in hippocampal pyramidal cells.', *The Journal of neuroscience : the official journal of the Society for Neuroscience*, 12, pp. 4122–4132.

Polissidis, A. *et al.* (2013) 'The cannabinoid CB1 receptor biphasically modulates motor activity and regulates dopamine and glutamate release region dependently.', *The international journal of neuropsychopharmacology / official scientific journal of the Collegium Internationale Neuropsychopharmacologicum (CINP)*, 16(2), pp. 393–403. doi: 10.1017/S1461145712000156.

Porter, A. C. *et al.* (2002) 'Characterization of a novel endocannabinoid, virodhamine, with antagonist activity at the CB1 receptor.', *The Journal of pharmacology and experimental therapeutics*, 301(3), pp. 1020–1024. doi: 10.1124/jpet.301.3.1020.

Proksch, R. *et al.* (2016) 'Practical loss tangent imaging with amplitude-modulated atomic force microscopy', *Journal of Applied Physics*, 119(13). doi: 10.1063/1.4944879.

Redondo, R. L. and Morris, R. G. M. (2011) 'Making memories last: the synaptic tagging and capture hypothesis', *Nature Reviews Neuroscience*, 12(1), pp. 17–30. doi: 10.1038/nrn2963.

Reggio, P. (2010) 'Endocannabinoid Binding to the Cannabinoid Receptors: What Is Known and

What Remains Unknown', *Current Medicinal Chemistry*. Bentham Science Publishers Ltd., 17(14), pp. 1468–1486. doi: 10.2174/092986710790980005.

Rey, A. A. *et al.* (2012) 'Biphasic effects of cannabinoids in anxiety responses: CB1 and GABA(B) receptors in the balance of GABAergic and glutamatergic neurotransmission.', *Neuropsychopharmacology : official publication of the American College of Neuropsychopharmacology*. Nature Publishing Group, 37(12), pp. 2624–34. doi: 10.1038/npp.2012.123.

Roberts, A., Li, W.-C. and Soffe, S. R. (2010) 'How neurons generate behavior in a hatchling amphibian tadpole: an outline.', *Frontiers in behavioral neuroscience*, 4, p. 16. doi: 10.3389/fnbeh.2010.00016.

Robinson, L. *et al.* (2007) 'The synthetic cannabinoid HU210 induces spatial memory deficits and suppresses hippocampal firing rate in rats', *British Journal of Pharmacology*. Wiley/Blackwell (10.1111), 151(5), pp. 688–700. doi: 10.1038/sj.bjp.0707273.

Rubino, T. *et al.* (2008) 'CB1 receptor stimulation in specific brain areas differently modulate anxiety-related behaviour.', *Neuropharmacology*, 54(1), pp. 151–60. doi: 10.1016/j.neuropharm.2007.06.024.

Ryberg, E. *et al.* (2007) 'The orphan receptor GPR55 is a novel cannabinoid receptor.', *British journal of pharmacology*, 152, pp. 1092–1101. doi: 10.1038/sj.bjp.0707460.

Sala, C. and Segal, M. (2014) 'Dendritic spines: the locus of structural and functional plasticity.', *Physiological reviews*, 94(1), pp. 141–88. doi: 10.1152/physrev.00012.2013.

Salio, C. *et al.* (2002) 'CB1 cannabinoid receptors in amphibian spinal cord: Relationships with some nociception markers', *Journal of Chemical Neuroanatomy*, 24, pp. 153–162. doi: 10.1016/S0891-0618(02)00040-6.

Sánchez-Blázquez, P., Rodríguez-Muñoz, M. and Garzón, J. (2014) 'The cannabinoid receptor 1 associates with NMDA receptors to produce glutamatergic hypofunction: implications in psychosis and schizophrenia.', *Frontiers in pharmacology*, 4, p. 169. doi:

10.3389/fphar.2013.00169.

Sánchez-Pastor, E. *et al.* (2007) 'Effects of cannabinoids on synaptic transmission in the frog neuromuscular junction.', *The Journal of pharmacology and experimental therapeutics*. American Society for Pharmacology and Experimental Therapeutics, 321(2), pp. 439–45. doi: 10.1124/jpet.106.116319.

Sañudo-Peña, M. C. *et al.* (2000) 'Activational role of cannabinoids on movement', *European Journal of Pharmacology*, 391(3), pp. 269–274. doi: 10.1016/S0014-2999(00)00044-3.

Schubart, C. D. *et al.* (2014) 'Cannabidiol as a potential treatment for psychosis', *European Neuropsychopharmacology*. Elsevier, 24(1), pp. 51–64. doi: 10.1016/J.EURONEURO.2013.11.002.

Session, A. M. *et al.* (2016) 'Genome evolution in the allotetraploid frog Xenopus laevis', *Nature*, 538(7625), pp. 336–343. doi: 10.1038/nature19840.

Shi, P., Huang, Y. and Hong, J. (2014) 'Automated three-dimensional reconstruction and morphological analysis of dendritic spines based on semi-supervised learning', *Biomedical Optics Express*, 5(5), p. 1541. doi: 10.1364/BOE.5.001541.

Shibata, M. *et al.* (2015) 'Long-tip high-speed atomic force microscopy for nanometer-scale imaging in live cells', *Scientific Reports*. Nature Publishing Group, 5(1), p. 8724. doi: 10.1038/srep08724.

Song, J. *et al.* (2015) 'Motor neurons control locomotor circuit function retrogradely via gap junctions', *Nature*. doi: 10.1038/nature16497.

Song, J., Kyriakatos, A. and El Manira, A. (2012) 'Gating the polarity of endocannabinoid-mediated synaptic plasticity by nitric oxide in the spinal locomotor network.', *The Journal of neuroscience : the official journal of the Society for Neuroscience*, 32(15), pp. 5097–105. doi: 10.1523/JNEUROSCI.5850-11.2012.

Starowicz, K., Nigam, S. and Di Marzo, V. (2007) 'Biochemistry and pharmacology of

endovanilloids.', *Pharmacology & therapeutics*, 114(1), pp. 13–33. doi: 10.1016/j.pharmthera.2007.01.005.

Staubli, U. and Lynch, G. (1990) 'Stable depression of potentiated synaptic responses in the hippocampus with 1-5 Hz stimulation.', *Brain research*, 513(1), pp. 113–8.

Stauffer, B. *et al.* (2011) 'CRIP1a switches cannabinoid receptor agonist/antagonist-mediated protection from glutamate excitotoxicity.', *Neuroscience letters*, 503(3), pp. 224–8. doi: 10.1016/j.neulet.2011.08.041.

Steindel, F. *et al.* (2013) 'Neuron-type specific cannabinoid-mediated G protein signalling in mouse hippocampus.', *Journal of neurochemistry*, 124(6), pp. 795–807. doi: 10.1111/jnc.12137.

Støving, R. K. *et al.* (2009) 'Leptin, ghrelin, and endocannabinoids: Potential therapeutic targets in anorexia nervosa', *Journal of Psychiatric Research*. Pergamon, 43(7), pp. 671–679. doi: 10.1016/J.JPSYCHIRES.2008.09.007.

Sulcova, E. (1998) 'Biphasic Effects of Anandamide', *Pharmacology Biochemistry and Behavior*, 59(2), pp. 347–352. doi: 10.1016/S0091-3057(97)00422-X.

Tononi, G. and Cirelli, C. (2014) 'Sleep and the price of plasticity: from synaptic and cellular homeostasis to memory consolidation and integration.', *Neuron*. NIH Public Access, 81(1), pp. 12–34. doi: 10.1016/j.neuron.2013.12.025.

Tononi, G. and Cirelli, C. (2016) 'Sleep and Synaptic Down-Selection', in. Springer, Cham, pp. 99–106. doi: 10.1007/978-3-319-28802-4_8.

Tóth, A., Blumberg, P. M. and Boczán, J. (2009) 'Anandamide and the vanilloid receptor (TRPV1).', *Vitamins and hormones*, 81, pp. 389–419. doi: 10.1016/S0083-6729(09)81015-7.

Tsou, K. *et al.* (1998) 'Immunohistochemical distribution of cannabinoid CB1 receptors in the rat central nervous system', *Neuroscience*, 83, pp. 393–411. doi: 10.1016/S0306-4522(97)00436-3.

Tzavara, E. T., Wade, M. and Nomikos, G. G. (2003) 'Biphasic effects of cannabinoids on acetylcholine release in the hippocampus: site and mechanism of action.', *The Journal of neuroscience : the official journal of the Society for Neuroscience*, 23(28), pp. 9374–9384. doi: 23/28/9374 [pii].

Vanderklish, P. W. and Edelman, G. M. (2002) 'Dendritic spines elongate after stimulation of group 1 metabotropic glutamate receptors in cultured hippocampal neurons.', *Proceedings of the National Academy of Sciences of the United States of America*. National Academy of Sciences, 99(3), pp. 1639–44. doi: 10.1073/pnas.032681099.

Vaughn, L. K. *et al.* (2010) 'Endocannabinoid signalling: Has it got rhythm?', *British Journal of Pharmacology*, pp. 530–543. doi: 10.1111/j.1476-5381.2010.00790.x.

van Versendaal, D. *et al.* (2012) 'Elimination of inhibitory synapses is a major component of adult ocular dominance plasticity.', *Neuron*, 74(2), pp. 374–83. doi: 10.1016/j.neuron.2012.03.015.

Vincent, P., Armstrong, C. M. and Marty, A. (1992) 'Inhibitory synaptic currents in rat cerebellar Purkinje cells: modulation by postsynaptic depolarization.', *The Journal of physiology*, 456, pp. 453–471.

Viveros, M. P., Marco, E. M. and File, S. E. (2005) 'Endocannabinoid system and stress and anxiety responses.', *Pharmacology, biochemistry, and behavior*, 81(2), pp. 331–42. doi: 10.1016/j.pbb.2005.01.029.

Wang, H. *et al.* (2016) 'Metabotropic Glutamate Receptors Induce a Form of LTP Controlled by Translation and Arc Signaling in the Hippocampus', *The Journal of Neuroscience*, 36(5), pp. 1723–1729. doi: 10.1523/JNEUROSCI.0878-15.2016.

Wang, S. J. and Gean, P. W. (1999) 'Long-term depression of excitatory synaptic transmission in the rat amygdala.', *The Journal of neuroscience : the official journal of the Society for Neuroscience*, 19(24), pp. 10656–63.

Watabe, A. M., Carlisle, H. J. and O'Dell, T. J. (2002) 'Postsynaptic Induction and Presynaptic Expression of Group 1 mGluR-Dependent LTD in the Hippocampal CA1 Region', *Journal of*

Neurophysiology, 87(3), pp. 1395–1403. doi: 10.1152/jn.00723.2001.

Weber, S. *et al.* (2002) 'Photoactivation of the flavin cofactor in Xenopus laevis (6-4) photolyase: Observation of a transient tyrosyl radical by time-resolved electron paramagnetic resonance', *Proceedings of the National Academy of Sciences of the United States of America*, 99(3), pp. 1319–1322. doi: 10.1073/pnas.032469399.

Wessendorf, M. (2004) 'Autofluorescence: Causes and Cures', *Internet*, pp. 1–8.
Wiley, J. L. *et al.* (2005) 'CB1 cannabinoid receptor-mediated modulation of food intake in mice.', *British journal of pharmacology*, 145(3), pp. 293–300. doi: 10.1038/sj.bjp.0706157.

Willard, S. S. and Koochekpour, S. (2013) 'Glutamate, glutamate receptors, and downstream signaling pathways.', *International journal of biological sciences*. Ivyspring International Publisher, 9(9), pp. 948–59. doi: 10.7150/ijbs.6426.

Yang, Y. and Calakos, N. (2013) 'Presynaptic long-term plasticity.', *Frontiers in synaptic neuroscience*, 5, p. 8. doi: 10.3389/fnsyn.2013.00008.

Yazejian, B., Yazejian, R. M., *et al.* (2013) 'Simultaneous pre- and post-synaptic electrophysiological recording from Xenopus nerve-muscle co-cultures.', *Journal of visualized experiments : JoVE*. MyJoVE Corporation, (73). doi: 10.3791/50253.

Yin, D., Yuan, X. and Brunk, U. T. (1995) 'Test-tube simulated lipofuscinogenesis. Effect of oxidative stress on autophagocytotic degradation', *Mechanisms of Ageing and Development*, 81(1), pp. 37–50. doi: 10.1016/0047-6374(94)01580-F.

Younts, T. J. and Castillo, P. E. (2014) 'Endogenous cannabinoid signaling at inhibitory interneurons', *Current Opinion in Neurobiology*, pp. 42–50. doi: 10.1016/j.conb.2013.12.006.

Zhang, H.-Y. *et al.* (2015) 'Mechanisms underlying the activity-dependent regulation of locomotor network performance by the Na+ pump', *Scientific Reports*. Nature Publishing Group, 5(1), p. 16188. doi: 10.1038/srep16188.

Zhang, H.-Y. and Sillar, K. T. (2012) 'Short-Term Memory of Motor Network Performance via

Activity-Dependent Potentiation of Na+/K+ Pump Function', *Current Biology*, 22(6), pp. 526–531. doi: 10.1016/j.cub.2012.01.058.

Zhang, L., Huang, Y. and Hu, B. (2016) 'Olfactory experiences dynamically regulate plasticity of dendritic spines in granule cells of Xenopus tadpoles in vivo.', *Scientific reports*. Nature Publishing Group, 6, p. 35009. doi: 10.1038/srep35009.